9-13-2016 12:00 AM

Contribution of the Primate Frontal Cortex to Eye Movements and Neuronal Activity in the Superior Colliculus

Tyler R. Peel, *The University of Western Ontario*

Supervisor: Dr. Brian Corneil, *The University of Western Ontario*

A thesis submitted in partial fulfillment of the requirements for the Doctor of Philosophy degree in Neuroscience

Abstract

Humans and non-human primates must precisely align the eyes on an object to view it with high visual acuity. An important role of the oculomotor system is to generate accurate eye movements, such as saccades, toward a target. Given that each eye has only six muscles that rotate the eye in three degrees of freedom, this relatively simple volitional movement has allowed researchers to well-characterize the brain areas involved in their generation. In particular, the midbrain Superior Colliculus (SC), is recognized as having a primary role in the generation of visually-guided saccades via the integration of sensory and cognitive information.

One important source of sensory and cognitive information to the SC is the Frontal Eye Fields (FEF). The role of the FEF and SC in visually-guided saccades has been well-studied using anatomical and functional techniques, but only a handful of studies have investigated how these areas work together to produce saccades. While it is assumed that the FEF exerts its influence on saccade generation though the SC, it remains unknown what happens in the SC when the FEF is suddenly inactivated. To test this prediction, I use the combined approach of FEF cryogenic inactivation and SC neuronal recordings, although it also provides a valuable opportunity to understand how FEF inputs to the SC govern saccade preparation. Nonetheless, it was first necessary to characterize the eye movement deficits following FEF inactivation, as it was unknown how a

large and reversible FEF inactivation would influence saccade behaviour, or whether cortical areas influence fixational eye movements (e.g. microsaccades).

Four major results emerged from this thesis. First, FEF inactivation delayed saccade reaction times (SRT) in both directions. Second, FEF inactivation impaired microsaccade generation and also selectively reduced microsaccades following peripheral cues. Third, FEF inactivation decreased visual, cognitive, and saccade-related activity in the ipsilesional SC. Fourth, the delayed onset of saccade-related SC activity best explained SRT increases during FEF inactivation, implicating one mechanism for how FEF inputs govern saccade preparation. Together, these results provide new insights into the FEF's role in saccade and microsaccade behaviour, and how the oculomotor system commits to a saccade.

Keywords: saccade, microsaccade, frontal eye field, superior colliculus, reversible inactivation, primate, oculomotor system

Co-Authorship Statement

Tyler Peel, the primary author of all chapters, was responsible for designing the experiments, constructing the cryoloops, performing surgical procedures, data collection and analysis, constructing the figures, writing and editing the manuscripts. **Brian Corneil** supervised all projects and contributed to the experimental design, surgical procedures, the interpretation of the results, and manuscript revisions. **Stephen Lomber** was primarily responsible for surgically implanting cryoloops into the arcuate sulcus, and also assisted in editing each manuscript. **Kevin Johnston** assisted in the interpretation of the results, and editing the manuscript in Chapter 2. **Ziad Hafed** contributed to the experimental design, provided modeling data, the interpretation of results, and manuscript revisions in Chapter 3. Finally**, Suryadeep Dash** collected data, assisted in interpreting the results, and the revision of manuscripts from Chapters 3 and 4.

Acknowledgments

For the past seven years, my supervisor Dr. Corneil has been an extraordinary mentor and colleague. My advice for any Ph.D. student is to find a supervisor you can not only trust, but also one whom enjoys research. I can say that Dr. Corneil's passion for research is certainly bar-none, and what is even more impressive is how he can precisely and effectively communicate his thoughts. I know that I received the best mentorship imaginable, and I'm thankful to Brian for allowing me to be his student. I'm sure my many years in the lab will serve me well in the years to come.

I'm also grateful to my collaborators on these manuscripts, and everyone in Dr. Corneil's lab. Most notably, Surya has been a fantastic colleague these past couple years. I'm in his debt for all his constructive comments, and advice he has given me. I'd also like to thank Scott, Mike, Brendan, and Sam for welcoming me into the lab when I first started, Sebastian for productive evenings outside the lab, Chao for keeping up to date on reality, and Becca for her infectious enthusiasm. Of course, I need to acknowledge the fine work of our animal care staff, Darren and Kat, for taking excellent care of Mookie, Alex, Diaz, Gruber, Ozzie, and the rest of the boys. I'm also very appreciative of the guidance and assistance from Ziad, Steve, Stefan, and Kevin J, and I hope to continue learning from these exceptional researchers.

Finally, I'd like to mention that I could have never accomplished this feat without the support of my loving girlfriend Julia, and my family: Mom, Dad, Tina, Travis, Ryan, Sean, Grandmas, Grandpa, and my close friends in Ontario and abroad. Hopefully, I'll see you soon!

Table of Contents

List of Figures

List of Abbreviations

~ - approximately

˚ - degree of visual angle

˚C - degrees Celsius

ANOVA - analysis of variance

cm - centimeter

DLPFC - dorsolateral prefrontal cortex

EBN - excitatory burst neuron

ft - foot

FEF - frontal eye field

GABA - gamma-aminobutyric acid

Hz - hertz

iSC - intermediately layers of the superior colliculus

IBN - inhibitory burst neuron

IA - inferior arm

kHz - kilohertz

kg - kilogram

LLBN - long-lead burst neuron

LIP - lateral intraparietal area

LGN - lateral geniculate nucleus

LED - light-emitting diode

LATER - Linear Approach to Threshold with Ergodic Rate

mm - millimeter

ms - millisecond

MRF - midbrain reticular formation

MN - motoneuron

MD - medial dorsal nucleus of thalamus

MRI - magnetic resonance image

MΩ - megaohms

nPH - nucleus prepositus hypoglossi

OPN - omnipause neuron

PPRF - paramedian pontine reticular formation

s - second

SA - superior arm

SRT - saccade reaction time

SC - superior colliculus

sSC - superficial layers of the superior colliculus

SBN - saccadic burst neuron

SNr - substantia nigra pars reticulata

µA - microamp

V1 - primary visual cortex

V4 - extrastriate visual cortex

List of Appendices

Chapter 1

General Introduction

1.1: Preamble

From scanning for food to performing actions like reaching, humans and non-human primates depend upon sight to perceive and interact with our surroundings. One phylogenetically novel aspect of the visual system of primates is that central vision is better represented than peripheral vision. Indeed, the eye contains a centralized fovea with an increased number of light-sensitive cells and optic nerve fibers compared to the outer regions of the retina (Stone and Johnston, 1981; Curcio and Allen, 1990). Consequently, the visual axis of the eye must be reorientated to observe a new image in fine visual detail.

The role of the *oculomotor system* is to reorient the eyes, and maintain active fixation of a visual target. While the oculomotor system generates many types of eye movements, rapid and conjugate movements of both eyes, called *saccades*, are largely responsible for reorienting the visual axis to a new target. Such saccadic eye movements followed by short durations of fixation permit the efficient analysis of the visual scene, but recurring eye movements during fixation are also essential for vision. For instance, the oculomotor system can generate *microsaccades* during fixation to precisely reorientate the fovea towards the target in high acuity tasks, such as threading a needle (Ko et al.,

2010). Because such small and repetitive microsaccades (typically <2˚ occurring ~2/s) refresh a visual image onto the retina, they may also counteract visual adaptation where the absence of movements reduces the visual perception of peripheral objects (Martinez-Conde et al., 2006). Consistent with this, microsaccades impact visual processing and visually-guided movements (Martinez-Conde et al., 2006; Rolfs et al., 2006; Hafed et al., 2015).

For visually-guided saccades, visuospatial information related to the target must be converted to a motor command, collectively called the sensorimotor transformation. However, natural environments usually contain many, constantly changing stimuli, thus cognitive control is required to decide which target to attend to, what visuospatial information to retain, and when to initiate a movement. In the oculomotor system, such flexible visually-guided movements depend on the convergence of sensory (e.g. visuospatial information) and cognitive processes (e.g. attention, memory, task goals) in the intermediate and deep layers of the Superior Colliculus (iSC). This midbrain structure has a primary role in generating visually-guided saccades, which has been well-studied within the primate animal model (Robinson, 1972; Wurtz and Goldberg, 1972a, 1972b; Sparks, 1975; Munoz and Wurtz, 1995; Dorris et al., 1997; Wurtz et al., 2001). This is due to the fact that invasive techniques can be used in non-human primates (e.g. lesions, electrical stimulation, neuronal

recordings), and both humans and non-human primates similarly contain a fovea within each eye that is reoriented by the six oculomotor muscles.

The primate frontal eye field (FEF) represents another well-studied brain area in saccade generation (Bruce and Goldberg, 1985; Bruce et al., 1985; Schall, 1991; Hanes and Schall, 1996; Hanes et al., 1998; Schlag et al., 1998; Brown et al., 2008), and importantly, the integrity of one of the FEF and iSC is required to generate saccades (Schiller et al., 1980). However, compared to the numerous studies that have studied the role of either the FEF or iSC to saccade behaviour, only a handful of studies have used combined approaches to investigate how these oculomotor areas work together to produce saccades. In one such study, Hanes and Wurtz (2001) showed that iSC inactivation abolished evoked saccades from the FEF, consistent with the FEF influencing saccade preparation though its projections to the ipsilateral iSC. Moreover, by stimulating the iSC to antidromically-identify FEF neurons with neuronal recordings, a few studies have demonstrated that FEF neurons projecting directly to the iSC contain sensory and cognitive information (Segraves and Goldberg, 1987; Everling and Munoz, 2000; Sommer and Wurtz, 2000). While the FEF is thought to be a key source of frontal inputs to the iSC, the iSC also receives sensory and cognitive information from other important oculomotor areas (Hikosaka and Wurtz, 1983a; Paré and Wurtz, 1997; Johnston and Everling, 2006). Because it remains unknown what happens in the iSC when the FEF is suddenly inactivated, we still do not know

how FEF inputs to the iSC (i.e. those pertaining to sensory or cognitive processes) govern saccade preparation, or how the iSC is involved in the decision to commit to a saccade. Interestingly, studies using inactivation of other brain areas have revealed unexpected findings about oculomotor function (Zénon and Krauzlis, 2012b; Johnston et al., 2014; Katz et al., 2016), stressing how important combining casual techniques (i.e. inactivation) with neuronal recordings are to support predictions.

In this thesis, I address the FEF's functional contribution to saccades and microsaccades, and neuronal activity in the downstream iSC using the combined approach of cryogenic FEF inactivation and iSC neuronal recordings. I begin by describing the important characteristics of saccades and microsaccades, and the role of the brainstem in generating these particular eye movements. Then I discuss previous research pertaining to sensory and cognitive processes in the iSC, and how the FEF could be a key cortical source of visual, cognitive, and saccade-related signals underlying these processes. Finally, I cover the specific objectives for this thesis, and the important methodological considerations when examining the function contribution of an individual brain area to behaviour and neuronal activity in the oculomotor system.

1.2: Oculomotor behaviour

1.2.1: Saccades

Saccades are ballistic movements with highly stereotypical kinematics. Specifically, saccade peak velocity or duration increases non-linearly with its amplitude (Zuber and Stark, 1965). These *main sequence relationships* (see **Fig. 1-1**) hold for the natural range of saccades from microsaccadic amplitudes < 2˚ to saccades of ~15˚ (Bahill et al., 1975), and suggest that the brainstem circuitry is optimized to tradeoff saccade amplitude and duration. Since saccade durations are typically very short (~50 ms), the trajectories are largely insensitive to visual or proprioceptive feedback during the movement; thus, saccades are characterized as *ballistic* movements (Keller and Robinson, 1971; Burr et al., 1994). While the ability to efficiently analyze the visual scene largely depends on saccade metrics (amplitude and direction) and dynamics (peak velocity or duration), another important determinant is the time taken to initiate a saccade.

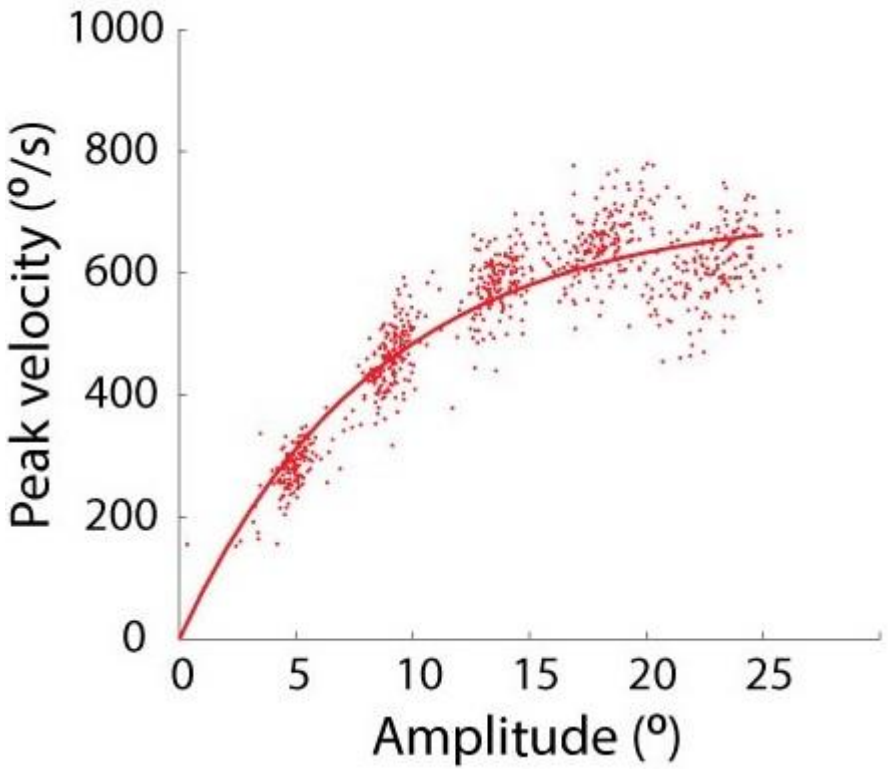

Figure 1-1. Main sequence relationship of saccade amplitude and peak velocity. Each dot represents an individual saccade. A non-linear regression is fitted to the data. Own figure from a monkey performing visually-guided saccades.

Saccade reaction time (SRT) is a fundamental and well-studied measure of the sensorimotor transformation (Fischer and Ramsperger, 1984; Munoz et al., 1998; Reddi and Carpenter, 2000; Taylor and Klein, 2000). In many experimental designs, the SRT indicates the time taken to initiate a saccade relative to a go-cue for each trial (e.g. appearance of a peripheral visual target, or extinguishing of a central fixation target). Even with the exact same stimuli and saccade response, the SRT is highly variable, ranging from 60 to 1000 ms, suggesting that the SRT is under volitional control. Nonetheless, properties of the stimuli can systematically influence SRT; for example, saccades are initiated quicker toward a bright stimuli compared to a dim one (Boch et al., 1984). Together, this evidence is consistent with the SRT being influenced by both sensory and cognitive processes.

The influence of sensory and cognitive processes on SRT can be studied more directly using specific saccade tasks. For instance, a sensory influence is revealed when comparing delayed visually- and memory-guided saccades. Saccades are more rapidly initiated towards persistent rather than extinguished visual targets (Becker and Fuchs, 1969), reflecting the additional sensory information available when preparing for a saccade. Importantly, a cognitive process is nonetheless required to recall the location of the extinguished target for memory-guided saccades. Similarly, an interaction of sensory and cognitive influences is exhibited in the pro- or anti-saccade task, which instructs subjects in

advance to either generate a saccade toward or diametrically away from a presented visual target, respectively. Anti-saccades have increased SRTs compared to pro-saccades (Hallett and Adams, 1980), reflecting a cognitive process that acts to suppress the natural tendency for a pro-saccade and then generate an anti-saccade toward an internally-generated target (Funahashi et al., 1993; Everling et al., 1998).

The LATER (Linear Approach to Threshold with Ergodic Rate) model for saccade initiation is a well-established, *rise-to-fixed threshold* model that captures the aforementioned aspects (e.g. variability of SRT, availability of information, and decision criteria) of saccade behaviour (**Fig. 1-2**; (Carpenter and Williams, 1995; Carpenter et al., 2009)). According to this model, a decision signal, beginning at some starting level, rises to a fixed threshold at which point a saccade is triggered. Interestingly, trial-by-trial variability in the accumulation rate can explain for experimental data when using the reciprocal of SRT. Moreover, changes to SRT resulting from the availability of information or task instructions have been successfully explained by altering the model's mean rate of accumulation or threshold, respectively (Reddi and Carpenter, 2000; Ludwig et al., 2004; Lo and Wang, 2006). This rise-to-fixed threshold framework is also remarkably similar to neuronal activity in oculomotor areas preparing to initiate a saccade. Specifically, previous reports have found that FEF and iSC neurons exhibit presaccadic activity rising to a fixed threshold, and the timing this

saccade-related activity is strongly correlated to SRT (Hanes and Schall, 1996; Dorris et al., 1997; Ratcliff et al., 2007). However, recent neurophysiological evidence suggests that saccade thresholds can vary (Heitz and Schall, 2012; Jantz et al., 2013), and the onset time of saccade-related activity is also an important factor in the underlying mechanism of saccade initiation (Pouget et al., 2011). Thus, while this rise-to-fixed threshold model may accurately reflect behaviour, and some aspects of FEF and iSC activity, it is perhaps an oversimplification of the underlying decision mechanism.

In all, preexisting models of saccade initiation (i.e. rise-to-threshold) and generation (i.e. main sequence relationship) provide a useful way to examine how oculomotor brain areas contribute to saccade behaviour. An important objective in this thesis is to study how large regions of the FEF contribute to saccade reaction time, metrics, and dynamics. By characterizing the saccadic deficits following FEF inactivation, this enabled us to make predictions based from preexisting models of saccade behaviour for testing the underlying neuronal mechanisms.

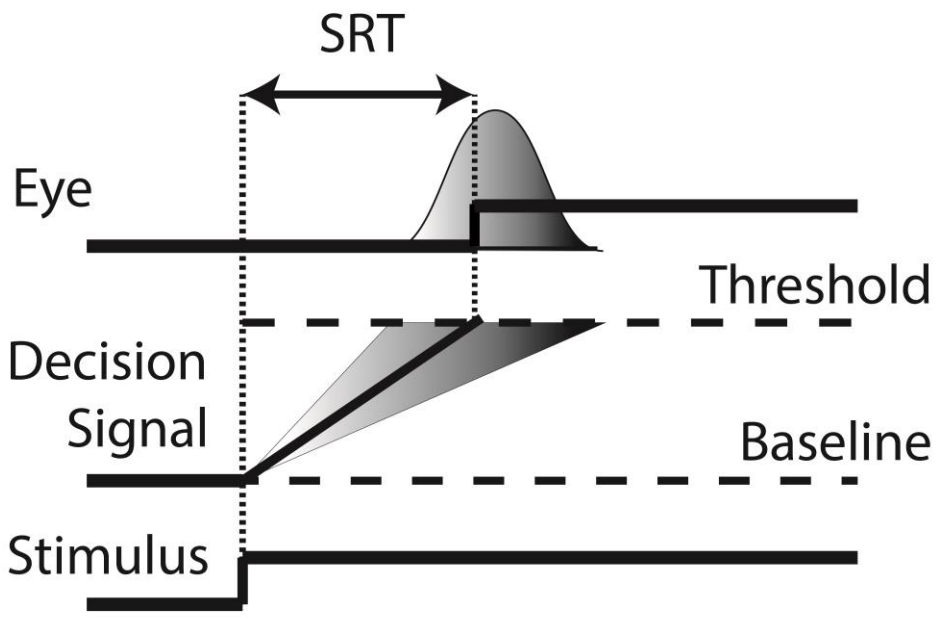

Figure 1-2. Rise-to-threshold model of saccade initiation. In this model, a decision signal related to the stimulus rises from a starting level to a threshold level, at which point a saccade is triggered. Trial-by-trial variability in the accumulation rate can account for the normal physiological variability of SRT.

1.2.2: Microsaccades

Microsaccades are similar to small amplitude saccades, but are involuntary generated during active fixation of a visual target. Nonetheless, microsaccades can be strategically deployed in high acuity tasks by reorienting the fovea toward an object (Ko et al., 2010; Poletti et al., 2013), and impact neuronal activity in the visual system (Bair and O'Keefe, 1998; Leopold and Logothetis, 1998; Martinez-Conde et al., 2000, 2002; Snodderly et al., 2001; Kagan et al., 2008), suggesting that the oculomotor system can also aid vision by microsaccade deployment. Importantly, microsaccades have ballistic and accurate movements similar to larger saccades (Land et al., 1999; Ko et al., 2010), and both types of eye movements follow the same main sequence relationships (Zuber and Stark, 1965); therefore the brain areas involved in saccade generation presumably also have a role for microsaccade generation. Consistent with this idea, the occurrence of microsaccades delays the SRT of visually-guided saccades (Rolfs et al., 2006), and recent studies inactivating the iSC largely support the notion that this structure is involved in generating both saccades and microsaccades (see (Hafed et al., 2009; Hafed, 2011)). However, there is a complete lack of studies investigating the cortical substrates of microsaccade generation. A key objective in this thesis is examine whether the FEF influences microsaccade generation.

The appearance of peripheral stimuli impart very robust time-varying influences on microsaccade rate and direction, which can be altered by either cognitive and sensory processes. The *microsaccadic rate signature* is characterized by a decline in microsaccade rate ~100-200 ms after stimuli onset, followed by a rate rebound lasting ~200 ms then returning to baseline rates (**Fig. 1-3**). Such *rebound microsaccades* exhibit different rates depending upon whether endogenous (implicit information) or exogenous cues (explicit information) specify visuospatial targets for saccades (Laubrock et al., 2005). Moreover, these rebound microsaccades are thought to reflect covert shifts of attention (Hafed and Clark, 2002; Engbert and Kliegl, 2003; Laubrock et al., 2005). Consequently, examining the FEF's contribution to microsaccades generated before and after peripheral cues could lead to a better understanding for how cue-induced or cognitive processes influences microsaccade deployment.

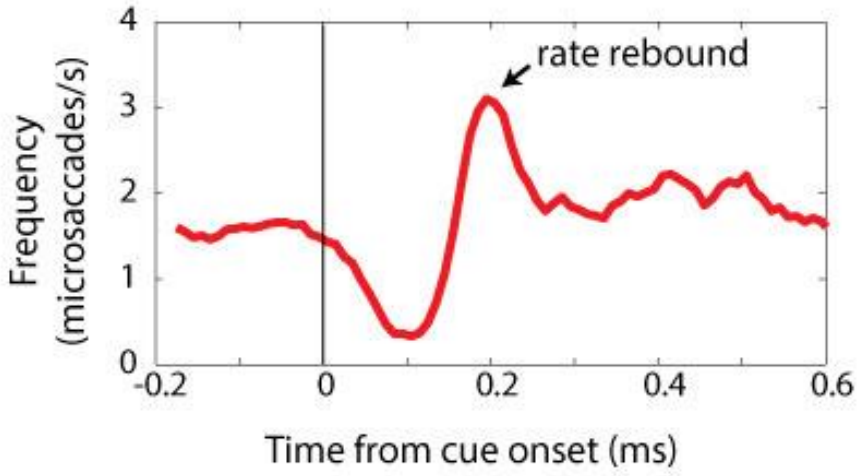

Figure 1-3. Peripheral cues impart a characteristic microsaccadic rate signature. From a baseline microsaccade rate, microsaccade rate dropped ~100 ms following cue onset, and subsequently rebounded ~250 ms following cue onset. Own figure from a monkey performing delayed saccades.

1.3: Oculomotor system

1.3.1: The extraocular muscles, and its motoneurons

The coordinated efforts of the extraocular muscles and the motor neurons in the brainstem and are responsible for generating saccades and microsaccades. Historically, the mechanics of the extraocular muscles (Robinson, 1964), and corresponding signals from its innervated motoneurons have provided a solid basis for understanding how the brain generates these particular eye movements (Robinson, 1970; Schiller, 1970; Fuchs and Luschei, 1971).

In general, the eye rotates about the vertical, horizontal, and visual axes (line of sight) to produce horizontal, vertical, and torsional eye movements, respectively. The six extraocular muscles are orthogonally paired such that one pair primarily controls a specific direction of eye movement (see Fig. 1 of Sparks, 2002). For example, contractions of the medial and lateral recti produce horizontal eye movements. Moreover, vertical and torsional eye movements are controlled by a combination of the remaining extraocular muscles (i.e. superior and inferior recti, and superior and inferior oblique muscles).

The extraocular muscles are innervated by three cranial nerves originating from the brainstem. For example, the abducens nerve (cranial nerve VI) innervates the lateral rectus to induce a horizontal eye rotation away from the nose (abducting movements; (Fuchs and Luschei, 1970)). Likewise, the

trochlear nerve (cranial nerve IV) also innervates a single muscle (superior oblique), but projects to the contralateral eye (Fuchs and Luschei, 1971). The oculomotor nerve (cranial nerve III) ultimately divides into four branches to innervate all other extraocular muscles (medial, inferior rectus, inferior oblique of the ipsilateral eye, and the superior rectus of the contralateral eye; (Robinson, 1970; Schiller, 1970)). Notably, the abducens nuclei also contains internuclear neurons projecting to the oculomotor nuclei that ensure coordinated horizontal saccadic eye movements from the lateral and medial recti (Büttner-Ennever and Akert, 1981).

Despite ongoing debates about the role of the oculomotor plant in rotating the eyes (see Demer, 2006), motoneurons clearly provide the necessary signals from a mechanistic perspective to generate saccades and microsaccades (Robinson, 1964; Sylvestre and Cullen, 1999; Van Horn and Cullen, 2009). Since the inertia of the eye is negligible, eye movements are only required to overcome the viscous drag and elastic restoring forces. Indeed, motoneurons exhibit both a *pulse* and *step* of activity that contribute to saccades and the holding of the eye position in its orbit, respectively (Fuchs and Luschei, 1970; Robinson, 1970; Schiller, 1970; Scudder et al., 2002). In particular, these motoneurons contain brief pulses of activity up to ~500 spikes/s, and sustained steps of activity at an order of a magnitude less. I next examine the brainstem

areas providing the pulse and step of activity to motoneurons for saccadic eye movements.

1.3.2: Brainstem areas involved in eye movement control

Specific brainstem areas project to abducens, trochlear, and oculomotor nuclei, and contribute the pulse and step of activity to motoneurons for saccadic eye movements. Importantly, the majority of neurons in these brainstem areas display temporal-coded activity, such as an on/off response, which is tightly coupled to the saccade produced.

For instance, saccadic burst neurons (SBN) within the brainstem burst generator exhibit a pulse of activity during the saccade. SBN comprise both excitatory burst neurons (EBN) and inhibitory burst neurons (IBN), which work together to produce a favourable contraction-relaxation of the paired extraocular muscles (**Fig. 1-4**). For example, EBNs projecting to the abducens nuclei for horizontal saccadic eye movements originate from the paramedian pontine reticular formation (PPRF; (Sparks and Travis, 1971; Cohen and Henn, 1972; Strassman et al., 1986b)). Lesions to the PPRF abolish the ability to generate horizontal saccades (Cohen et al., 1968), thus confirming the critical role for EBN in saccade generation. The IBN for horizontal saccadic eye movements are contained in the medullary reticular formation, which silence motoneurons in the contralateral abducens nuclei (Strassman et al., 1986a;

Scudder et al., 1988). For the vertical and torsional components of saccadic eye movements, the SBN are found in the midbrain reticular formation (MRF; (Büttner et al., 1977; King and Fuchs, 1979)). SBN bursts of activity start ~10-20 ms before saccade onset (Strassman et al., 1986b), and its number of spikes and peak activity are related to saccade amplitude and peak velocity, respectively. Thus, this evidence is consistent with the tight coupling of SBN activity and saccade initiation and generation.

The step of activity in motoneurons is supplied by other oculomotor brainstem areas. These brainstem structures integrate the pulse command from the EBN to encode a new position signal enabling the eyes to hold their orbital position. The nucleus prepositus hypoglossi (nPH) serves as the *neural integrator* for horizontal eye movements (McFarland and Fuchs, 1992), and receives the appropriate signals from the PPRF (**Fig. 1-4**). Moreover, the interstitial nucleus of Cajal integrates pulses originating from the MRF for steps in vertical eye position (King et al., 1981; Crawford et al., 1991). Lesions to their areas disrupt the ability to hold the eyes at a new position following a saccade, consistent with a role of these areas in providing a step command to the motoneurons (Cannon and Robinson, 1987).

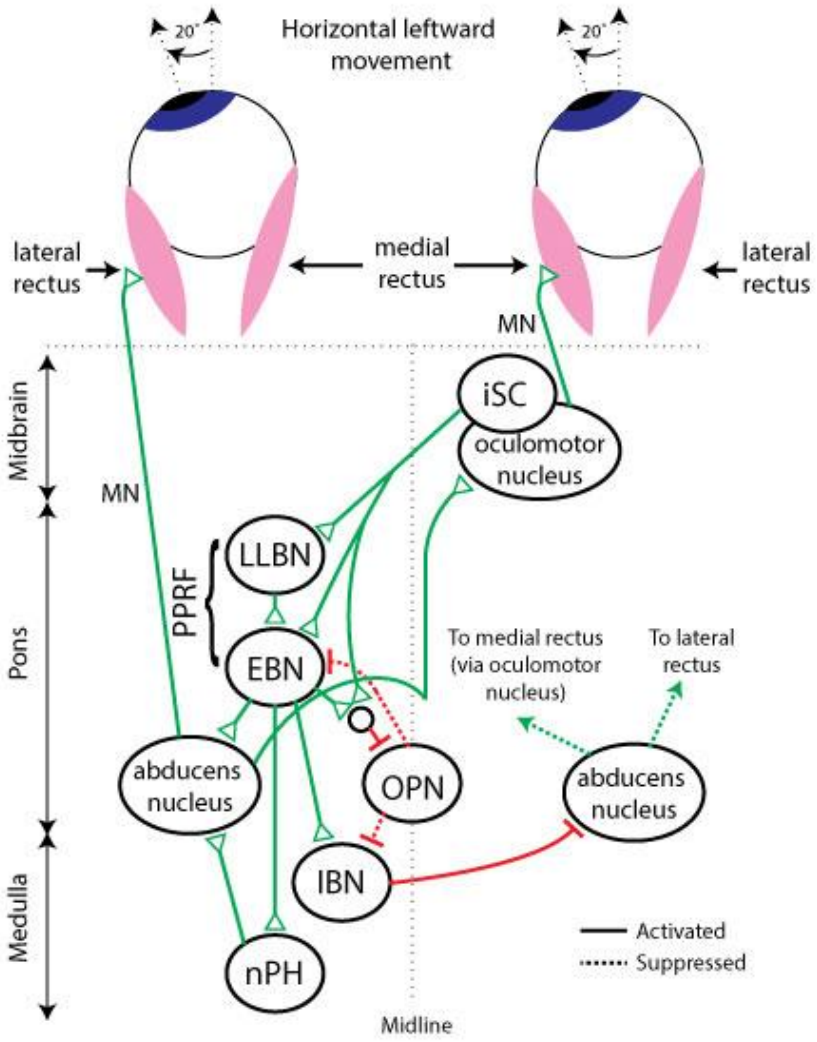

Figure 1-4. Brainstem circuitry for horizontal saccades. A pulse of activity originating from the right iSC triggers the abducens motoneurons on the contralateral side via the PPRF, which contracts the lateral rectus to abduct the left eye. Together, the iSC, and PPRF inhibit the OPN via inhibitory interneurons, which releases SBN from tonic inhibition. Internuclear neurons from the abducens nucleus project to the contralateral oculomotor nucleus to also contract the medial rectus. The nPH integrates the EBN pulse command to provide a tonic step of a activity to abducens motoneurons for maintaining the new eye position. Finally, IBN silences the contralateral abducens nucleus to relax the left medial and right lateral recti. (SBN, saccadic burst neuron; EBN, excitatory burst neuron; IBN, inhibitory burst neuron; LLBN, long-lead burst neuron, MN, motoneuron, nPH, nucleus prepositus hypoglossi, OPN, omnipause neuron; PPRF, paramedian pontine reticular formation).

While functionally similar to the SBN, the long-lead burst neurons (LLBN) distributed throughout the PPRF (**Fig. 1-4**), appear to have a more supervisory role on saccadic eye movements. Similar to SBN, LLBN can provide a pulse of activity directly to the motoneurons (Strassman et al., 1986a), but differ because of the much advanced (~200-20 ms) activity before saccade onset (Munoz et al., 2000). Thus, the LLBN are a possible candidate for removing the tonic influence of the omnipause neurons (OPN) on the SBN (see **Fig. 1-4**). While the role of the LLBN remains unclear, the LLBN at the very least represent a key functional connection between the iSC, FEF, and other subcortical areas for saccade generation (Scudder et al., 1996; Keller et al., 2000).

Despite these brainstem areas having a critical role for saccade generation, they are normally triggered by the iSC and/or cortical FEF to generate a saccade with a specific vector (Schiller et al., 1980; van Opstal and Kappen, 1993). This permits the oculomotor system to incorporate visuospatial information and cognitive processes for the generation of saccades towards visual targets.

1.3.3: Convergence of sensory and cognitive information in the intermediate layers of the superior colliculus

Together, the midbrain iSC and cortical FEF drive the downstream brainstem circuitry for saccade generation, although the FEF likely exerts much of its influence on saccade generation through the iSC (Segraves and Goldberg, 1987; Hanes and Wurtz, 2001). Thus while the iSC and FEF have parallel projections to the brainstem (Harting, 1977; Stanton et al., 1988a), the FEF brainstem pathway that bypasses the SC likely only has subtle influences on saccade generation. Neurons within either the FEF and iSC contain visual-, cognitive-, or saccade-related responses, reflecting the sensorimotor transformation (Schiller and Koerner, 1971; Bruce and Goldberg, 1985), and the FEF sends all these responses to the SC (Segraves and Goldberg, 1987; Everling and Munoz, 2000; Sommer and Wurtz, 2000), thus the FEF is a likely a key source of frontal inputs to the SC. I'll next describe the functional organization of the iSC, and how neurons within this structure respond after cues, or before saccades for the sensorimotor transformation.

First, the iSC contains a functional topography with each neuron encoding a restricted region of visual space (response field) and/or an ideal saccade vector (movement field). As first described by Robinson (1972), the rostral and caudal aspects of the iSC represent foveal or peripheral visual space, respectively (**Fig. 1-5**). Visual response and movement fields are highly aligned in the iSC, thus

these rostral and caudal aspects also encode microsaccades and large saccades, respectively. This continuum from small to large saccades in the iSC map follows a logarithmic relationship with more neurons representing either foveal visual space, smaller saccades, or fixation-related responses (Bergeron and Guitton, 2000; Hafed et al., 2009). Notably, each side of the iSC encodes contralateral visual space or saccades, and the medial-lateral iSC axis represents the entire directional range between vertical-upward to vertical-downward visual space or saccades. Together, this suggests that the iSC drives the brainstem circuitry with a specific saccade command.

Second, iSC neurons typically display a continuum of responses representative of a sensorimotor transformation, from visual to saccade-related bursts of activity starting in advance of the saccade (**Fig. 1-6**). Approximately 50 ms after a visual target appears, many iSC neurons encoding that region of space exhibit a clear burst of spikes. The timing and magnitude of this visual-related activity is related to the luminosity of the visual stimuli (Bell et al., 2006), thus largely reflects a sensory signal for the visual target. If this visual target is also the goal of saccade command, then many of these same iSC neurons display a second burst of spikes with its peak activity occurring around the time of saccade initiation (Munoz and Wurtz, 1995; Dorris et al., 1997). This saccade-related activity can be clearly dissociated from visual-related activity in delayed saccade tasks (Mays and Sparks, 1980), which requires subjects to saccade towards the

target after a certain time interval or if instructed by a go-cue (e.g. extinguishing of a central fixation target).

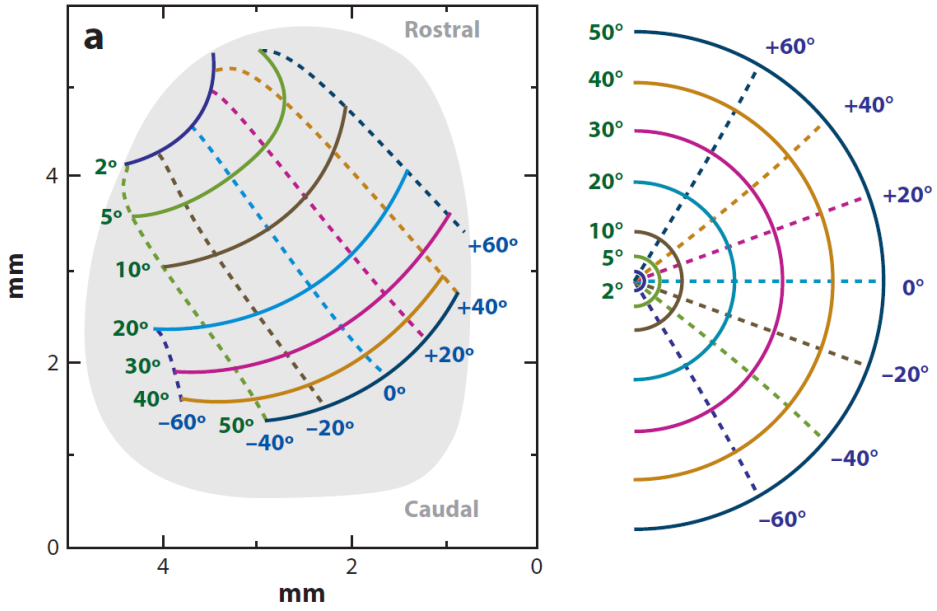

Figure 1-5. Topographic map of visual response or saccade movement fields in the iSC. Neurons in the left iSC encode the contralateral or right visual space. From (Gandhi and Katnani, 2011).

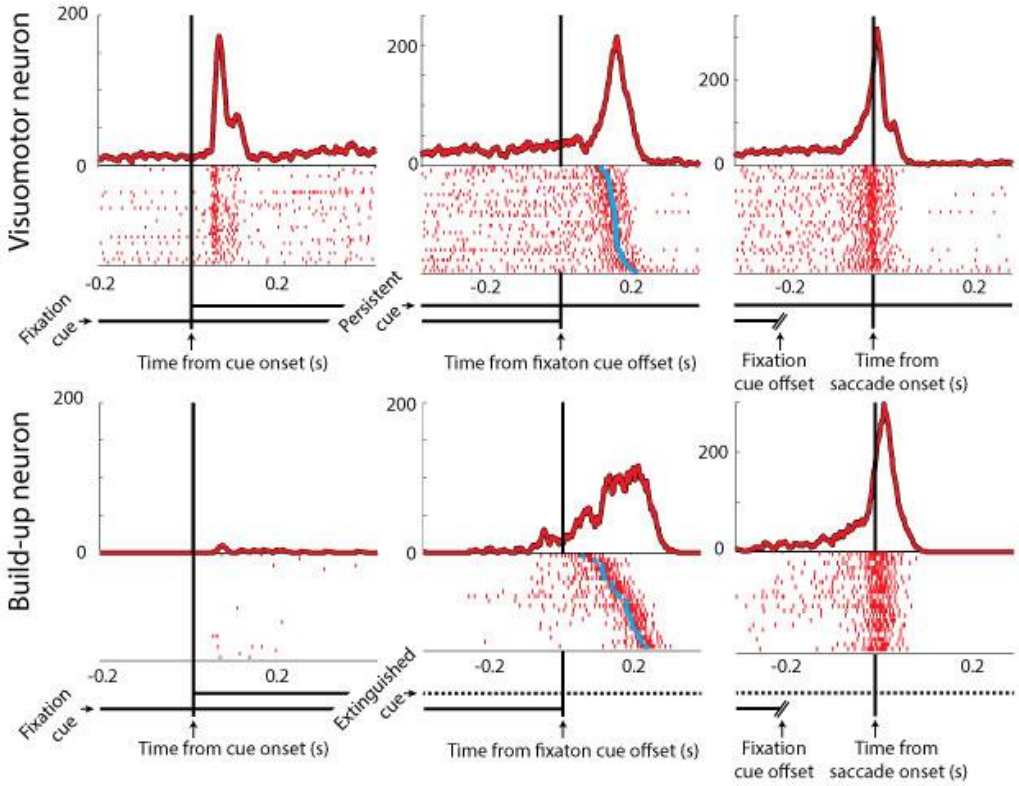

Figure 1-6. Firing patterns of two example iSC neurons displaying visual, delay-period, and/or saccade-related activity. The first, a visuomotor neuron, exhibits visual-related activity following cue onset (left), and during the delay-period (middle), and also a burst of activity starting immediately before saccade onset (right). The second neuron displays delay-period activity, in the absence of a visual cue, building up to peak of activity around saccade onset. Cyan dots indicate the SRT for each trial. Own figure from dataset of iSC neurons with a monkey performing delayed saccades (see **Chapter 4**).

Third, iSC neurons can also exhibit task-related activity, which is important for flexible visual-guided saccades. For example, iSC neurons can exhibit low-frequency spikes following the appearance of a visual stimuli that reflects its the behavioural relevance (Everling et al., 1999), and the probability of initiating a saccade toward it (Basso and Wurtz, 1998). For certain iSC neurons containing a saccade-related response, their activity can accumulate or *build-up* once a go-cue for a saccade has been given, starting at least 100 ms before saccade onset (Munoz and Wurtz, 1995). Consistent with this observation, electrical stimulation at sub-saccadic currents enhances the selection of a contralateral rather than ipsilateral target for saccadic responses (Carello and Krauzlis, 2004). Similarly, the presence of the visual target strengthens the resulting saccade-related activity compared to visually absent targets (Munoz and Wurtz, 1995; Edelman and Keller, 1996), thus the saccade command issued by the iSC ultimately reflects the convergence of both sensory and cognitive information.

In all, this evidence suggests that the iSC is a key oculomotor area for the cognitive control of saccades and microsaccades. This view has been reinforced by iSC inactivation studies, which provide a critical test the iSC's role for saccade and microsaccade behaviour.

1.3.4: Role of the intermediate layers of superior colliculus in saccade and microsaccade behaviour

The integrity of the iSC is important for the generation of saccades and microsaccades. For instance, caudal iSC inactivation causes a triad of deficits (i.e. increased SRT, decreased accuracy, and peak velocity) for contralateral saccades directed towards the affected region of the visual field (Hikosaka and Wurtz, 1985, 1986; Quaia et al., 1998). Similarly, rostral iSC inactivation greatly diminished the overall frequency of microsaccades generated in both directions (Hafed et al., 2009; Goffart et al., 2012). While the iSC contributes to both saccade and microsaccade generation, this oculomotor structure is also particularly key in cognitively demanding saccade tasks, and cognitive influences on microsaccade deployment. I emphasize each of these two iSC contributions to illustrate its role for the cognitive control of oculomotor behavior.

For instance, caudal iSC inactivation causes a more pronounced triad of deficits and performance errors, such as incorrectly initiated saccades (e.g. before the go-cue) or completely neglecting to saccade, for memory-guided than visually-guided saccades (Hikosaka and Wurtz, 1985, 1986; Quaia et al., 1998). Moreover, in a covert visuospatial attention task where peripheral cues guide behavioural responses, monkeys ignored cues in the affected region of the visual field during caudal iSC inactivation (McPeek and Keller, 2004). Importantly, attentional deficits occurred independently of impairments in saccade

generation (McPeek and Keller, 2004), which suggests that the iSC is directly involved in the mechanism governing visuospatial attention. Interestingly, caudal iSC inactivation causes similar impairments in visuospatial attention without perturbing mechanisms involving the visual cortex (Zénon and Krauzlis, 2012a), consistent with the iSC having a particularly important role in processing visuospatial information.

Although microsaccade behaviour is related to the convergence of sensory and cognitive information, the contribution of oculomotor areas, including the iSC, to its underlying mechanisms have been less studied. Only one study to date has investigated the causal role of caudal iSC to microsaccade deployment following peripheral cues (Hafed et al., 2013). Recall that peripheral stimuli impart a very specific rate signature on microsaccade behaviour (Hafed and Clark, 2002; Engbert and Kliegl, 2003; Laubrock et al., 2005). Intriguingly, inactivating portions of the iSC encoding peripheral stimuli do not affect the rate of microsaccades, but causes microsaccades to be biased away following visual targets. Inactivating the FEF could help clarify the role of each structure to microsaccade deployment.

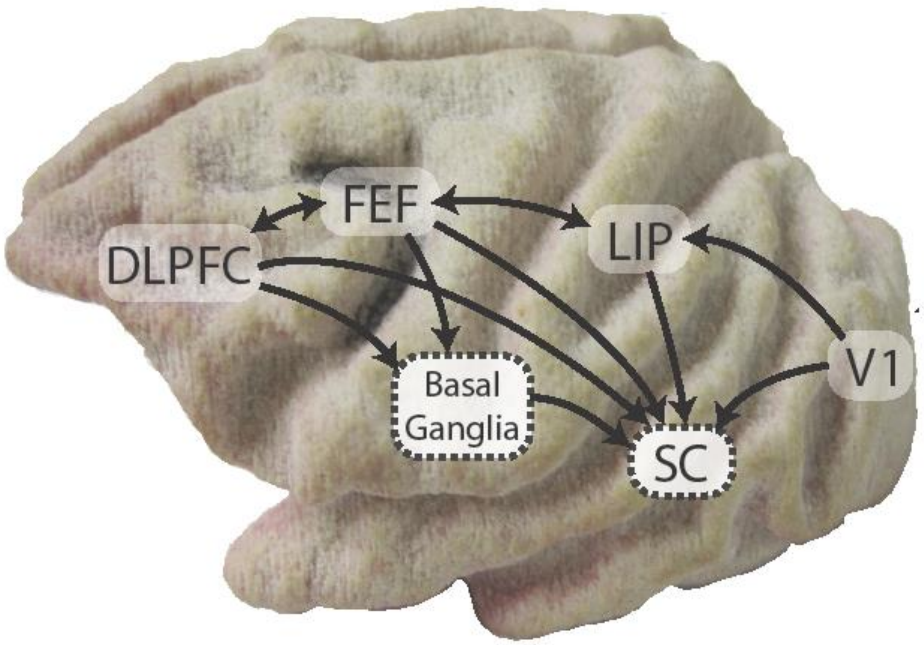

Figure 1-7. Convergence of sensory and cognitive information in the FEF and iSC. Visuospatial information is primary relayed through the cortex to converge on oculomotor areas implicated in saccade generation (i.e. FEF and iSC). Alternatively, cognitive information from the DLPFC passes through the frontal cortex or basal ganglia to these same oculomotor areas. (V1, primary visual cortex; LIP, lateral intraparietal area; FEF, frontal eye field; DLPFC, dorsolateral prefrontal cortex; SC, superior colliculus)

1.3.5: Frontal eye fields sends sensory and cognitive information to the intermediate layers of superior colliculus

What is the source of sensory and cognitive information to the iSC? The FEF is a possible substrate for how cortical processes influence the oculomotor mechanisms in the iSC (**Fig. 1-7**). The FEF is a functionally defined area in the frontal lobe that evokes saccadic eye movements with very low stimulation currents of <50 μA (Bruce et al., 1985), which anatomically corresponds to the anterior bank of the arcuate sulcus in the non-human primate. Similar to the iSC, the FEF contains a topographic map of visual response fields, and saccade movement fields in the contralateral direction, however FEF neurons are occasionally tuned in the ipsilateral direction (Bruce and Goldberg, 1985; Crapse and Sommer, 2009). Despite early antidromic studies reporting that FEF corticotectal neurons (FEF neurons projecting directly to the ipsilateral iSC; (Kuenzle et al., 1976; Stanton et al., 1988a, 1989)) contained only saccade-related signals (Segraves and Goldberg, 1987), it is now known that FEF corticotectal neurons project to topographically similar iSC neurons, and exhibit a diverse set of responses, including task-related signals from cognitive processes (Everling and Munoz, 2000; Sommer and Wurtz, 2000, 2001; Helminski and Segraves, 2003).

For example, the pre-stimulus, visual and saccade-related activity of FEF corticotectal neurons is modulated by a cognitive process that integrates task goals to modify saccade behaviour. In correctly performed anti-saccade trials, FEF neurons displayed reduced pre-stimulus, and visual activity, and a suppression of saccade-related activity for presented targets in its response field compared to pro-saccades (Everling and Munoz, 2000). In contrast, when monkeys generated an erroneous pro-saccade in an anti-saccade trial, FEF neurons had presaccadic activity more reflective of correctly performed pro-saccades than anti-saccades. Therefore, the binding of task goals to saccade behaviour was exhibited by FEF corticotectal neurons projecting directly to the iSC.

Importantly, inactivation studies have provided causal evidence that the FEF has an important contribution to the generation of visually-guided saccades. Analogous to the effects of iSC inactivation, FEF inactivation produces a triad of contralateral deficits for saccades directed toward the affected region of the visual field, and causes more pronounced deficits for memory-guided than visually-guided saccades (Sommer and Tehovnik, 1997; Dias and Segraves, 1999). Interestingly, FEF inactivation also increases the incidence of performance errors similar to those observed following caudal iSC inactivation, but FEF inactivation additionally causes an inability to suppress saccades towards ipsilateral cues.

Given that FEF corticotectal neurons project to topographically similar iSC neurons, what is an mechanistic explanation for these ipsilesional saccades? One possible reason is that inactivating small FEF regions, usually achieved by pharmacological modulations in these previous reports (Sommer and Tehovnik, 1997; Dias and Segraves, 1999), may bias the contribution of ipsilateral tuned FEF neurons. Indeed, ipsilateral tuned neurons are relatively more scattered in the FEF than neurons turned in the contralateral direction (Bruce and Goldberg, 1985); thus, large-volume inactivations could help clarify the FEF's role for saccade generation, particularly in the ipsilateral direction.

Interestingly, there is mounting evidence that the FEF is involved in visuomotor processing for both directions. First, evidence exists of functional connections from the FEF to both sides of iSC. In addition to the aforementioned ipsilateral projections, the lateral aspect of the FEF corticotectal neurons clearly projects to the contralateral iSC (Distel and Fries, 1982). Moreover, FEF neurons can be activated by electrical stimulation from each side of the iSC (Sommer and Wurtz, 2004; Crapse and Sommer, 2009), and exhibit tuning fields that could be predicted based on these iSC inputs. For example, FEF neurons with connections to contralateral iSC had lateralized tuning fields in the ipsilateral direction, whereas tuning fields could be in any direction if FEF neurons had inputs from both iSC. Second, FEF neurons, in either hemisphere, exhibit temporal firing patterns highly dependent on their visual response fields. Specifically, FEF

neurons with overlapping or non-overlapping visual response fields had positive or negative spike timing correlations, respectively (Cohen et al., 2010). This cooperation and competition among FEF neurons in both hemispheres was heightened following the appearance of peripheral cues, thus could be a potential mechanism for selecting a single target in either visual hemisphere for a potential saccade. Third, communication between the FEFs may also play an important role in generating a specific saccade vector. While electrical stimulation in the FEF evoked a saccade with a set vector, it also dynamically impacted saccade-related activity in the contralateral FEF (Schlag et al., 1998). In particular, stimulation excited or inhibited contralateral FEF neurons with response fields similar or different to the evoked saccade, respectively. This suggests that FEF neurons in each hemisphere may modulate one another to drive the generation of a specific saccade vector.

Based on the diverse set of signals relayed by FEF corticotectal neurons, and SRT increases following FEF inactivation, the FEF would certainly be expected to have an important contribution to saccade initiation in the downstream iSC. Both FEF and iSC neurons exhibit activity reflective of a rise-to-fixed threshold process for saccade initiation (Hanes and Schall, 1996; Paré and Hanes, 2003; Ratcliff et al., 2007), but recent neurophysiological evidence suggests that this mechanism also depends on factors such as the onset time of the rise (Pouget et al., 2011). Specifically, Pouget and colleagues (2011) found

that increases in onset time of saccade-related activity in either the FEF and iSC could largely explain the systematic increases in SRT following stop-signal trials in a countermanding task. Consequently, inactivating the FEF provides a valuable opportunity to test the iSC-mediated mechanisms of saccade initiation.

1.3.6: Additional sources of visual, cognitive, and saccade-related signals to the intermediate layers of superior colliculus

Although the FEF is presumably a key source of visual, cognitive, and saccade-related signals to the iSC, other oculomotor areas could serve this role. For example, the superficial layers of the SC (sSC), and primary visual cortex (V1) are two additional sources of visual-related inputs to the iSC (see **Fig. 1-7**). Moreover, the substantia nigra pars reticulata (SNr) of the basal ganglia, lateral intraparietal area (LIP), and dorsolateral prefrontal cortex (DLPFC) may also provide cognitive or saccade-related signals.

Despite the superficial and intermediate layers of the SC having largely overlapping visual response fields, they are largely distinct functional areas (Schiller and Koerner, 1971; Schiller and Stryker, 1972). Indeed, sSC neurons usually display short-latency (~40 ms), and transient visual responses (Goldberg and Wurtz, 1972), and have afferents predominantly from visual areas such as the retina, and V1 (Finlay et al., 1976; Schiller and Malpeli, 1977). Interestingly, the sSC has vertical topographic connections to the deeper iSC neurons, and this

pathway has been proposed to mediate the generation of short-latency saccades, or *express saccades* (Fischer and Boch, 1983; Doubell et al., 2003; Saito and Isa, 2003; Helms et al., 2004). Functionally, this pathway is sufficient to activate iSC neurons when released from the tonic inhibition of the rostral iSC (Munoz and Istvan, 1998) and the SNr (Hikosaka and Wurtz, 1983a; Isa et al., 1998), and does in fact play an important role in generating visually-guided saccades following V1 lesions (Kato et al., 2011). Thus, in an intact oculomotor system, the sSC could potentially contribute to iSC activity via intrinsic connections within the SC.

Additionally, the iSC receives visuospatial information from V1 through corticotectal neurons contain short-latency visual signals (Finlay et al., 1976). Since V1 receives visuospatial information from the lateral geniculate nucleus (LGN), and visuospatial information flows anteriorly to several cortical areas with corticotectal neurons, including the LIP, FEF, and DLPFC (Leonard et al., 2011; Siegel et al., 2015), these cortical areas may contribute to visual-related responses in the iSC. Importantly, ablation or reversible inactivation of either the V1 or LGN abolishes visual-related responses in iSC neurons (Schiller et al., 1974, 1979), implying that the integrity of these structures is necessary for sensory influences to be integrated in the iSC.

The SNr of the basal ganglia tonically inhibits iSC activity via GABA-mediated projections (Jayaraman et al., 1977; Hikosaka and Wurtz, 1983a). Importantly, SNr neurons exhibit visual, cognitive, and saccade-related responses, pausing this tonic activity, which may ultimately activate iSC neurons (Hikosaka and Wurtz, 1983a, 1983b). The FEF can inhibit SNr activity via the caudate nucleus (Stanton et al., 1988b), thus providing evidence that the FEF or other areas projecting to the SNr can indirectly influence iSC activity.

LIP is another oculomotor area that relays a diverse set of visual, cognitive, and saccade-related signals directly to the iSC (Paré and Wurtz, 1997). Similar to the FEF and iSC, LIP neurons exhibit responses representative of the sensorimotor transformation (Blatt et al., 1990; Barash et al., 1991a, 1991b), and LIP inactivation causes deficits in contralateral saccades, particularly for memory-guided saccades (Li et al., 1999). A comparison of FEF and LIP corticotectal neurons found that LIP corticotectal neurons displayed a similar set of visual, cognitive, and saccade-related signals, but its delay-period activity was more related to the visuospatial cue than the saccade towards it (Paré and Wurtz, 2001; Wurtz et al., 2001). Consequently, this suggests that LIP corticotectal neurons may have a distinct contribution to iSC activity.

Interestingly, DLPFC inactivation has been used to directly address its contribution to neuronal activity in the downstream iSC (Koval et al., 2011;

Johnston et al., 2014). The DLPFC has been implicated in cognitive processes (Curtis and D'Esposito, 2003; Wallis and Miller, 2003; Barraclough et al., 2004; Johnston et al., 2007), and directly sends task-related signals to the iSC (Johnston and Everling, 2006). While DLPFC inactivation increased SRT for correct contralesional pro- and anti-saccades, generally more erroneous ipsilesional saccades occurred. Such behavioural effects were accompanied by intriguing changes in iSC activity: delayed onsets of saccade-related activity in the ipsilesional iSC, and increases in contralesional iSC activity. This was contrary to assumptions of cognitive control that cortical areas had an inhibitory influence on the downstream iSC; thus, these reports provided novel insights into the mechanisms underlying the cognitive influence of DLPFC on saccade behaviour.

In all, the iSC receives visual, cognitive, and saccade-related signals directly from several oculomotor areas including the FEF. Given this, and the fact that the FEF has reciprocal projections to many of these areas (Schall et al., 1995; Siegel et al., 2015), the FEF's contribution to iSC activity cannot be estimated based solely on FEF corticotectal neurons. Consequently, an important objective in this thesis is to uncover the FEF's individual contribution to neuronal activity in either the ipsilateral or contralateral iSC. Such an endeavor could provide novel insights into the individual contributions of the FEF and iSC to mechanisms of saccade initiation and generation.

1.4: Objectives

1.4.1: Role of frontal eye fields in saccade behaviour

While previous studies have described how small FEF regions contribute to saccade generation (Sommer and Tehovnik, 1997; Dias and Segraves, 1999), the contribution of the large FEF regions in an intact oculomotor system remain unclear. This particularly useful as it could potentially reveal the contribution of ipsiversive-tuned FEF neurons that are dispersed, and rarely encountered compared to the contraversive-tuned ones (Bruce and Goldberg, 1985). **Chapter 2** addresses the contribution of large unilateral FEF regions to saccade behaviour, using cryogenic reversible inactivation, while monkeys performed one of two saccade tasks. In the first task, we examined how large FEF inactivation affected saccades towards various targets placed in the contralateral and ipsilateral visual hemifield. The second task enabled us to better understand the influence of large FEF regions in tasks requiring visuospatial memory. To accomplish this, we compared saccade behaviour between interleaved delayed visually- and memory-guided saccades. The results of these experiments may reveal the contribution of large FEF regions to saccade behaviour, and provide a necessary foundation for examining the FEF's contribution to the underlying neuronal mechanisms in the iSC.

1.4.2: Role of frontal eye fields in microsaccade behaviour

Microsaccades are strategically deployed to aid vision. While some mechanisms underlying microsaccade generation have been elucidated in the iSC (Hafed et al., 2009, 2013; Hafed, 2011; Goffart et al., 2012; Hafed and Krauzlis, 2012), cerebellum (Arnstein et al., 2015), and brainstem saccadic burst generator (Van Gisbergen et al., 1981; Brien et al., 2009; Van Horn and Cullen, 2012), no study has addressed the involvement of any cortical area in microsaccade generation. Nonetheless, the involvement of cortical areas would explain why microsaccade deployment is impacted by cognitive and sensory processes, particularly following peripheral stimuli (Hafed and Clark, 2002; Engbert and Kliegl, 2003; Laubrock et al., 2005). **Chapter 3** investigates how FEF inactivation influenced microsaccades generated before or after cue onset while monkeys performed delayed saccades. We utilize either unilateral and bilateral FEF inactivation, and carefully characterize its impact on microsaccade behaviour (i.e. metrics, dynamics, rate, and direction), either before or after peripheral stimuli. These results could determine if the FEF is a plausible substrate for cognitive influences on microsaccades.

1.4.3: Role of frontal eye fields to neuronal activity in the downstream superior colliculus

The FEF and iSC are the two key, and best-studied, brain areas for the cognitive control of saccadic eye movements (Wurtz and Goldberg, 1972b, 1972c; Sparks et al., 1976; Sparks, 1978; Mays and Sparks, 1980; Schiller et al., 1980; Bruce and Goldberg, 1985; Bruce et al., 1985; Munoz and Wurtz, 1995). The FEF and iSC both project to the brainstem areas containing the oculomotor nuclei (Raybourn and Keller, 1977; Schnyder et al., 1985; Huerta et al., 1986; Sparks, 1986), but the FEF likely exerts much of its cognitive influence on saccade and microsaccade generation through an intact iSC (Leichnetz et al., 1981; Komatsu and Suzuki, 1985; Segraves and Goldberg, 1987; Everling and Munoz, 2000; Sommer and Wurtz, 2000, 2001; Hanes and Wurtz, 2001). Surprisingly, the mechanisms underlying this important influence remain poorly understood. **Chapter 4** addresses the impact of unilateral cryogenic FEF inactivation on ipsilateral or contralateral iSC neuronal activity in monkeys performing either delayed visually- or memory guided saccades. Since these tasks discriminated visual and cognitive activity in the delay-period, and the subsequent saccade-related activity of iSC neurons, they enabled the critical test of the FEF's cognitive contribution to the downstream iSC neurons. Importantly, this also provides a valuable opportunity to examine the mechanisms in the iSC underlying saccade generation without its primary functional input.

1.5: Methodological considerations

1.5.1: Studying oculomotor behaviour using permanent versus reversible inactivations

A permanent lesion or reversible inactivation of a brain area is typically performed to directly address its contribution to saccade behaviour, however each approach has benefits and limitations. For example, neuronal plasticity is one limitation of using brain lesions, whereby other oculomotor areas take over to compensate for loss of the lesioned area, confounding any interpretation of attributing a behaviour to one brain area. Further complicating the interpretation, functional recovery between the time of surgery and experimentation may also underestimate the contribution of a lesioned area to behaviour. In the oculomotor system, this influence is demonstrated by the progressive recovery of deficits for visually- or memory-guided saccades following either FEF or iSC lesions (Schiller et al., 1980, 1987; Deng et al., 1986; Hanes et al., 2005). After approximately one month from such lesions, *only* memory-guided saccades exhibit lasting, yet modest, deficits. This strikingly contrasts with the clear triad of deficits during reversible inactivation of either of these structures using less invasive injections of pharmacological modulations such as lidocaine or muscimol (Hikosaka and Wurtz, 1983c; Sommer and Tehovnik, 1997; Quaia et al., 1998; Dias and Segraves, 1999). Importantly, this

also implies a particular important benefit of using reversible inactivation: no permanent neuronal plastic changes in the oculomotor system.

1.5.2: Studying oculomotor behaviour using large versus small-volume inactivations

Permanent lesions typically disrupt much larger volumes of tissue than reversible inactivation techniques, which can be advantageous in some situations. For example, large-volume inactivations are more applicable to models of cerebrovascular stroke (Karnath et al., 2004), which can assist its diagnosing or treatment. Furthermore, large-volume inactivations are similar to important translational, non-invasive techniques used on humans to study brain function (e.g. transcranial magnetic stimulation, functional magnetic imagining), which have less spatial resolution about an area of interest than many invasive techniques (i.e. electrical stimulation, neuronal recordings). Moreover, large-volume inactivations can potentially reveal the contribution of neurons dispersed throughout a given brain region. In the FEF, a small fraction of neurons contain ipsilateral response fields, but they are relatively more scattered than neurons turned in the contralateral direction (Bruce and Goldberg, 1985); thus large-volume inactivations could help clarify the FEF's role for ipsiversive saccades. One important limitation of large-volume inactivations is the potential impact on areas adjacent to a region of interest, thus the contribution of each area must be considered in the interpretation of the results.

Reversible inactivations, commonly achieved by pharmacological modulations, achieve a smaller and more selective volume inactivation of tissue (Tehovnik and Sommer, 1997), hence do not usually intrude on surrounding functional areas. The selectivity of this approach can also be beneficial when studying certain subclasses of neurons (e.g. muscimol activates inhibitory neurons via a GABA agonist), or dissociating contributions from regions within a functional topographic map (e.g. rostral versus caudal iSC). Indeed, small-volume inactivations may perturb existing functional interactions between brain areas or topographic regions (Munoz and Istvan, 1998), perhaps explaining why reversible inactivation of the rostral, but not caudal, iSC causes premature saccades (Munoz and Wurtz, 1993).

1.6: References

Arnstein D, Junker M, Smilgin A, Dicke PW, Thier P (2015) Microsaccade control signals in the cerebellum. J Neurosci 35:3403–3411.

Bahill AT, Adler D, Stark L (1975) Most naturally occurring human saccades have magnitudes of 15 degrees or less. Invest Ophthalmol 14:468–469.

Bair W, O'Keefe LP (1998) The influence of fixational eye movements on the response of neurons in area MT of the macaque. Vis Neurosci 15:779–786.

Barash S, Bracewell RM, Fogassi L, Gnadt JW, Andersen RA (1991a) Saccade-related activity in the lateral intraparietal area. I. J Neurophysiol 66:1095–1107.

Barash S, Bracewell RM, Fogassi L, Gnadt JW, Andersen R a (1991b) Saccade-related activity in the lateral intraparietal area. II. Spatial properties. J Neurophysiol 66:1109–1124.

Barraclough DJ, Conroy ML, Lee D (2004) Prefrontal cortex and decision making in a mixed-strategy game. Nat Neurosci 7:404–410.

Basso MA, Wurtz RH (1998) Modulation of neuronal activity in superior colliculus by changes in target probability. J Neurosci 18:7519–7534.

Becker W, Fuchs AF (1969) Further properties of the human saccadic system: eye movements and correction saccades with and without visual fixation points. Vision Res 9:1247–1258.

Bell AH, Meredith MA, Van Opstal AJ, Munoz DP (2006) Stimulus intensity modifies saccadic reaction time and visual response latency in the superior colliculus. Exp Brain Res 174:53–59.

Bergeron A, Guitton D (2000) Fixation neurons in the superior colliculus encode distance between current and desired gaze positions. Nat Neurosci 3:932–939.

Blatt GJ, Andersen RA, Stoner GR (1990) Visual receptive field organization and cortico-cortical connections of the lateral intraparietal area (area LIP) in the macaque. J Comp Neurol 299:421–445.

Boch R, Fischer B, Ramsperger E (1984) Express-saccades of the monkey: reaction times versus intensity, size, duration, and eccentricity of their targets. Exp brain Res 55:223–231.

Brien DC, Corneil BD, Fecteau JH, Bell AH, Munoz DP (2009) The behavioral and neurophysiological modulation of microsaccades in monkeys. J Eye Mov Res 3:1–12.

Brown JW, Hanes DP, Schall JD, Stuphorn V (2008) Relation of frontal eye field activity to saccade initiation during a countermanding task. Exp Brain Res 190:135–151.

Bruce CJ, Goldberg ME (1985) Primate frontal eye fields. I. Single neurons discharging before saccades. J Neurophysiol 53:603–635.

Bruce CJ, Goldberg ME, Bushnell MC, Stanton GB (1985) Primate frontal eye fields. II. Physiological and anatomical correlates of electrically evoked eye movements. J Neurophysiol 54:714–734.

Burr DC, Morrone MC, Ross J (1994) Selective suppression of the magnocellular visual pathway during saccadic eye movements. Nature 371:511–513.

Büttner-Ennever JA, Akert K (1981) Medial rectus subgroups of the oculomotor nucleus ant their abducens internuclear input in the monkey. J Comp Neurol 197:17–27.

Büttner U, Büttner-Ennever JA, Henn V (1977) Vertical eye movement related unit activity in the rostral mesencephalic reticular formation of the alert monkey. Brain Res 130:239–252.

Cannon SC, Robinson D a (1987) Loss of the neural integrator of the oculomotor system from brain stem lesions in monkey. J Neurophysiol 57:1383–1409.

Carello CD, Krauzlis RJ (2004) Manipulating intent: Evidence for a causal role of the superior colliculus in target selection. Neuron 43:575–583.

Carpenter RH, Williams ML (1995) Neural computation of log likelihood in control of saccadic eye movements. Nature 377:59–62.

Carpenter RHS, Reddi BAJ, Anderson AJ (2009) A simple two-stage model predicts response time distributions. J Physiol 587:4051–4062.

Cohen B, Henn V (1972) Unit activity in the pontine reticular formation associated with eye movements. Brain Res 46:403–410.

Cohen B, Komatsuzaki A, Bender MB (1968) Electrooculographic syndrome in monkeys after pontine reticular formation lesions. Arch Neurol 18:78–92.

Cohen JY, Crowder EA, Heitz RP, Subraveti CR, Thompson KG, Woodman GF, Schall JD (2010) Cooperation and Competition among Frontal Eye Field Neurons during Visual Target Selection. J Neurosci 30:3227–3238.

Crapse TB, Sommer MA (2009) Frontal eye field neurons with spatial representations predicted by their subcortical input. J Neurosci 29:5308–5318.

Crawford J, Cadera W, Vilis T (1991) Generation of torsional and vertical eye position signals by the interstitial nucleus of Cajal. Science 252:1551–1553.

Curcio CA, Allen KA (1990) Topography of ganglion cells in human retina. J Comp Neurol 300:5–25.

Curtis CE, D'Esposito M (2003) Persistent activity in the prefrontal cortex during working memory. Trends Cogn Sci 7:415–423.

Demer JL (2006) Current concepts of mechanical and neural factors in ocular motility. Curr Opin Neurol 19:4–13.

Deng SYY, Goldberg M. E, Segraves MAA, Ungerleider LGG, Mishkin M (1986) The effect of unilateral ablation of the frontal eye fields on saccadic performance in the monkey. In: Adaptive Processes in the Visual and Oculomotor Systems, pp 201–208. Elsevier.

Dias EC, Segraves MA (1999) Muscimol-induced inactivation of monkey frontal eye field: effects on visually and memory-guided saccades. J Neurophysiol 81:2191–2214.

Distel H, Fries W (1982) Contralateral cortical projections to the superior colliculus in the macaque monkey. Exp brain Res 48:157–162.

Dorris MC, Paré M, Munoz DP (1997) Neuronal activity in monkey superior colliculus related to the initiation of saccadic eye movements. J Neurosci 17:8566–8579.

Doubell TP, Skaliora I, Baron J, King AJ (2003) Functional connectivity between the superficial and deeper layers of the superior colliculus: an anatomical substrate for sensorimotor integration. J Neurosci 23:6596–6607.

Edelman JA, Keller EL (1996) Activity of visuomotor burst neurons in the superior colliculus accompanying express saccades. J Neurophysiol 76.

Engbert R, Kliegl R (2003) Microsaccades uncover the orientation of covert attention. Vision Res 43:1035–1045.

Everling S, Dorris MC, Klein RM, Munoz DP (1999) Role of primate superior colliculus in preparation and execution of anti-saccades and pro-saccades. J Neurosci 19:2740–2754.

Everling S, Dorris MC, Munoz DP (1998) Reflex suppression in the anti-saccade task is dependent on prestimulus neural processes. J Neurophysiol 80:1584–1589.

Everling S, Munoz DP (2000) Neuronal correlates for preparatory set associated with pro-saccades and anti-saccades in the primate frontal eye field. J Neurosci 20:387–400.

Finlay BL, Schiller PH, Volman SF (1976) Quantitative studies of single-cell properties in monkey striate cortex. IV. Corticotectal cells. J Neurophysiol 39:1352–1361.

Fischer B, Boch R (1983) Saccadic eye movements after extremely short reaction times in the monkey. Brain Res 260:21–26.

Fischer B, Ramsperger E (1984) Human express saccades: extremely short reaction times of goal directed eye movements. Exp Brain Res 57:191–195.

Fuchs AF, Luschei ES (1970) Firing patterns of abducens neurons of alert monkeys in relationship to horizontal eye movement. J Neurophysiol 33:382–392.

Fuchs AF, Luschei ES (1971) The activity of single trochlear nerve fibers during eye movements in the alert monkey. Exp Brain Res 13:78–89.

Funahashi S, Chafee M V, Goldman-Rakic PS (1993) Prefrontal neuronal activity in rhesus monkeys performing a delayed anti-saccade task. Nature 365:753–756.

Gandhi NJ, Katnani HA (2011) Motor functions of the superior colliculus. Annu Rev Neurosci 34:205–231.

Goffart L, Hafed ZM, Krauzlis RJ (2012) Visual Fixation as Equilibrium: Evidence

from Superior Colliculus Inactivation. J Neurosci 32:10627–10636.

Goldberg ME, Wurtz RH (1972) Activity of superior colliculus in behaving monkey. I. Visual receptive fields of single neurons. J Neurophysiol 35:542–559.

Hafed ZM (2011) Mechanisms for generating and compensating for the smallest possible saccades. Eur J Neurosci 33:2101–2113.

Hafed ZM, Chen C, Tian X (2015) Vision, perception, and attention through the lens of microsaccades: mechanisms and implications. Front Syst Neurosci 9.

Hafed ZM, Clark JJ (2002) Microsaccades as an overt measure of covert attention shifts. Vision Res 42:2533–2545.

Hafed ZM, Goffart L, Krauzlis RJ (2009) A neural mechanism for microsaccade generation in the primate superior colliculus. Science 323:940–943.

Hafed ZM, Krauzlis RJ (2012) Similarity of superior colliculus involvement in microsaccade and saccade generation. J Neurophysiol 107:1904–1916.

Hafed ZM, Lovejoy LP, Krauzlis RJ (2013) Superior colliculus inactivation alters the relationship between covert visual attention and microsaccades. Eur J Neurosci 37:1169–1181.

Hallett PE, Adams BD (1980) The predictability of saccadic latency in a novel voluntary oculomotor task. Vision Res 20:329–339.

Hanes DP, Patterson WF, Schall JD (1998) Role of frontal eye fields in countermanding saccades: visual, movement, and fixation activity. J Neurophysiol 79:817–834.

Hanes DP, Schall JD (1996) Neural control of voluntary movement initiation. Science 274:427–430.

Hanes DP, Smith MK, Optican LM, Wurtz RH (2005) Recovery of saccadic dysmetria following localized lesions in monkey superior colliculus. Exp Brain Res 160:312–325.

Hanes DP, Wurtz RH (2001) Interaction of the frontal eye field and superior colliculus for saccade generation. J Neurophysiol 85:804–815.

Harting JK (1977) Descending pathways from the superior collicullus: an autoradiographic analysis in the rhesus monkey (Macaca mulatta). J Comp Neurol 173:583–612.

Heitz RP, Schall JD (2012) Article Neural Mechanisms of Speed-Accuracy Tradeoff.

Helminski JO, Segraves MA (2003) Macaque Frontal Eye Field Input to Saccade-Related Neurons in the Superior Colliculus. J Neurophysiol 90:1046–1062.

Helms MC, Ozen G, Hall WC (2004) Organization of the intermediate gray layer of the superior colliculus. I. Intrinsic vertical connections. J Neurophysiol 91:1706–1715.

Hikosaka O, Wurtz R (1986) Saccadic eye movements following injection of lidocaine into the superior colliculus. Exp Brain Res 61:531–539.

Hikosaka O, Wurtz RH (1983a) Visual and oculomotor functions of monkey substantia nigra pars reticulata. IV. Relation of substantia nigra to superior colliculus. J Neurophysiol 49:1285–1301.

Hikosaka O, Wurtz RH (1983b) Visual and oculomotor functions of monkey substantia nigra pars reticulata. III. Memory-contingent visual and saccade responses. J Neurophysiol 49:1268–1284.

Hikosaka O, Wurtz RH (1983c) Effects on eye movements of a GABA agonist and antagonist injected into monkey superior colliculus. Brain Res 272:368–372.

Hikosaka O, Wurtz RH (1985) Modification of saccadic eye movements by GABA-related substances. II. Effects of muscimol in monkey substantia nigra pars reticulata. J Neurophysiol 53:292–308.

Huerta MF, Krubitzer LA, Kaas JH (1986) Frontal eye field as defined by intracortical microstimulation in squirrel monkeys, owl monkeys, and macaque monkeys: I. Subcortical connections. J Comp Neurol 253:415–439.

Isa T, Endo T, Saito Y (1998) The visuo-motor pathway in the local circuit of the rat superior colliculus. J Neurosci 18:8496–8504.

Jantz JJ, Watanabe M, Everling S, Munoz DP (2013) Threshold mechanism for saccade initiation in frontal eye field and superior colliculus. J Neurophysiol 109:2767–2780.

Jayaraman A, Batton RR, Carpenter MB (1977) Nigrotectal projections in the monkey: An autoradiographic study. Brain Res 135:147–152.

Johnston K, Everling S (2006) Monkey dorsolateral prefrontal cortex sends task-selective signals directly to the superior colliculus. J Neurosci 26:12471–12478.

Johnston K, Koval MJ, Lomber SG, Everling S (2014) Macaque Dorsolateral Prefrontal Cortex Does not Suppress Saccade-Related Activity in the Superior Colliculus. Cereb Cortex 24:1373–1388.

Johnston K, Levin HM, Koval MJ, Everling S (2007) Top-Down Control-Signal Dynamics in Anterior Cingulate and Prefrontal Cortex Neurons following Task Switching. Neuron 53:453–462.

Kagan I, Gur M, Snodderly DM (2008) Saccades and drifts differentially modulate neuronal activity in V1: effects of retinal image motion, position, and extraretinal influences. J Vis 8:19.1-25.

Karnath HO, Berger MF, Kuker W, Rorden C (2004) The anatomy of spatial neglect based on voxelwise statistical analysis: A study of 140 patients. Cereb Cortex 14:1164–1172.

Kato R, Takaura K, Ikeda T, Yoshida M, Isa T (2011) Contribution of the retino-tectal pathway to visually guided saccades after lesion of the primary visual cortex in monkeys. Eur J Neurosci 33:1952–1960.

Katz LN, Yates JL, Pillow JW, Huk AC (2016) Dissociated functional significance of decision-related activity in the primate dorsal stream. Nature 535:285–288.

Keller EL, McPeek RM, Salz T (2000) Evidence against direct connections to PPRF

EBNs from SC in the monkey. J Neurophysiol 84:1303–1313.

Keller EL, Robinson DA (1971) Absence of a stretch reflex in extraocular muscles of the monkey. J Neurophysiol 34:908–919.

King WM, Fuchs AF (1979) Reticular control of vertical saccadic eye movements by mesencephalic burst neurons. J Neurophysiol 42:861–876.

King WM, Fuchs AF, Magnin M (1981) Vertical eye movement-related responses of neurons in midbrain near interstitial nucleus of Cajal. J Neurophysiol 46:549–562.

Ko H-K, Poletti M, Rucci M (2010) Microsaccades precisely relocate gaze in a high visual acuity task. Nat Neurosci 13:1549–1553.

Komatsu H, Suzuki H (1985) Projections from the functional subdivisions of the frontal eye field to the superior colliculus in the monkey. Brain Res 327:324–327.

Koval MJ, Lomber SG, Everling S (2011) Prefrontal cortex deactivation in macaques alters activity in the superior colliculus and impairs voluntary control of saccades. J Neurosci 31:8659–8668.

Kuenzle H, Akert K, Wurtz RH (1976) Projection of area 8 (frontal eye field) to superior colliculus in the monkey. An autoradiographic study. Brain Res 117:487–492.

Land M, Mennie N, Rusted J (1999) The roles of vision and eye movements in the control of activities of daily living. Perception 28:1311–1328.

Laubrock J, Engbert R, Kliegl R (2005) Microsaccade dynamics during covert attention. Vision Res 45:721–730.

Leichnetz GR, Spencer RF, Hardy SGP, Astruc J (1981) The prefrontal corticotectal projection in the monkey; An anterograde and retrograde horseradish peroxidase study. Neuroscience 6:1023–1041.

Leonard CJ, Luck SJ, Schmolesky MT, Wang Y, Hanes DP, Thompson KG, Leutgeb S, Schall JD, Leventhal AG (2011) Signal Timing Across the Macaque Visual System Signal Timing Across the Macaque Visual System. :3272–3278.

Leopold DA, Logothetis NK (1998) Microsaccades differentially modulate neural activity in the striate and extrastriate visual cortex. Exp Brain Res 123:341–345.

Li CS, Mazzoni P, Andersen R a (1999) Effect of reversible inactivation of macaque lateral intraparietal area on visual and memory saccades. J Neurophysiol 81:1827–1838.

Lo C-C, Wang X-J (2006) Cortico-basal ganglia circuit mechanism for a decision threshold in reaction time tasks. Nat Neurosci 9:956–963.

Ludwig CJH, Gilchrist ID, McSorley E (2004) The influence of spatial frequency and contrast on saccade latencies. Vision Res 44:2597–2604.

Martinez-Conde S, Macknik SL, Hubel DH (2000) Microsaccadic eye movements and firing of single cells in the striate cortex of macaque monkeys. Nat Neurosci 3:251–258.

Martinez-Conde S, Macknik SL, Hubel DH (2002) The function of bursts of spikes during visual fixation in the awake primate lateral geniculate nucleus and primary visual cortex. Proc Natl Acad Sci U S A 99:13920–13925.

Martinez-Conde S, Macknik SL, Troncoso XG, Dyar TA (2006) Microsaccades counteract visual fading during fixation. Neuron 49:297–305.

Mays LE, Sparks DL (1980) Dissociation of visual and saccade-related responses in superior colliculus neurons. J Neurophysiol 43:207–232.

McFarland JL, Fuchs AF (1992) Discharge patterns in nucleus prepositus hypoglossi and adjacent medial vestibular nucleus during horizontal eye movement in behaving macaques. J Neurophysiol 68:319–332.

McPeek RM, Keller EL (2004) Deficits in saccade target selection after inactivation of superior colliculus. Nat Neurosci 7:757–763.

Munoz DP, Broughton JR, Goldring JE, Armstrong IT (1998) Age-related performance of human subjects on saccadic eye movement tasks. Exp Brain Res 121:391–400.

Munoz DP, Dorris MC, Paré M, Everling S (2000) On your mark, get set: brainstem circuitry underlying saccadic initiation. Can J Physiol Pharmacol 78:934–944.

Munoz DP, Istvan PJ (1998) Lateral inhibitory interactions in the intermediate layers of the monkey superior colliculus. J Neurophysiol 79:1193–1209.

Munoz DP, Wurtz RH (1993) Fixation cells in monkey superior colliculus. II. Reversible activation and deactivation. J Neurophysiol 70:576–589.

Munoz DP, Wurtz RH (1995) Saccade-related activity in monkey superior colliculus. I. Characteristics of burst and buildup cells. J Neurophysiol 73:2313–2333.

Paré M, Hanes DP (2003) Controlled movement processing: superior colliculus activity associated with countermanded saccades. J Neurosci 23:6480–6489.

Paré M, Wurtz RH (1997) Monkey posterior parietal cortex neurons antidromically activated from superior colliculus. J Neurophysiol 78:3493–3497.

Paré M, Wurtz RH (2001) Progression in neuronal processing for saccadic eye movements from parietal cortex area lip to superior colliculus. J Neurophysiol 85:2545–2562.

Poletti M, Listorti C, Rucci M (2013) Microscopic eye movements compensate for nonhomogeneous vision within the fovea. Curr Biol 23:1691–1695.

Pouget P, Logan GD, Palmeri TJ, Boucher L, Paré M, Schall JD (2011) Neural Basis of Adaptive Response Time Adjustment during Saccade Countermanding. J Neurosci 31:12604–12612.

Quaia C, Aizawa H, Optican LM, Wurtz RH (1998) Reversible inactivation of monkey superior colliculus. II. Maps of saccadic deficits. J Neurophysiol 79:2097–2110.

Ratcliff R, Hasegawa YT, Hasegawa RP, Smith PL, Segraves M a (2007) Dual

diffusion model for single-cell recording data from the superior colliculus in a brightness-discrimination task. J Neurophysiol 97:1756–1774.

Raybourn MS, Keller EL (1977) Colliculoreticular organization in primate oculomotor system. J Neurophysiol 40:861–878.

Reddi BA, Carpenter RH (2000) The influence of urgency on decision time. Nat Neurosci 3:827–830.

Robinson D (1972) Eye movements evoked by collicular stimulation in the alert monkey. Vision Res 12:1795–1808.

Robinson DA (1964) the Mechanics of Human Saccadic Eye Movement. J Physiol 174:245–264.

Robinson DA (1970) Oculomotor unit behavior in the monkey. J Neurophysiol 33:393–403.

Rolfs M, Laubrock J, Kliegl R (2006) Shortening and prolongation of saccade latencies following microsaccades. Exp Brain Res 169:369–376.

Saito Y, Isa T (2003) Local excitatory network and NMDA receptor activation generate a synchronous and bursting command from the superior colliculus. J Neurosci 23:5854–5864.

Schall JD (1991) Neuronal activity related to visually guided saccadic eye movements in the supplementary motor area of rhesus monkeys. J Neurophysiol 66:530–558.

Schall JD, Morel A, King DJ, Bullier J (1995) Topography of visual cortex connections with frontal eye field in macaque: convergence and segregation of processing streams. J Neurosci 15:4464–4487.

Schiller PH (1970) The discharge characteristics of single units in the oculomotor and abducens nuclei of the unanesthetized monkey. Exp Brain Res 10:347–362.

Schiller PH, Koerner F (1971) Discharge characteristics of single units in superior colliculus of the alert rhesus monkey. J Neurophysiol 34:920–936.

Schiller PH, Malpeli JG (1977) Properties and tectal projections of monkey retinal ganglion cells. J Neurophysiol 40:428–45.

Schiller PH, Malpeli JG, Schein SJ (1979) Composition of geniculostriate input ot superior colliculus of the rhesus monkey. J Neurophysiol 42:1124–1133.

Schiller PH, Sandell JH, Maunsell JH (1987) The effect of frontal eye field and superior colliculus lesions on saccadic latencies in the rhesus monkey. J Neurophysiol 57:1033–1049.

Schiller PH, Stryker M (1972) Single-unit recording and stimulation in superior colliculus of the alert rhesus monkey. J Neurophysiol 35:915–924.

Schiller PH, Stryker M, Cynader M, Berman N (1974) Response characteristics of single cells in the monkey superior colliculus following ablation or cooling of visual cortex. J Neurophysiol 37:181–194.

Schiller PH, True SD, Conway JL (1980) Deficits in eye movements following

frontal eye-field and superior colliculus ablations. J Neurophysiol 44:1175–1189.

Schlag J, Dassonville P, Schlag-Rey M (1998) Interaction of the two frontal eye fields before saccade onset. J Neurophysiol 79:64–72.

Schnyder H, Reisine H, Hepp K, Henn V (1985) Frontal eye field projection to the paramedian pontine reticular formation traced with wheat germ agglutinin in the monkey. Brain Res 329:151–160.

Scudder CA, Fuchs AF, Langer TP (1988) Characteristics and functional identification of saccadic inhibitory burst neurons in the alert monkey. J Neurophysiol 59:1430–1454.

Scudder CA, Kaneko CR, Fuchs AF (2002) The brainstem burst generator for saccadic eye movements: A modern synthesis. Exp Brain Res 142:439–462.

Scudder CA, Moschovakis AK, Karabelas AB, Highstein SM (1996) Anatomy and physiology of saccadic long-lead burst neurons recorded in the alert squirrel monkey. II. Pontine neurons. J Neurophysiol 76:353–370.

Segraves MA, Goldberg ME (1987) Functional properties of corticotectal neurons in the monkey's frontal eye field. J Neurophysiol 58:1387–1419.

Siegel M, Buschman TJ, Miller EK (2015) Cortical information flow during flexible sensorimotor decisions. Science (80-) 348:1352–1355.

Snodderly DM, Kagan I, Gur M (2001) Selective activation of visual cortex neurons by fixational eye movements: implications for neural coding. Vis Neurosci 18:259–277.

Sommer M a, Wurtz RH (2004) What the brain stem tells the frontal cortex. II. Role of the SC-MD-FEF pathway in corollary discharge. J Neurophysiol 91:1403–1423.

Sommer MA, Tehovnik EJ (1997) Reversible inactivation of macaque frontal eye field. Exp brain Res 116:229–249.

Sommer MA, Wurtz RH (2000) Composition and topographic organization of signals sent from the frontal eye field to the superior colliculus. J Neurophysiol 83:1979–2001.

Sommer MA, Wurtz RH (2001) Frontal eye field sends delay activity related to movement, memory, and vision to the superior colliculus. J Neurophysiol 85:1673–1685.

Sparks DL (1975) Response properties of eye movement-related neurons in the monkey superior colliculus. Brain Res 90:147–152.

Sparks DL (1978) Functional properties of neurons in the monkey superior colliculus: Coupling of neuronal activity and saccade onset. Brain Res 156:1–16.

Sparks DL (1986) Translation of sensory signals into commands for control of saccadic eye movements: role of primate superior colliculus. Physiol Rev 66:118–171.

Sparks DL (2002) The brainstem control of saccadic eye movements. Nat Rev

Neurosci 3:952–64.

Sparks DL, Holland R, Guthrie BL (1976) Size and distribution of movement fields in the monkey superior colliculus. Brain Res 113:21–34.

Sparks DL, Travis RP (1971) Firing patterns of reticular formation neurons during horizontal eye movements. Brain Res 33:477–481.

Stanton GB, Deng SY, Goldberg ME, McMullen NT (1989) Cytoarchitectural characteristic of the frontal eye fields in macaque monkeys. J Comp Neurol 282:415–427.

Stanton GB, Goldberg ME, Bruce CJ (1988a) Frontal eye field efferents in the macaque monkey: II. Topography of terminal fields in midbrain and pons. J Comp Neurol 271:493–506.

Stanton GB, Goldberg ME, Bruce CJ (1988b) Frontal eye field efferents in the macaque monkey: I. Subcortical pathways and topography of striatal and thalamic terminal fields. J Comp Neurol 271:473–492.

Stone J, Johnston E (1981) The topography of primate retina: a study of the human, bushbaby, and new- and old-world monkeys. J Comp Neurol 196:205–223.

Strassman A, Highstein S, McCrea R (1986a) Anatomy and Physiology of Saccadic Burst Neurons in the Alert Squirrel Monkey. II. Inhibitory Burst Neurons. J Comp Neurol 76:353–370.

Strassman A, Highstein SM, McCrea RA (1986b) Anatomy and physiology of saccadic burst neurons in the alert squirrel monkey. I. Excitatory burst neurons. J Comp Neurol 249:337–357.

Sylvestre PA, Cullen KE (1999) Quantitative analysis of abducens neuron discharge dynamics during saccadic and slow eye movements. J Neurophysiol 82:2612–2632.

Taylor TL, Klein RM (2000) Visual and motor effects in inhibition of return. J Exp Psychol Hum Percept Perform 26:1639–1656.

Tehovnik EJ, Sommer MA (1997) Effective spread and timecourse of neural inactivation caused by lidocaine injection in monkey cerebral cortex. J Neurosci Methods 74:17–26.

Van Gisbergen JA, Robinson DA, Gielen S (1981) A quantitative analysis of generation of saccadic eye movements by burst neurons. J Neurophysiol 45:417–442.

Van Horn MR, Cullen KE (2009) Dynamic characterization of agonist and antagonist oculomotoneurons during conjugate and disconjugate eye movements. J Neurophysiol 102:28–40.

Van Horn MR, Cullen KE (2012) Coding of Microsaccades in Three-Dimensional Space by Premotor Saccadic Neurons. J Neurosci 32:1974–1980.

van Opstal a, Kappen H (1993) A two-dimensional ensemble coding model for spatial-temporal transformation of saccades in monkey superior colliculus. Netw Comput Neural Syst 4:19–38.

Wallis JD, Miller EK (2003) Neuronal activity in primate dorsolateral and orbital prefrontal cortex during performance of a reward preference task. Eur J Neurosci 18:2069–2081.

Wurtz RH, Goldberg ME (1972a) Activity of superior colliculus in behaving monkey. IV. Effects of lesions on eye movements. J Neurophysiol 35:587–596.

Wurtz RH, Goldberg ME (1972b) Activity of superior colliculus in behaving monkey. 3. Cells discharging before eye movements. J Neurophysiol 35:575–586.

Wurtz RH, Goldberg ME (1972c) Activity of superior colliculus in behaving monkey. IV. Effects of lesions on eye movements. J Neurophysiol 35:587–596.

Wurtz RH, Sommer MA, Paré M, Ferraina S (2001) Signal transformations from cerebral cortex to superior colliculus for the generation of saccades. Vision Res 41:3399–3412.

Zénon A, Krauzlis RJ (2012b) Attention deficits without cortical neuronal deficits. Nature 489:434–437.

Zénon A, Krauzlis RJ (2012a) Attention deficits without cortical neuronal deficits. Nature 489:434–437.

Zuber BL, Stark L (1965) Microsaccades and the velocity-amplitude relationship for saccadic eye movements. Science 150:1459–1460.

Chapter 2

Bilateral saccadic deficits following large and reversible inactivation of unilateral frontal eye field

Tyler R. Peel[1,2], Kevin Johnston[1,3,4], Stephen G. Lomber[1-4] , Brian D. Corneil[1-5]

[1]The Brain and Mind Institute, University of Western Ontario, London, ON, N6A 5B7, Canada
[2]Graduate Program in Neuroscience, University of Western Ontario, London, ON, N6A 3K7, Canada
[3]Department of Physiology & Pharmacology, University of Western Ontario, London, ON, N6A 3K7, Canada
[4]Department of Psychology, University of Western Ontario, London, ON, N6A 3K7, Canada
[5]Robarts Research Institute, London, ON, N6A 5B7, Canada

Keywords: frontal eye field, reversible inactivation, saccade generation

Peel TR, Johnston K, Lomber SG, Corneil BD (2014) Bilateral saccadic deficits following large and reversible inactivation of unilateral frontal eye field. J Neurophysiol 111:415–433.

2.1: Introduction

The primate frontal eye field (FEF) is a key brain area involved in the generation of saccadic eye movements (for review see (Schall, 2002)). The functional role for the FEF in oculomotor control has been reinforced by a series of inactivation studies, which have described a triad of contralateral saccadic deficits (increased reaction time, decreased accuracy and peak velocity) and performance errors (e.g., neglect, premature saccades, and an inability to maintain fixation) following permanent FEF ablations (Latto and Cowey, 1971; Schiller et al., 1980; Collin et al., 1982; Deng et al., 1986; van der Steen et al., 1986; Lynch, 1992; Schiller and Chou, 1998) or reversible pharmacological FEF inactivation (Dias et al., 1995; Sommer and Tehovnik, 1997; Shi et al., 1998; Dias and Segraves, 1999). Each mode of inactivation has both advantages and disadvantages (Lomber, 1999). Ablations lesion a large volume of tissue permanently, with assessments of oculomotor deficits occurring after weeks to months of recovery. The remaining oculomotor capabilities therefore reflect both what was lost due to the FEF lesion, and the plastic capacity of the oculomotor network to recover over time. Reversible pharmacological inactivation is less invasive and enables study of the oculomotor system unconfounded by plastic recovery, however the volume of inactivation is substantially smaller and varies with time as the drug diffuses and is metabolized. The effects of inactivating a large volume of the FEF on saccade behaviour, unconfounded by recovery, remains unknown.

The goal of this study is to evaluate the FEF's contribution to visually-, delayed-, and memory-guided saccadic behaviour via an assessment of oculomotor behaviour before, during, and after large and reversible inactivation of unilateral FEF. To do this, we use the cryogenic inactivation technique (Lomber et al., 1999), wherein cryoloops (see **Fig. 2-1**) are implanted into the brain to permit controlled lowering of tissue temperature to a point where it is synaptically inactive yet viable upon rewarming. Here, we designed our cryoloops to reversibly inactivate a volume of tissue (~162 mm^3) that is substantially larger than other reversible inactivation techniques (~14 -33 mm^3; (Sommer and Tehovnik, 1997; Dias and Segraves, 1999). The cryogenic technique also enables collection of large, repeated datasets that facilitate statistical analysis of saccadic deficits. Here, we describe the effects of unilateral cryogenic inactivation of the FEF on bilateral saccadic performance in two tasks. In the *step saccade task* (**Fig. 2-2A**) a briefly flashed saccadic target is presented at one of 32 locations, allowing us to describe the saccadic deficits associated with targets distributed throughout the visual field. In addition to the expected contralateral saccadic deficits, we are also particularly interested in any ipsilateral saccadic deficits that may arise with a large but reversible lesion, given that FEF neurons with ipsilateral response fields are sparsely distributed throughout the FEF (Bruce and Goldberg, 1985; Funahashi et al., 1991; Segraves, 1992; Crapse and Sommer, 2009). In the *interleaved memory-guided and delayed saccade task* (**Fig. 2-2B**), the monkeys had to first withhold a saccadic response, and look to

either a remembered or persistent visual cue after offset of a central fixation point. This task permitted a direct comparison of the effects of FEF inactivation on tasks with differing requirements for spatial working memory. We are particularly interested in the preponderance of premature saccades to ipsilateral-presented cues in this task, as such errors are prevalent following reversible pharmacological inactivation (Dias et al., 1995; Sommer and Tehovnik, 1997; Dias and Segraves, 1999), but not permanent ablations (Deng et al., 1986). It therefore remains unclear whether premature saccades occur only when a small volume of the FEF is inactivated, perhaps because of disinhibition of a focal, corresponding region of the non-inactivated FEF (Schlag et al., 1998), or whether premature saccades are not seen following permanent ablations because of functional recovery.

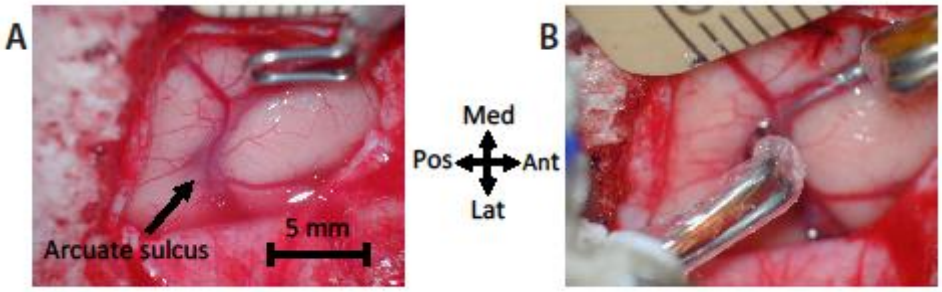

Figure 2-1. Surgical insertion of two cryoloops into the right arcuate sulcus. A) A 5 x 3 mm cryoloop is positioned over the superior aspect of the arcuate sulcus before insertion. B) An additional 7 x 3 mm cryoloop is inserted into the inferior aspect of the arcuate sulcus.

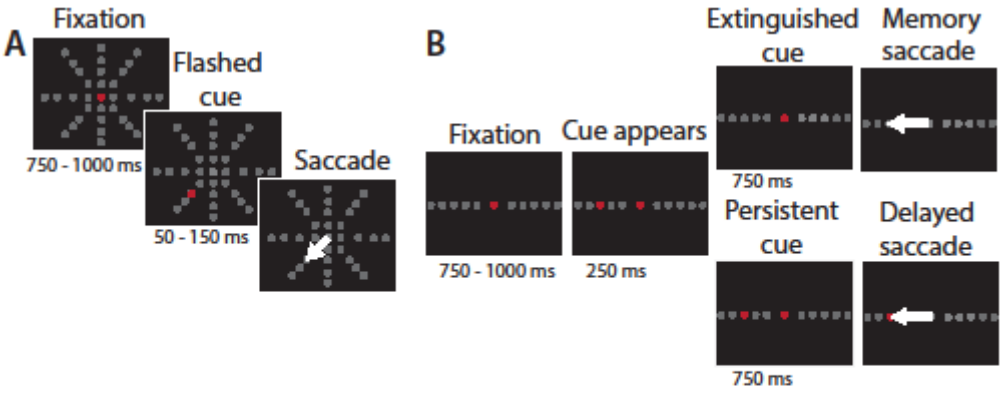

Figure 2-2. Experimental saccade tasks used: A) Step saccade task with cues distributed throughout the visuomotor field. Thirty-two cue locations are arranged in eight directions with eccentricities ranging from 4 to 20 degrees (grey circles represent potential cue locations). B) Interleaved memory and delayed saccade task to contralateral and ipsilateral presented cues. Five cues are confined to the horizontal axis on both sides of the central fixation LED with eccentricities of 4 to 20 degrees.

Consistent with previous FEF inactivation studies, we observed the triad of contralateral saccadic deficits that usually accompany the inactivation of oculomotor structures (increased reaction time, decreased accuracy and peak velocity). We also found moderate, yet consistent, increases in reaction times for ipsiversive saccades, even though these saccades had normal saccade accuracy and dynamics. Surprisingly, we did not observe any consistent increases in premature saccades with ipsilateral cues, which differ markedly from the substantial increases reported by reversible pharmacological inactivation studies.

Some results have been reported previously in abstract form (Peel et al., 2010).

2.2: Methods

2.2.1: Subjects and physiological procedures

Two male monkeys (*Macaca mulatta*, monkeys M and G, weighing 8.7 and 11.1 kg, respectively) were used in these experiments. All training, surgical, and experimental procedures were in accordance with the Canadian Council on Animal Care policy on the use of laboratory animals (Olfert et al., 1993) and approved by the Animal Use Subcommittee of the University of Western Ontario Council on Animal Care. The monkeys' weights were monitored daily and their health was under the close supervision of the university veterinarians.

Each monkey underwent an aseptic procedure to implant two stainless steel cryoloops into the right arcuate sulcus as shown in **Figure 2-1**. We customized the cryoloops based on an anatomical magnetic resonance image (MRI) obtained from each monkey, implanting in each case a 3 X 7 mm and 3 X 5 mm (depth X length) cryoloop in the inferior and superior aspects of the arcuate sulcus (inferior arm: IA, superior arm: SA), respectively. We performed a small 2.25 cm^2 craniotomy at the stereotaxic coordinates of the arcuate sulcus spur to allow for insertion of both IA and SA cryoloops. A detailed technical report of the cryoloop technique has been described before (Lomber et al., 1999), and previous studies have implanted cryoloops in monkey cortical sulci to reversibly inactivate brain areas (Ponce et al., 2011; Nassi et al., 2013; Johnston et al., 2014). The typical drug regimen and other surgical details in the lab have been described previously (Elsley et al., 2007). In addition, monkeys were given dexamethasone post-operatively to minimize potential brain swelling.

2.2.2: Experimental procedures

The monkeys were placed with their heads restrained in a customized primate chair (Crist Instruments) for the duration of the experiment. We conducted experiments in a dark, sound-attenuated room, and infrared cameras were used to monitor body movements. The chair was secured at the center of a 3-ft^3 coil system (CNC Engineering), with the monkey facing an rectilinear grid of greater

than 500 red LEDs covering ± 35˚ of the horizontal and vertical visual field. All aspects of the experiment were controlled by customized real-time LabView programs on a PXI controller (National Instruments) operating at a rate of 1 kHz. We collected eye position signals from either a gaze-tracking coil system or a single, chair-mounted eye tracker (EyeLink II) in monkey M and G, respectively. An experimental dataset consisted of pre- (active), peri- (inactivated), and post-cooling (re-activated) sessions, with each session containing 200 or 150 correct trials (~ 10 minutes) for monkey M and G, respectively. Following the pre-cooling session, we turned on the cooling pumps, initiating the flow of chilled methanol through the lumen of the cryoloops. We began the peri-cooling session when cryoloop temperature attained a temperature of 0-3˚C for at least 3 minutes. The temperature of the cryoloop was monitored via a wired connection from a microthermocouple to a digital thermometer. Cryoloop temperatures of 0-3˚C silences post-synaptic activity in surrounding neurons up to 1.5 mm away without influencing fibers of passage (Lomber et al., 1999). Cooling both the IA and SA cryoloops provided an inactivation volume of approximately 162 mm^3, which is approximately 5 to 10 times larger than previous FEF pharmacological inactivation studies (Dias et al., 1995; Sommer and Tehovnik, 1997; Dias and Segraves, 1999). Note that this volume estimate does not include the volume of inactivated tissue in the posterior bank of the arcuate sulcus, as inactivation of this region does not appear to affect saccadic behaviour. Once we finished trial collection for the peri-cooling session, the cooling pumps were turned off, which

allowed the tissue to rapidly rewarm. We commenced the post-cooling session when cryoloop temperatures were within 1˚C of temperatures observed in the pre-cooling session (~37˚C) for at least 3 minutes. The monkeys continued to perform the behavioural task throughout the cooling and rewarming transitions, but this data is not reported in this manuscript. We also conducted sham control sessions where experimental conditions were identical to actual cooling days, with the exception that the flow of chilled methanol bypassed the cryoloops so that the cryoloops remained at physiological temperatures. To avoid any possible biases, we collected only one complete cooling or sham control dataset per day.

2.2.3: Behavioural tasks

We trained monkeys to perform two behavioural tasks: a step saccade task and an interleaved memory and delayed saccade task (**Fig. 2-2**). These tasks were always performed on separate days. The step saccade task allowed us to evaluate saccades to cue locations distributed throughout the visual field. After the monkey maintained fixation of a central LED for 750 - 1000 ms, a briefly flashed peripheral cue appeared simultaneously with the offset of the central LED, which signaled the monkey to generate a saccade towards the cue within 1000 ms. Since preliminary data showed only subtle saccadic deficits towards persistent visual cues, we flashed cues in order to increase the cognitive demands for this task, since previous research has demonstrated that greater

deficits during FEF inactivation accompany more demanding tasks (Deng et al., 1986; Sommer and Tehovnik, 1997; Dias and Segraves, 1999). We chose flash period durations of 50 or 150 ms for monkey M and G, respectively, selecting a duration that was usually sufficient for the monkey to generate a saccade (monkeys often neglected shorter flash durations during FEF inactivation). Thirty-two possible cue locations were distributed within ±20˚ of visual angle from the central fixation LED (positive values denote right or up location). Both monkeys completed 4 to 7 correct saccade trials to each cue location per session. These cues were arranged in eight evenly spaced directions (rotated at 0˚, 45˚, 90˚ … 315˚ of straight right) at four different eccentricities (4, 10, 16, and 20˚), with the smallest amplitude varying slightly for cardinal (4˚) or oblique (5.7˚) directions. Acceptance windows around the target were relatively large (2.8 - 14˚) with the diameter equal to 70 % of the target's visual angle. Monkeys were required to maintain eye position within this window for 250 ms to be rewarded with water delivered via a sipper tube. Larger acceptance windows were necessary in this study to ensure that the monkey could be rewarded despite some degree of inaccuracy during FEF inactivation.

We utilized the interleaved memory and delayed saccade task to compare the saccadic deficits towards remembered or persistent visual cues following a delay period, which enabled a more comprehensive description of various saccade errors. We also used this task to study saccade dynamics via

construction of velocity-amplitude main sequence relationships. Following an initial fixation period of 750 to 1000 ms, a peripheral cue was presented on the horizontal axis, which was either extinguished after 250 ms or persisted throughout a 1000 ms delay-period where the monkey was required to maintain central fixation. The central fixation LED was then extinguished, which signaled the monkey to generate a memory- or delayed- saccade to either the extinguished or persistent cue location, respectively, within 1000 ms. Both monkeys completed 15 to 20 correct trials to each cue location per session. Cue locations were arranged along the horizontal meridian either contralateral or ipsilateral to the central fixation LED at five different eccentricities (4, 8, 12, 16 and 20˚). The acceptance windows around the fixation point and cue were the same as in the step saccade task, as was the required fixation duration at the cue.

2.2.4: Data analysis

Eye position traces were scanned by computer algorithms in MatLab (Mathworks) to determine the onset and offset times of saccades using a velocity criterion of 30˚/s. We analyzed the first saccade following fixation LED disappearance. Visual inspection of the data off-line by the experimenter verified if these onset and offset marks were appropriate for saccades towards the target location, and re-classified rewarded trials where the first saccade went in the direction opposite to the cue as misdirected saccade error trials. We also

discarded correct trials that had saccade endpoints greater than two times the target window (less than 1 % of trials). Furthermore, trials with reaction times less than 60 ms were classified as premature saccade error trials.

We calculated saccade targeting error and endpoint scatter for each saccade using formulae described by White and colleagues (1994). The saccade targeting error represents the mean angular distance between the displacements of cue location and individual saccade endpoints from the central fixation position, and is defined as:

$$TE_{saccade} = \sqrt{(X - x_i)^2 + (Y - y_i)^2}$$

where

X = horizontal displacement, in degrees, of cue location

Y = vertical displacement, in degrees, of cue location

x = horizontal displacement, in degrees, of saccade endpoint

y = vertical displacement, in degrees, of saccade endpoint

Saccade endpoint scatter represents the mean angular distance between the displacements of mean and individual saccade endpoints from the central fixation position, and is defined as:

$$ES_{saccade} = \sqrt{(\bar{x} - x_i)^2 + (\bar{y} - y_i)^2}$$

where

$\bar{x}$ = mean horizontal displacement, in degrees, of saccade endpoints

$\bar{y}$ = mean vertical displacement, in degrees, of saccade endpoints

x = horizontal displacement, in degrees, of saccade endpoint

y = vertical displacement, in degrees, of saccade endpoint

Trials that were not successfully completed were also included in the analysis of performance errors. We observed three main error types that increased during FEF inactivation: neglect (no saccade generated), misdirected saccades (defined as saccades that were rotated more than 90˚ clockwise or counterclockwise from the appropriate saccade direction), and premature saccades (saccades initiated in any direction before or up to 60 ms after the fixation LED was extinguished). Since neglect or misdirected saccades error types occurred after the offset of the fixation LED, we combined these error types for statistical analyses. Our rationale for grouping these errors was also motivated by the observation that misdirected saccades generally occurred much later than correct saccades for both monkeys and tasks; therefore, both neglect and misdirected saccades error trials had a prolonged period following fixation point offset where no saccade was generated. The RTs of misdirected saccades were 144 ms and 100 ms longer than correct memory saccade trials for monkey M and G, respectively. These average RTs for misdirected saccades are 4.7 or 2.3 standard deviations larger than the mean RTs for correctly performed trials for monkeys M and G, respectively, and the differences between distributions were significant (monkey M: $P < 0.005$, monkey G: $P < 0.05$; Wilcoxon singed-rank test).

For analyses of saccadic reaction time and performance errors, we first collapsed data by saccade direction, and then calculated statistics within each session. For analyses of saccade trajectory (e.g., targeting errors and saccade scatter) and peak velocity, we calculated the statistics on data pooled across all sessions. We compared the effects of conditions (FEF or sham cooling), tasks (when comparing delayed-, and memory-saccades), sessions (pre-, peri-, post-cooling), and cue or saccade directions (contra-, and ipsi-lateral) on each of these saccade and performance measures. In cases where behavioural measures are compared across sessions, a paired test was used with a Bonferroni correction for multiple comparisons (corrected $\alpha = 0.05/2 = 0.025$), whereas repeated measures ANOVAs were used to compare the effects of cooling across conditions, tasks, and directions ($\alpha = 0.05$). Alternatively for cases where there are multiple comparisons across cue locations, a two sample t-test was used with a Bonferroni correction (corrected $\alpha = 0.05/32 = 0.00156$). To calculate statistics for the velocity-amplitude main sequence relationship, we pooled saccades across datasets for each session, and fit a non-linear regression to independently measure changes to saccade peak velocities across sessions. To determine significant changes in saccade peak velocities independent of amplitude, we first performed a bootstrap analysis using 5000 sets of randomly sampled saccades with replacement in a non-linear regression fit for the function and its initial coefficients a and b defined as:

$$y = a\left(1 - e^{\frac{-x}{b}}\right);\ a = 800\ ;\ b\ = 35$$

where

y = saccade peak velocity, in degrees per second

x = saccade amplitude, in degrees

The non-linear regression fit returned coefficient estimates for each of the 5000 sets of randomly sampled saccades, which we then used to extract the peak velocities at 10˚, 15˚, and 20˚. Finally, we calculated the standard error and 95 % confidence intervals of session distribution means, and determined significant differences between distributions using Welch's t-tests with a Bonferroni correction for multiple comparisons (corrected $\alpha = 0.025$).

2.3: Results

2.3.1: Description of dataset

We tested the effects of cryogenic FEF inactivation on saccadic behaviour by cooling one or both of the IA and SA cryoloops. From monkey M, we collected 7 sets of pre-, peri-, and post-cooling sessions of both cryoloops from the step saccade task, and 10 sets from the memory and delayed saccade task. We also performed sham controls where the cryoloops remained warm throughout time-controlled sessions, and collected 5 and 8 sets of sessions from the step or memory and delayed saccade task, respectively. From monkey G, we collected 7 sets of cooling sessions of both cryoloops in the step saccade task, while 8 sets were collected in the memory and delayed saccade task. Similarly, we also collected 7 and 12 sets of sham control sessions in the step or memory and

delayed saccade task, respectively. In addition, we collected 22 and 37 sets of sessions from individual (IA or SA) cryoloop cooling from monkey M and monkey G, respectively. For simplicity, we only report the effects of cooling both cryoloops together, since saccadic deficits were only quantitatively, and not qualitatively, less severe when cooling individual cryoloops. Briefly, cooling only the IA cryoloop caused greater saccadic deficits than cooling the SA cryoloop alone, and produced a deficit ~70 % as severe as that observed when cooling both cryoloops.This estimate includes the increases in ipsiversive saccade reaction times we observed with cooling both cryoloops. Furthermore, with the exception of neglect errors, the effects of cooling both cryoloops were well predicted by adding the effects of cooling individual cryoloops alone. In contrast, neglect errors tended to be rare during cooling of individual IA or SA cryoloops, but much more frequent with combined cooling of the cryoloops (see below). In sum, we found larger FEF inactivation volumes produced larger saccadic deficits, although saccadic deficits were more apparent with a FEF inactivation in the inferior compared to the superior arm of the arcuate sulcus. For the rest of the results, we focus the effects of cooling both cryoloops.

2.3.2: Behavioural deficits profile following unilateral FEF inactivation

We observed a broad and consistent profile of saccadic deficits during unilateral FEF cryogenic inactivation on every cooling day, which at least partially recovered upon rewarming. For this manuscript, we emphasize saccadic deficits that: i) were consistent in both monkeys, ii) showed some tendency for recovery upon FEF rewarming, and iii) were greater than trends observed during sham inactivation, and hence could not simply be attributed to satiation or decreased motivation. Saccadic deficits included increases in bilateral-directed saccade reaction time, decreases in contraversive (leftward) saccade accuracy, peak velocity and amplitude, and increases in several performance errors (neglect, and misdirected saccades). We first describe saccadic deficits towards flashed cues distributed throughout the visual field in the step-saccade task, and then describe the changes in saccade behaviour in the interleaved memory- and delay saccade task. Overall, both monkeys continued to perform well during FEF inactivation, even though performance errors increased. Additionally, we did not see any increases in the proportion of missed trials during FEF inactivation (e.g. where the monkey failed to initiate the trial by not looking at the central fixation LED). During FEF inactivation, we also did not observe any substantial (>1˚) changes in fixation eye position nor propensity for erroneous saccades in the fixation interval preceding cue presentation. We also did not detect any abnormalities in monkeys' non-saccadic behaviour during FEF inactivation,

although we acknowledge that we did not specifically test limb or hand movements. Indeed, non-saccadic deficits are likely since the inactivation volume extended to the posterior bank of the arcuate sulcus, encompassing functional areas in the premotor cortex related to coordinated visually-guided arm and hand movements (Moll and Kuypers, 1977; Halsband and Passingham, 1982; Weinrich and Wise, 1982; Weinrich et al., 1984).

2.3.3: Unilateral FEF inactivation increased targeting errors for contraversive saccades

We first describe saccade trajectories and errors to flashed cue locations distributed throughout the visual field following unilateral inactivation of the right FEF. Before FEF inactivation, both monkeys could generate accurate saccades to all briefly-flashed cue locations (**Fig. 2-3A,B**). Saccade amplitudes scaled with cue eccentricity, although monkey G's rightward (ipsilateral) saccades showed substantial hypometria (**Fig. 2-3B**). Recall that this figure only shows the first saccade; we confirmed that monkey G attained all flashed cues with a subsequent saccade(s). Monkey G also generated normometric saccades to persistent visual targets (see **Fig. 2-9B** bottom). In both monkeys, FEF inactivation increased hypometria and endpoint scatter for saccades toward contralateral cues (**Fig. 2-3C,D**; these changes are difficult to resolve for monkey M given the scaling, but will be analyzed quantitatively in the next section). Hypometria tended to be greatest for more eccentric contralateral cues,

whereas less eccentric cues primarily exhibited increased endpoint scatter. Monkey G displayed quantitatively larger deficits with more pronounced hypometria to contralateral cue locations, and to upward and downward locations as well. Upon rewarming, both monkeys showed considerable recovery in saccade amplitude and endpoint scatter, particularly for those cues most affected by FEF inactivation (**Fig. 2-3E,F**). In summary, both monkeys had increased targeting errors for contralateral cues during FEF inactivation characterized by hypometria and increased endpoint scatter towards flashed contralateral cues, which showed substantial recovery upon FEF rewarming.

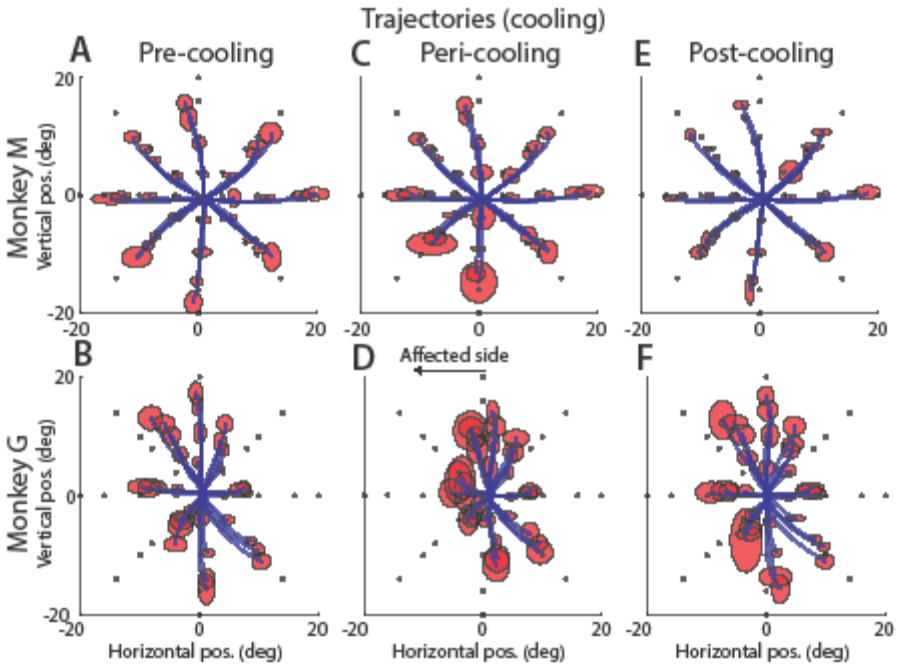

Figure 2-3. Saccade trajectories and endpoints to briefly flashed cues distributed throughout the visual field before (A/B), during (C/D) and after (E/F) unilateral FEF inactivation for each monkey. Mean saccade trajectory (blue curve) was calculated from individual trajectories pooled across days for each session. Red ellipses represent ±1 standard deviation of the horizontal and vertical saccade endpoint scatter.

2.3.4: Quantitative comparison of saccade targeting error across all cue locations

To quantify and compare these trajectory deficits across all cue locations and to sham control sessions, we constructed contour plots representing the change in targeting error for each cue location. The change in saccade targeting error is computed for the cooling and warming transitions as:

Change across cooling transition: $\overline{TE}_{during} / \overline{TE}_{before}$

Change across rewarming transition: $\overline{TE}_{after} / \overline{TE}_{during}$

Since increases in targeting errors following transitions produce ratios greater than 1, larger values represent situations where saccades become more inaccurate across the transition. We observed significant increases in the targeting error for 33 % (4/12) and 92 % (11/12) of contralateral cues for monkey M (**Fig. 2-4A**) and monkey G (**Fig. 2-4B**), respectively (two sample t-tests, Bonferroni corrected for multiple comparisons; this analysis excludes saccades to purely vertical cues). Targeting error ratio increases mainly arose from saccade hypometria, and could increase by a value of 1.5 or more, particularly for contralateral cues. Both monkeys exhibited increased targeting error ratios for contralateral, downward, and select ipsilateral cues. A trend for an increasing degree of hypometria for more eccentric cues was also apparent in both monkeys. Statistically significant hypometria was observed for cue eccentricities > 12˚ in 38 % (6/16) and 63 % (10/16) cases for monkey M and G, respectively, whereas hypometria only reached significance for cue eccentricities < 12˚ in 13 %

(2/16) and 44 % (7/16) cases for monkey M and G, respectively. Upon FEF rewarming, targeting error ratios recovered to some degree in both monkeys, especially for those cue locations most affected during FEF inactivation (**Fig. 2-4C,D**). Such recovery reached significance only in monkey G for 14 of the 18 cue locations significantly affected by FEF inactivation. In contrast to the changes in the targeting error ratio seen with actual cooling and rewarming of the FEF, sham inactivation produced only minimal and largely non-significant changes in the targeting error ratio for each monkey across any transition (**Fig. 2-4E,F,G,H**). Thus, the increases in hypometria for contraversive saccades during FEF inactivation are not simply attributable to satiation or decreased motivation.

We next investigated the changes in saccade endpoint scatter across cue locations, by constructing contour plots using saccade endpoint scatter ratio for each monkey in a similar manner. The change in saccade endpoint scatter is computed for the cooling and warming transitions as:

Change across cooling transition: $\overline{ES}_{during} \,/\, \overline{ES}_{before}$

Change across rewarming transition: $\overline{ES}_{after} \,/\, \overline{ES}_{during}$

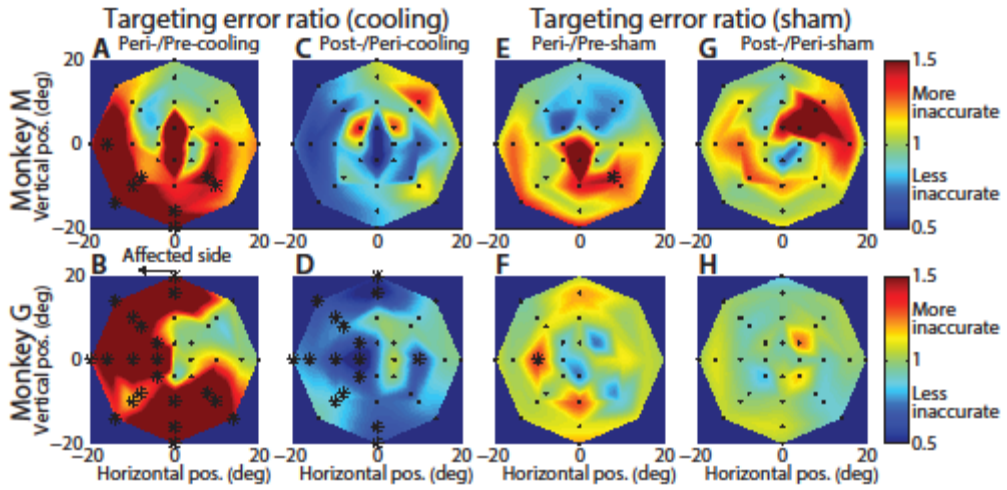

Figure 2-4. The relative change of saccade targeting error to briefly flashed cues distributed throughout the visual field following unilateral FEF inactivation for monkey M (A) and monkey G (B), and upon FEF rewarming for monkey M (C) and monkey G (D). For comparison, the relative change of saccade targeting error is shown following a sham inactivation for monkey M (E) and monkey G (F), and upon reversal for monkey M (G) and monkey G (H). The targeting error ratio was calculated for each of the 32 target locations across cooling days. Increases in saccade targeting error ratio are indicated by red tints, decreases by blue tints, and negligible changes by green tints. Significant changes in saccade targeting error ratio are represented by asterisks for each target location using a paired t-test with a Bonferroni correction ($P < 0.00156$).

Since increases in endpoint scatter following transitions produce ratios greater than 1, larger values represent situations where saccades become more variable across the transition. Following FEF inactivation, we observed increases of the saccade endpoint scatter ratio exceeding 1.5 to several contralateral cue locations, including some of those that also had concomitant large increases in targeting error ratio (**Fig. 2-5A,B**). Significant increases in the saccade endpoint scatter ratio was observed for 17 % (2/12) and 42 % (5/12) of contralateral cues for monkey M and G, respectively (paired t-tests, Bonferroni corrected for multiple comparisons; excluding vertical saccades). While monkey M exhibited a similar spatial profile in the changes of the targeting error ratio and saccade endpoint scatter ratio, for monkey G significant increases in saccade endpoint scatter tended to be restricted to less eccentric contralateral cues, unlike the spatial profile observed for targeting error ratio. This result may be related to the larger degree of hypometria exhibited by this monkey, or the greater propensity for this monkey to neglect eccentric contralateral cues (see below). Upon rewarming, the changes in saccade endpoint scatter generally recovered, primarily for those cue locations most affected during FEF inactivation (**Fig. 2-5C,D**), with significant recovery of endpoint scatter being observed in monkey G at 5 of the 8 cue locations significantly affected by FEF inactivation. Again, sham inactivation produced little consistent effect on saccade scatter across any transition (**Fig. 2-5E,F,G,H**).

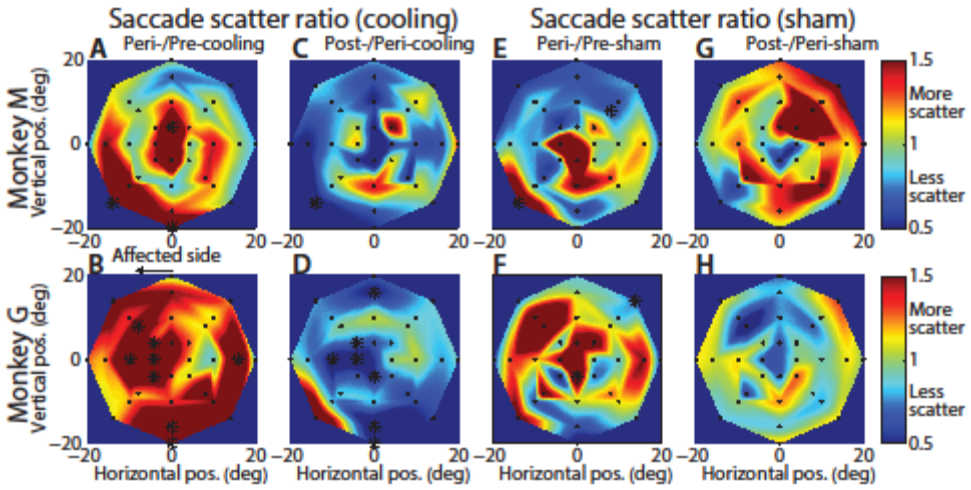

Figure 2-5. The relative change of saccade scatter to briefly flashed cues distributed throughout the visual field with unilateral FEF inactivation. Same format as **Figure 2-4**.

In summary, unilateral FEF inactivation in both monkeys increased hypometria and endpoint scatter to almost all contralateral cues, and to some ipsilateral cues close to the vertical midline. In both monkeys, these deficits tended to be more severe for more eccentric cues.

2.3.5: Unilateral FEF inactivation increases SRTs towards flashed cues bilaterally

We next evaluated the changes in SRTs following unilateral FEF inactivation. First, we represent the SRTs pooled across contralateral or ipsilateral locations (**Fig. 2-6A,B**; excluding vertical cues). During FEF inactivation, both contralateral- and ipsiversive SRTs significantly increased for monkey M (contra- $P < 0.0001$, ipsi- $P < 0.05$) and monkey G (contra- $P < 0.0001$, ipsi- $P < 0.01$, paired t-tests, Bonferroni-corrected for multiple comparisons), with greater SRT increases accompanying contralateral versus ipsilateral cues (SRTs increased to contralateral cues by 54 and 134 ms for monkey M and G, respectively, and for ipsilateral cues by 44 and 21 ms for monkey M and G, respectively). Upon rewarming, bilateral-directed SRTs deficits showed some recovery, although only the SRT decrease for monkey G's contraversive saccades reached significance ($P < 0.0001$). The absence of consistent SRT recovery may be partly due to the monkeys' satiation, since SRTs also increased during sham inactivation, and again upon reversal. However, the increase in SRT seen during FEF inactivation was far greater than that observed during sham inactivation as revealed by a two-way

ANOVA for both monkeys using only data from the FEF and sham inactivation session. For monkey M during FEF/sham inactivation, we found significant effects for saccade directions (contra- and ipsilateral; $P < 0.0001$) and conditions (cooling and sham; $P < 0.0001$) on SRTs. A similar ANOVA analysis for monkey G during FEF/sham inactivation revealed significant effects for saccade directions ($P < 0.0001$) and conditions ($P < 0.0001$) on SRTs. We also found a significant two-way interaction of saccade direction and condition ($P < 0.0001$). In general, we found bilateral-directed SRT increases for both monkeys during FEF inactivation, with greater increases accompanying contraversive saccades.

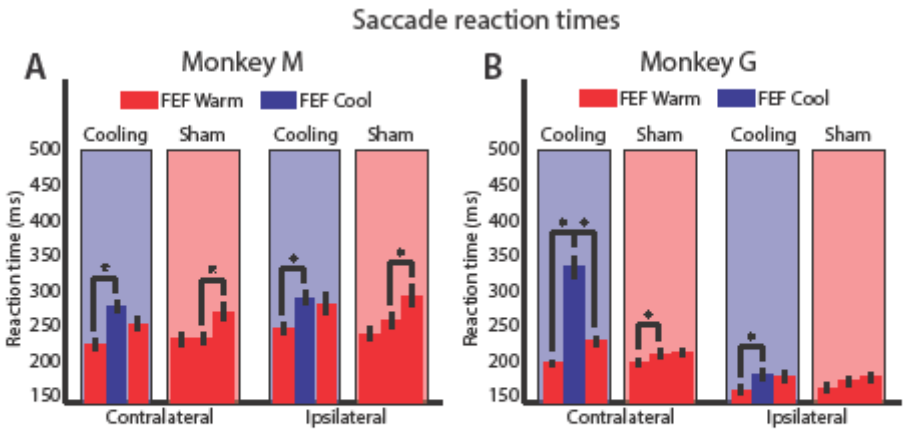

Figure 2-6. Comparison of SRTs (mean ± standard error) toward contralateral and ipsilateral briefly flashed cues for cooling (blue highlight) and sham conditions (red highlight) before, during, and after unilateral FEF inactivation. Sessions where the FEF is active or inactivated are shown by red or blue, respectively. Significant differences across transitions are indicated by asterisks if significance is reached by a t-test with a Bonferroni correction ($P < 0.025$).

2.3.6: Quantitative comparison of SRT changes across all cue locations

We also investigated the changes in SRT at each cue location by constructing contour plots of the change in SRTs across cooling and rewarming (**Fig. 2-7**). Following FEF inactivation, we observed SRT increases at most cue locations, with the largest increases accompanying contraversive saccades (**Fig. 2-7A,B**). Such SRT increases reached significance for 50 % (6/12) and 100 % (12/12) of contralateral cue locations for monkey M and G, respectively (two sample t-tests, Bonferroni corrected for multiple comparisons; excluding vertical cues). SRTs towards these cue locations increased in the range of 50-100 and 50-200 ms for monkey M and G, respectively. For monkey M, SRT increases tended to be greatest for more eccentric and upward contralateral cues. For monkey G, SRT increases tended to be greatest for downward contralateral cues. Upon FEF rewarming, SRTs for both monkeys tended to either recover or remain stable (**Fig. 2-7C,D**). Such recovery only reached significance in monkey G, doing so in 76% (13/17) of the cases where significant SRT increases were seen with FEF inactivation. In contrast to the large and spatially contiguous SRT changes with FEF inactivation, we observed mostly patchy, and insignificant changes in SRTs during sham inactivation (**Fig. 2-7E,F,G,H**), which we attribute to the effects of satiation or decreased motivation. In summary, SRTs increased for both monkeys during FEF inactivation, particularly for contralateral locations.

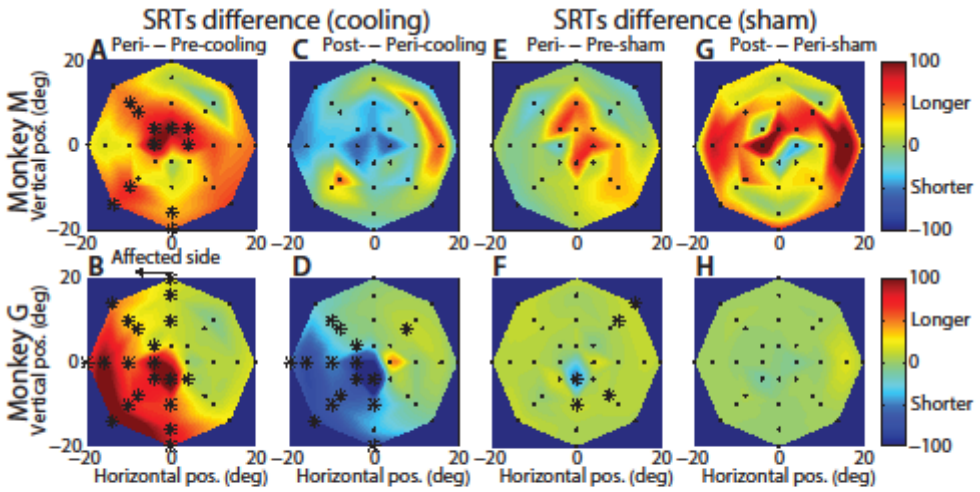

Figure 2-7. The absolute difference of SRTs to briefly flashed cues distributed throughout the visual field with an unilateral FEF inactivation. Same format as **Figure 2-4**.

2.3.7: Increased neglect and misdirected saccades for flashed contralateral cues during unilateral FEF inactivation

During FEF inactivation, two types of errors were commonly observed in the step saccade task. Monkeys often neglected to look at a flashed cue (a *neglect* error), or looked in the opposite direction (a *misdirected saccade* error). Before FEF inactivation, both monkeys had low levels of combined neglect and misdirected saccade errors (<5%; **Fig. 2-8**). During unilateral FEF inactivation, monkey G displayed a marked increase in the tendency to either neglect contralateral cues, or look in the opposite direction (**Fig. 2-8B**; $P < 0.025$, paired t-tests, Bonferroni-corrected for multiple comparisons). In contrast, monkey M had a mild, yet significant increase in errors towards ipsilateral cues (**Fig. 2-8A**; $P < 0.025$). Following FEF rewarming, monkey G's error rate substantially recovered, nearly reaching significance ($P = 0.05$), while monkey M's error rate increased, possibly due to satiation as similar increases were seen in the sham condition. A two-way ANOVA for monkey G during FEF/sham inactivation revealed significant effects of cue directions (contra- and ipsilateral; $P < 0.01$) and conditions (cooling and sham; $P < 0.01$) on combined neglect and misdirected saccade error rate. We also found a significant two-way interaction of cue direction and condition ($P < 0.005$). Using a similar ANOVA analysis for monkey M during FEF/sham inactivation, we found no significant effects of factors on error rate, nor significant interactions of factors.

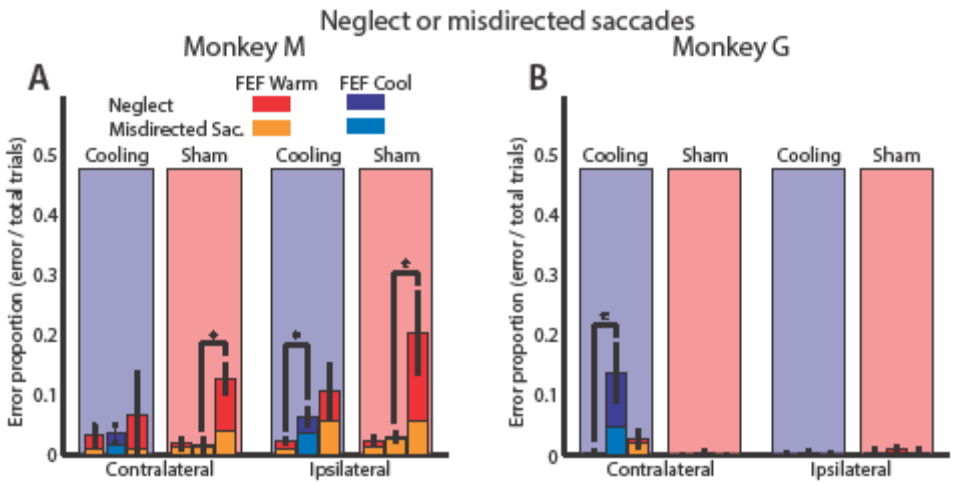

Figure 2-8. Comparison of neglect or misdirected saccade errors across contralateral and ipsilateral briefly flashed cues for cooling (blue highlight) and sham conditions (red highlight) before, during, and after an unilateral FEF inactivation. Same format as **Figure 2-6**. Values represent the proportion of error trials divided by total trials in a session (mean ± standard error ratio). Proportions of neglect errors are represented by red and dark blue with an active (FEF warm) and inactivated FEF (FEF cool), respectively. Misdirected saccade errors are represented by orange and light blue with an active and inactivated FEF, respectively. Significant differences within the both loop and sham cooling groups are indicated by asterisks if significance is reached by a t-test with a Bonferroni correction ($P < 0.025$).

2.3.8: Summary of saccadic deficits for step saccade task

We used the step saccade task during unilateral FEF inactivation to quantify saccadic deficits towards flashed cue locations across the visual field. Unilateral FEF inactivation increased saccade targeting errors, endpoint scatter, reaction times, and in one monkey neglect and misdirected saccades. In general, we found greater impairments towards contralateral cue locations than ipsilateral locations, however moderate deficits were observed for oblique ipsiversive saccades. We also found greater increases of saccadic deficits for saccades towards eccentric cue locations throughout the visual field compared to near locations. Both monkeys presented similar saccadic deficit profile during FEF inactivation, but the severity of saccadic deficits were greater in monkey G versus M. Monkey G also displayed a greater propensity for neglect and misdirected saccade errors. Although data is not shown for saccade peak velocity and amplitude relationship for this task, we did find decreases in both monkeys' saccade peak velocity independent of its amplitude during FEF inactivation for contraversive saccades only.

2.3.9: Memory saccades showed greater increases in targeting errors and endpoint scatter than delayed saccades during FEF inactivation

We now describe changes in saccadic behaviour with unilateral FEF inactivation in a task that requires a delayed response to either a remembered (*memory saccades*) or persistent (*delayed saccades*) visual target. Here, we compared the effects of FEF inactivation on saccade trajectories and endpoints between memory and delayed saccades. In the pre-cooling session, both monkeys displayed greater hypometria towards remembered cue locations (**Fig. 2-9A,B**), although monkey G had relatively greater hypometria towards rightward than leftward targets. We attribute this rightward hypometria to an idiosyncrasy in his normal behaviour since he could generate normometric delayed saccades (**Fig. 2-9B** bottom). During FEF inactivation, memory and delayed saccades from both monkeys showed increased hypometria and endpoint scatter, primarily for contralateral cue locations (**Fig. 2-9C,D**). In addition, for both monkeys, we found greater targeting errors for memory than delayed saccades, and saccade targeting errors were more severe for peripheral, contralateral cue locations than cues near the central fixation target. During FEF inactivation, we also found mild increases in endpoint scatter for both monkeys' ipsiversive saccades, particularly for saccades directed towards cue locations near the central fixation target. In order to determine the quantitative differences in saccade targeting error and endpoint scatter following FEF inactivation, we calculated the ratio of

error values across the cooling transition for each of the 5 contralateral and ipsilateral cue locations. In both monkeys and tasks, we found significant increases in target error ratios primarily towards contralateral cue locations. Specifically, for memory saccades, we found significant increases of ~1.5 at 4 of 5 and 2 of 5 contralateral cue locations for monkey M and G, respectively. For delayed saccades, we found significant increases of ~1.6 at 3 of 5 contralateral cue locations for both monkeys. Similarly, we found increases in endpoint scatter primarily towards contralateral cue locations, which reached significance only for memory saccades in both monkeys (ratios increased by ~1.3, reaching significance for 2 of 5 cue locations). Upon rewarming, for both monkeys, saccade targeting error and endpoint scatter errors decreased, and their saccades had comparable metrics to the pre-cooling session (**Fig. 2-9E,F**).

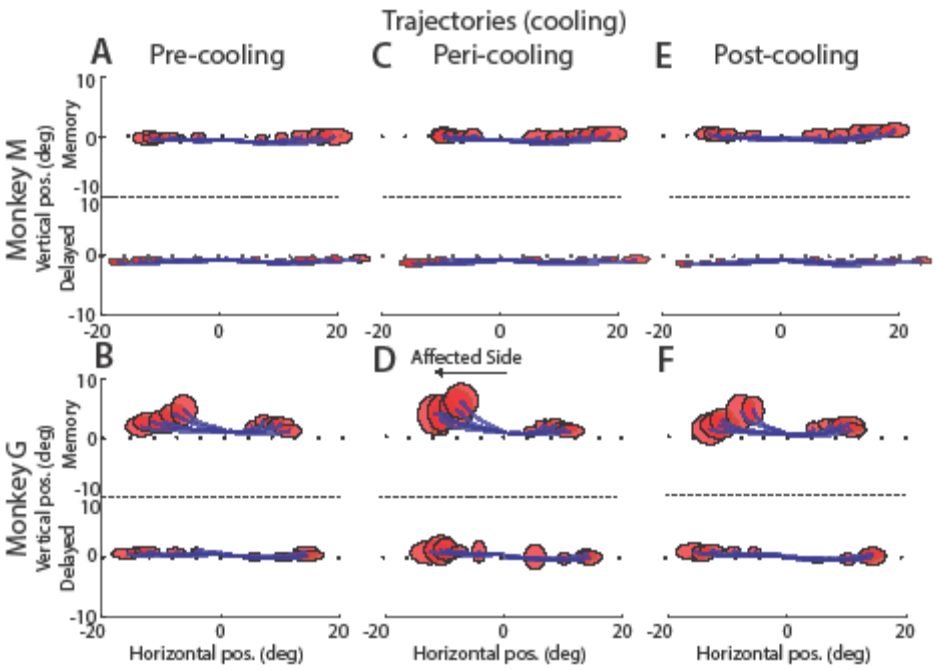

Figure 2-9. Trajectories and endpoints of memory (top row) and delayed (bottom row) saccades. Same format as **Figure 2-3**.

2.3.10: Unilateral FEF inactivation preferentially impaired SRTs towards remembered cues bilaterally

Next, we describe the changes in the SRT in this task, measured from the time of the offset of the central fixation LED. Unilateral FEF inactivation produced greater increases in contraversive SRTs towards remembered compared to persistent visual cue locations for both monkeys (**Fig. 2-10**), increasing for monkey M by 106 and 44 ms for memory and delayed saccades, respectively (memory and delay Ps < 0.0001, paired t-tests, Bonferroni-corrected for multiple comparisons) and for monkey G by 64 and 52 ms, for memory and delayed saccades, respectively (memory and delayed Ps < 0.0001). We also observed significant SRT increases for ipsiversive saccades, particularly for memory saccades, although these increases were smaller than that observed for contraversive saccades. For monkey M, ipsiversive SRTs significantly increased by 65 and 25 ms for memory and delayed saccades, respectively (both Ps < 0.0001), and for monkey G ipsiversive SRTs significantly increased by 32 and 29 ms, for memory or delayed saccades, respectively (memory P < 0.01, delayed P < 0.0001). To determine significant effects and interactions of cooling conditions (cooling and sham), tasks (memory and delayed saccades), and saccade direction (contra- and ipsilateral) on SRTs, we used a three-way ANOVA using data only during FEF/sham inactivation. For monkey M, we found significant effects of saccade conditions (P < 0.0001) and tasks (P < 0.0001), but no significant effects of directions on SRTs. We also found significant two-way interactions of

condition and task ($P < 0.001$) and saccade direction and condition ($P < 0.001$). A similar ANOVA analysis for monkey G during FEF inactivation revealed significant effects for tasks ($P < 0.0001$) and cooling conditions ($P < 0.001$) on SRTs. We found a significant two-way interactions of saccade direction and condition ($P < 0.05$). Upon FEF rewarming, SRTs for both monkeys partly recovered to similar levels observed in the sham inactivation post-session. In summary, both monkeys presented greater increases in bilateral-directed SRTs for memory versus delayed saccades, with the greatest increases in SRTs accompanying contraversive saccades.

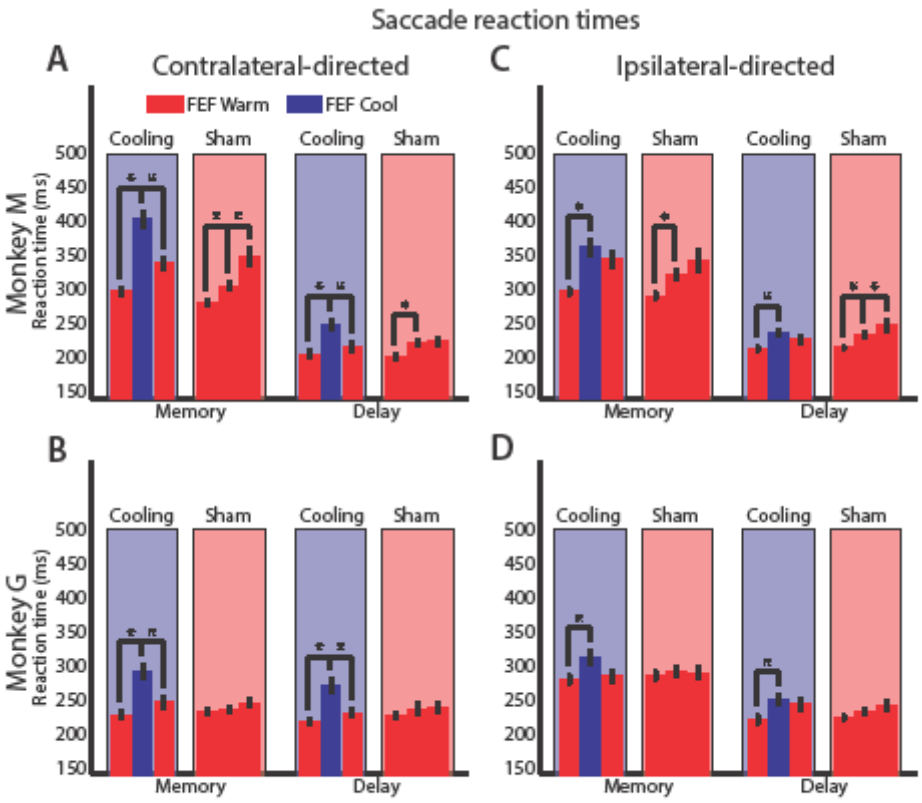

Figure 2-10. Comparison of SRTs (mean ± standard error) of memory and delayed saccades for cooling (blue highlight) and sham conditions (red highlight) before, during, and after an unilateral FEF inactivation. Contraversive saccades are shown for monkey M (A) and monkey G (B), and ipsiversive saccades for monkey M (C) and monkey G (D). Same format as **Figure 2-6**.

2.3.11: Unilateral FEF inactivation slowed all saccades towards contralateral cues

We also studied the velocity-amplitude main sequence, and compared any changes with FEF inactivation across task and direction. During FEF inactivation, we observed substantial downward shifts in a nonlinear function fit to the velocity-amplitude main sequence relationships for contraversive memory-guided saccades that recovered upon rewarming (**Fig. 2-11A,C**). Importantly, this downward shift did not depend on any accompanying hypometria, as changes in peak velocity are evident even for saccades of moderate amplitude (e.g., 10˚). To determine significant differences in peak velocities with FEF inactivation, we performed a bootstrap analysis of a non-linear regression model, which we used to extract the peak velocities at 10˚, 15˚, and 20˚ in amplitude. For saccade peak velocities extracted at 10˚ or 15˚ in amplitude, we found significant peak velocity decreases of contraversive saccades during FEF inactivation for both monkey M (10˚ and 15˚, Ps < 0.001) and G (10˚, P < 0.001; 15˚, P < 0.01). In addition, FEF inactivation resulted in significant decreases in peak velocities extracted at 20˚ in amplitude for only monkey M (P < 0.001). In contrast, no significant changes were found for ipsiversive saccades for both monkeys using extracted peak velocities at 10˚, 15˚, and 20˚ in amplitude (**Fig. 2-11C,D**). Upon rewarming, peak velocities of contraversive saccades extracted at 10˚, 15˚, or 20˚ in amplitude significantly increased in both monkey M (10˚, 15˚ and 20˚, Ps < 0.001) and G (10˚and 15˚, Ps < 0.001; and 20˚, P < 0.01) . Furthermore, we also found

significant downward shifts in the saccade peak velocity-amplitude main sequence relationship for both monkeys' contraversive delayed saccades at 10˚, 15˚, and 20˚ in amplitude (**Fig. 2-12A,B**; Ps < 0.001), which also recovered upon rewarming (Ps < 0.001). In contrast, FEF inactivation did not significantly influence the main sequence relationships for ipsiversive delayed saccades (**Fig. 2-12C,D**). Thus, in contrast to the bilateral effects of FEF inactivation on SRTs, the effects of FEF inactivation of velocity-amplitude relationships are unilateral, selectively shifting the relationship down for contraversive memory or delayed saccades.

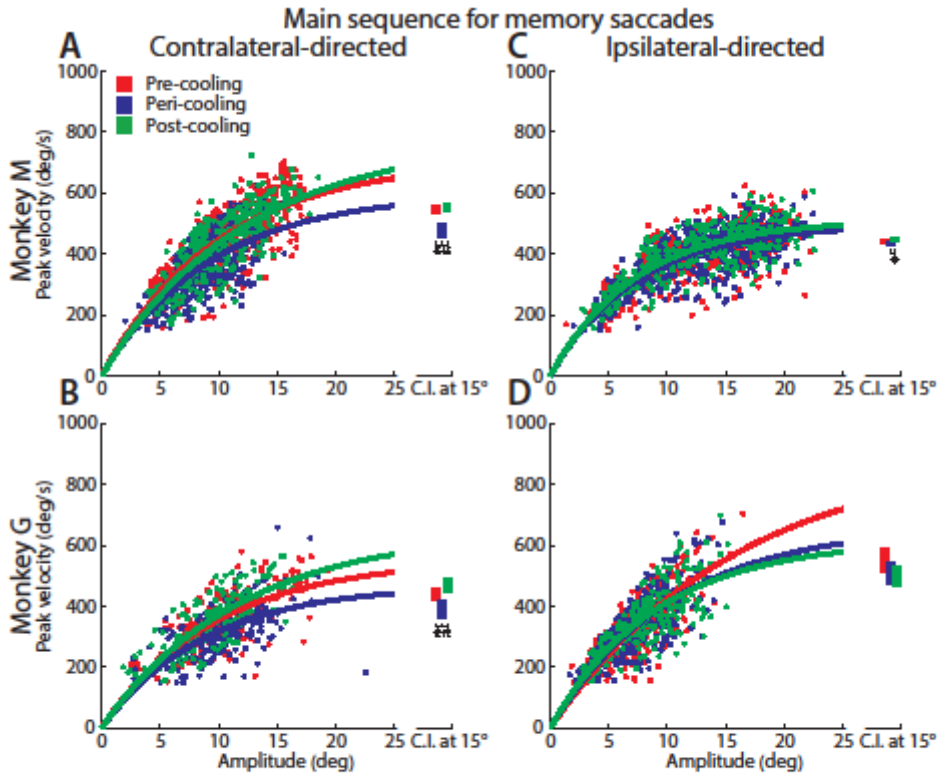

Figure 2-11. Peak velocity-amplitude main sequence relationship for memory-guided saccades to contralateral and ipsilateral targets before (red lines and symbols), during (blue), and after (red) unilateral FEF inactivation. Contraversive saccades are shown first for monkey M (A) and monkey G (B), and ipsiversive saccades for monkey M (C) and monkey G (D). For each session, an exponential regression function fitted the main sequence relationship, and its confidence interval at 15˚ is shown on the right using a bootstrap analysis. Significant differences in peak velocity at 15˚ across transitions are shown by asterisks, which are located below the confidence intervals.

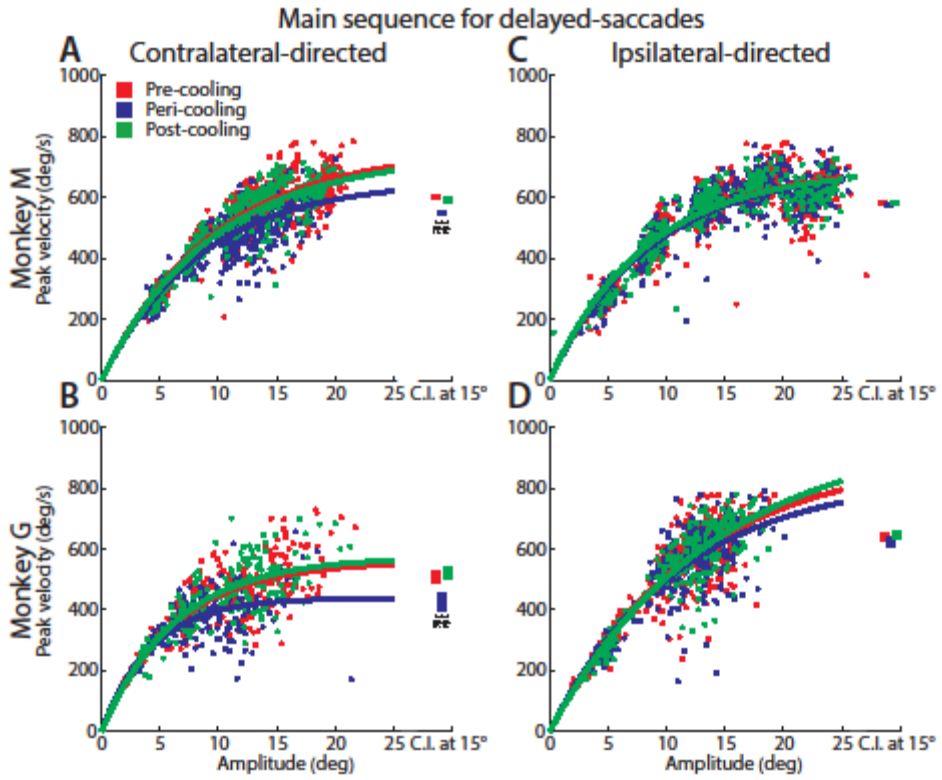

Figure 2-12. Peak velocity-amplitude main sequence relationship for delayed saccade main sequence. Same format as **Figure 2-10**.

2.3.12: Preferential increase in neglect and misdirected during unilateral FEF inactivation for contraversive memory saccades

For a variety of error classes, we computed the frequency of errors before, during, and after unilateral FEF inactivation, beginning first with neglect and misdirected saccades. During unilateral FEF inactivation, both monkeys frequently either neglected to look to a remembered contralateral cue, or looked in the wrong direction after disappearance of the central fixation LED (**Fig. 2-13A,B**). Since both neglect and misdirected saccades errors occurred after offset of central fixation LED and were significantly delayed compared to SRTs for correct trials, we pooled them together for statistical analysis. We found both monkeys had significant increases in error frequency during FEF inactivation in memory saccade trials using paired t-tests, Bonferroni-corrected for multiple comparisons (monkey M $P < 0.005$, monkey G $P < 0.01$). In contrast, we observed less dramatic increases in neglect and misdirected saccade errors for delayed saccades to persistent visual, contralateral cues, which approached significance for both monkeys (monkey M $P = 0.042$, monkey G $P = 0.13$). Interestingly, we found significant increases in errors only for monkey M's memory saccade trials towards ipsilateral cues (**Fig. 2-13C,D**). With a three-way ANOVA for monkey M during FEF/sham inactivation, we found significant effects of cue locations (contra- and ipsilateral; $P < 0.01$), tasks (memory and delayed saccades; $P < 0.0001$), and conditions (cooling and sham; $P < 0.0001$) on combined neglect and misdirected error rate. We also found significant two-way interactions of cue

direction and condition ($P < 0.05$) and task and condition ($P < 0.005$). A similar ANOVA analysis for monkey G during FEF/sham inactivation revealed significant effects of only tasks ($P < 0.0001$) on error rate. We also found a significant two-way interaction of cue direction and condition ($P < 0.025$). Following FEF rewarming, monkey M and monkey Gs' neglect and misdirected errors considerably decreased, nearly reaching significance (monkey M $P = 0.14$, monkey G $P = 0.07$). In sum, we found both monkeys exhibited an increased tendency upon FEF inactivation to make errors of neglect or misdirected saccades primarily in trials with contralateral, remembered cues.

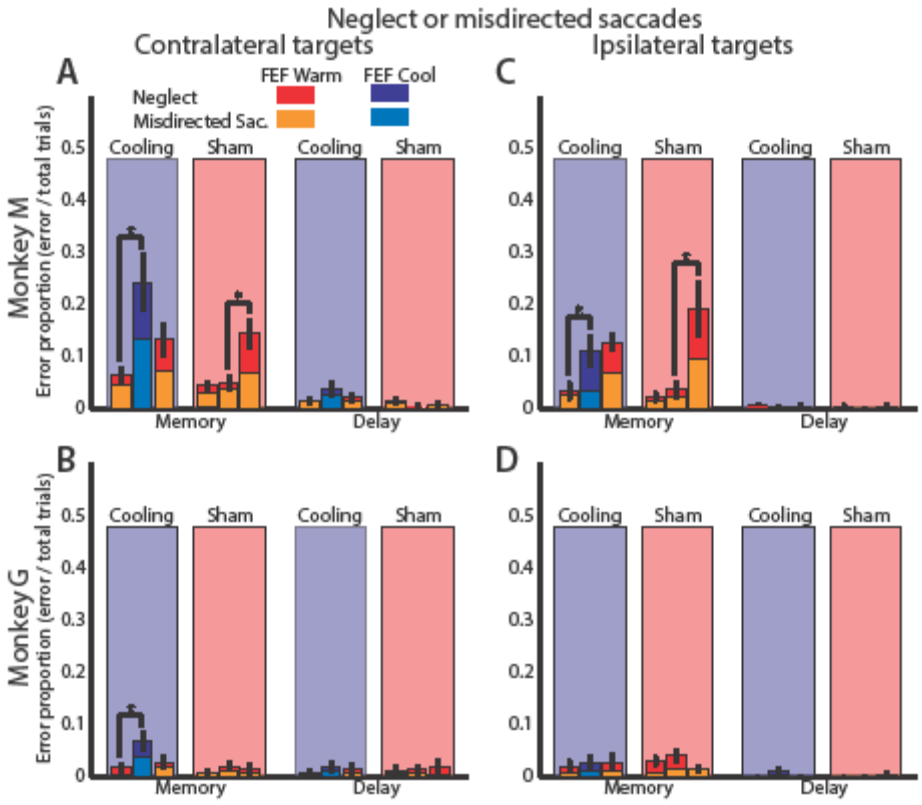

Figure 2-13. Comparison of errors in neglect or misdirected saccades between memory and delayed saccade trials. Same format as **Figure 2-8**.

2.3.13: Unilateral FEF inactivation had mild and inconsistent effects on premature saccade errors

Finally, we describe the effects of FEF inactivation on saccades generated prematurely (the interval for premature saccades spans from the time of cue presentation until 60 ms after disappearance of the fixation LED). During FEF inactivation, we observed only mild and inconsistent increases of premature saccade errors for both monkeys towards ipsilateral presented cues (**Fig. 2-14C,D**) with the only evidence being the nearly significant increases occurring in delay saccade trials for monkey M ($P = 0.05$; paired t-test, Bonferroni-corrected for multiple comparisons). In contrast, we found no significant increases in premature saccade errors for both monkeys in contralateral cue trials (**Fig. 2-14A,B**), nor any recovery upon rewarming. Although we found no significant increases across the cooling transitions, monkey M had significantly greater premature saccade errors with FEF inactivation compared to the sham condition. Using a three-way ANOVA for monkey M during FEF/sham inactivation, we found significant effects of cue locations (contra- and ipsilateral; $P < 0.05$), tasks (memory and delayed saccades; $P < 0.001$), and conditions (cooling and sham; $P < 0.001$) on premature saccade error rate. In contrast, a similar analysis for monkey G during FEF/sham inactivation revealed significant effects of only tasks ($P < 0.0001$) on error rate.

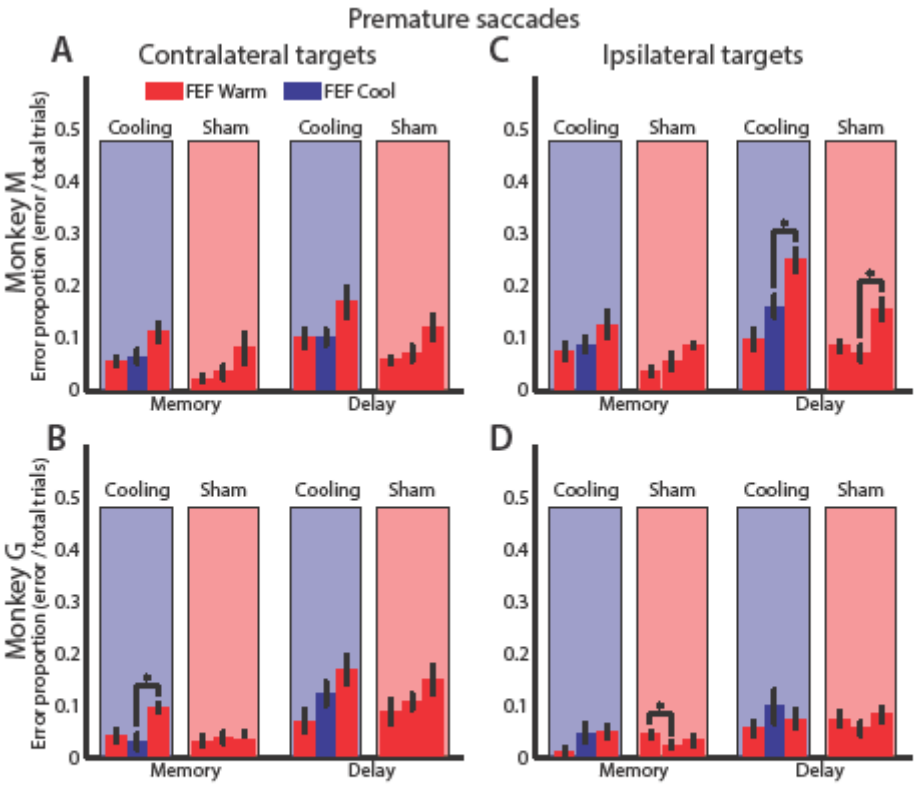

Figure 2-14. Comparison of premature saccades for memory and delayed saccades. Same format as **Figure 2-6**. Values represent the proportion of error trials divided by total trials in a session (mean ± standard error ratio).

2.3.14: Summary of saccadic deficits for memory and delayed saccade task

We used the interleaved memory and delayed saccade task during unilateral FEF inactivation to compare saccadic deficits and performance errors towards remembered and persistent visual cues, and investigate the velocity-amplitude main sequence relationship. Unilateral FEF inactivation increased bilateral-directed SRTs preferentially towards remembered cues, decreased peak velocities of all contraversive saccades, and increased performance errors. We also investigated the saccade accuracy in this task, and found increases in both monkeys' saccade targeting error and endpoint scatter during FEF inactivation primarily for contraversive saccades. An analysis of performance errors during FEF inactivation revealed monkeys tended to neglect or look in the wrong direction of extinguished, contralateral cues, and surprisingly, had few prematurely generated saccades towards ipsilateral cues.

2.4: Discussion

2.4.1: Summary of results

We examined the effects of a large and reversible FEF inactivation on saccadic behaviour separate from any long-term recovery. To accomplish this, we analyzed the saccadic deficits and performance errors in three saccade tasks before, during and after reversible cryogenic inactivation of the unilateral FEF. We observed many of the contralateral saccadic deficits and neglect errors

expected from previous reversible pharmacological inactivation studies, with greater deficits accompanying tasks with a greater working memory load. Importantly, we also observed consistent, albeit smaller, increases in reaction times to ipsilateral targets that have not been previously reported. In addition, we found premature ipsilateral saccade errors only slightly increased with FEF inactivation, in contrast to what had been expected from previous results with pharmacological inactivation. Together, these results add to the body of knowledge concerning the functional contribution of the FEF to saccades in both directions, and attest to the differential effect of inactivating different volumes of the FEF.

2.4.2: Comparison of cryogenic inactivation to pharmacological inactivation and lesions studies

Cryogenic inactivation provides the dual advantages of inactivating a large volume of tissue in a reversible manner. Based on the dimensions of our constructed cryoloops and assuming that 3˚C inactivates the entire depth of the gray matter, we estimated that cooling inactivated a volume of 162 mm^3. This volume is much larger than that assumed to be inactivated by pharmacological means (~14 -33 mm^3 with a radius of 1 - 2 mm from the injection site; (Sommer and Tehovnik, 1997; Dias and Segraves, 1999), and comparable to studies using permanent ablations (~125 mm^3 circumscribing a triangular surface region of 6

mm along both the inferior and superior arms of the arcuate sulcus with a depth of 8 mm into the arcuate sulcus; (Bruce et al., 1985; Schiller and Chou, 1998).

In light of the large volume that is presumably inactivated, the residual abilities that both animals displayed in generating contraversive saccades may seem somewhat surprising. Indeed, the residual abilities for animals to generate contraversive saccades following permanent ablations of the FEF are usually attributed to intact oculomotor areas taking over via parallel pathways (Schiller et al., 1980). While plastic recovery undoubtedly plays a role following permanent ablation, it is also clear that the oculomotor system can continue to operate during large but reversible inactivation of the FEF.

A methodological consideration inherent to cryogenic inactivation is that of loop placement. Our protocol involved inserting two loops oriented medial and lateral from the spur of the arcuate sulcus, which corresponds to the superior and inferior aspect of the arcuate sulcus, respectively. We selected this strategy based on previous literature, and based on the location of the other FEF for monkey M as determined in a previous study (Elsley et al., 2007). One caveat in this strategy is the unintended inactivation of adjacent areas outside of the traditional FEF. Our loops were specifically designed to inactivate tissue within the arcuate sulcus, and hence inactivation did not extend to the premotor oculomotor regions described by Fujii and colleagues (1998, 2000) that lie on the gyri either posterior to the inferior arm of the arcuate (Fujii et al., 1998), or

medial to the superior arm of the arcuate sulcus (Fujii et al., 2000), between the frontal and supplementary eye fields. Cooling within the acruate sulcus also did not extend to the premotor regions that lie on the gyrus between the arcuate and central sulci, from where a variety of defensive or multi-segmental movements that can include an oculomotor component can be evoked via microstimulation (Graziano et al., 2002; Boulanger et al., 2009). Cooling the loops certainly inactivated the posterior bank of the arcuate sulcus, and while we cannot completely rule out the possibility that some of our observed deficits may be related to this, previous studies suggest that this area is not critical for saccade generation. Monkeys with either permanent (Rizzolatti et al., 1983) or reversible (Schieber, 2000) lesions to premotor areas found within the posterior bank of the arcuate sulcus do not display the constellation of oculomotor deficits that we observed here, even though such lesions perturbed skeletomotor behaviours in a variety of tasks. It is possible that inactivated tissue extended into the fundus, which has been linked to smooth pursuit eye movements (Gottlieb et al., 1994) and from where ~20% of neurons have pre-saccade responses (Tanaka and Fukushima, 1998). However, muscimol inactivation of FEF sites physiologically characterized to be related to smooth pursuit severely compromised smooth pursuit without influencing saccades (Shi et al., 1998). Thus, although functional imaging and neuroanatomical techniques demonstrate a large portion of the premotor cortex is active during visually-guided saccades (Koyama et al., 2004; Moschovakis et al., 2004), the preponderance of evidence

from other studies leads us to think that the majority of the saccadic deficits we observed arise from cryogenic inactivation of the anterior bank of the arcuate sulcus.

2.4.3: Changes to contraversive saccade behaviour: spatial specificity, and impact on saccade RT, accuracy, and saccade velocity

In both tasks, unilateral FEF inactivation consistently decreased saccade accuracy (manifested as increased hypometria and/or endpoint scatter), decreased saccade velocities, and increased saccadic reaction times. This triad of contralateral saccadic deficits is commonly seen following either pharmacological FEF inactivation (Dias et al., 1995; Sommer and Tehovnik, 1997; Dias and Segraves, 1999) or ablations in monkeys (Latto and Cowey, 1971; Schiller et al., 1980; Collin et al., 1982; Deng et al., 1986; van der Steen et al., 1986; Lynch, 1992; Schiller and Chou, 1998), and also in human patients presenting with unilateral loss of the FEF (Pierrot-Deseilligny et al., 1991; Rivaud et al., 1994; Gaymard et al., 1999).

The spatial distribution of saccadic deficits we observed encompassed contraversive saccades with or without an oblique component, with smaller deficits accompanying smaller saccade amplitudes. Such relative sparing of smaller amplitude saccades may relate to the logarithmic coding of oculocentric

space, with proportionally more tissue devoted to smaller amplitude saccades (Schwartz, 1980; Bruce and Goldberg, 1985). Alternatively (or perhaps additionally), our protocol for cryoloop placement may not have been optimal to influence the more ventrolateral portions of the FEF preferentially involved in small amplitude saccades (Bruce and Goldberg, 1985).

In all tasks, we consistently found that FEF inactivation decreased contraversive saccade peak velocities, with greater decreases occurring if the target was extinguished during the memory- versus delayed-saccade paradigm. Previous studies using pharmacological inactivation have observed such contraversive decreases in peak velocity (Dias and Segraves, 1999), although others had only inconsistent effects (Sommer and Tehovnik, 1997). Dias and Segraves (1999) postulated that the lack of effects on saccade dynamics found by Sommer and Tehovnik (1997) was due to generally slower peak velocities, possibly from the dark environment, which could result in less peak velocity differences between before and after FEF inactivation. This discrepancy may also be due to the use of primarily lidocaine in the Sommer and Tehovnik (1997) study versus muscimol in the Dias and Segraves (1999) study. Regardless of the mechanism, our results confirm that a large volume of FEF inactivation influences saccade dynamics.

All contralateral saccadic deficits tended to be greater in the memory-guided versus delayed-saccade paradigm, attesting to the FEF's increased role on more cognitively-demanding tasks. This result is also consistent with the greater and longer lasting performance deficits for memory-guided saccades compared to visually-guided saccades following either ablations (Deng et al., 1986) or pharmacological inactivation (Sommer and Tehovnik, 1997; Dias and Segraves, 1999) of FEF. Cognitive signals in the FEF, including delay period activity, appear to play a prominent role in the sensorimotor transformation for saccades. Indeed, a sample of FEF neurons projecting to the superior colliculus (SC) contain visuomotor delay activity that is modulated by Go/Nogo task instructions for only memory-guided saccades; therefore this delay activity may be a correlate of working memory (Sommer and Wurtz, 2001).

Finally, a surprising aspect of our results was the negligible effect of unilateral cryogenic inactivation on gross fixation behaviour, particularly given the previous pharmacological inactivation study by Dias and Segraves (1999) which showed increased scatter during fixation, and modest ipsilateral shifts in spontaneous eye position, neither of which was apparent in either monkey. In addition, Sommer and Tehovnik (1997) reported that monkeys with pharmacological FEF inactivations had difficulty maintaining fixation of peripheral contralateral targets. Fixation-related neurons and sites where electrical stimulation increased bilateral-directed saccade reaction times tend to

be preferentially located more lateral in the arcuate sulcus, and ventrally towards the fundus (Burman and Bruce, 1997; Izawa et al., 2004a, 2004b, 2009). This suggests that either our volume of inactivation did not encompasses these lateral and/or ventral FEF sub-regions, or a more focal FEF inactivation preferentially causes fixation-related deficits. Note however that we did not require our monkeys to fixate eccentrically for a sustained period of time, as was done by Sommer and Tehovnik (1997), hence it is possible that fixation deficits could have been revealed in our monkeys had we used a modified task or required different behaviours.

2.4.4: Increased ipsiversive SRTs without concomitant changes to accuracy or saccade velocity

In addition to contralateral saccadic deficits, large and reversible inactivation of the unilateral FEF also impacted the generation of ipsiversive saccades. Importantly, the impact of inactivation is restricted to increased RTs, with negligible impact on saccade accuracy or dynamics. In all tasks for both monkeys we observed significant increases in ipsiversive SRTs of ~25-50 ms, and while this is less than the RT increase for contraversive saccades, it always exceeded the RT increases observed in the same time interval for sham cooling sessions. Previous FEF inactivation studies have reported only subtle or negligible effects on ipsiversive saccades using either lesions (Latto and Cowey, 1971; Schiller et al., 1980; Collin et al., 1982; Deng et al., 1986; van der Steen et al., 1986; Lynch,

1992; Schiller and Chou, 1998) or injected pharmaceuticals (Sommer and Tehovnik, 1997; Dias and Segraves, 1999), leading us to speculate that the ipsilateral saccade deficits are unique to large and reversible FEF inactivation.

Two potential mechanisms could produce increased ipsilateral SRTs upon inactivation without changing metrics or dynamics. One mechanism could be the relatively sparse distribution of FEF neurons that exhibit ipsilateral responses fields (Bruce and Goldberg, 1985). Because of such a sparse distribution, the functional contribution of these neurons to ipsiversive saccades would only be revealed with a large volume of inactivation, which may be why pharmacological inactivation studies have not observed consistent effects. The functional contribution of ipsilateral-related FEF neurons may be also fundamentally different from the canonical contralateral saccade-related neurons in the FEF; specifically, ipsilateral-related FEF neurons may exert their influence on ipsiversive SRTs through projections that bypass the SC (e.g. indirectly via basal ganglia, or to the brainstem oculomotor areas; see section on potential neuronal mechanisms below), influencing target selection or saccade initiation without influencing the vigor or representation of the oculomotor drive in the brainstem. Although recent work by Crapse and Sommer (2009) has identified some of the inputs to these ipsilateral-related FEF neurons, their functional contribution to oculomotor control remains to be determined.

Alternatively, a large lesion of one FEF may produce widespread disinhibition of the other FEF, with the consequence of somewhat paradoxically prolonging the target selection process for ipsilateral saccades. The FEFs in each hemisphere have connections with each other (Pandya and Vignolo, 1971), and the influence of these connections is thought to be mostly inhibitory (Schlag et al., 1998; Seidemann et al., 2002). Our observation of broadly *increased* ipsiversive SRTs is all the more surprising in light of what is usually thought about interhemispheric FEF communication, which would have predicted *decreased* ipsiversive SRTs. However, the FEF is known to be a key area for saccade target selection (for review, see (Schall, 2002)), instantiating a gradual discrimination between representations of a target from distractors. Such selection is thought to involve inter- and intrahemispheric FEF networks, supporting cooperative or competitive interactions between FEF neurons that share overlapping or non-overlapping response fields (Cohen et al., 2010). If a large portion of one FEF is broadly disinhibited due to a large-volume inactivation of the other FEF, it would presumably take longer for the target selection processes to resolve into a single choice, but once resolved the saccade would have normal metrics and dynamics. In contrast, if a focal portion of one FEF is inactivated, only the mirror location of the other FEF would be disinhibited, leading to shorter ipsilateral RTs only for that location.

These two explanations need not be mutually exclusive. What they do provide is a potential explanation of why increased ipsilateral SRTs are unique to large and reversible FEF lesions, and occur without concomitant changes in saccade metrics or dynamics.

2.4.5: Increased contralateral neglect, but no increased tendency for premature ipsiversive saccades

The functional contribution of the FEF to saccades can also be revealed through an analysis of various error types in different tasks. We observed a markedly increased tendency for both monkeys to either neglect (i.e., not respond) or look in the opposite direction to contralateral-presented stimuli in the memory-guided saccade task. This tendency was greatly reduced in both monkeys if the stimulus remained on in the delayed-saccade task, reinforcing the increased contribution of the FEF in tasks with a greater working memory requirement. Previous FEF studies have found similar observations using pharmacological inactivation (Dias et al., 1995; Sommer and Tehovnik, 1997; Dias and Segraves, 1999) or ablations (Latto and Cowey, 1971; Schiller et al., 1980; Collin et al., 1982; Deng et al., 1986; van der Steen et al., 1986; Lynch, 1992; Schiller and Chou, 1998). These observations of neglect do not appear attributable to inabilities of detecting or remembering contralateral cues. Using monkeys trained in a memory-guided saccade task that spatially dissociated the saccadic response from cue location, Lee and colleagues (2012) found FEF

pharmacological inactivation resulted in no marked differences in monkeys' performance for spatially dissociated responses following contralateral cue presentation. Alternatively when the required responses were not spatially dissociated from contralateral cues, monkeys frequently neglected to generate saccades or looked in the wrong direction, which is in agreement with our own results.

In contrast to previous pharmacological FEF inactivation studies, we found essentially no consistent tendency for either monkey to generate premature ipsiversive saccades during FEF inactivation in the memory-guided or delayed-saccade paradigms, particularly when compared to the results with sham inactivation (**Fig. 2-14**). To put our observations in perspective with previous results, Sommer and Tehovnik (1997) reported that the tendency to generate premature saccades to ipsilateral cues increased from ~5% before pharmacological inactivation to ~50% during FEF inactivation in a memory-guided saccade task. Similarly, Dias and Segraves (1999) reported that the tendency to generate premature saccades to ipsilateral stimuli in a similar task increased progressively from <2% before inactivation to almost 100% ~2 hours after muscimol injection. The marked differences between our results with studies using pharmacological inactivation appears to be another example of the effect of FEF inactivation volume; a more focal FEF inactivation results in

increased difficulty in suppressing inappropriate saccades towards ipsilateral cues at the mirror location.

2.4.6: Predictions of neuronal activity in the downstream oculomotor areas

The triad of contralateral saccadic deficits following large volume unilateral FEF inactivation is largely consistent with the robust and topographically organized projections from FEF to the SC (Leichnetz et al., 1981; Sommer and Wurtz, 2000). FEF neurons do not appear to encode saccadic metrics and dynamics per se (Segraves and Park, 1993), although there are correlations with saccadic reaction time (Segraves and Park, 1993; Hanes et al., 1998; Purcell et al., 2012). Instead, oculocentric signals relayed to downstream oculomotor areas convert these signals into saccadic vectors (Dassonville et al., 1992). Neural activity within the intermediate and deep layers of the SC relates to saccade timing, metrics and dynamics (Mays and Sparks, 1980; Munoz et al., 2000), and reversible inactivation or ablations of the SC produce the same triad of saccadic deficits (Wurtz and Goldberg, 1972; Schiller et al., 1980; Albano and Wurtz, 1982; Albano et al., 1982; Hikosaka and Wurtz, 1983, 1986; Aizawa and Wurtz, 1998; Quaia et al., 1998; Cavanaugh et al., 2012b). Based on the contralateral saccadic deficits we observed, it is likely that saccade-related activity in the ipsilateral SC takes longer to reach threshold, is spatially displaced and variable from the representation of the target before cooling, and reaches a lower peak firing rate.

What remains an open question is how SC activity outside of the peri-saccadic interval is influenced by FEF inactivation, particularly during memory-guided and delayed saccades; preliminary results of ours indicate that visual- and delay-period activity in the ipsilateral SC largely decreases during FEF inactivation (Peel et al., 2012), which suggests the FEF functionally contributes to all aspects of ipsilateral SC activity.

In addition to the robust and topographic projections to the SC, descending projections from the FEF also go through the basal ganglia (Künzle and Akert, 1977) and other brainstem centers downstream from the SC. The direct influence of the basal ganglia on brainstem saccadic activity is thought to be predominantly relayed through the substantia nigra pars reticulata (SNr), which has projections to the ipsilateral and contralateral SC via uncrossed (Jayaraman et al., 1977; Graybiel and Ragsdale, 1978; Chevalier et al., 1981; Hikosaka and Wurtz, 1983) and crossed (Beckstead et al., 1981; Jiang et al., 2003; Liu and Basso, 2008) pathways, respectively. Although both the uncrossed and crossed projections are inhibitory, Jiang and colleagues (2003) found these projections also differ in several respects (e.g., spatial distributions of SNr neurons, spontaneous activity, conduction velocities, and response fields); therefore, they suggested that coordination of these pathways (i.e., inhibition by crossed pathway, and disinhibition of uncrossed pathway) could facilitate pre-saccadic activity in the SC. Previously, Hikosaka and Wurtz (1983) had

investigated the influence of the SNr on pre-saccadic activity in the ipsilateral SC (i.e., uncrossed pathway). Liu and Basso (2008) showed that electrical stimulation in SNr transiently decreases pre-saccadic activity in both contralateral and ipsilateral SC neurons. While the functional role of the crossed pathway for oculomotor behaviour remains to be determined, the crossed pathway provides a substrate by which FEF activity can indirectly influence the SC on the other side. Based on our results, we speculate that any influence on the contralateral SC would be limited to the timing of the saccade-related activity.

A similar degree of uncertainty exists when trying to predict the impact of FEF inactivation on the signals conveyed directly to the brainstem, downstream from the SC. FEF neurons project to the ipsilateral oculomotor regions of the pons, including both the omni-pause and saccadic burst generation regions (Leichnetz et al., 1984; Schnyder et al., 1985; Huerta et al., 1986; Stanton et al., 1988a, 1988b; Segraves, 1992), and contain functional signals that largely resemble those sent directly to the SC (Segraves and Goldberg, 1987; Segraves, 1992). However, the ability to electrically evoke saccades directly from the FEF depends on the integrity of the SC (Hanes and Wurtz, 2001), suggesting that the direct projections from the FEF to the oculomotor brainstem are either insufficient to evoke saccades, or that an additional signal from the SC is required in downstream structures. Alternatively, FEF signals that are sent

directly to the brainstem may participate in ongoing saccadic preparation via cortico-cerebellar loops. The first part of the cortico-cerebellar loop consists of a corticopontocerebellar disynaptic pathway that innervates the cerebellar hemispheric lobule VII (Huerta et al., 1986; Schmahmann and Pandya, 1997; Xiong et al., 2002) and the adjacent dentate nucleus via Purkinje neurons (Xiong et al., 2002). The loop is closed by ascending disynaptic projections from the dentate nucleus to the FEF through the ventralateral nucleus of the thalamus (Lynch et al., 1994), although the dentate nucleus also projects to several other oculomotor areas, including the SC (May et al., 1990) and LIP (Prevosto et al., 2010). Using reversible inactivation of ventrolateral nucleus, Tanaka (2006) reported increased reaction times of self-timed saccades, and suggested that these ascending projections back to cortex are important for the timing of self-triggered saccades. Subsequently, Tanaka (2007) found delay-period activity in neurons of the ventrolateral nucleus, and this activity was correlated to saccade generation when tasks required internal monitoring of time (i.e., self-triggered saccades), or were associated with predictive cues related to saccade timing (i.e., disappearance of fixation light in delayed- or memory-saccades). Recently, Ashmore and Sommer (2013) suggested that one probable source of this delay-period activity is the dentate nucleus. They found delay-period activity in neurons of the dentate nucleus, and this activity was related to the initiation and directionality (but not accuracy or dynamics) of self-triggered saccades. One implication of this finding is that cortico-cerebellar loops appear to play a role in

self-triggered saccades, therefore FEF inactivation may result in impairments of self-triggered saccades by removing a key source of inputs and recipient area of signals from cortico-cerebellar loops.

How then do we explain the changes to ipsiversive saccade behaviour? The increase in ipsiversive SRTs without concomitant changes in saccade metrics or dynamics, as well as the lack of any consistent increase is the tendency to generate premature saccades to ipsilateral stimuli in either the memory-guided or delayed-saccade task, suggests a mechanism whose influence is restricted to saccade timing, rather than saccade generation per se. Such changes may speak to the functional contribution of ipsilateral-related neurons in the FEF contributing to saccade timing but not metrics and dynamics. Although speculative, altered signaling from these neurons through either the basal ganglia (e.g., delayed disinhibition via the crossed pathway) or directly to the oculomotor brainstem (e.g., a delayed pause of the omni-pause neurons, or impairments to cortico-cerebellar loops) could explain our results. Alternatively, as described above, large-volume FEF inactivation may cause broad disinhibition of the contralateral FEF neurons, disrupting the balance of cooperative and competitive interactions among local FEF neurons in the target selection process.

2.4.7: Differential effects of focal versus large-volume inactivation?

One implication of our results compared to those obtained with more focal, pharmacologically-mediated inactivation is that the volume of inactivation may have an important impact on both contralateral- and ipsiversive saccades. In particular, focal inactivation may promote a degree of disinhibition in the mirroring location via a loss of interhemispheric inhibition that is not obtained with large volume inactivation. Large volume inactivation may exert a different impact on saccade behaviour, perhaps because of its proportionally greater impact on functional classes of neuron (like ipsilateral-related neurons) that have a more disbursed distribution in the FEF, because of differences in inter-hemispheric inhibition, or because of the properties of downstream circuits (e.g., in the basal ganglia). To further complicate matters, finer details of receptive field structures in the FEF continue to emerge (e.g., (Cavanaugh et al., 2012a)) making it even harder to predict the comparative changes in the FEF with progressively greater volumes of inactivation. An appreciation of the potential differences between focal and large volume inactivation is particularly relevant for experiments which aim to record in one structure while inactivating the other; in the oculomotor network in particular, the problem with aligning the recorded and inactivated response fields is largely avoided with large-volume inactivation. We are currently conducting such studies to directly investigate the impact of large-volume FEF inactivation on neuronal activity in the SC.

2.5: References

Aizawa H, Wurtz RH (1998) Reversible inactivation of monkey superior colliculus. I. Curvature of saccadic trajectory. J Neurophysiol 79:2082–2096.

Albano JE, Mishkin M, Westbrook LE, Wurtz RH (1982) Visuomotor deficits following ablation of monkey superior colliculus. J Neurophysiol 48:338–351.

Albano JE, Wurtz RH (1982) Deficits in eye position following ablation of monkey superior colliculus, pretectum, and posterior-medial thalamus. J Neurophysiol 48:318–337.

Ashmore RC, Sommer M a (2013) Delay activity of saccade-related neurons in the caudal dentate nucleus of the macaque cerebellum. J Neurophysiol 109:2129–2144.

Beckstead M, Edwards B, Beckstead RM, Edwards SB, Frankfurter A (1981) A comparison of the intranigral distribution of nigrotectal neurons labeled with horseradish peroxidase in the monkey, cat, and rat. J Neurosci 1:121–125.

Boulanger M, Bergeron A, Guitton D (2009) Ipsilateral head and centring eye movements evoked from monkey premotor cortex. Neuroreport 20:669–673.

Bruce CJ, Goldberg ME (1985) Primate frontal eye fields. I. Single neurons discharging before saccades. J Neurophysiol 53:603–635.

Bruce CJ, Goldberg ME, Bushnell MC, Stanton GB (1985) Primate frontal eye fields. II. Physiological and anatomical correlates of electrically evoked eye movements. J Neurophysiol 54:714–734.

Burman DD, Bruce CJ (1997) Suppression of task-related saccades by electrical stimulation in the primate's frontal eye field. J Neurophysiol 77:2252–2267.

Cavanaugh J, Joiner WM, Wurtz RH (2012a) Suppressive Surrounds of Receptive Fields In Monkey Frontal Eye Field. J Neurosci 32:12284–12293.

Cavanaugh J, Monosov IE, McAlonan K, Berman R, Smith MK, Cao V, Wang KH, Boyden ES, Wurtz RH (2012b) Optogenetic Inactivation Modifies Monkey Visuomotor Behavior. Neuron 76:901–907.

Chevalier G, Deniau JM, Thierry AM, Feger J (1981) The nigro-tectal pathway. An electrophysiological reinvestigation in the rat. Brain Res 213:253–263.

Cohen JY, Crowder EA, Heitz RP, Subraveti CR, Thompson KG, Woodman GF, Schall JD (2010) Cooperation and Competition among Frontal Eye Field Neurons during Visual Target Selection. J Neurosci 30:3227–3238.

Collin NG, Cowey A, Latto R, Marzi C (1982) The role of frontal eye-fields and superior colliculi in visual search and non-visual search in rhesus monkeys.

Behav Brain Res 4:177–193.

Crapse TB, Sommer MA (2009) Frontal eye field neurons with spatial representations predicted by their subcortical input. J Neurosci 29:5308–5318.

Dassonville P, Schlag J, Schlag-Rey M (1992) The frontal eye field provides the goal of saccadic eye movement. Exp Brain Res 89:300–310.

Deng SYY, Goldberg M. E, Segraves MAA, Ungerleider LGG, Mishkin M (1986) The effect of unilateral ablation of the frontal eye fields on saccadic performance in the monkey. In: Adaptive Processes in the Visual and Oculomotor Systems, pp 201–208. Elsevier.

Dias EC, Kiesau M, Segraves MA (1995) Acute activation and inactivation of macaque frontal eye field with GABA-related drugs. J Neurophysiol 74:2744–2748.

Dias EC, Segraves MA (1999) Muscimol-induced inactivation of monkey frontal eye field: effects on visually and memory-guided saccades. J Neurophysiol 81:2191–2214.

Elsley JK, Nagy B, Cushing SL, Corneil BD (2007) Widespread presaccadic recruitment of neck muscles by stimulation of the primate frontal eye fields. J Neurophysiol 98:1333–1354.

Fujii N, Mushiake H, Tanji J (1998) An oculomotor representation area within the ventral premotor cortex. Proc Natl Acad Sci U S A 95:12034–12037.

Fujii N, Mushiake H, Tanji J (2000) Rostrocaudal distinction of the dorsal premotor area based on oculomotor involvement. J Neurophysiol 83:1764–1769.

Funahashi S, Bruce CJ, Goldman-Rakic PS (1991) Neuronal Activity Related to Saccadic Eye Movements in the Monkey's Dorsolateral Prefrontal Cortex. J Neurophysiol 65:1464–1483.

Gaymard B, Ploner CJ, Rivaud-Péchoux S, Pierrot-Deseilligny C (1999) The frontal eye field is involved in spatial short-term memory but not in reflexive saccade inhibition. Exp Brain Res 129:288–301.

Gottlieb JP, MacAvoy MG, Bruce CJ (1994) Neural responses related to smooth-pursuit eye movements and their correspondence with electrically elicited smooth eye movements in the primate frontal eye field. J Neurophysiol 72:1634–1653.

Graybiel AM, Ragsdale CW (1978) Histochemically distinct compartments in the striatum of human, monkeys, and cat demonstrated by acetylthiocholinesterase staining. Proc Natl Acad Sci U S A 75:5723–5726.

Graziano MSA, Taylor CSR, Moore T (2002) Complex movements evoked by microstimulation of precentral cortex. Neuron 34:841–851.

Halsband U, Passingham R (1982) The role of premotor and parietal cortex in the direction of action. Brain Res 240:368–372.

Hanes DP, Patterson WF, Schall JD (1998) Role of frontal eye fields in countermanding saccades: visual, movement, and fixation activity. J Neurophysiol 79:817–834.

Hanes DP, Wurtz RH (2001) Interaction of the frontal eye field and superior colliculus for saccade generation. J Neurophysiol 85:804–815.

Hikosaka O, Wurtz R (1986) Saccadic eye movements following injection of lidocaine into the superior colliculus. Exp Brain Res 61:531–539.

Hikosaka O, Wurtz RH (1983) Effects on eye movements of a GABA agonist and antagonist injected into monkey superior colliculus. Brain Res 272:368–372.

Huerta MF, Krubitzer LA, Kaas JH (1986) Frontal eye field as defined by intracortical microstimulation in squirrel monkeys, owl monkeys, and macaque monkeys: I. Subcortical connections. J Comp Neurol 253:415–439.

Izawa Y, Suzuki H, Shinoda Y (2004a) Suppression of visually and memory-guided saccades induced by electrical stimulation of the monkey frontal eye field. I. Suppression of ipsilateral saccades. J Neurophysiol 92:2261–2273.

Izawa Y, Suzuki H, Shinoda Y (2004b) Suppression of visually and memory-guided saccades induced by electrical stimulation of the monkey frontal eye field. II. Suppression of bilateral saccades. J Neurophysiol 92:2261–2273.

Izawa Y, Suzuki H, Shinoda Y (2009) Response properties of fixation neurons and their location in the frontal eye field in the monkey. J Neurophysiol 102:2410–2422.

Jayaraman A, Batton RR, Carpenter MB (1977) Nigrotectal projections in the monkey: An autoradiographic study. Brain Res 135:147–152.

Jiang H, Stein BE, McHaffie JG (2003) Opposing basal ganglia processes shape midbrain visuomotor activity bilaterally. Nature 423:982–986.

Johnston K, Koval MJ, Lomber SG, Everling S (2014) Macaque Dorsolateral Prefrontal Cortex Does not Suppress Saccade-Related Activity in the Superior Colliculus. Cereb Cortex 24:1373–1388.

Koyama M, Hasegawa I, Osada T, Adachi Y, Nakahara K, Miyashita Y (2004) Functional magnetic resonance imaging of macaque monkeys performing visually guided saccade tasks: Comparison of cortical eye fields with humans. Neuron 41:795–807.

Künzle H, Akert K (1977) Efferent connections of cortical, area 8 (frontal eye field) in Macaca fascicularis. A reinvestigation using the autoradiographic technique. J Comp Neurol 173:147–164.

Latto R, Cowey A (1971) Visual field defects after frontal eye-field lesions in monkeys. Brain Res 30:1–24.

Lee KM, Ahn KH, Keller EL (2012) Saccade generation by the frontal eye fields in Rhesus monkeys is separable from visual detection and bottom-up attention shift. PLoS One 7.

Leichnetz GR, Spencer RF, Hardy SGP, Astruc J (1981) The prefrontal corticotectal projection in the monkey; An anterograde and retrograde horseradish peroxidase study. Neuroscience 6:1023–1041.

Leichnetz GR, Spencer RF, Smith DJ (1984) Cortical projections to nuclei adjacent to the oculomotor complex in the medial dien-mesencephalic tegmentum in the monkey. J Comp Neurol 228:359–387.

Liu P, Basso M a (2008) Substantia nigra stimulation influences monkey superior colliculus neuronal activity bilaterally. J Neurophysiol 100:1098–1112.

Lomber SG (1999) The advantages and limitations of permanent or reversible deactivation techniques in the assessment of neural function. J Neurosci Methods 86:109–117.

Lomber SG, Payne BR, Horel JA (1999) The cryoloop: An adaptable reversible cooling deactivation method for behavioral or electrophysiological assessment of neural function. J Neurosci Methods 86:179–194.

Lynch JC (1992) Saccade initiation and latency deficits after combined lesions of the frontal and posterior eye fields in monkeys. J Neurophysiol 68:1913–1916.

Lynch JC, Hoover JE, Strick PL (1994) Input to the primate frontal eye field from the substantia nigra, superior colliculus, and dentate nucleus demonstrated by transneuronal transport. Exp Brain Res 100:181–186.

May PJ, Hartwich-Young R, Nelson J, Sparks DL, Porter JD (1990) Cerebellotectal pathways in the macaque: Implications for collicular generation of saccades. Neuroscience 36:305–324.

Mays LE, Sparks DL (1980) Dissociation of visual and saccade-related responses in superior colliculus neurons. J Neurophysiol 43:207–232.

Moll L, Kuypers HG (1977) Premotor cortical ablations in monkeys: contralateral changes in visually guided reaching behavior. Science 198:317–319.

Moschovakis AK, Gregoriou GG, Ugolini G, Doldan M, Graf W, Guldin W, Hadjidimitrakis K, Savaki HE (2004) Oculomotor areas of the primate frontal lobes: a transneuronal transfer of rabies virus and [14C]-2-deoxyglucose functional imaging study. J Neurosci 24:5726–5740.

Munoz DP, Dorris MC, Paré M, Everling S (2000) On your mark, get set: brainstem circuitry underlying saccadic initiation. Can J Physiol Pharmacol 78:934–944.

Nassi JJ, Lomber SG, Born RT (2013) Corticocortical feedback contributes to surround suppression in V1 of the alert primate. J Neurosci 33:8504–8517.

Olfert E, Cross B, McWilliam A (1993) Guide to the care and use of experimental animals.

Pandya DN, Vignolo L a (1971) Intra- and interhemispheric projections of the precentral, premotor and arcuate areas in the rhesus monkey. Brain Res 26:217–233.

Peel TR, Lomber SG, Corneil BD (2010) Behavioural effects of unilateral cryogenic inactivation of primate frontal eye fields. In: Society for Neuroscience Abstracts, pp 779.17.

Peel TR, Lomber SG, Corneil BD (2012) The functional contribution of the frontal eye fields to activity in the intermediate superior colliculus. In: Society for Neuroscience Abstracts. New Orleans, LA.

Pierrot-Deseilligny C, Rivaud S, Gaymard B, Agid Y (1991) Cortical control of reflexive visually-guided saccades. Brain 114:1473–1485.

Ponce CR, Hunter JN, Pack CC, Lomber SG, Born RT (2011) Contributions of indirect pathways to visual response properties in macaque middle temporal area MT. J Neurosci 31:3894–3903.

Prevosto V, Graf W, Ugolini G (2010) Cerebellar inputs to intraparietal cortex areas LIP and MIP: Functional frameworks for adaptive control of eye movements, reaching, and arm/eye/head movement coordination. Cereb Cortex 20:214–228.

Purcell BA, Heitz RP, Cohen JY, Schall JD (2012) Response Variability of Frontal Eye Field Neurons Modulates with Sensory Input and Saccade Preparation but not Visual Search Salience. J Neurophysiol 7817:2737–2750.

Quaia C, Aizawa H, Optican LM, Wurtz RH (1998) Reversible inactivation of monkey superior colliculus. II. Maps of saccadic deficits. J Neurophysiol 79:2097–2110.

Rivaud S, Müri RM, Gaymard B, Vermersch a I, Pierrot-Deseilligny C (1994) Eye movement disorders after frontal eye field lesions in humans. Exp brain Res 102:110–120.

Rizzolatti G, Matelli M, Pavesi G (1983) Deficits in attention and movement following the removal of postarcuate (area 6) and prearcuate (area 8) cortex in macaque monkeys. Brain 106:655–673.

Schall JD (2002) The neural selection and control of saccades by the frontal eye field. Philos Trans R Soc Lond B Biol Sci 357:1073–1082.

Schieber MH (2000) Inactivation of the ventral premotor cortex biases the laterality of motoric choices. Exp Brain Res 130:497–507.

Schiller PH, Chou IH (1998) The effects of frontal eye field and dorsomedial frontal cortex lesions on visually guided eye movements. Nat Neurosci 1:248–253.

Schiller PH, True SD, Conway JL (1980) Deficits in eye movements following frontal eye-field and superior colliculus ablations. J Neurophysiol 44:1175–1189.

Schlag J, Dassonville P, Schlag-Rey M (1998) Interaction of the two frontal eye fields before saccade onset. J Neurophysiol 79:64–72.

Schmahmann JD, Pandya DN (1997) Anatomic organization of the basilar pontine projections from prefrontal cortices in rhesus monkey. J Neurosci 17:438–458.

Schnyder H, Reisine H, Hepp K, Henn V (1985) Frontal eye field projection to the paramedian pontine reticular formation traced with wheat germ agglutinin in the monkey. Brain Res 329:151–160.

Schwartz EL (1980) Computational anatomy and functional architecture of striate cortex: a spatial mapping approach to perceptual coding. Vision Res 20:645–669.

Segraves MA (1992) Activity of monkey frontal eye field neurons projecting to oculomotor regions of the pons. J Neurophysiol 68:1967–1985.

Segraves MA, Goldberg ME (1987) Functional properties of corticotectal neurons in the monkey's frontal eye field. J Neurophysiol 58:1387–1419.

Segraves MA, Park K (1993) The relationship of monkey frontal eye field activity to saccade dynamics. J Neurophysiol 69:1880–1889.

Seidemann E, Arieli A, Grinvald A, Slovin H (2002) Dynamics of depolarization and hyperpolarization in the frontal cortex and saccade goal. Science 295:862–865.

Shi D, Friedman HR, Bruce CJ (1998) Deficits in smooth-pursuit eye movements after muscimol inactivation within the primate's frontal eye field. J Neurophysiol 80:458–464.

Sommer MA, Tehovnik EJ (1997) Reversible inactivation of macaque frontal eye field. Exp brain Res 116:229–249.

Sommer MA, Wurtz RH (2000) Composition and topographic organization of signals sent from the frontal eye field to the superior colliculus. J Neurophysiol 83:1979–2001.

Sommer MA, Wurtz RH (2001) Frontal eye field sends delay activity related to movement, memory, and vision to the superior colliculus. J Neurophysiol 85:1673–1685.

Stanton GB, Goldberg ME, Bruce CJ (1988a) Frontal eye field efferents in the macaque monkey: II. Topography of terminal fields in midbrain and pons. J Comp Neurol 271:493–506.

Stanton GB, Goldberg ME, Bruce CJ (1988b) Frontal eye field efferents in the macaque monkey: I. Subcortical pathways and topography of striatal and

thalamic terminal fields. J Comp Neurol 271:473–492.

Tanaka M (2006) Inactivation of the central thalamus delays self-timed saccades. Nat Neurosci 9:20–22.

Tanaka M (2007) Cognitive signals in the primate motor thalamus predict saccade timing. J Neurosci 27:12109–12118.

Tanaka M, Fukushima K (1998) Neuronal responses related to smooth pursuit eye movements in the periarcuate cortical area of monkeys. J Neurophysiol 80:28–47.

van der Steen J, Russell IS, James GO (1986) Effects of unilateral frontal eye-field lesions on eye-head coordination in monkey. J Neurophysiol 55:696–714.

Weinrich M, Wise SP (1982) The premotor cortex of the monkey. J Neurosci 2:1329–1345.

Weinrich M, Wise SP, Mauritz KH (1984) A neurophysiological study of the premotor cortex in the rhesus monkey. Brain 107:385–414.

White JM, Sparks DL, Stanford TR (1994) Saccades to remembered target locations: An analysis of systematic and variable errors. Vision Res 34:79–92.

Wurtz RH, Goldberg ME (1972) Activity of superior colliculus in behaving monkey. IV. Effects of lesions on eye movements. J Neurophysiol 35:587–596.

Xiong G, Hiramatsu T, Nagao S (2002) Corticopontocerebellar pathway from the prearcuate region to hemispheric lobule VII of the cerebellum: an anterograde and retrograde tracing study in the monkey. Neurosci Lett 322:173–176.

Chapter 3

A causal role for the cortical frontal eye fields in microsaccade deployment

Tyler R. Peel[1,2], Ziad M. Hafed[3], Suryadeep Dash[1,4], Stephen G. Lomber[1,4,5], Brian D. Corneil[1,4-6]

[1]The Brain and Mind Institute, University of Western Ontario, London, ON, N6A 5B7, Canada

[2]Graduate Program in Neuroscience, University of Western Ontario, London, ON, N6A 3K7, Canada

[3]Physiology of Active Vision Laboratory, Werner Reichardt Centre for Integrative Neuroscience, Tuebingen University, Tuebingen, 72076, Germany

[4]Department of Physiology & Pharmacology, University of Western Ontario, London, ON, N6A 3K7, Canada

[5]Department of Psychology, University of Western Ontario, London, ON, N6A 3K7, Canada

[6]Robarts Research Institute, London, ON, N6A 5B7, Canada

Keywords: frontal eye fields, reversible inactivation, microsaccades, fixational eye movements

Peel T.R., Hafed Z.M., Dash S., Lomber S.G., and Corneil B.D. (2016) A causal role for the cortical frontal eye fields in microsaccade deployment. *PLoS Biol 14:775-786*.

3.1: Introduction

Microsaccades, which frequently occur during gaze fixation, translate retinal images by only a few photoreceptors. Despite their modest size, microsaccades strongly impact visual perception (Martinez-Conde et al., 2006; Rucci et al., 2007; Hafed et al., 2011, 2015; Hafed, 2013) and visually-guided behavior (Rolfs et al., 2006; Hafed and Krauzlis, 2010; Hermens et al., 2010). Indeed, visual responses in a number of brain structures are dynamically influenced by either the production or consequence of microsaccades, with responses being enhanced immediately before microsaccades (Chen et al., 2015), suppressed during or just after microsaccades (Leopold and Logothetis, 1998; Snodderly et al., 2001; Hafed and Krauzlis, 2010), and then subsequently enhanced (Bair and O'Keefe, 1998; Leopold and Logothetis, 1998; Martinez-Conde et al., 2000, 2002; Snodderly et al., 2001; Kagan et al., 2008). While some mechanisms underlying microsaccade generation have been elucidated in the superior colliculus (SC; (Hafed et al., 2009, 2013; Hafed, 2011; Goffart et al., 2012; Hafed and Krauzlis, 2012)), cerebellum (Arnstein et al., 2015), and brainstem saccadic burst generator (Van Gisbergen et al., 1981; Brien et al., 2009; Van Horn and Cullen, 2012), no study has addressed the involvement of any cortical area in microsaccade generation. This gap in knowledge is all the more surprising given the strategic deployment of microsaccades in tasks requiring high visual acuity (Ko et al., 2010; Poletti et al., 2013), the impacts of microsaccades on visuomotor processing noted above, and the interest in microsaccades as a potential

biomarker for visuospatial attention (Hafed and Clark, 2002; Engbert and Kliegl, 2003; Pastukhov and Braun, 2010; Corneil and Munoz, 2014; Tian et al., 2016).

Here, we directly examined the causal role of the frontal eye fields (FEF), a key cortical oculomotor structure that projects strongly to the SC (Stanton et al., 1988; Schall, 2002), in microsaccade generation. To address this, we reversibly inactivated large volumes of either the unilateral or bilateral FEF using cryoloops implanted in the arcuate sulcus, and examined the changes in microsaccade behavior, focusing primarily on how FEF inactivation alters the well-known evolution of microsaccades that occurs following peripheral stimulus onset (Hafed and Clark, 2002; Engbert and Kliegl, 2003; Valsecchi et al., 2007; Hafed and Ignashchenkova, 2013). Our results show that the role for the FEF in microsaccades is distinct from that for the SC, and that the FEF provides a plausible substrate for how microsaccades can be strategically deployed.

3.2: Results

3.2.1: Description of dataset

The FEF was reversibly inactivated using cryogenic techniques either unilaterally (3 monkeys) or bilaterally (2 of the 3 monkeys) while monkeys performed delayed visually- or memory-guided saccades (see **Materials and Methods**). These tasks required the monkeys to maintain fixation before and after

peripheral cues were presented, allowing us to study pre- and post-cue microsaccadic modulations during otherwise steady fixation. We analyzed 74,650 microsaccades from 44,225 trials across monkeys, sessions (*i.e.,* pre-, peri-, and post-cooling), and inactivation configurations (*i.e.,* left or right unilateral inactivation, and bilateral inactivation). In this paper, we present representative results from monkey DZ during unilateral inactivation of the left FEF (7,791 trials) or bilateral FEF inactivation (7,378 trials), and we also summarize results from all monkeys. To ensure that the effects of FEF inactivation were not due to satiation or other time-dependent factors, we combined pre- and post-cooling trials into the *FEF warm* condition and compared it to the *FEF cool* condition.

As expected, large-volume FEF inactivation impacted many aspects of (large) saccadic behavior. In a previous report (Peel et al., 2014), we described the effects of unilateral cryogenic FEF inactivation on immediate and delayed saccades to peripheral targets located 4˚ or more from the fixation point. Briefly, unilateral FEF inactivation increased reaction times for delayed visually- or memory-guided saccades in either direction, and decreased accuracy and peak velocity (*i.e.*, decreased the velocity-amplitude main sequence relationship) of contralesional but not ipsilesional saccades. These effects were replicated in the current study, and are consistent with the geometry and positioning of the cryogenic loops within the arcuate sulcus relative to FEF's topography (Bruce et

al., 1985; Peel et al., 2014). We also found that bilateral FEF inactivation exacerbated all effects, such that saccades in either direction were generated at increased reaction times with lower peak velocities and accuracy. Despite these effects, the monkeys continued to perform well, with error rates increasing by less than 10%. Having established this, we now turn to the specific effects of FEF inactivation on microsaccades.

3.2.2: FEF inactivation increased microsaccade amplitude and decreased microsaccade peak velocity

Across our sample, we found consistent alterations in microsaccade amplitude and peak velocity, regardless of whether the microsaccade was generated before or after peripheral cue onset in our tasks. **Fig 3-1A** shows the effects of unilateral FEF inactivation on ipsilesional and contralesional microsaccade amplitude for our representative dataset. When the FEF was not inactivated, microsaccades had relatively small amplitudes (median: 0.51˚) compared to the fixation window, which likely relates to the small size of our fixation cue (Thaler et al., 2013). During FEF inactivation, the amplitude distributions for both ipsi- and contralesional microsaccades were shifted towards larger amplitudes ($p < 0.0001$, Wilcoxon rank sum test), with greater shifts for contralesional (increased by 21%) versus ipsilesional (increased by 10%) microsaccades. Regardless of increases in microsaccade amplitude during FEF inactivation, the vast majority of microsaccades remained < 1.5°. Across our sample, contralesional microsaccade

amplitudes increased significantly in 4 of 5 configurations; ipsilesional microsaccade amplitude increased significantly in 2 of 5 configurations (**Fig 3-1B**). During bilateral FEF inactivation, the amplitudes of both leftward and rightward microsaccades also increased significantly (**Fig 3-1B**). Importantly, microsaccade amplitude increased regardless of whether microsaccades were generated before or after cue presentation (**Fig 3-1C**, and see **Fig 3-3** and **Materials and Methods** for definitions of pre-cue and rebound periods).

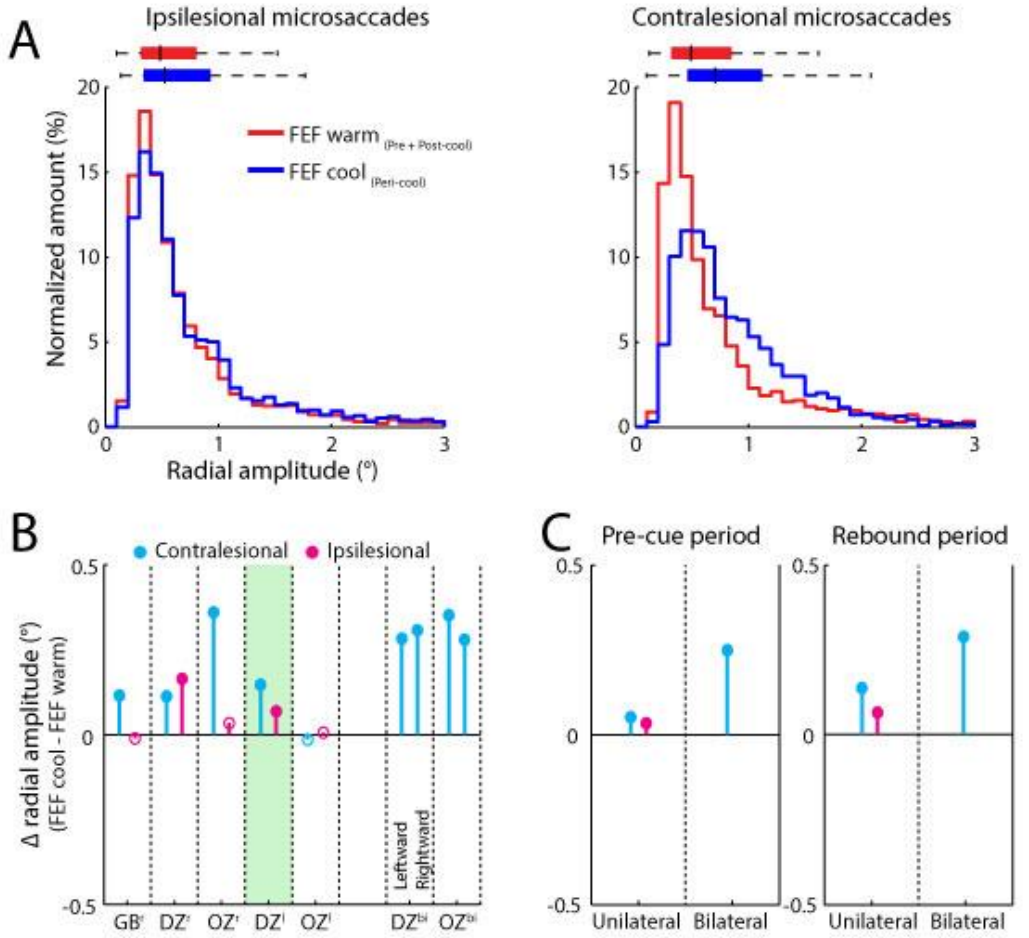

Figure 3-1. FEF inactivation increased ipsilesional and contralesional microsaccade amplitudes independently of peripheral cueing. (**A**) Unilateral (left) FEF inactivation shifted distributions towards larger amplitudes for each microsaccade direction from example monkey DZ, although we observed larger increases for contralesional microsaccades. Colored bars above the distributions indicate the median, and 25th and 75th percentiles with whiskers extending outwards to the 1st and 99th percentiles. (**B**) Microsaccade amplitudes increased for each monkey (GB, DZ, and OZ) and unilateral (X^{r} or X^{l}) or bilateral (X^{bi}) inactivation configurations, but unilateral FEF inactivation more consistently increased contralesional amplitudes. The shaded area in **B** indicates microsaccades from our example monkey. (**C**) Across monkeys, unilateral or bilateral FEF inactivation increased microsaccade amplitudes in both the pre-cue (left) and rebound (right) periods. Filled symbols in **B** and **C** indicate statistically significant differences using a Wilcoxon rank sum test ($p < 0.05$).

Could these increases in microsaccade amplitude be a simple consequence of a biased fixation position? We analyzed fixation position with and without FEF inactivation, and found that unilateral FEF inactivation biased fixation position by less than 1˚ towards the intact visual hemifield (**Fig 3-S1A**). However, this bias persisted before, during, and after cue presentation (**Fig 3-S1B,C**), meaning that any changes in microsaccade behavior due to FEF inactivation were not sufficient to correct for a biased fixation position. This observation is consistent with the idea that FEF inactivation introduces a new balance point for eye position, as observed during SC inactivations (Hafed et al., 2008; Goffart et al., 2012), rather than a mechanism that acts to correct for the biased fixation position since unilateral FEF inactivation also increased ipsilesional microsaccade amplitudes (**Fig 3-1**). Similarly, we observed increased microsaccade amplitudes in both directions during bilateral FEF inactivation (**Fig 3-1B,C**), despite a fixation position bias only toward one side (**Fig 3-S1C**).

More compelling evidence against a simple compensatory mechanism based on a bias in fixation position is provided by microsaccade peak velocity, which decreased independent of increased microsaccade amplitude or fixation offset. Such decreases in peak velocity are shown in the velocity-amplitude main sequence relationships in **Fig 3-2A** for both ipsilesional and contralesional microsaccades; note how both main sequence relationships are shifted downward during unilateral FEF inactivation. To determine the significance of

such changes, we fitted a linear regression to 5,000 bootstrapped samples of microsaccades for both the FEF warm and FEF cool conditions, and then extracted peak velocities from each relationship at amplitudes of 0.4 to 1.0˚ with 0.1˚ increments. We found significantly decreased peak velocities across this entire range of amplitudes for both ipsilesional and contralesional microsaccades (insets of **Fig 3-2A**, each $p < 0.01$, Welch's t-tests). **Fig 3-2B** shows how FEF inactivation alters the kinematic profiles of microsaccades matched for radial amplitudes (*e.g.,* between 0.40 and 0.45˚, see shaded region of **Fig 3-2A**), by lowering peak velocity and significantly increasing microsaccade duration (ipsilesional, $p < 0.05$; contralesional, $p < 0.0001$, Wilcoxon rank sum test). Such changes in kinematics and duration are consistent with FEF inactivation altering the drive to brainstem circuits generating microsaccades. To analyze any changes across our sample, we extracted peak velocities at 2˚, and found significant decreases of 9 and 23% for ipsilesional and contralesional microsaccades during FEF inactivation, respectively (**Fig 3-2C**, each $p < 0.0001$, Welch's t-tests). Unilateral FEF inactivation significantly decreased contralesional peak velocity in all 5 configurations, and significantly decreased ipsilesional peak velocity in 3 of 5 configurations (**Fig 3-2C**). Bilateral FEF inactivation significantly decreased peak velocity for both leftward and rightward microsaccades in both monkeys (**Fig 3-2C**). Once again, such bilateral decreases in microsaccade peak velocity occurred regardless of whether microsaccades were generated in the pre-cue or rebound

period (**Fig 3-2D**), and despite a unilateral bias in fixation position during bilateral inactivation (**Fig 3-S1C**).

Therefore, even prior to any task-related stimulus, FEF inactivation had a measurable impact on microsaccade metrics and kinematics, with such an impact often influencing even ipsilesional microsaccades. We next describe an even larger impact of FEF inactivation on the rate of cue-induced microsaccades.

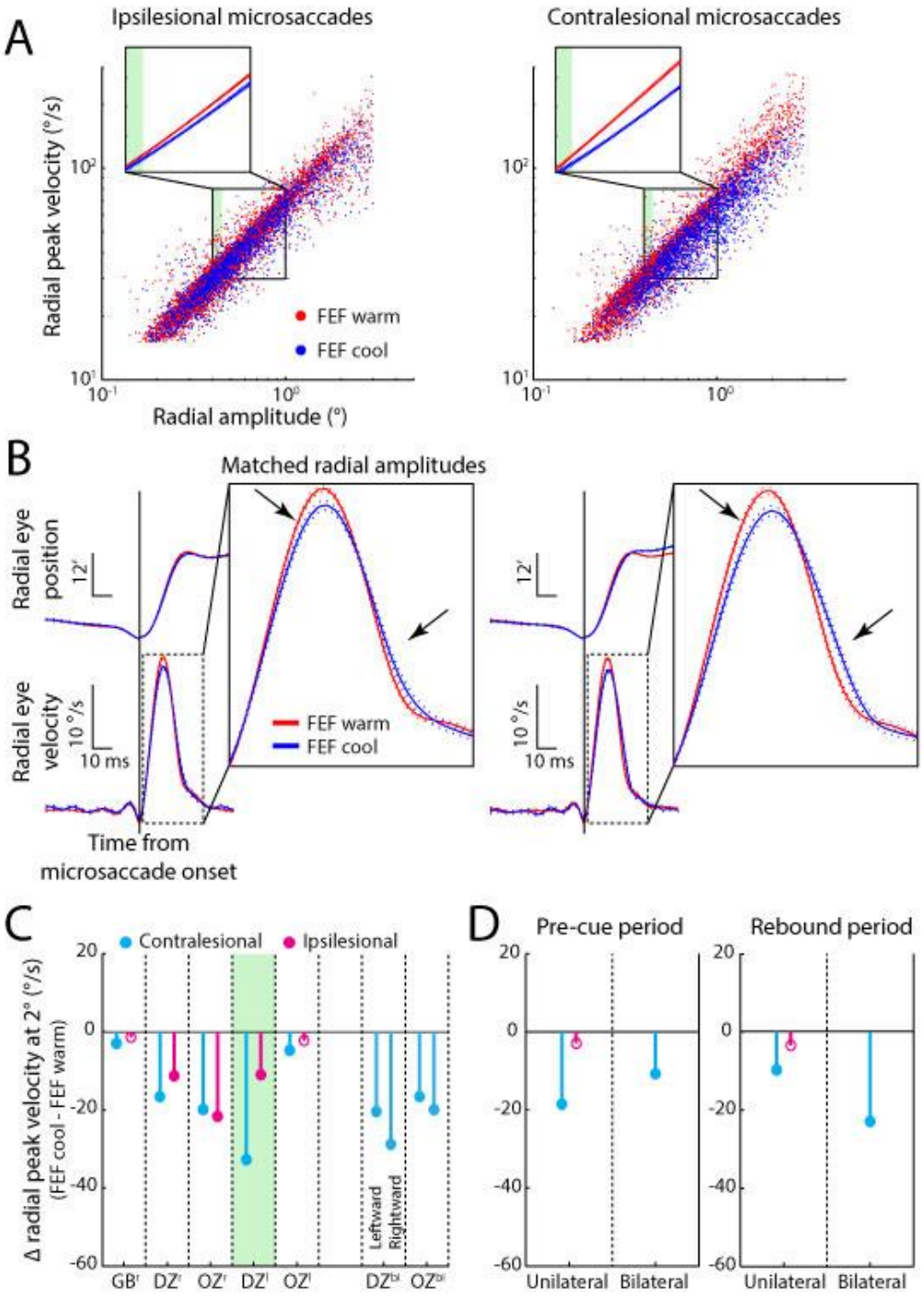

Figure 3-2. FEF inactivation decreased ipsilesional and contralesional microsaccade peak velocities, both before and after cue onset. (**A**) Unilateral (left) FEF inactivation reduced peak velocity for contralesional microsaccades independently of amplitude in our example monkey DZ, and also decreased peak

velocities for ipsilesional microsaccades. As shown in each inset, decreased peak velocities were associated with a downward shift in the main sequence relationship (+/- 95% confidence intervals). (**B**) FEF inactivation reduced peak velocity for microsaccades matched for radial amplitude, here shown for monkey DZ by averaging radial eye position and velocity traces (+/- standard error) aligned to microsaccade onset. As indicated by the shaded regions in **A**, we selected ipsilesional and contralesional microsaccades having radial amplitudes between 0.40 and 0.45˚. The bilateral influence of FEF inactivation on amplitude-matched microsaccades is demonstrated by decreased peak velocity and increasing duration within the enlarged radial velocity traces (see arrows). (**C**) Peak velocity extracted at 2˚ decreased for contralesional microsaccades across monkeys and inactivation configurations, and occasionally decreased for ipsilesional microsaccades. Distributions of peak velocities at 2˚ were obtained by bootstrapping 5,000 random samples of microsaccades, and extracting the peak velocity at 2˚ from each linear regression. (**D**) Across monkeys, unilateral and bilateral FEF inactivation produced similar decreases in contralesional peak velocity at 2˚ in both the pre-cue and rebound periods. Filled symbols in **C** and **D** indicate statistically significant differences using a Welch's t-test ($p < 0.05$) with 5,000 bootstrapped samples from each of the FEF warm and FEF cool conditions.

3.2.3: FEF inactivation blunted the rate of cue-induced microsaccades

Microsaccade rate shows robust and highly repeatable modulations after peripheral cue onsets, decreasing ~50 ms after cue onset and then rebounding before returning to baseline (Engbert and Kliegl, 2003; Hafed et al., 2011; Hafed and Ignashchenkova, 2013). To analyze the effects of FEF inactivation on microsaccade rate, we divided our data into three periods: pre-cue, microsaccadic inhibition, and rebound (**Fig 3-3**; see **Materials and Methods** for how these periods were defined; microsaccade rate was calculated within a sliding ±50 ms window with step size of 5 ms). As shown in our representative data, the influence of unilateral FEF inactivation was largely specific to the rebound period (**Fig 3-3A,B**): note how the rate of such *rebound microsaccades* decreased from 1.08 to 0.70 microsaccades/s with FEF inactivation, and then recovered to 0.87 microsaccades/s with FEF rewarming (both changes significant, $p < 0.0001$, Welch's t-test). In contrast, microsaccade rate in the pre-cue period decreased from 1.11 to 0.91 microsaccades/s ($p < 0.0001$) with FEF inactivation, and decreased further to 0.76 microsaccades/s ($p < 0.01$) when the FEF was rewarmed, suggesting that this effect may have been due to satiation with increasing trial count. Microsaccade rate during the inhibition period was unchanged. We also analyzed both the start and end of microsaccadic inhibition, and the timing of the first rebound microsaccade after cue presentation (see **Materials and Methods**). FEF inactivation had no influence on the start of

microsaccadic inhibition following cue onset (59 ms for both pre- and peri-cool), nor its end (152 versus 158 ms for FEF pre- versus peri-cool, $p = 0.74$, Wilcoxon rank sum test). In contrast, the timing of the first rebound microsaccades increased from 264 to 291 ms with FEF inactivation, and then recovered to 266 ms when the FEF was rewarmed (**Fig 3-S2A**, both $p < 0.0001$; Wilcoxon rank sum test).

For each of the three monkeys, unilateral FEF inactivation systematically decreased microsaccade rate during the rebound period (**Fig 3-3D**, significant in 4 of 5 configurations), but not the pre-cue period (**Fig 3-3C**). Bilateral FEF inactivation further reduced microsaccade rate during the rebound period (**Fig 3-3D**), but unlike unilateral inactivation, also significantly decreased microsaccade rate during the pre-cue period (**Fig 3-3C**). Thus, with bilateral inactivation, there was a generalized decrease in microsaccades. Across our sample, the decrease in microsaccade rate in the rebound period averaged 24% with unilateral inactivation, and 54% with bilateral inactivation. Consistent with a generally exacerbated effect of bilateral versus unilateral FEF inactivation, we also found a relatively greater increase in the timing of the first microsaccade in the rebound period during bilateral (44 ms) versus unilateral (7 ms; **Fig 3-S2B**). These results indicate that FEF integrity is critical for cue-induced microsaccades, and that larger bilateral inactivation volumes can further impact microsaccades generated before cue presentation. These effects on cue-induced microsaccade rate are

also categorically different from those reported during pharmacological inactivation of the SC, where cue-induced microsaccade rates remained unchanged (Hafed et al., 2013).

Because FEF inactivation also introduced a bias in fixation position, we wondered whether this could explain the changes in microsaccade rate during the rebound period. To investigate this, we repeated our analysis of microsaccade rate after performing a median split of FEF warm and FEF cool trials based on their radial fixation error in the pre-cue period (**Fig 3-4A**). This analysis exploits the substantial overlap in fixation positions with or without FEF inactivation (**Fig 3-S1A**), and in fact fixation error was significantly larger for the higher-than-median FEF warm trials than for the lower-than-median FEF cool trials (**Fig 3-4A,** fixation error for FEF $warm_{high}$ = 0.82˚; fixation error for FEF $cool_{low}$ = 0.53˚). As shown in **Fig 3-4B**, the robust decrease in rebound microsaccades during FEF inactivation persisted regardless of this split in fixation error. To quantify this across our sample, we calculated the change in rebound microsaccades from FEF $warm_{high}$ trials to FEF $cool_{low}$ trials. If the changes in rebound microsaccades during inactivation arose because of a greater fixation error, then we should observe no decrease in rebound microsaccades across these subsets of data, since fixation offset was greater in FEF $warm_{high}$ trials. However, as shown in **Fig 3-4C**, we still observed a profound decrease in

microsaccade rate during the rebound period with FEF inactivation. Therefore, the effects of **Fig 3-3** cannot be due to fixation error.

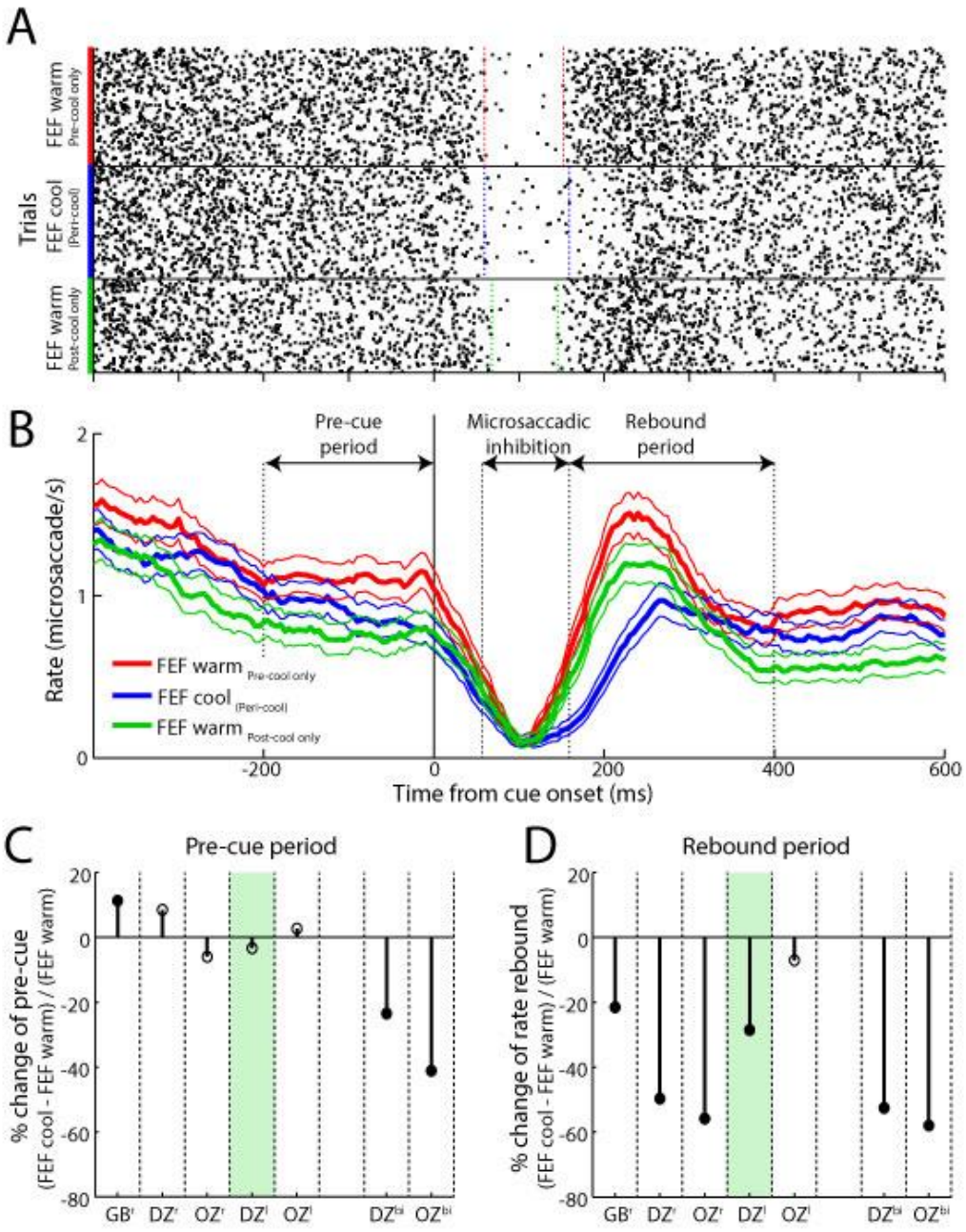

Figure 3-3. FEF inactivation markedly reduced microsaccades in the rebound period. (**A**) Microsaccade onset times relative to cue onset for individual pre-, peri-, and post-cooling trials from our example monkey with a unilateral (left) FEF inactivation. Each dot is a microsaccade onset time, and each row is a trial. (**B**) Corresponding time-courses of mean microsaccade rate (+/- 95% confidence intervals) for each of the pre-, peri-, and post-cooling sessions. In our example monkey unilateral FEF inactivation exerted its greatest impact on microsaccade rate during the rebound period (*i.e.,* 140-400 ms after cue onset) with no changes occurring in the pre-cue period (*i.e.,* 200 ms period before cue onset) nor the microsaccadic inhibition period (*i.e.,* 60-140 ms after cue onset). (**C**)

Across monkeys, we found consistent microsaccade rate decreases in the pre-cue period with bilateral, but not unilateral inactivation configurations. (**D**) In contrast, both unilateral and bilateral FEF inactivation consistently decreased microsaccade rate in the rebound period. Same format as **Fig 3-2C**.

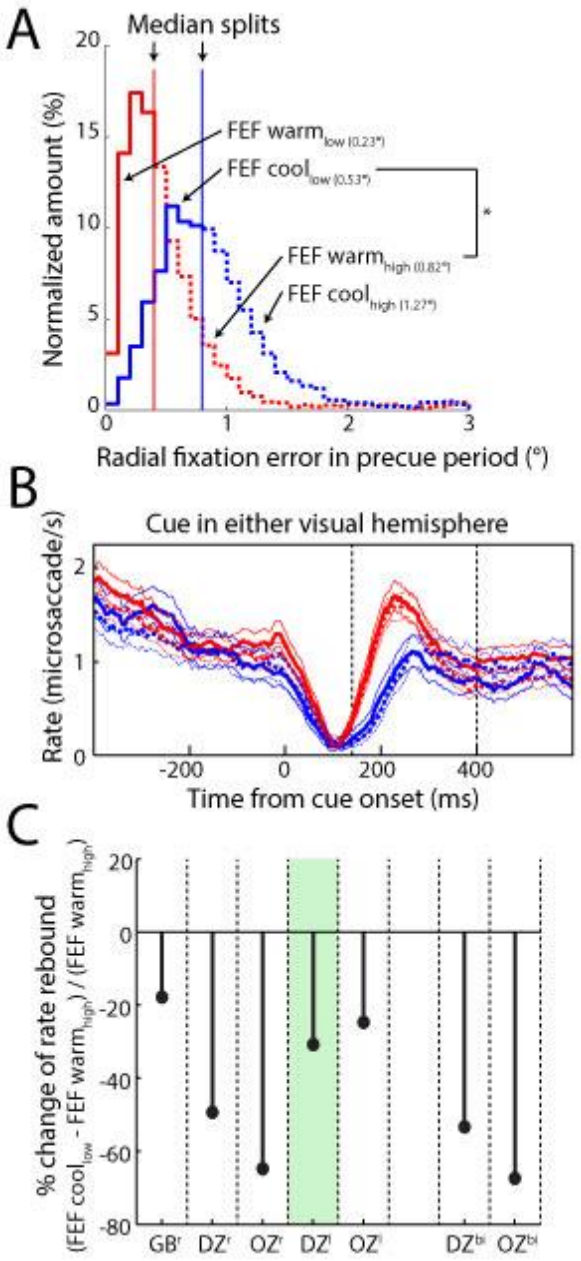

Figure 3-4. FEF inactivation decreased rebound microsaccades despite increases in fixation error. (**A**) Unilateral (left) FEF inactivation increased radial fixation error before cue onset in our example monkey DZ, largely due to shift in fixation position towards the intact side (see **Fig 3-S1**). (**B**) For this same monkey, FEF inactivation reduced microsaccade rate in the rebound period for both trials with high (higher-than- median values) and low (lower-than-median values) radial fixation error in the pre-cue period. Importantly, FEF inactivation reduced rebound microsaccades despite a significantly greater fixation error in FEF $warm_{high}$ (0.82˚) compared to the FEF $cool_{low}$ (0.53˚). (**C**) Across all monkeys and cooling configurations, FEF inactivation consistently reduced microsaccade rate

in the rebound period when comparing FEF $warm_{high}$ and FEF $cool_{low}$ trials. Same format as **Fig 3-2C**.

Finally, these analyses lead us to investigate whether FEF inactivation impacted eye position drift, and not just overall bias. Even though our eye tracker was not well suited to study drift at a higher resolution, to the extent that we could measure it, eye position drift before cue onset was not influenced by FEF inactivation (**Fig 3-S3**). FEF inactivation also did not influence dependencies between drift and microsaccades. Specifically, we analyzed the relationship between eye position drift and microsaccades, as previous work has shown that drift speed is lower before as compared to after a microsaccade (Chen and Hafed, 2013). However, we observed no systematic influence of FEF inactivation on this relationship (**Fig 3-S4**). Thus, we conclude that the effects shown in **Fig 3-3** on FEF inactivation on microsaccade rate could not be attributed to biases in fixation position or drift in the pre-cue period.

3.2.4: Unilateral FEF inactivation decreased microsaccade rate regardless of the side of the cue

Next, we investigated whether the effects of FEF inactivation on microsaccade rate only occurred when cues were presented contralateral to the side of inactivation. To our surprise, we found that unilateral FEF inactivation decreased microsaccade rate during the rebound period regardless of the side of the cue (**Fig 3-5A**, shown for our representative data during left FEF inactivation). Despite an idiosyncratically higher rate of rebound microsaccades for cues presented in the intact (left) hemifield even before inactivation, unilateral FEF

inactivation significantly reduced microsaccade rate during the rebound period for cues presented in both the intact (left; 41% decrease, $p < 0.001$, Welch's t-test) and affected (right; 12% decrease, $p < 0.05$) hemifield (see arrows). We observed such robust decreases in microsaccade rate during the rebound period during unilateral FEF inactivation across our sample, regardless of the side of the cue relative to the side of inactivation (**Fig 3-5C**). Such decreases were even greater during bilateral FEF inactivation (**Fig 3-5B**; both hemifields are presumably affected in this configuration; **Fig 3-5C**).

We also compared the influence of unilateral or bilateral FEF inactivation on microsaccade rate during the pre-cue and rebound periods (**Fig 3-5D**). This analysis again revealed that each cooling configuration robustly decreased the rate of microsaccades in the rebound period regardless of the side of the cue, but that only bilateral FEF inactivation decreased microsaccade rate before cue onset. Together with **Fig 3-3**, these results demonstrate the importance of FEF integrity when microsaccades are deployed, particularly after cue onset.

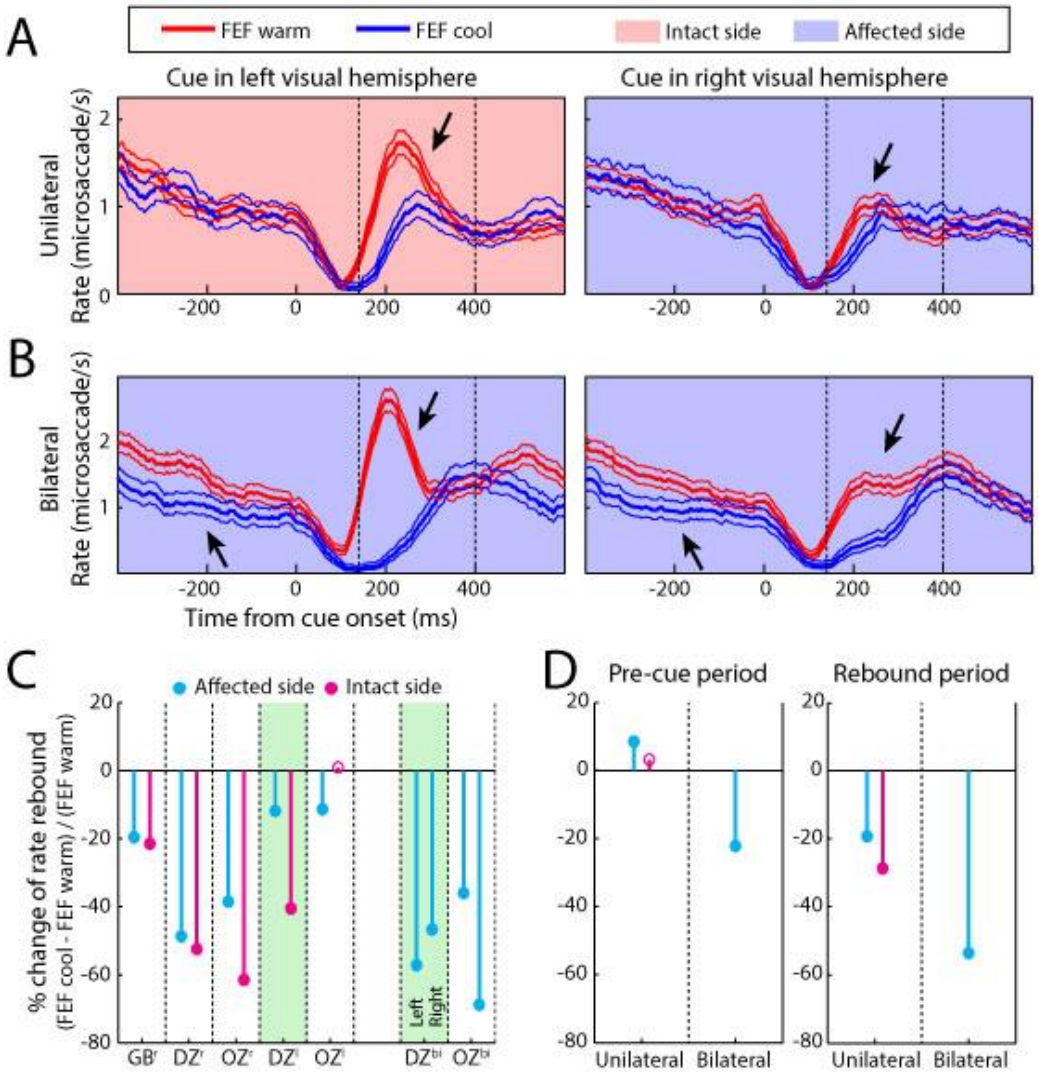

Figure 3-5. FEF inactivation decreased microsaccade rate in response to cues appearing in either visual hemifield. (**A**) Time-courses of mean microsaccade rate (+/- 95% confidence intervals) in response to cues either in the affected or intact visual hemifield for unilateral FEF warm and FEF cool conditions from our example monkey DZ. As indicated by arrows, unilateral (left) FEF inactivation decreased microsaccade rate in the rebound period for cues appearing in both the intact and affected visual hemifield. (**B**) Bilateral FEF inactivation produced similar, but quantitatively larger, decreases in microsaccade rate in response to cues in either affected visual hemifield from this same monkey (downward arrows). Bilateral FEF inactivation also decreased microsaccade rate in the pre-cue independent of subsequent cue location (upward arrows). (**C**) Microsaccade rate in the rebound period consistently decreased for both the intact and affected side across monkeys and inactivation configurations, with somewhat larger effects accompanying bilateral versus unilateral FEF inactivation. (**D**) Across monkeys only bilateral FEF inactivation decreased microsaccade rate in

the pre-cue period, and had a quantitatively larger impact on rate in the rebound period compared to unilateral FEF inactivation. Same format as **Fig 3-2C**.

3.2.5: FEF inactivation altered the directions of microsaccades

Cue presentation is known to briefly bias microsaccade direction toward and then away from the cue (Hafed and Clark, 2002; Engbert and Kliegl, 2003; Valsecchi et al., 2007; Hafed and Ignashchenkova, 2013); will FEF inactivation alter such directional modulations? Our monkeys exhibited strong idiosyncratic tendencies in microsaccade direction even before FEF inactivation, which complicates our interpretation. However, we still observed consistencies across our sample, especially when examining how FEF inactivation impacted the fraction of microsaccades towards the cue during the rebound period.

In general, unilateral FEF inactivation biased microsaccades towards the affected side, with this bias becoming more pronounced following contralesional cues. For example, before FEF inactivation, monkey DZ had a strong idiosyncratic tendency to make leftward microsaccades which was perturbed for ~400 ms after cue presentation (**Fig 3-6A**). Left FEF inactivation increased the tendency for rightward microsaccades even before cue onset (*i.e.,* the blue line lies above the red line for rightward cues, but below the red line for leftward cues), perhaps to correct for an altered fixation position. During the microsaccade rebound period, FEF inactivation exacerbated this effect only when cues were presented in the affected hemifield (arrow in **Fig 3-6A**). To quantify this effect, we measured how FEF inactivation altered the fraction of microsaccades towards cues in the rebound period, segregated by the side of the cue. This

fraction significantly increased from 40 to 62% during unilateral FEF inactivation for cues in the affected hemifield ($p < 0.0001$, Welch's t-test), but only increased from 6 to 11% for cues in the intact hemifield ($p = 0.08$). Across our sample, such an increase was seen in 3 of 5 unilateral configurations for cues in the affected hemifield, but never for cues presented in the intact hemifield (**Fig 3-6C**). Thus, FEF inactivation influenced microsaccade directionality after contralesional but not ipsilesional cues. Interestingly, this directional profile differs from how FEF inactivation influenced microsaccade rate for both contralesional and ipsilesional cues (**Figs 3-3** and **3-5**).

For bilateral FEF inactivation, pre-existing biases in microsaccade direction following cue onset were delayed and magnified. For example, in monkey DZ (**Fig 3-6B**), bilateral FEF inactivation did not alter the general idiosyncratic tendency of the monkey (*e.g.,* before or long after cue onset), but it instead prolonged and exaggerated the transient modulation of microsaccades after the cue. Quantitatively, the fraction of microsaccades towards the cue during the rebound period changed from 7 to 4% for leftward cues ($p = 0.08$, Welch's t-test) and from 45 to 7% for rightward cues ($p < 0.0001$, see arrow).

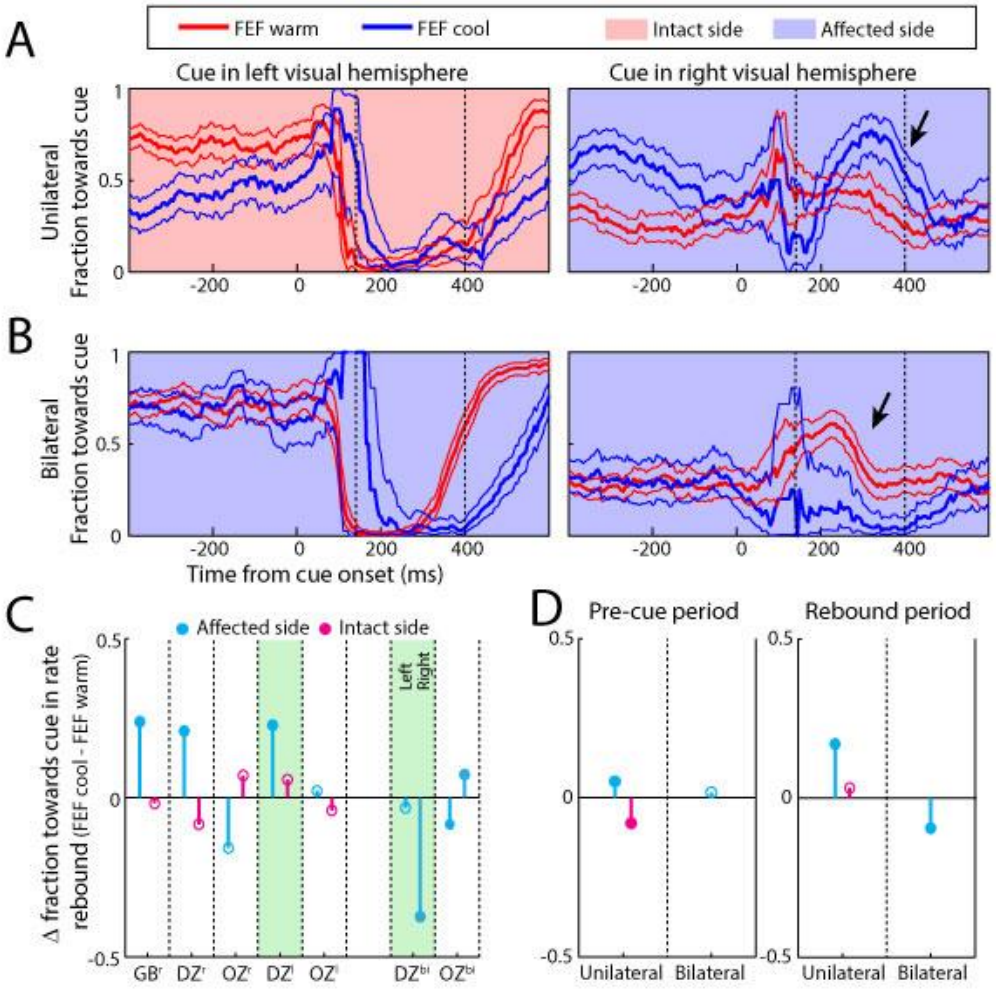

Figure 3-6. Unilateral FEF inactivation biased microsaccades towards the affected side, whereas bilateral FEF inactivation rescued this effect and delayed and magnified any pre-existing cue-induced directional modulations. (**A**) Time-courses of mean microsaccade directionality (*i.e.,* fraction towards cue +/- 95% confidence intervals) in response to cues either in the affected or intact visual hemifield for unilateral FEF warm and FEF cool conditions from our example monkey DZ. While unilateral FEF inactivation biased microsaccades towards the affected field before cue onset, a change in post-cue microsaccades only accompanied cues for the affected visual hemifield (see arrow). (**B**) Bilateral FEF inactivation did not bias microsaccades in the pre-cue period, but delayed and magnified the pre-existing directional biases in the microsaccadic inhibition and rebound periods (see arrow). (**C**) 3 of 5 unilateral FEF inactivation configurations had similar effects, whereas bilateral FEF inactivation in both monkeys produced no pre-cue directional bias, and a magnification of pre-existing biases in the rebound period. (**D**) A pre-cue bias towards the affected side was consistent across monkeys only with unilateral FEF inactivation, whereas unilateral and bilateral FEF inactivation impacted cue-induced

microsaccade directionality following cues in the affected side. Same format as **Fig 3-2C**.

Across our sample, unilateral FEF inactivation biased microsaccade directions towards the affected side even before cue onset (**Fig 3-6D**). This is again different from SC inactivation (Hafed et al., 2013), but it could be related to the altered fixation position. However, the bilateral inactivation data shows that altered fixation position does not produce directional biases in the pre-cue period. Interestingly, changes in microsaccade directionality after cue onset only occurred in the affected hemifield during unilateral inactivation (**Fig 3-6C**), but even these changes were not consistently seen in our sample. Taken together, all of our results emphasize that the main effect of FEF inactivation on microsaccade deployment is through modulations of rate, rather than microsaccade directionality. This profile differs completely from that seen following inactivation of the SC, which robustly and consistently altered microsaccade direction without influencing microsaccade rate (Hafed et al., 2013).

3.3: Discussion

3.3.1: Summary of results

Our study demonstrates a causal role for the FEF in microsaccade generation, particularly following cue onset. A number of our results are novel, given that this is the first study of any cortical area being involved in microsaccade production. First, unilateral FEF inactivation increased microsaccade amplitude

and decreased microsaccade peak velocity, particularly for contralesional microsaccades; this suggests a role for the FEF in contributing to brainstem signals during microsaccade generation, independent of peripheral cues. Second, unilateral FEF inactivation severely impaired cue-induced microsaccades for cues appearing in either hemifield; therefore, changes in microsaccade generation with unilateral FEF inactivation are not the result of impaired processing of a contralateral visual stimulus, but rather attest to the FEF's role in deploying microsaccades following any peripheral cue. Third, bilateral FEF inactivation exacerbated the effects of unilateral FEF inactivation, consistent with the FEF contributing to microsaccades generated towards either hemifield. In this discussion, we consider the implications of these results in the context of what is known about microsaccade generation and deployment, known properties of FEF activity, and the emerging view that microsaccades are an essential component of optimal sampling of a visual scene (Rucci et al., 2007; McCamy et al., 2014; Rucci and Victor, 2015).

3.3.2: Substrates for top-down control of microsaccades

Microsaccades can be strategically deployed in tasks requiring high visual acuity (Ko et al., 2010; Poletti et al., 2013), but the substrates responsible for such top-down influences on microsaccades are poorly understood. Previous studies have demonstrated a critical role for the SC in microsaccade generation and deployment (Hafed et al., 2009, 2013; Goffart et al., 2012). Frontal inputs into

the SC may enable cognitive processes to influence microsaccade behavior. The results of FEF inactivation, which preferentially impacted the rate of microsaccades following peripheral cue onset, are largely consistent with this idea. Further, the FEF has been implicated in covert visuospatial attention (Moore and Fallah, 2001; Wardak et al., 2006), and sends visual, cognitive, and saccade-related signals directly to the SC (Sommer and Wurtz, 2000). We are not suggesting that the FEF is the sole source of frontal input into the SC for microsaccade control, but it may well serve as an important interface between the SC and other prefrontal areas.

We were also intrigued by the differences in how FEF or SC inactivation impacted microsaccades generated after peripheral cue onset. Specifically, FEF inactivation decreased microsaccade rate without having an equally large impact on direction; in contrast, inactivation of the caudal SC (which represents peripheral cue locations) impacted microsaccade direction without influencing rate (Hafed et al., 2013). There are a number of potential, and not mutually exclusive, explanations for these comparative results. They may speak to a particularly important role for the FEF in intervals requiring top-down control of microsaccades, in this case providing signals related to when a microsaccade should be generated. Alternatively, our cryogenic inactivation of the FEF inactivated a much larger volume of tissue compared to the more focal pharmacological techniques used to inactivate the SC (see below). Such

differences in inactivation volume are likely even more important considering that the strength of topographic organization in the FEF tends to be less than that observed in the SC. FEF neurons tuned for small retinal errors, which are akin to those found in the rostral SC, tend to be diffusely distributed throughout the FEF and not just confined to the most lateral portion (Sommer and Wurtz, 2000; Izawa et al., 2009). Thus, methodological differences between inactivation techniques hinder the functional conclusions about the comparative role of each area in microsaccade behavior. Nevertheless, the impact of FEF inactivation on the microsaccade rate signature can help us better understand the underlying neural mechanisms.

3.3.3: Implications of our findings on the microsaccade rate signature

The microsaccade rate signature describes the well-known and highly-replicable inhibition and then rebound of microsaccade rate following presentation of any stimulus (Hafed and Clark, 2002; Engbert and Kliegl, 2003; Valsecchi et al., 2007; Rolfs et al., 2008; Hafed and Ignashchenkova, 2013). Despite the large volume of inactivated FEF tissue, unilateral inactivation delayed and blunted microsaccade production only during the rebound period (**Fig 3-3**), without affecting the baseline rate of microsaccades before cue onset, or the start of the microsaccadic inhibition period. Perhaps most surprisingly, such effects were observed regardless of the side of cue presentation. Hence, they cannot simply

be explained by impaired processing or neglect of a contralesional stimulus. The temporal specificity of FEF inactivation, impairing the rebound but not baseline nor inhibition periods, demonstrates that recovery of microsaccades after disruption by sensory transients requires frontal inputs, and hence is not simply a passive process. Consistent with this, the direction of microsaccades in the rebound period tends to be opposite to those preceding reflexive microsaccades directed towards the cue (Tian et al., 2016). Following the same logic, FEF inputs do not seem to be involved in the onset of microsaccade inhibition, as inhibition onset was not influenced by FEF inactivation. Based on our results, it appears that different portions of the microsaccade rate signature are attributable to different neural substrates (*e.g.,* non-frontal inputs to microsaccade inhibition, and frontal inputs to the rebound).

Interestingly, a role for frontal inputs in the first microsaccade after inhibition is consistent with recent models regarding microsaccade generation. In a model by Hafed and Ignaschenkova (Hafed and Ignashchenkova, 2013) that utilizes the framework of a recurring rise-to-threshold process, the process initiating the first microsaccade after inhibition has a faster rate of rise to threshold. Similarly, in a model by Engbert (Engbert et al., 2011; Engbert, 2012) that considers spatiotemporal dynamics of SC activity, the rebound from inhibition is associated with a change in threshold that integrates sensory and attentional inputs. While both of these models are agnostic as to the source of

signals that change microsaccade behavior in the rebound period, attributing either a faster rate of rise (in the Hafed and Ignaschenkova model) or attentional signals (in the Engbert model) to frontal sources is broadly consistent with the impact of FEF inactivation on the microsaccade rate signature. Note however that our reasoning regarding the impact of unilateral FEF inactivation on the Engbert model hinges on the assumption that a large unilateral inactivation can produce bilateral effects (see below). In support of our contention that frontal sources are involved in rebound microsaccades, simulations of the Hafed and Ignaschenkova model where we reduced the rate of rise related to the first microsaccade after inhibition produced results very similar to those produced by FEF inactivation (**Supplemental Information** and **Fig 3-S5**).

While we observed strong influences of FEF inactivation on microsaccade rate, we observed little systematic influence of FEF inactivation on microsaccade direction. This finding may be attributable to the idiosyncracies of our subjects, but perhaps more fundamentally, we only studied microsaccades during the performance of delayed-saccade tasks. The strongest evidence linking microsaccade direction to the allocation of visuospatial attention has come from tasks where covert attention needs to be allocated precisely to perform the task (Hafed and Clark, 2002; Engbert and Kliegl, 2003; Laubrock et al., 2005; Pastukhov and Braun, 2010; Hafed et al., 2011). Recent psychophysical results have demonstrated a dissociation between microsaccade rate and direction

effects in attention paradigms (Pastukhov and Braun, 2010), and experiments inactivating the SC have shown that rate and direction may not necessarily be affected by the same neural mechanism (Hafed et al., 2013). In light of these findings, it will be of considerable future interest to see the comparative effect of FEF inactivation on microsaccade rate and direction in other paradigms.

3.3.4: Unilateral FEF inactivation produces bilateral effects on microsaccades

The FEF has an important role in the generation of saccades and deployment of visuospatial attention into the contralateral visual hemifield (Moore and Fallah, 2001; Wardak et al., 2006), and the effects of FEF inactivation on contralesional microsaccades are consistent with the extension of this role for the FEF into the range of the smallest amplitude saccades. How then do we explain the impact of FEF inactivation on the peak velocity of ipsilesional microsaccades, and on microsaccades deployed after the onset of ipsilesional cues?

The response fields for neurons in the rostral SC can cover portions of both contralateral and ipsilateral fields (Hafed et al., 2009). If homologous FEF neurons tuned for small amplitudes also cover both hemifields, then inactivation of such neurons may contribute to the decreases in ipsilesional microsaccade peak velocity with unilateral FEF inactivation. Consistent with this, the lateral portion of one FEF, which preferentially represents small amplitude saccades,

also projects to the contralateral SC (Distel and Fries, 1982). A preferential projection from the lateral but not medial FEF to the contralateral SC may explain why unilateral FEF inactivation did not decrease the peak velocity of larger ipsilesional saccades (Peel et al., 2014).

Further, recent findings suggest a more nuanced role in how the FEF contributes to spatially-guided behavior. For example, while focal FEF inactivation increases or decreases the reaction times of contralesional or ipsilesional saccades respectively (Sommer and Tehovnik, 1997; Dias and Segraves, 1999; Wardak et al., 2006), larger volume temporary or permanent lesions of the FEF raise saccade reaction times bilaterally (Peel et al., 2014; Kunimatsu et al., 2015). In our previous work (Peel et al., 2014), we estimated that the volume inactivated via cooling is conservatively at least four times larger than that typically achieved using pharmacological modulations or optogenetics (Cavanaugh et al., 2012; Goffart et al., 2012; Hafed et al., 2013). In light of this large inactivation volume, we speculated (Peel et al., 2014) that bilateral reaction time increases may arise from differences in how the FEF commits to a saccadic decision via widespread disinhibition of the intact FEF, or to the presence of diffusely-distributed FEF neurons with ipsilateral response fields (Bruce and Goldberg, 1985) whose contribution is only revealed by large-volume inactivation. Similarly, inactivation of diffusely-distributed FEF neurons tuned to small retinal errors (Sommer and Wurtz, 2000; Izawa et al., 2009) may delay the

generation of microsaccades during the rebound period, regardless of the side of the cue (*e.g.,* **Fig 3-S4**), thereby delaying and blunting the rebound period.

3.3.5: Conclusions

The FEF has been implicated in the deployment of covert visuospatial attention via top-down signals to extrastriate visual cortex (Moore and Armstrong, 2003; Ekstrom et al., 2009; Gregoriou et al., 2009), and was recently shown to contribute to pupil dilation (Lehmann and Corneil, 2016). Our discovery of a role for the FEF in microsaccade deployment raises the interesting possibility that the FEF can also influence visual processing in still more ways, for example by strategically deploying microsaccades, or via pre-microsaccadic modulations that shape visual processing before the arrival of re-afferent visual input (Chen et al., 2015). Our findings set the stage for future experiments that distinguish how cognitive processes optimize visual processing via the preparation and generation of microsaccades, or by coordinating such microsaccades with other components of the orienting response (Corneil and Munoz, 2014).

3.4: Materials and Methods

3.4.1: Subjects and physiological procedures

Three male monkeys (*Macaca mulatta*, monkeys GB, DZ, and OZ weighing 11.1, 9.8, and 8.6 kg respectively) were used in these experiments. Only monkey GB

contributed data to our previous manuscript (Peel et al., 2014). All training, surgical, and experimental procedures conformed to the policies of the Canadian Council on Animal Care and National Institutes of Health on the care and use of laboratory animals, and were approved by the Animal Use Subcommittee of the University of Western Ontario Council on Animal Care. We monitored the monkeys' weights daily and their health was under the close supervision of the university veterinarians.

Each monkey underwent one surgery to enable reversible cryogenic inactivation of one or both frontal eye fields (FEF). Monkeys DZ and OZ were implanted with bilateral FEF cryoloops, whereas monkey GB was only implanted with unilateral FEF cryoloops in the right hemisphere. Our surgical procedures of implanting cryoloops in the arcuate sulcus have been previously described (Lomber et al., 1999; Peel et al., 2014). Briefly, we performed a small 2.25 cm^2 craniotomy at the stereotaxic coordinates of the arcuate sulcus spur, and implanted two customized, stainless steel cryoloops (each 8-5 mm in length, and extending 3 mm into the sulcus) into each arcuate sulcus, which allowed for the cooling of tissue adjacent to the superior and inferior arms of the arcuate sulcus. Cryoloop temperatures of 3˚C silence post-synaptic activity in tissue up to 1.5 mm away without influencing the propagation of action potentials in nearby axons (Lomber et al., 1999). For this manuscript, we only collected data using the cryoloop in the inferior arm of the arcuate sulcus, which provided an estimated

volume of inactivation of 90 mm^3 in the anterior bank of the arcuate sulcus. Cooling only the cryoloop in the inferior arm of the arcuate sulcus produced the expected triad of contralateral saccadic deficits (*i.e.,* decreases in peak velocity, accuracy, and increases in reaction time), which was approximately 70% of the total saccadic deficits observed from cooling both cryoloops (Peel et al., 2014).

3.4.2: Data collection

Head-restrained monkeys were placed in front of a rectilinear grid of 500+ red LEDs covering ±35˚ of the horizontal and vertical visual field. We conducted experiments in a dark, sound-attenuated room and recorded each monkey's eye position using a single, chair-mounted eye tracker (EyeLink II). The behavioral tasks were controlled by customized real-time LabView programs on a PXI controller (National Instruments) at a rate of 1 kHz.

A single experimental dataset consisted of a pre-, peri-, and post-cooling session with each session containing the same number of correct trials. The number of trials for a given dataset ranged from 180 to 480 correct trials depending upon the number of cue locations. Our experimental procedure for cryogenic inactivation of the FEF has been previously described (Peel et al., 2014). Briefly, following the completion of the pre-cooling session, chilled methanol was pumped through the lumen of the cryoloops, decreasing the cryoloop temperature. Once the cryoloop temperature was stable at 3˚C for at

least 3 minutes, we began the peri-cooling session. Upon finishing the peri-cooling session, we turned off the cooling pumps, which allowed the cryoloop temperature to rapidly return to normal. When the cryoloop temperature had reached 35˚C for at least 3 minutes, we started the post-cooling session. Since we simultaneously recorded neurons in the intermediate layers of the superior colliculus (iSC) with FEF inactivation, it was necessary to minimize the amount of time for transitions (*i.e.,* shorter than 3 minutes between pre- and peri-cooling and peri- and post-cooling sessions) to ensure continued isolation of an iSC neuron throughout the full dataset. However, cryoloop temperatures rapidly decreased or increased when the cooling pumps were turned on and off, respectively, and we still found similar effects on saccadic behavior with slightly reduced transition durations. The effects of FEF inactivation on neuronal activity within the iSC will be described in a future manuscript.

3.4.3: Behavioral tasks

Monkeys performed memory and visually-guided saccades towards peripheral cues after a delayed response period. Following a variable fixation period of 750 to 1000 ms where monkeys maintained fixation within a +/- 3˚ window of a central cue, a peripheral cue appeared in either visual hemifield. Monkeys were required to maintain fixation of the central cue, and delay their saccadic response until the central cue was extinguished. Note that despite the large fixation window in our experiments, our central cue was 0.63˚ in diameter,

explaining why most microsaccades were significantly smaller than 1˚ (**Fig 3-1A**). Peripheral cues were either extinguished either 150 or 250 ms after onset or remained on for the ensuing memory or visually-guided saccade, respectively. After a delayed response period of at least 750 ms, monkeys were rewarded with a liquid reward if they generated a saccade towards the location of the remembered or persistent peripheral cue within 1000 ms of the offset of the central cue. This response window allowed us to differentiate trials with increased saccade reaction times from neglect of the peripheral cue during FEF inactivation, although monkeys had very few saccade reaction times > 500 ms. When we were also recording iSC activity, the location of one peripheral cue coincided with the peak of the response field of an isolated iSC neuron; the other peripheral cue was placed in the diametrically opposite position. In this report, peripheral cues were always located within 45˚ radial angle relative to the horizontal meridian, and more than 5˚ in radial eccentricity from the central cue. Analysis of microsaccade rate and directionality in the 500 ms window surrounding cue onset revealed no differences depending on the location of the peripheral cue, or depending on whether the peripheral cue remained illuminated or not. Accordingly, we pooled all trials together, subdividing data based only on the side of the cue relative to the side of FEF inactivation.

3.4.4: Data analysis

Offline, we screened all trials for microsaccades in a customized graphics user interface made in MatLab (Mathworks) that automatically detected microsaccade onset and offset using velocity (10˚/s) and acceleration (600˚/s^2) criteria. We only accepted trials where the monkey maintained fixation of the central cue for the full delayed period, and removed any trial where we identified any blinks, or other aberrant changes in eye position or velocity (*e.g.,* due to fatigue or inattention). We verified the onset and offset marks for each microsaccade, and removed any microsaccades with amplitudes greater than 3˚, or severe curvatures in their trajectories (*i.e.,* ratio of maximal to final displacement greater than 2). To differentiate microsaccades from drift, we also removed any microsaccades with onset accelerations lower than 1000˚/s^2. We considered all microsaccades generated for each monkey actively fixating the central cue (*i.e.,* fixation and delayed response periods), regardless of whether they correctly looked to the location of the peripheral cue. Similar results were observed if we constrained our analysis only to successfully performed trials. While our amplitude limit of 3˚ is very liberal, we wanted to ensure that any reduction of microsaccade occurrence during FEF inactivation (see **Results**) was not due to a coinciding increase in microsaccade amplitude above an arbitrary limit. Despite this liberal definition of microsaccade amplitude, and despite the specifics of our task and fixation window size, for each monkey, we found that the distribution of microsaccade amplitudes (*e.g.,* median microsaccade

amplitude of 0.51˚ for our example monkey in the FEF warm condition, see **Fig 3-1A**) was in good agreement with previous studies in monkeys and humans (reviewed in (Martinez-Conde et al., 2009)). Perhaps most importantly, all of the results of FEF inactivation still held if we reduced our amplitude limit to 2˚.

We investigated the contribution of the FEF to multiple aspects of microsaccade behavior in this manuscript. *Microsaccade rate* was defined as the number of microsaccades within a sliding ±50 ms rectangular window (in steps of 5 ms) divided by the number of all acceptable trials. Based on observations across monkeys, we used fixed time windows to quantify the microsaccade rate for the pre-cue period (*i.e.,* 200 ms preceding cue onset), microsaccadic inhibition period (*i.e.,* 60-140 ms after cue onset), and rate rebound period (*i.e.,* 140-400 ms after cue onset; see **Fig 3-3B** for depiction of these periods). In order to investigate the timing of cue-induced microsaccades, we defined the *microsaccade response time*, as the mean latency of the first microsaccade generated following cue onset during the rate rebound period. We defined the *microsaccade amplitude* as the angular vectorial displacement from microsaccade onset to offset. The *microsaccade peak velocity* was defined as the maximal vectorial velocity during its movement. To characterize changes in peak velocity, we constructed velocity-amplitude main sequence relationships, and then extracted the *peak velocity for 2˚ microsaccades* from a fitted linear regression. We also investigated *microsaccade directionality* as the fraction of

microsaccades towards the cue (*i.e.,* sum of microsaccades towards the cue divided by the sum of microsaccades directed either toward or away from the cue); therefore microsaccade directionality was independent of rate. Microsaccades directed within ±45˚ of the cue or diametrically opposite location of the cue were classified as towards, or away from the cue, respectively. Finally, we also determined the specific timing of the microsaccade rate signature for each monkey. For this analysis, we first counted microsaccades across the full trial duration in ±50 ms bins, and then calculated a threshold number of microsaccades that corresponded to 20% of the mean number in the pre-cue period. We determined the start of microsaccadic inhibition and rebound periods by incrementing bins backwards and forwards from 100 ms after cue onset in 1 ms steps, respectively, to find the next bin that exceeded the threshold number.

To determine the time-course and statistics of microsaccade rate and directionality, we performed sliding window analyses where we calculated a given measure within a ±50 ms window, and incrementally shifted this window every 5 ms for the full trial duration. The 95% confidence intervals of the mean microsaccade rate and peak velocity at 2˚ were calculated using 5,000 bootstrapped samples of randomly selected trials with replacement, while for directionality we used a binomial probability function. For statistical comparisons of specific time periods and/or conditions between bootstrapped distributions,

we performed Welch's t-tests ($p < 0.05$). For all other microsaccade measures, we determined statistical significance using Wilcoxon rank sum tests ($p < 0.05$).

3.5: References

Arnstein D, Junker M, Smilgin A, Dicke PW, Thier P (2015) Microsaccade control signals in the cerebellum. J Neurosci 35:3403–3411.

Bair W, O'Keefe LP (1998) The influence of fixational eye movements on the response of neurons in area MT of the macaque. Vis Neurosci 15:779–786.

Brien DC, Corneil BD, Fecteau JH, Bell AH, Munoz DP (2009) The behavioral and neurophysiological modulation of microsaccades in monkeys. J Eye Mov Res 3:1–12.

Bruce CJ, Goldberg ME (1985) Primate frontal eye fields. I. Single neurons discharging before saccades. J Neurophysiol 53:603–635.

Bruce CJ, Goldberg ME, Bushnell MC, Stanton GB (1985) Primate frontal eye fields. II. Physiological and anatomical correlates of electrically evoked eye movements. J Neurophysiol 54:714–734.

Cavanaugh J, Monosov IE, McAlonan K, Berman R, Smith MK, Cao V, Wang KH, Boyden ES, Wurtz RH (2012) Optogenetic Inactivation Modifies Monkey Visuomotor Behavior. Neuron 76:901–907.

Chen C, Ignashchenkova A, Thier P, Hafed ZM (2015) Neuronal Response Gain Enhancement prior to Microsaccades. Curr Biol 25:2065–2074.

Chen CY, Hafed ZM (2013) Postmicrosaccadic enhancement of slow eye movements. Ann Intern Med 158:5375–5386.

Corneil BD, Munoz DP (2014) Overt responses during covert orienting. Neuron 82:1230–1243.

Dias EC, Segraves MA (1999) Muscimol-induced inactivation of monkey frontal eye field: effects on visually and memory-guided saccades. J Neurophysiol 81:2191–2214.

Distel H, Fries W (1982) Contralateral cortical projections to the superior colliculus in the macaque monkey. Exp brain Res 48:157–162.

Ekstrom LB, Roelfsema PR, Arsenault JT, Kolster H, Vanduffel W (2009) Modulation of the contrast response function by electrical microstimulation of the macaque frontal eye field. J Neurosci 29:10683–10694.

Engbert R (2012) Computational Modeling of Collicular Integration of Perceptual Responses and Attention in Microsaccades. J Neurosci 32:8035–8039.

Engbert R, Kliegl R (2003) Microsaccades uncover the orientation of covert attention. Vision Res 43:1035–1045.

Engbert R, Mergenthaler K, Sinn P, Pikovsky A (2011) An integrated model of fixational eye movements and microsaccades. Proc Natl Acad Sci 108:E765–E770.

Goffart L, Hafed ZM, Krauzlis RJ (2012) Visual Fixation as Equilibrium: Evidence from Superior Colliculus Inactivation. J Neurosci 32:10627–10636.

Gregoriou GG, Gotts SJ, Zhou H, Desimone R (2009) High-frequency, long-range

coupling between prefrontal and visual cortex during attention. Science (80-) 324:1207–1210.

Hafed ZM (2011) Mechanisms for generating and compensating for the smallest possible saccades. Eur J Neurosci 33:2101–2113.

Hafed ZM (2013) Alteration of Visual Perception prior to Microsaccades. Neuron 77:775–786.

Hafed ZM, Chen C, Tian X (2015) Vision, perception, and attention through the lens of microsaccades: mechanisms and implications. Front Syst Neurosci 9.

Hafed ZM, Clark JJ (2002) Microsaccades as an overt measure of covert attention shifts. Vision Res 42:2533–2545.

Hafed ZM, Goffart L, Krauzlis RJ (2008) Superior colliculus inactivation causes stable offsets in eye position during tracking. J Neurosci 28:8124–8137.

Hafed ZM, Goffart L, Krauzlis RJ (2009) A neural mechanism for microsaccade generation in the primate superior colliculus. Science 323:940–943.

Hafed ZM, Ignashchenkova A (2013) On the dissociation between microsaccade rate and direction after peripheral cues: microsaccadic inhibition revisited. J Neurosci 33:16220–16235.

Hafed ZM, Krauzlis RJ (2010) Microsaccadic suppression of visual bursts in the primate superior colliculus. J Neurosci 30:9542–9547.

Hafed ZM, Krauzlis RJ (2012) Similarity of superior colliculus involvement in microsaccade and saccade generation. J Neurophysiol 107:1904–1916.

Hafed ZM, Lovejoy LP, Krauzlis RJ (2011) Modulation of Microsaccades in Monkey during a Covert Visual Attention Task. J Neurosci 31:15219–15230.

Hafed ZM, Lovejoy LP, Krauzlis RJ (2013) Superior colliculus inactivation alters the relationship between covert visual attention and microsaccades. Eur J Neurosci 37:1169–1181.

Hermens F, Zanker JM, Walker R (2010) Microsaccades and preparatory set: A comparison between delayed and immediate, exogenous and endogenous pro- and anti-saccades. Exp Brain Res 201:489–498.

Izawa Y, Suzuki H, Shinoda Y (2009) Response properties of fixation neurons and their location in the frontal eye field in the monkey. J Neurophysiol 102:2410–2422.

Kagan I, Gur M, Snodderly DM (2008) Saccades and drifts differentially modulate neuronal activity in V1: effects of retinal image motion, position, and extraretinal influences. J Vis 8:19.1-25.

Ko H-K, Poletti M, Rucci M (2010) Microsaccades precisely relocate gaze in a high visual acuity task. Nat Neurosci 13:1549–1553.

Kunimatsu J, Miyamoto N, Ishikawa M, Shirato H, Tanaka M, J. K, N. M, M. I, H. S, M. T (2015) Application of radiosurgical techniques to produce a primate model of brain lesions. Front Syst Neurosci 9:67.

Laubrock J, Engbert R, Kliegl R (2005) Microsaccade dynamics during covert

attention. Vision Res 45:721–730.

Lehmann SJ, Corneil BD (2016) Transient Pupil Dilation after Subsaccadic Microstimulation of Primate Frontal Eye Fields. J Neurosci 36:3765–3776.

Leopold DA, Logothetis NK (1998) Microsaccades differentially modulate neural activity in the striate and extrastriate visual cortex. Exp Brain Res 123:341–345.

Lomber SG, Payne BR, Horel JA (1999) The cryoloop: An adaptable reversible cooling deactivation method for behavioral or electrophysiological assessment of neural function. J Neurosci Methods 86:179–194.

Martinez-Conde S, Macknik SL, Hubel DH (2000) Microsaccadic eye movements and firing of single cells in the striate cortex of macaque monkeys. Nat Neurosci 3:251–258.

Martinez-Conde S, Macknik SL, Hubel DH (2002) The function of bursts of spikes during visual fixation in the awake primate lateral geniculate nucleus and primary visual cortex. Proc Natl Acad Sci U S A 99:13920–13925.

Martinez-Conde S, Macknik SL, Troncoso XG, Dyar TA (2006) Microsaccades counteract visual fading during fixation. Neuron 49:297–305.

Martinez-Conde S, Macknik SL, Troncoso XG, Hubel DH (2009) Microsaccades: a neurophysiological analysis. Trends Neurosci 32:463–475.

McCamy MB, Otero-Millan J, Di Stasi LL, Macknik SL, Martinez-Conde S (2014) Highly informative natural scene regions increase microsaccade production during visual scanning. J Neurosci 34:2956–2966.

Moore T, Armstrong KM (2003) Selective gating of visual signals by microstimulation of frontal cortex. Nature 421:370–373.

Moore T, Fallah M (2001) Control of eye movements and spatial attention. Proc Natl Acad Sci USA 98:1273–1276.

Pastukhov A, Braun J (2010) Rare but precious: Microsaccades are highly informative about attentional allocation. Vision Res 50:1173–1184.

Peel TR, Johnston K, Lomber SG, Corneil BD (2014) Bilateral saccadic deficits following large and reversible inactivation of unilateral frontal eye field. J Neurophysiol 111:415–433.

Poletti M, Listorti C, Rucci M (2013) Microscopic eye movements compensate for nonhomogeneous vision within the fovea. Curr Biol 23:1691–1695.

Rolfs M, Kliegl R, Engbert R (2008) Toward a model of microsaccade generation: the case of microsaccadic inhibition. J Vis 8:5.1-23.

Rolfs M, Laubrock J, Kliegl R (2006) Shortening and prolongation of saccade latencies following microsaccades. Exp Brain Res 169:369–376.

Rucci M, Iovin R, Poletti M, Santini F (2007) Miniature eye movements enhance fine spatial detail. Nature 447:851–854.

Rucci M, Victor JD (2015) The unsteady eye: an information-processing stage, not a bug. Trends Neurosci 38:195–206.

Schall JD (2002) The neural selection and control of saccades by the frontal eye field. Philos Trans R Soc Lond B Biol Sci 357:1073–1082.

Snodderly DM, Kagan I, Gur M (2001) Selective activation of visual cortex neurons by fixational eye movements: implications for neural coding. Vis Neurosci 18:259–277.

Sommer MA, Tehovnik EJ (1997) Reversible inactivation of macaque frontal eye field. Exp brain Res 116:229–249.

Sommer MA, Wurtz RH (2000) Composition and topographic organization of signals sent from the frontal eye field to the superior colliculus. J Neurophysiol 83:1979–2001.

Stanton GB, Goldberg ME, Bruce CJ (1988) Frontal eye field efferents in the macaque monkey: II. Topography of terminal fields in midbrain and pons. J Comp Neurol 271:493–506.

Thaler L, Schütz AC, Goodale MA, Gegenfurtner KR (2013) What is the best fixation target? The effect of target shape on stability of fixational eye movements. Vision Res 76:31–42.

Tian X, Yoshida M, Hafed ZM (2016) A Microsaccadic Account of Attentional Capture and Inhibition of Return in Posner Cueing. Front Syst Neurosci 10:23.

Valsecchi M, Betta E, Turatto M (2007) Visual oddballs induce prolonged microsaccadic inhibition. Exp Brain Res 177:196–208.

Van Gisbergen JA, Robinson DA, Gielen S (1981) A quantitative analysis of generation of saccadic eye movements by burst neurons. J Neurophysiol 45:417–442.

Van Horn MR, Cullen KE (2012) Coding of Microsaccades in Three-Dimensional Space by Premotor Saccadic Neurons. J Neurosci 32:1974–1980.

Wardak C, Ibos G, Duhamel J-R, Olivier E (2006) Contribution of the monkey frontal eye field to covert visual attention. J Neurosci 26:4228–4235.

3.6: Supplemental Information

3.6.1 Simulating the effects of reducing top-down drive in a model of microsaccade deployment

To help interpret our results, we wondered whether an existing model of cue-induced microsaccade deployment by Hafed and Ignashchenkova (2013) could be modified to produce microsaccade rate results similar to what we observed during FEF inactivation. According to the model (Hafed and Ignashchenkova, 2013), cue onsets influence microsaccades in a manner similar to how sudden visual transients influence large saccades (Reingold and Stampe, 2002): resetting ongoing saccadic activity, which subsequently recovers to its normal behavior. Implied in this model is the idea that microsaccades immediately after cue onset are generated by a reflexive sensory mechanism, whereas the latter microsaccades in the rebound period are produced by top-down recovery from this cue-induced disruption. Moreover, these rebound microsaccades have a faster rate of rise to threshold, due to a 'facilitation factor', compared to other microsaccades. Given this framework, we tested whether reducing the top-down drive in the model, and hence slowing the rate of rise of rebound microsaccades, could reproduce the experimentally-observed effects of FEF inactivation on rebound microsaccades.

To simulate a reduced top-down drive, we created a unilateral inactivation model in which we scaled down the model's facilitation factor for rebound microsaccades (r_B in the normal model by a factor of 0.65). We predicted that this single parameter change would be sufficient to generate microsaccade rate modulations similar to our unilateral FEF inactivation experiments. This prediction is supported by **Fig 3-S5A**, in which we simulated the original model (red) and the unilateral inactivation model with reduced top-down drive (blue) for 4,000 trials each. As can be seen, the modified model captured the delay and reduction of rebound microsaccades that we observed experimentally during FEF inactivation (compare to **Fig 3-3B** and **Fig 3-5A**). Notably, this model does not introduce any directional biases, and it thus produced similar effects regardless of where the cue appeared. Therefore, a reduced top-down drive within the model's framework is consistent with the effects of FEF inactivation on rebound microsaccades.

Since we altered a single parameter that specifically affects rebound microsaccades, our unilateral inactivation model did not perturb microsaccade rate before cue onset, consistent with our experimental results. However, bilateral FEF inactivation decreased pre-cue microsaccade rate, thus we hypothesized that a general decrease in the overall FEF drive, presumably due to the larger cortical inactivation, could account for these discrepancies. We tested this in our bilateral inactivation model with the same modification that reduced

top-down drive as in the unilateral inactivation model, but we also scaled down the slope in the rise-to-threshold process for all microsaccades independent of when they occurred (*i.e.,* this slope reduction to 0.65 of the normal model influenced both pre-cue and rebound microsaccades). Critically, the bilateral inactivation model captured both the decrement in pre-cue microsaccade rate, and a further blunting of rebound microsaccade rate (**Fig 3-S5B**), similar to our experimental manipulations (compare to **Fig 3-5B**). Accordingly, our modified models with reduced top-down drive are conceptually compatible with the decreased rate of microsaccades during FEF inactivation, particularly after cue onset.

Hafed ZM, Ignashchenkova A (2013) On the dissociation between microsaccade rate and direction after peripheral cues: microsaccadic inhibition revisited. J Neurosci 33:16220–16235.

Reingold EM, Stampe DM (2002) Saccadic inhibition in voluntary and reflexive saccades. J Cogn Neurosci 14:371–388.

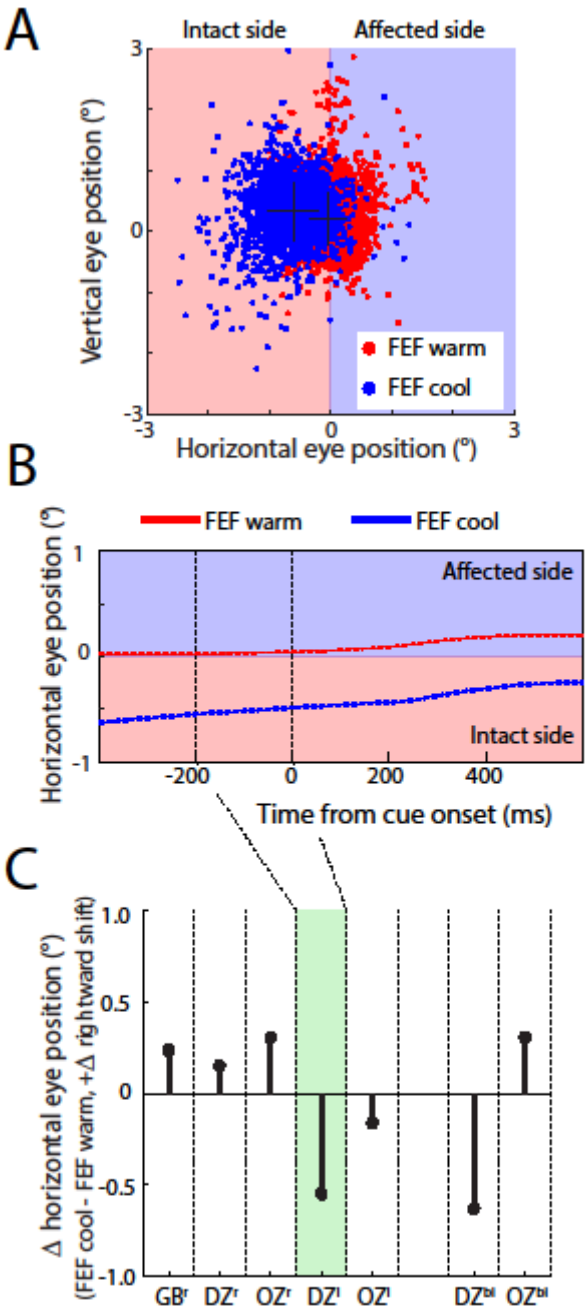

Figure 3-S1. FEF inactivation biased fixation position. (**A**) Unilateral FEF inactivation biased fixation position towards the intact side. Mean horizontal and vertical eye position in pre-cue-period for FEF warm and FEF cool trials from our example monkey DZ with a unilateral (left) FEF inactivation after removing any outliers (>3 standard deviation). Lines indicate the mean +/- standard deviation for each condition. (**B**) This bias in horizontal eye position toward the intact side (+/- standard error) during FEF inactivation was largely stable before and after cue onset. (**C**) Consistent horizontal biases towards the intact side occurred for each monkey (GB, DZ, and OZ) and unilateral (X^r or X^l) inactivation configuration,

whereas bilateral FEF inactivation (X^{bi}) consistently biased fixation positions to one affected side. All differences in position offset were statistically significant using a Wilcoxon rank sum test ($p < 0.05$).

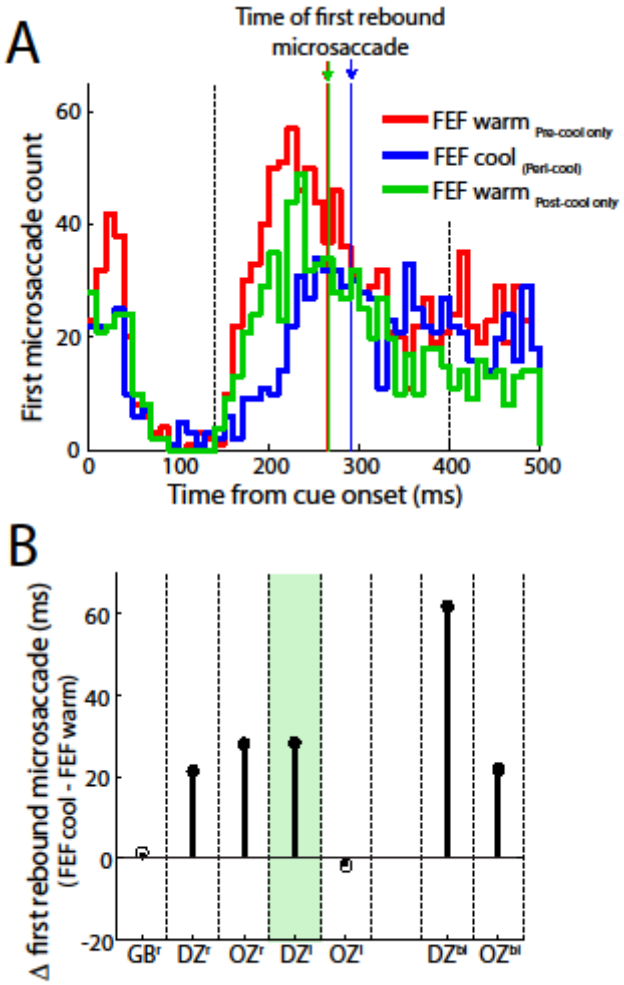

Figure 3-S2. FEF inactivation prolonged the onset of the first microsaccade in the rebound period. (**A**) Number of the first rebound microsaccades across pre-, peri-, and post-cooling trials from our example monkey DZ. FEF inactivation increased the response time for microsaccades specifically occurring within the rebound period. Vertical lines indicate the mean response time for rebound microsaccades. (**B**) Microsaccadic response time increased across monkeys in 3 of 5 unilateral inactivation configurations, whereas bilateral FEF inactivation produced a quantitatively larger and more consistent increase in microsaccadic response time. Same format as **Fig 3-S1C**.

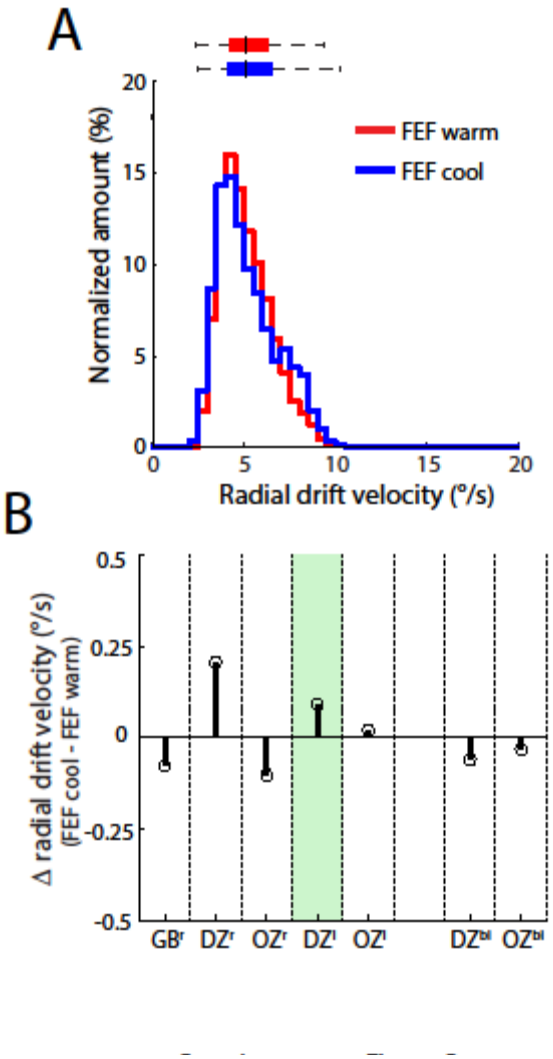

Figure 3-S3. FEF inactivation did not influence drift velocity before cue onset. (**A**) Unilateral (left) inactivation had no effect on radial drift velocity within the 750 ms before cue onset in our example monkey DZ. For this analysis, we calculated the mean radial velocity from each trial after removing any intervals with microsaccades (10 ms before to 10 ms after) and artifacts (radial velocity > 20˚/s). (**B**) Across monkeys, FEF inactivation did not significantly influence radial drift velocity with absolute differences always less than 0.25˚/s. Same format as **Fig 3-S1C**. Note that our eye tracker was not well suited to study drift at a higher resolution, thus it is possible that FEF inactivation caused effects on drift beyond the limits of our eye tracking technology.

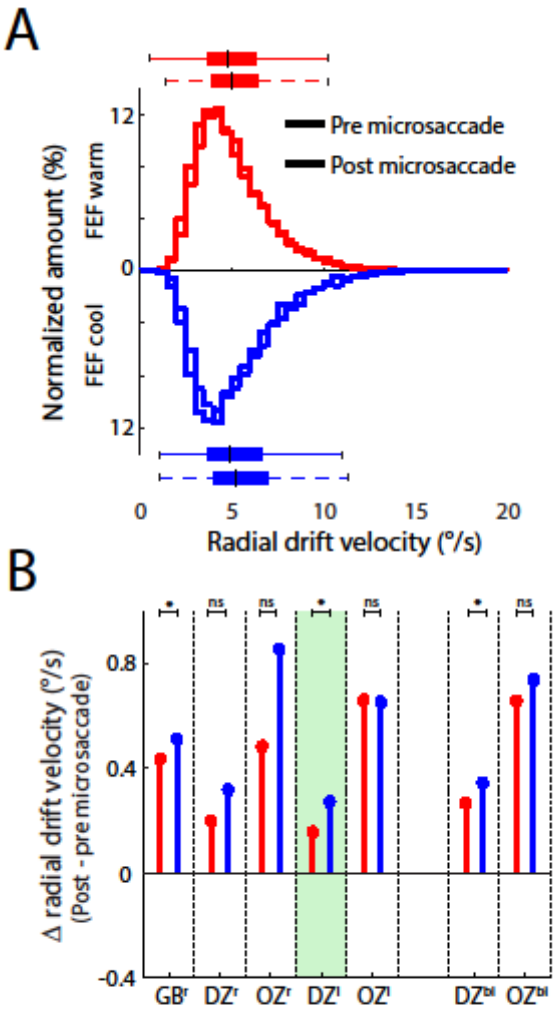

Figure 3-S4. FEF inactivation had no effect on the post-microsaccadic increase in drift velocity. (**A**) Radial drift velocity somewhat increased following microsaccades in our example monkey DZ, but FEF inactivation did not alter this relationship. Pre- and post-microsaccade radial drift velocity were calculated from 60 to 10 ms before microsaccade onset and 10 to 60 ms after microsaccade offset, respectively, although we first removed any time-points with artifacts (radial velocity > 20˚/s). (**B**) Across monkeys, we observed a similar post-microsaccadic increase of radial drift velocity for FEF warm trials. While FEF inactivation sometimes produced significant effects on the post-microsaccadic increases (indicated by asterisks above differences, Wilcoxon rank sum test, $p < 0.025$), such effects were either marginal (< 0.25˚/s) or not consistently observed across monkeys. Same format as **Fig 3-S1C**.

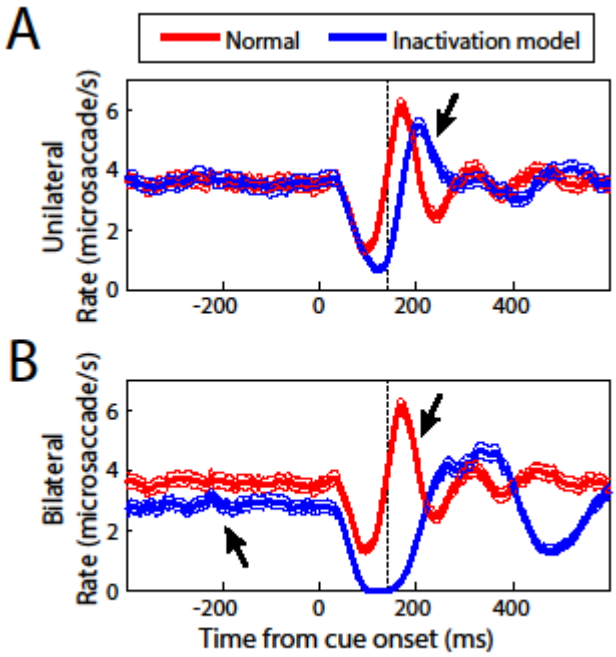

Figure 3-S5. Reducing the top-down drive in an existing model of cue-induced microsaccade deployment captures our experimentally observed effects on microsaccade rate. (**A** and **B**) Time-courses of mean microsaccade rate (+/- 95% confidence intervals) in response to cues for unilateral and bilateral inactivation simulations, respectively. Microsaccade rate is shown for the normal model (red) and with parameter changes to reflect reduced FEF drive (blue). Our unilateral inactivation model implemented only a simple reduction in the facilitation factor (*i.e.,* top-down drive) that is specific for rebound microsaccades, which delayed and reduced their occurrence after cue onset similar to our experimental results (see **Fig 3-5A**). The bilateral inactivation model additionally implemented a reduction in overall drive for all microsaccades, and simulated both a decrease in pre-cue microsaccade rate, and a further blunting of rate for rebound microsaccades comparable to the effects of bilateral FEF inactivation (see **Fig 3-5B**). Note that both models simulated identical results for cues in either visual hemi-field, and we used the same procedures to determine the time-course and statistics for our modeling data, except that we implemented a ±25 ms window instead, which more precisely represented our observed post-cue microsaccade modulations in FEF warm trials.

Chapter 4

Cortical Control of Saccade Initiation: Frontal Eye Field Inactivation Delays the Onset of Saccade-related Accumulation in the Superior Colliculus

Tyler R. Peel[1,5], Suryadeep Dash[1,2], Stephen G. Lomber[1,2,3], Brian D. Corneil[1,2,3,4]

[1]The Brain and Mind Institute, University of Western Ontario, London, ON, Canada
[2]Department of Physiology & Pharmacology, University of Western Ontario, London, ON, Canada
[3]Department of Psychology, University of Western Ontario, London, ON, Canada
[4]Robarts Research Institute, London, ON, Canada
[5]Graduate Program in Neuroscience, University of Western Ontario, London, ON, Canada

Keywords: frontal eye field, reversible inactivation, superior colliculus, saccade

In preparation for Cerebral Cortex.

4.1: Introduction

How does the brain commit to a voluntary action? The oculomotor system that moves our line of sight provides an ideal substrate to study this question, given what is known about the saccadic premotor circuits within the lower brainstem (for review, see Scudder et al., 2002; Sparks, 2002). The primate frontal eye fields (FEF) and intermediate layers of the superior colliculus (iSC) are two of the most studied structures within this system (Wurtz and Goldberg, 1972a, 1972b; Sparks et al., 1976; Sparks, 1978; Mays and Sparks, 1980; Schiller et al., 1980; Bruce and Goldberg, 1985; Bruce et al., 1985; Munoz and Wurtz, 1995; Wurtz et al., 2001), and while at least one of these structures needs to be intact for long-term recovery of saccadic behavior following ablations (Schiller et al., 1980), integrity of the iSC is required for saccades to be evoked from the FEF in the intact animal (Hanes and Wurtz, 2001). Despite this work, simple yet fundamental questions about the oculomotor system remain unresolved. For example, what happens in the iSC when FEF is suddenly abolished or compromised, and perhaps more importantly, how do changes in iSC activity relate to increases in saccadic reaction times (SRTs) that accompany FEF inactivation (Deng et al., 1986; Dias et al., 1995; Sommer and Tehovnik, 1997; Dias and Segraves, 1999; Peel et al., 2014, 2016)? The answers to such questions would provide considerable insight into how the oculomotor system commits to a saccade, but are surprisingly hard to predict for a variety of reasons.

First, these structures are highly interconnected, by virtue of monosynaptic corticotectal projections, and polysynaptic descending (e.g., through the basal ganglia, or other cortical structures), ascending (e.g., through the thalamus or pulvinar), and callosal pathways (Pandya and Vignolo, 1971; Leichnetz et al., 1981; Komatsu and Suzuki, 1985; Sommer and Wurtz, 2004a, 2004b; Berman et al., 2009; Crapse and Sommer, 2009). Both the FEF and iSC also project directly to the brainstem saccadic burst generator (Raybourn and Keller, 1977; Schnyder et al., 1985; Huerta et al., 1986; Sparks, 1986), and antidromically-identified FEF neurons projecting to either the iSC (Segraves and Goldberg, 1987; Everling and Munoz, 2000; Sommer and Wurtz, 2000; Helminski and Segraves, 2003) or brainstem burst generator (Segraves, 1992) convey a diverse set of visual-, fixation-, delay-, and saccade-related signals. Finally, antidromically-identified neurons from other parietal, prefrontal and sub-cortical sources also relay signals spanning the sensorimotor continuum to the iSC (Hikosaka and Wurtz, 1983a; Paré and Wurtz, 2001; Johnston and Everling, 2006). Thus, oculomotor circuits above the level of the brainstem burst generator have a parallel nature, both in terms of anatomy and functional content of signals relayed between areas.

Second, it is also not clear how iSC activity would relate to increases in SRT. Until recently, it was largely believed that saccades occurred when FEF and/or iSC activity increased above a fixed threshold, so that increases in SRT or

decision-related variables arose primarily due to decreases in the rate at which activity accumulated and/or the baseline level of activity (Hanes and Schall, 1996; Basso and Wurtz, 1997; Dorris et al., 1997; Hanes et al., 1998; Horwitz and Newsome, 1999; Kim and Shadlen, 1999; Paré and Hanes, 2003; Stanford et al., 2010). These results largely conformed to the predictions of stochastic accumulator models for saccade initiation (Carpenter and Williams, 1995; Reddi and Carpenter, 2000; Mazurek et al., 2003; Ratcliff and Smith, 2004; Lo and Wang, 2006; Ratcliff and McKoon, 2008; Carpenter et al., 2009). However new evidence suggests that saccade threshold may not be fixed (Jantz et al., 2013) and can paradoxically decrease for longer SRTs (Heitz and Schall, 2012). Other parameters such as the onset of accumulation (Pouget et al., 2011), the speed of perceptual evaluation (Shankar et al., 2011; Costello et al., 2013), or the time period of integration (Heitz and Schall, 2012) can also impact when the oculomotor system commits to a saccade. These results, as well as other results during inactivation of oculomotor structures that differed from the expectations of ideas regarding oculomotor function (Zénon and Krauzlis, 2012; Johnston et al., 2014; Katz et al., 2016), reinforce the need to record neural activity in order to understand why SRT increases during FEF inactivation.

Here, we recorded activity from either the ipsi- or contra-lesional iSC before, during, and after large-volume unilateral FEF inactivation, while monkeys performed delayed visually- or memory-guided saccades. Consistent with a

generalized loss of one source of excitatory input, FEF inactivation diminished all aspects of ipsilesional iSC activity. Large-volume unilateral inactivation also increased SRTs for contraversive and often for ipsiversive saccades (Peel et al., 2014; Kunimatsu et al., 2015). To link such SRT increases to SCi activity, we first matched saccades made with and without FEF inactivation for metrics and peak velocity. Such matching is critical important to avoid confounds related to the generation of a different saccade, or differing degrees of saccade-related drive onto the brainstem burst generator (Yoshida et al., 1999). We then examined how changes in parameters extracted from iSC activity (e.g., baseline activity, onset and rate of accumulation, and saccade threshold) related to accompanying increases in SRT. Remarkably, we found that SRT increases during unilateral FEF inactivation were best explained by delays in the onset of accumulation of SCi saccade-related activity.

4.2: Methods

4.2.1: Subjects and physiological procedures

Four male monkeys (*Macaca mulatta*, monkeys M, G, D, and O weighing 8.7, 11.1, 9.8, and 8.6 kg respectively) were used in these experiments. All training, surgical, and experimental procedures conformed to the policies of the Canadian Council on Animal Care and National Institutes of Health on the care and use of laboratory animals, and were approved by the Animal Use Subcommittee of the University of Western Ontario Council on Animal Care. We

monitored the monkeys' weights daily and their health was under the close supervision of the university veterinarians.

Each monkey underwent two surgeries that allowed us to both reversibly inactivate large portions of the FEF and record extracellular activity from the iSC. In the first surgery, we implanted either unilateral (right side only; monkeys M and G) or bilateral cryoloops into the arcuate sulcus using surgical procedures previously described (Lomber et al., 1999; Peel et al., 2014). Briefly, we performed a small 2.25 cm^2 craniotomy above the spur of the arcuate sulcus, and implanted two customized, stainless steel cryoloops (each 5-8 mm in length, and 3 mm in depth) into the arcuate sulcus (**Fig. 4-1A**), which allowed for the cooling of tissue adjacent to the superior and inferior arms of the arcuate sulcus. Cryoloop temperatures of 3˚C silence post-synaptic activity in tissue up to 1.5 mm away without influencing axonal propagation of action potentials (Lomber et al., 1999). Thermal surface imaging of the exposed tissue revealed that pumping chilled methanol through the lumen of the cryoloops decreased temperatures only in the vicinity of the arcuate sulcus, and did not spread to adjacent gyri. In the second surgery, we anchored a recording chamber (Crist Instruments) within the acrylic implant to access the SC bilaterally. For this procedure, we placed the chamber stereotactically over a 19 mm midline craniotomy that allowed for a surface normal approach (38˚ posterior of vertical) to the SC (Rezvani and Corneil, 2008).

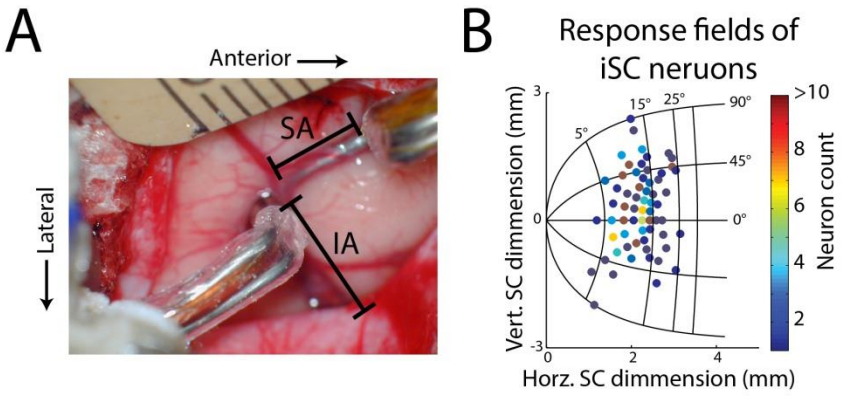

V = 44, VM = 63, M = 94, Tonic = 20, Other = 18, Total = 239

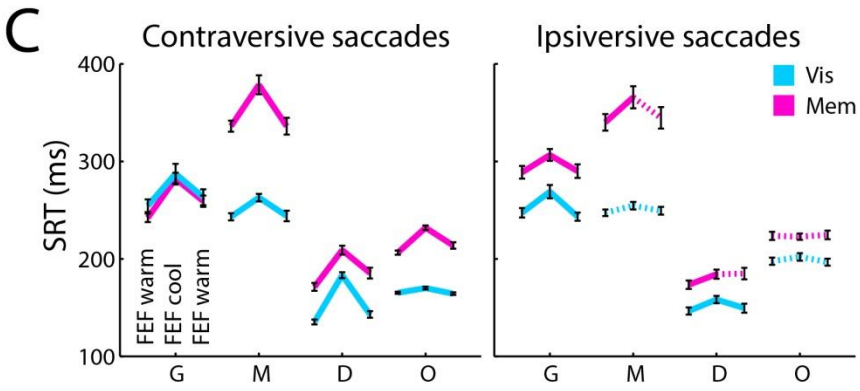

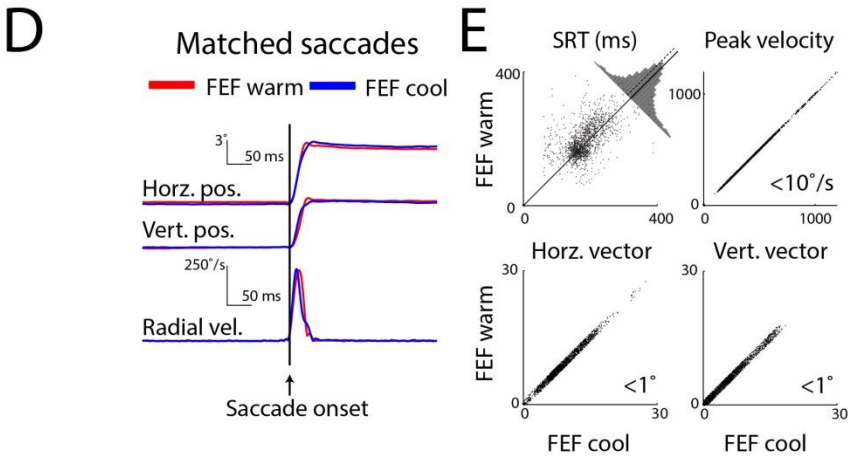

Figure 4-1. Description of methods. (A) Insertion of cryoloops into the arcuate sulcus. (B) Estimate of recording positions in the superior colliculus based on the central location of a neuron's response field. (C) FEF inactivation increased contraversive SRT for each monkey (*i.e.,* G, M, D, O), and occasionally also for ipsiversive saccades. For each direction and monkey, the mean visually- and memory-guided SRT (+/- standard error) is indicated for each of the pre-, peri-, and post-cooling sessions. Solid lines indicate significant differences by a Wilcoxon sign-rank test ($p < 0.05$). (D) Example of two matched saccades, one from each of the FEF warm and FEF cool conditions, having similar eye position and velocity traces. (E) Across all 2,145 matched saccades having horizontal and vertical displacements within 1˚, and peak velocities within 10˚/s, FEF inactivation still increased SRT.

4.2.2: Experimental procedures

Head-restrained monkeys were placed in front of a rectilinear grid of 500+ red LEDs covering ± 35˚ of the horizontal and vertical visual field. We conducted experiments in a dark, sound-attenuated room and sampled each monkey's eye position using a single, chair-mounted eye tracker at 500 Hz (EyeLink II). The behavioural tasks (see below) were controlled by customized real-time LabView programs on a PXI controller (National Instruments) at a rate of 1 kHz.

In this manuscript we only performed unilateral FEF inactivation, and on separate days inactivated either the right FEF in monkeys M, G, and D, or the left FEF in monkeys D, and O. Moreover, we only cooled the cryoloop in the inferior arm of the arcuate sulcus, which provided an estimated volume of inactivation of 90 mm^3 in the anterior bank of the arcuate sulcus. Our previous report showed that cooling only the cryoloop in the inferior arm of the arcuate sulcus resulted in a triad of contraversive saccade deficits (*i.e.,* decreases in peak velocity, accuracy, and increases in reaction time), with the magnitude of such deficits being ~70% of that observed when cooling both cryoloops (Peel et al., 2014).

Neuronal activity was recorded using tungsten microelectrodes (0.5 - 3.0 MΩ; FHC) on a MAP data acquisition system (Plexon). We lowered microelectrodes through 23 gauge guide tubes anchored in a Delrin grid (Crist

Instruments) using a motorized microdrive (NAN Instruments). For each monkey, guide tube lengths were customized to allow for a ~3 mm approach to the SC. Action potential waveforms that surpassed a user-defined threshold were amplified, low-cut filtered, sorted, and stored at 40 kHz. All neurons were recorded > 1 mm below the surface of the SC, where electrical stimulation (300 Hz, 100 ms, biphasic cathodal-first pulses with each phase 0.3 ms in duration) evoked saccades with currents < 50 μA; thus the majority of our recorded neurons were likely contained within the intermediate layers of the SC. We subsequently confirmed the isolation of single-unit neurons offline throughout cooling using both sorted and unsorted action potential waveforms, and ensured that the functional definition of a given neuron was maintained before and after FEF inactivation whenever possible.

Upon isolating an iSC neuron, we mapped its response field for visual cues presented at or saccades made to an array of cue locations. Across the 239 isolated neurons in our sample, response field centers were associated with visual cues presented at a mean visual eccentricity of 11.6 ± 4.7˚ (range: 4 to 25˚) and an angle relative to the horizontal axis of 12.8 ± 30.5˚ (range: -90 to 90˚) (**Fig. 4-1B**); thus, our recordings were confined to regions of the iSC encoding saccades >4˚. After identifying a neuron's response field, we attempted to collect a dataset consisting of a pre-, peri-, and post-cooling session (60 correct trials each), which required maintaining isolation for ~20 minutes. Our experimental

procedure for cryogenic inactivation of the FEF has been previously described (Peel et al., 2014), although in order to facilitate neuronal isolation throughout a dataset, we did not implement a 3 minutes transition time between cooling sessions. Following the completion of the pre-cooling session, chilled methanol was pumped through the lumen of the cryoloops, decreasing the cryoloop temperature. Once the cryoloop temperature was stable at 3˚C, we began the peri-cooling session. Upon finishing the peri-cooling session, we turned off the cooling pumps, which allowed the cryoloop temperature to rapidly return to normal. When the cryoloop temperature reached 35˚C, we began the post-cooling session. Even though saccadic behaviour and iSC activity rapidly recovered after rewarming, the post-cooling sessions likely had slight residual effects of cooling. We controlled for this and other time-dependent factors by combining trials from pre- and post-cooling sessions into the FEF warm condition. However for ~15% of datasets, isolation of an iSC neuron was lost after completion of the peri-cooling session. We excluded post-cooling trials from these sessions. Nonetheless, the effects of cooling in these sessions (based on comparing peri- to pre-cooling activity) were similar to those observed when isolation was maintained throughout the post-cool session).

4.2.3: Behavioural tasks

Monkeys performed visually- or memory-guided saccades after a delayed response period. Following a variable fixation period (750 to 1000 ms) where monkeys maintained fixation within ±3˚ of a central cue, a peripheral cue appeared in or diametrically opposite to the center of the response field of an isolated SC neuron (79% of datasets). In the remaining 21% of datasets, we collected data from intermixed visual- or memory-guided saccades, using peripheral cues placed only in the neuron's response field. Peripheral cues were either extinguished after 250 ms or remained on for memory- or visually-guided saccades, respectively. To receive a liquid reward, monkeys were required to maintain fixation throughout a delay-period of 1000 ms, and generate a saccade towards a target window (70% of the peripheral cue's visual angle) when the central cue was extinguished. Since FEF inactivation increased saccade scatter and targeting error particularly for memory-guided saccades (Peel et al., 2014), this large target window ensured that monkeys were rewarded during FEF inactivation.

In this study, unilateral (right or left) FEF inactivation consistently increased reaction times, and decreased the accuracy and peak velocities for contraversive saccades for each monkey. These effects recovered after FEF rewarming (left panel, **Fig. 4-1C**). FEF inactivation also produced similar, albeit less robust, reaction time increases for ipsiversive saccades, consistent with

previous reports using large-volume inactivations (Peel et al., 2014, 2016; Kunimatsu et al., 2015) (right panel, **Fig. 4-1C**). FEF inactivation had only a margin impact on the monkeys' ability to perform either task, with error rates increasing by less than 14%.

4.2.4: Data analysis

We categorized acceptable trials for analyses of visual, delay-period, build-up, and saccadic activity using customized computer algorithms in MatLab (Mathworks). For *visual activity*, we defined acceptable trials as those where the monkey maintained fixation of the central cue for the entire delay-period, and generated their first saccade towards the target as determined using a velocity criterion of 30˚/s. For *delay-period* and *build-up activity*, we applied the same criteria, but also removed any trial with anticipatory saccades (*i.e.,* reaction time less than 60 ms after fixation cue offset; ~12% of trials). Finally for *saccadic activity*, we used the same trials as those for the analysis of delay-period and build-up activity, but we additionally removed any trial where the monkey blinked during the first saccade (~11% of trials in this subset). We subsequently removed any dataset with less than 8 acceptable saccades into the response field of an isolated iSC neuron either before, during, or after FEF inactivation (~2% or ~9% of datasets removed for analyses on delay-period and saccadic activity, respectively).

We classified neurons as having visual, delay-period, build-up and/or saccadic activity if they achieved certain criteria. To quantify neuronal activity, we convolved spike times on individual trials (time-stamped with a 1 kHz resolution) with a spike density function that mimics an excitatory post-synaptic potential (rise-time of 1 ms, decay-time of 20 ms; (Thompson et al., 1996)). We confirmed that all of our results were the same if we convolved neural activity with a 10-ms Gaussian. To classify neurons with *visual activity*, we first required the detection of visual-related response using a Poisson analysis as described elsewhere (Hanes et al., 1995). Briefly, we compared the actual number of spikes within a time window to the number of spikes predicted by a Poisson distribution based on spiking activity across the entire trial. To calculate the latency of visual-related response within a trial, we utilized the time of the first burst of spikes greater than chance between 30 to 120 ms after cue onset. We determined the visual latency of a given neuron by averaging detected single-trial onsets of visual bursts across at least 8 trials. We subsequently classified neurons as having visual activity if their mean firing rates in the 50 ms interval after its visual latency were significantly greater than baseline activity integrated in the last 200 ms before cue onset ($p < 0.05$, Wilcoxon signed rank test; (Basso and Wurtz, 1998; McPeek and Keller, 2002)). Visual activity was defined as the difference between these firing rates, although we also calculated the peak magnitude of the visual response minus the baseline activity for complementary comparisons with previous studies. We did not separate the analysis of visual

activity for visual- or memory-guided saccades since each task was equivalent for 250 ms after cue onset.

We classified neurons as displaying *delay-period activity* if their mean firing rates in the last 100 ms of the delay-period were at least 5 spikes/s above baseline activity (i.*e.,* 200 ms before cue onset; $p < 0.05$, Wilcoxon signed rank test; (see Basso and Wurtz, 1998; McPeek and Keller, 2002)); the magnitude of delay-period activity was calculated as the difference in firing rates between these intervals. Neurons with *build-up activity* had mean firing rates 100 to 200 ms before saccade onset significantly greater than the 100 ms period immediately before (*i.e.,* 200 - 300 ms before saccade onset, $p < 0.05$, Wilcoxon signed rank test; (see Anderson et al., 1998)).

Finally, we classified neurons having *saccadic activity* if their mean peri-saccadic firing rates (defined as 8 ms before saccade onset to 8 ms prior to its end) were significantly greater than the last 100 ms of the delay-period ($p < 0.05$, Wilcoxon signed rank test), and if the increase in peri-saccadic activity above baseline activity in the 200 ms before cue onset exceeded 50 spikes/s (Munoz and Wurtz, 1995; McPeek and Keller, 2002). Saccadic activity was defined as the difference of mean peri-saccadic and baseline firing rates, although we also utilized the peak magnitude of this response minus baseline activity for complementary comparisons.

4.2.5: Matched saccade analysis

In order to examine iSC activity associated with saccade initiation and generation across FEF inactivation, it is imperative that the actual saccades are as similar as possible. Failure to perform such matching would mean that any differences that may arise could be due to confounds relating to the spatial coding of saccade metrics in the iSC (e.g., since a different saccade would be produced by a shifted population of iSC activity), or potential relationships between the vigor of iSC activity and peak saccade velocity (Waitzman et al., 1991; Stanford et al., 1996; Katnani and Gandhi, 2012), or the degree of saccade-related inhibition onto omni-pause neurons (Yoshida et al., 1999). To avoid these confound, for each neuron, we randomly matched each FEF cool trial with one trial from a set of corresponding FEF warm trials containing similar saccade metrics and dynamics (**Fig. 4-1D**). We specified that any such matched saccades had to have horizontal and vertical displacements within 1˚, and peak velocities within 10˚/s (**Fig. 4-1E**). Importantly, we matched saccades for both metrics and dynamics for all analyses on saccade-related activity, except where we investigated the relationship between the cumulative number of spikes of iSC neurons and saccade metrics. To analyze our sample, we only utilized neurons where we could match at least 5 trials in each of the FEF warm and FEF cool conditions. To allow us to assess the variability inherent to this procedure with and without FEF inactivation, we also performed the same matched saccade analysis utilizing only FEF warm trials.

4.2.6: Rise to threshold model of saccade initiation

To investigate how FEF inactivation affected parameters of iSC activity related to saccade onset (*i.e.,* onset of accumulation relative to a go-cue, accumulation rate, baseline activity, and threshold activity immediately before saccade onset), we fit convolved iSC activity with a rise-to-threshold model on a trial-by-trial basis. We determined the onset of accumulation using a rationale described elsewhere (Woodman et al., 2008; Pouget et al., 2011), modifying this procedure slightly to permit single-trial analysis. To do this, we first smoothed the spike density functions of individual trials using a moving average within a ± 20 ms window. Then, we moved a ± 10 ms sliding window (in steps of 1 ms) backward in time from peak activity until a significantly increasing Spearman correlation ($p < 0.05$) no longer occurred. If this point occurred where there was no activity (*e.g.,* **Fig. 4-5A**), the onset of accumulation was defined as the time (relative to fixation cue offset) where subsequent activity occurred; otherwise it corresponded to the time of any lower or equivalent activity in the subsequent 10 ms interval. To verify our onset results, we used an alternative analysis using a two-piece piecewise linear regression analysis (Cashaback et al., 2013; Goonetilleke et al., 2015), and found equivalent results. For threshold activity, we calculated the activity 18 to 8 ms prior to saccade onset (Jantz et al., 2013; Johnston et al., 2014), which is based on the minimum amount of time for the iSC to influence the brainstem circuits regulating saccade onset (Miyashita and Hikosaka, 1996). Finally we calculated the accumulation rate as the difference of

threshold and baseline activities at the onset of accumulation divided by the difference in saccade reaction time and the onset of accumulation time (Pouget et al., 2011).

4.3: Results

4.3.1: Description of dataset

We investigated the impact of unilateral FEF inactivation on visual, delay-period, build-up, and saccade-related activity in the iSC, and also investigate how changes in saccade-related iSC activity related to changes in SRT. We recorded a total of 239 iSC neurons (178 ipsilesional, 61 contralesional to FEF inactivation) in four monkeys, maintaining isolation before and during FEF inactivation, and usually (85%) through re-warming of the FEF. Of these neurons, 107 (45%) had visual activity, 144 (60%) had delay-period activity, 58 (24%) had build-up activity, 157 (66%) had saccade-related activity (note that a single neuron could contribute to multiple responses), and 18 neurons (8%) did not meet any of our selection criteria. Before FEF inactivation, neurons with visual activity had mean ± SD response latencies of 56 ± 9 ms (range: 42 to 99 ms), firing rates of 95 ± 49 spikes/s, and peak magnitudes of 150 ± 77 spikes/s; these agree with previous descriptions of visual responses in the iSC (Munoz and Wurtz, 1995; Basso and Wurtz, 1998; McPeek and Keller, 2002; Sommer and Wurtz, 2004a). 79% of these 107 visual neurons also exhibited either delay-period activity (70%), build-up (11%), or saccade-related activity (59%), which is consistent with most of these

visual neurons being recorded from the intermediate and not superficial layers of SC. For neurons classified as having saccade-related activity, we found mean ± SD firing rates of 181 ± 101 spikes/s, and peak magnitudes of 288 ± 138 spikes/s during visually-guided saccades, and corresponding activities of 130 ± 65 and 215 ± 85 spikes/s during memory-guided saccades. Moreover, 82% of 157 saccade-related neurons additionally exhibited either visual (40%), delay-period (68%), or build-up (27%) activity. Thus, our sample of iSC neurons contained a continuum of visuomotor responses similar to that reported previously (Munoz and Wurtz, 1995; Sommer and Wurtz, 2004a). Having established this, we now turn to the effects of FEF inactivation on iSC activity. As previously mentioned, we controlled for time-dependent factors by combining pre- and post-cooling trials into the FEF warm condition (red), which we compared to trials when the FEF was inactivated (*i.e.,* FEF cool, blue).

4.3.2: FEF inactivation reduced visual activity of ipsilesional iSC neurons

FEF inactivation robustly decreased visual activity of neurons in the ipsilesional iSC, but did not alter their visual burst latency. **Figure 4-2A** shows an example neuron from the ipsilesional iSC (neuron D1) which was maintained before, during, and after FEF inactivation. In the FEF warm condition, visual activity of neuron D1 started 87 ms after cues appeared in its response field, and averaged 174 spikes/s for the subsequent 50 ms period. We classified neuron D1

as a visual neuron with delay-period activity since it also remained active, albeit at a lower activity, when the cue remained on, and did not display saccade-related activity. FEF inactivation significantly decreased its visual activity from 174 to 103 spikes/s ($p < 0.0001$), but did not alter the visual burst latency (87 to 86 ms, $p = 0.82$). Across our sample of iSC neurons, FEF inactivation robustly decreased visual activity in the ipsilesional ($p < 0.01$, ~4% decrease in all 89 neurons, and ~24% decrease in the 23 neurons in which FEF inactivation significantly decreased visual activity), but not contralesional side ($p = 0.40$; **Fig. 4-2B**). Moreover, FEF inactivation had no impact on visual response latencies across our sample of ipsilesional ($p = 0.94$) or contralesional iSC neurons ($p = 0.40$; **Fig. 4-2C**). Thus, FEF inactivation impacted the magnitude but not latency of iSC visual activity. Importantly, FEF inactivation did not impact baseline activity in the 200 ms preceding cue onset in either the ipsilesional ($p = 0.85$) or contralesional ($p = 0.16$) iSC, nor in the subset of 23 ipsilesional iSC neurons ($p = 0.68$) exhibiting significantly reduced visual activity.

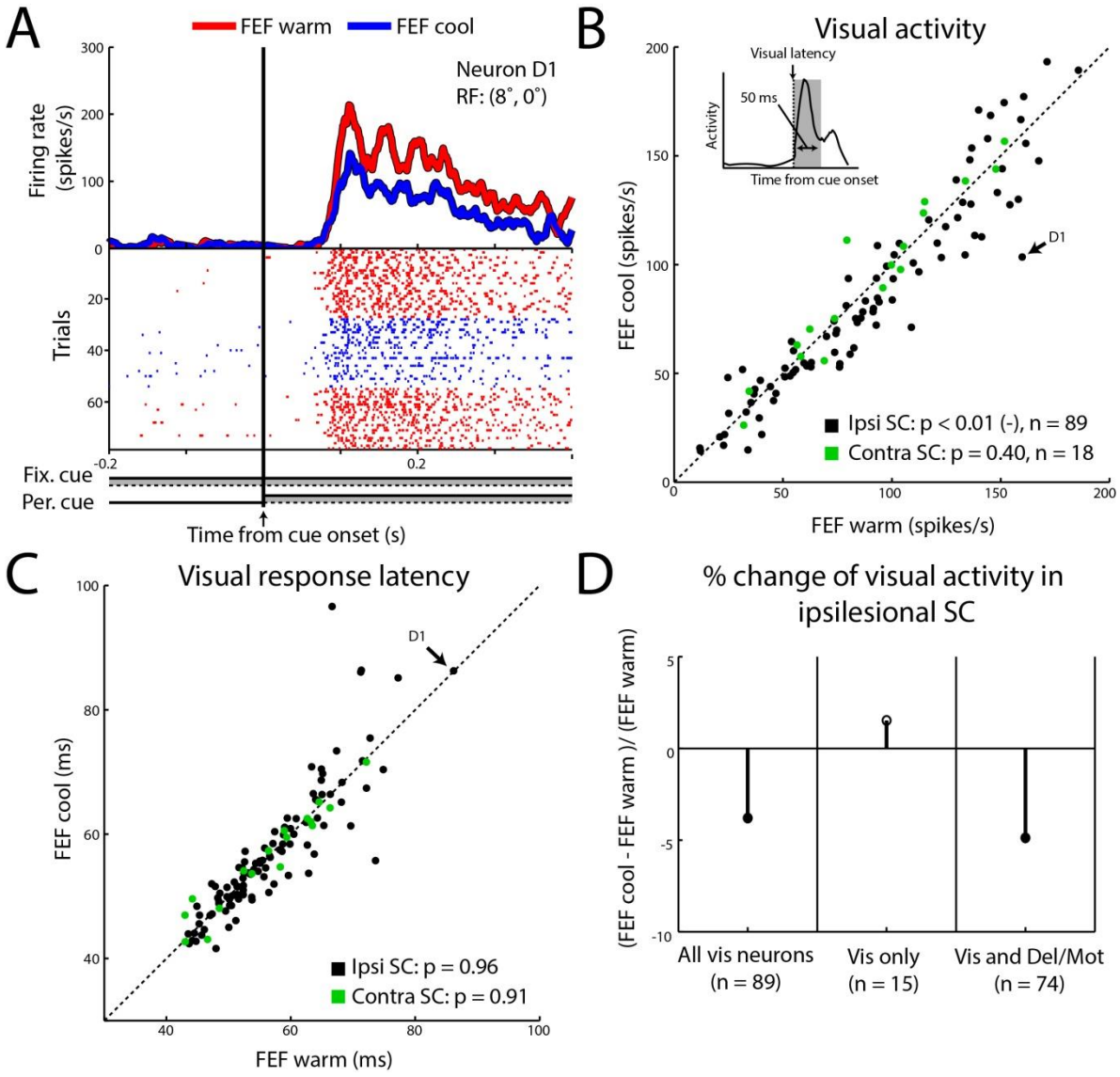

Figure 4-2. FEF inactivation decreased visual activity of ipsilesional iSC neurons. (A) Ipsilesional iSC neuron D1 demonstrates the reduced visual response following peripheral cue onset during FEF inactivation. (B) FEF inactivation consistently decreased visual activity in the 50 ms interval subsequent to its visual latency only across ipsilesional iSC neurons. (C) In contrast, FEF inactivation had no consistent effect on visual latencies on either ipsilesional or contralesional iSC neurons. (D) FEF inactivation decreased visual responses of neurons generally having additional responses. Filled circles represent significant effects using a Wilcoxon sign-rank test ($p < 0.05$).

Interestingly, FEF inactivation impacted on visual responses in iSC neurons which also displayed delay- and/or saccade-related activity. This is shown in **Fig. 4-2D**, where we subdivided our sample based on whether a neuron only exhibited a visual response (n = 15) or also exhibited delay- or saccade-related activity (n = 74). Similarly, 22 of 23 visually-responsive neurons significantly impacted by FEF inactivation exhibited delay- or saccade-related activity.

4.3.3: FEF inactivation decreased delay-period activity in ipsilesional iSC neurons, regardless of the presence or absence of the visual cue

We next investigated whether FEF inactivation impacted delay-period activity within iSC neurons, and found that FEF inactivation reduced delay-period activity in ipsilesional iSC neurons both in the presence (visually-guided saccades) and absence (memory-guided saccades) of peripheral cues, consistent with a contribution of the FEF to tonic visual activity and visuospatial memory in downstream iSC neurons. We show this result for two ipsilesional iSC neurons, neuron D2 (**Fig. 4-3A**) and O1 (**Fig. 4-3B**). In the FEF warm condition, neuron D2 displayed modest delay-period activity of ~12 spikes/s in the last 100 ms period before fixation cue offset, which continued to ramp up until saccade onset when peripheral cues were absent. Remarkably, FEF inactivation effectively abolished this delay-period activity with such activity decreasing from 12 to 0.2 spikes/s ($p < 0.0001$). Visuomotor neuron O1 was recorded during interleaved visually- and

memory-guided saccades, and exhibited far greater delay-period activity when the cue was present (76 spikes/s) than absent (11 spikes/s). FEF inactivation decreased delay-period activity both when cues were present (76 to 46 spikes/s) or absent (11 to 5 spikes/s), although we this effect only reached significance for visually-guided saccades ($p < 0.0001$). Across our sample, FEF inactivation robustly reduced delay-period activity in both saccade tasks, but only for the ipsilesional iSC (**Fig. 4-3C**; visually-guided, cyan, $p < 0.001$, 30% of the 76 neurons had significant decreases; memory-guided, magenta, $p < 0.0001$, 41% of the 44 neurons had significant decreases). While FEF inactivation had a similar impact on ipsilesional iSC neurons with (squares) or without (circles) build-up activity, FEF inactivation decreased activity to a larger extent in neurons when peripheral cues were absent (~35% decrease in all 44 neurons, or ~69% decrease in the 18 neurons with significant decreases) than present (~17% decrease in all 76 neurons, or ~52% decrease in the 23 neurons with significant decreases). In contrast, we observed no consistent effect of FEF inactivation on delay-period activity within contralesional iSC neurons (**Fig. 4-3D**).

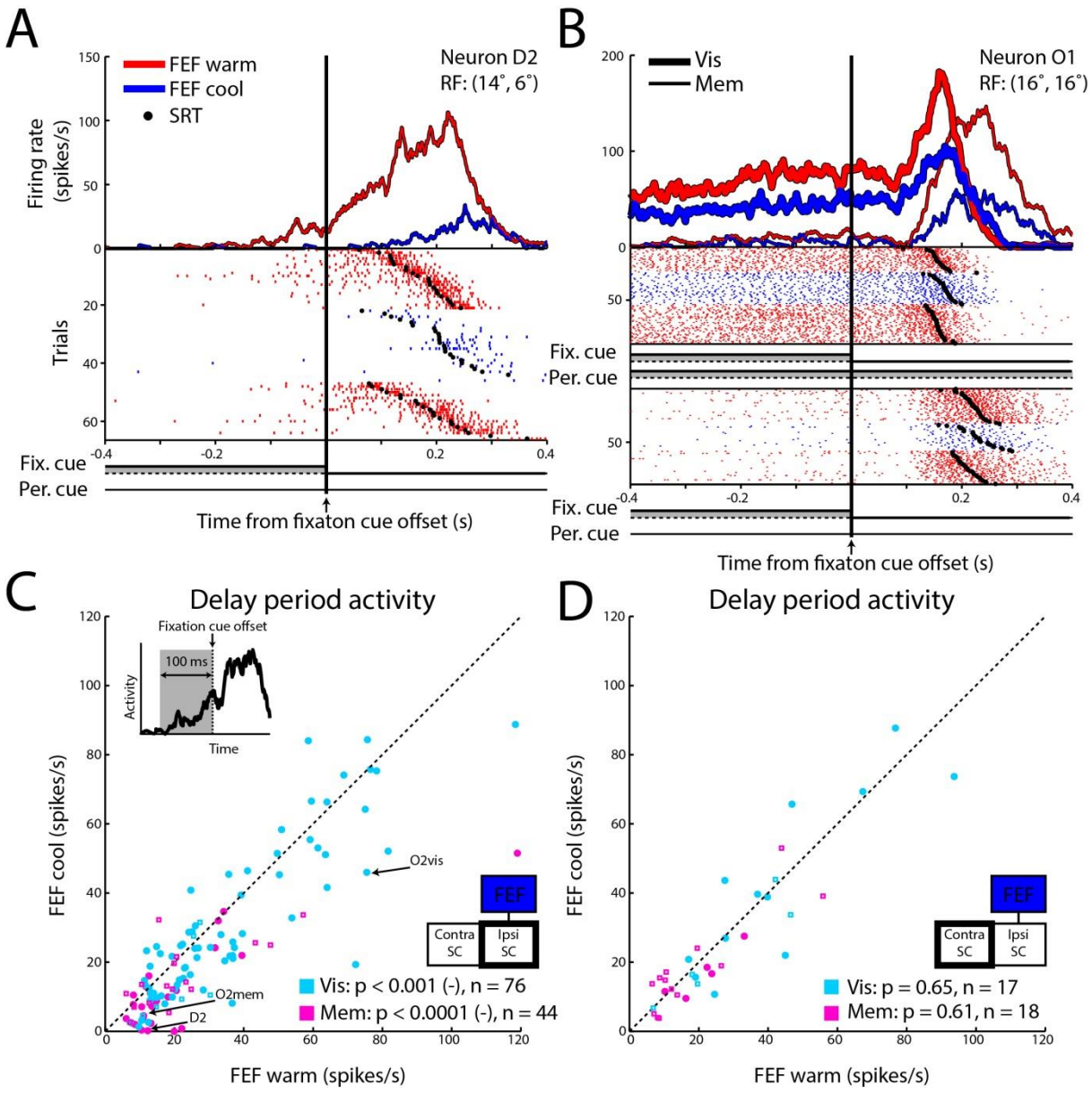

Figure 4-3. FEF inactivation decreased delay-period activity of ipsilesional iSC neurons, both in the presence and absence of peripheral cues. (A) While ipsilesional iSC neuron D2 exhibited modest delay-period activity in the absence of peripheral cues, FEF inactivation nearly abolished this delay-period activity. (B) Similarly FEF inactivation reduced delay-period activity both in the presence and the absence of peripheral cues in ipsilesional neuron O1. (C) FEF inactivation consistently decreased delay-period activity in the last 100 ms before peripheral cue offset for both visually- and memory-guided tasks in ipsilesional iSC neurons, including those displaying build-up activity (squares). (D) In contrast, we found no consistent influence of FEF inactivation across contralesional iSC neurons.

As previously mentioned, FEF inactivation selectively and broadly impacted visual neurons that also exhibited delay- or saccade-related activity. We found a similar pattern for the 111 ipsilesional iSC neurons with delay-period activity related to the presence or absence of the visual cue: 40 of 41 neurons exhibiting significantly reduced delay-period activity during FEF inactivation also exhibited either visual (63%), build-up (23%), or saccade-related activity (75%). Likewise, FEF inactivation consistently decreased these additional responses in this subset of 40 neurons (each $p < 0.05$, except for build-up activity prior to visually-guided saccades). Taken together with the pattern seen with visual responses, these results are consistent with identified FEF corticotectal neurons sending signals that span the visuomotor continuum to iSC neurons (Sommer and Wurtz, 2000, 2001).

4.3.4: FEF inactivation reduced saccade-related activity of ipsilesional iSC neurons, even for matched saccades

Next, we examined the FEF's contribution to saccade-related activity in the ipsi- and contralesional iSC. For this analysis, it is imperative that saccades generated during FEF inactivation be matched as closely as possible for metrics and velocity, otherwise any changes in saccade-related activity could simply be related to the generation of a different saccade. As described in the **Methods**, we matched saccades within 1˚ of horizontal and vertical displacement and within 10˚/s of radial peak velocity. Given the similarity in the metrics and

dynamics of saccades generated in the FEF warm or FEF cool conditions, one could have expected similar profiles of saccade-related iSC activity. Instead, we found that FEF inactivation decreased saccade-related activity (*i.e.,* 8 ms before onset to 8 ms before saccade offset) in ipsilesional iSC neurons even for matched visually- or memory-guided saccades. This result is illustrated by neuron O2 (**Fig. 4-4A**) where saccade-related activity significantly decreased from 375 to 320 spikes/s ($p < 0.01$), despite the generation of virtually-identical saccades. Across our sample, we observed a consistent decrease in saccade-related activity for ipsilesional iSC neurons, providing there were at least 5 matches, for either visually- or memory-guided saccades (each $p < 0.0001$, **Fig. 4-4B**). FEF inactivation decreased saccade-related activity more for memory- versus visually-guided saccades, both in terms of how much activity decreased (27 and 15% decrease, respectively) and in the proportion of neurons exhibiting significantly changed activity (35% of 55 neurons, and 14% of 70 neurons, respectively). Thus, even for matched saccades, the effects of FEF inactivation are greater on more complex oculomotor tasks, as reported previously (Sommer and Tehovnik, 1997; Dias and Segraves, 1999; Peel et al., 2014).

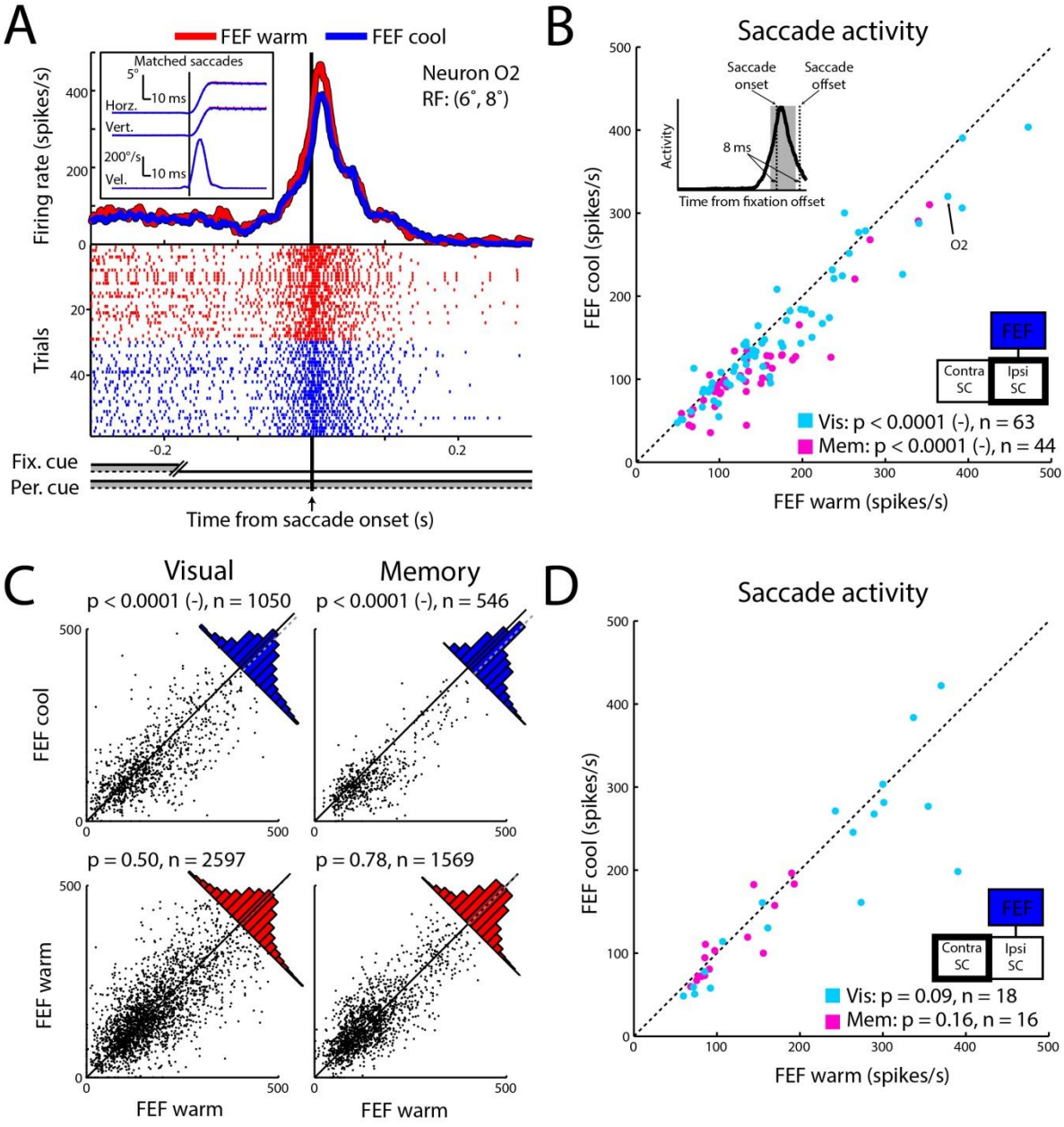
A
FEF warm
FEF cool
Matched saccades
5°
10 ms
Horz.
Vert.
200°/s
Vel.
10 ms
Neuron O2
RF: (6˚, 8˚)
Firing rate (spikes/s)
Trials
Fix. cue
Per. cue
Time from saccade onset (s)
B
Saccade activity
Saccade onset
Saccade offset
Activity
8 ms
Time from fixation offset
FEF cool (spikes/s)
FEF warm (spikes/s)
O2
FEF
Contra SC
Ipsi SC
Vis: p < 0.0001 (-), n = 63
Mem: p < 0.0001 (-), n = 44
C
Visual
Memory
p < 0.0001 (-), n = 1050
p < 0.0001 (-), n = 546
p = 0.50, n = 2597
p = 0.78, n = 1569
FEF cool
FEF warm
FEF warm
FEF warm
D
Saccade activity
FEF cool (spikes/s)
FEF warm (spikes/s)
FEF
Contra SC
Ipsi SC
Vis: p = 0.09, n = 18
Mem: p = 0.16, n = 16

Figure 4-4. FEF inactivation decreased saccade-related activity of ipsilesional iSC neurons matched for saccade metrics and dynamics. (A) For example neuron O2, FEF inactivation decreased saccade-related activity matched for visually-guided saccades. (B) FEF inactivation consistently decreased saccade-related activity (8 ms before saccade onset to 8 ms before saccade offset) consistently across ipsilesional iSC neurons for trials matched for visually- or memory-guided saccades. (C) Across all visually- and memory-guided saccades matched between FEF warm and FEF cool trials, FEF inactivation skewed the distributions of activity differences (blue) towards decreasing saccade-related activity. As a control, matching only FEF warm trials produced no skews in distributions of saccade-related activity (red). (D) We found that FEF inactivation had no consistent effect on saccade-related activity in contralesional iSC neurons with matched saccades.

Another way of analyzing the effects of FEF inactivation on saccade-related iSC activity is to directly compare activity for all matched saccades, pooled across all recorded neurons. The result of this analysis is shown in **Fig. 4-5C** (top row), where each point represents saccade-related activity for a matched saccade generated during the FEF cool versus FEF warm condition. The clustering of points below the line of unity in the top row of **Fig. 4-4C**, as well as the rightward skew of the blue histograms, reinforces the observation of decreasing iSC activity during FEF inactivation. We can also explore the variability in the saccade-matching procedure by matching saccades using on FEF warm trials; while there is considerable scatter in this analysis around the line-of-unity (lower rows in **Fig. 4-4C**), the resulting distributions of the red histograms were not skewed away from zero.

Finally, while FEF inactivation occasionally significantly decreased saccade-related activity neurons in the contralesional iSC (33 and 13% of neurons for visually- and memory-guided, respectively), such effects were not consistent across our sample (**Fig. 4-4D**).

4.3.5: FEF inactivation increased the onset time of saccade-related activity bilaterally in the iSC, which reflected changes in SRT

The preceding results shows that FEF inactivation reduces saccade-related activity in the ipsilesional iSC. This result is intriguing since it suggests that different profiles of iSC activity can still lead to the generation of an

equivalent, albeit longer latency, saccade. To investigate this further, we analyzed how FEF inactivation impacted the parameters of saccade-related activity derived from a rise-to-threshold model (*i.e.,* baseline and threshold activity, onset and rate of accumulation see **Methods** for details), and determined which parametric changes best reflected the changes in SRT. Within this model, increased SRTs for matched saccades could be related to decreases in baseline activity or rate of accumulation, or increases in onset of accumulation or saccade threshold.

We first focus on the onset of accumulation, since changes in this parameter best related to changes in SRT. For simplicity, we pooled data across visually- and memory-guided saccades, since similar results were obtained for each task. The influence of FEF inactivation on the onset of accumulation (empty circles) and SRT (black circles) is shown for a representative neuron in **Fig. 4-5A**, showing single-trial activity for one example of a matched saccade (**Fig. 4-5A**, top; the inset shows the position and velocity profiles for this match), and across all matches recorded from this neuron (**Fig. 4-5A**; bottom). For this example, FEF inactivation significantly increased the onset of accumulation from 139 to 162 ms after fixation cue offset ($p < 0.01$), and also significantly increased the SRT of matched memory-guided saccades from 207 to 233 ms ($p < 0.05$).

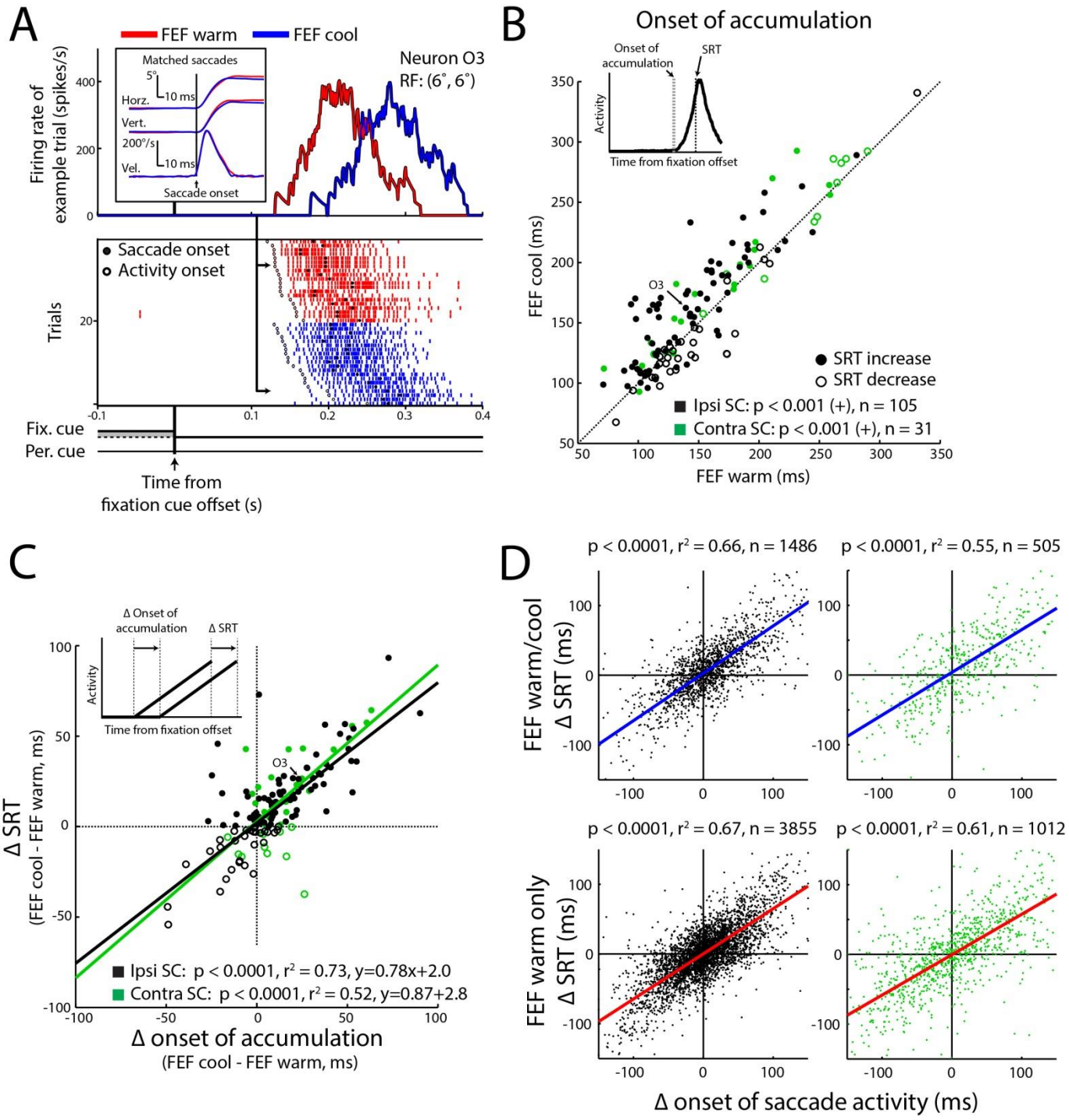
A
FEF warm
FEF cool
Neuron O3
RF: (6˚, 6˚)
Matched saccades
5˚
10 ms
Horz.
Vert.
200˚/s
10 ms
Vel.
Saccade onset
Firing rate of example trial (spikes/s)
Saccade onset
Activity onset
Trials
Fix. cue
Per. cue
Time from fixation cue offset (s)
B
Onset of accumulation
Onset of accumulation
SRT
Activity
Time from fixation offset
FEF cool (ms)
FEF warm (ms)
O3
SRT increase
SRT decrease
Ipsi SC: p < 0.001 (+), n = 105
Contra SC: p < 0.001 (+), n = 31
C
Δ Onset of accumulation
Δ SRT
Activity
Time from fixation offset
Δ SRT
(FEF cool - FEF warm, ms)
O3
Ipsi SC: p < 0.0001, r² = 0.73, y=0.78x+2.0
Contra SC: p < 0.0001, r² = 0.52, y=0.87+2.8
Δ onset of accumulation
(FEF cool - FEF warm, ms)
D
p < 0.0001, r² = 0.66, n = 1486
p < 0.0001, r² = 0.55, n = 505
FEF warm/cool Δ SRT (ms)
p < 0.0001, r² = 0.67, n = 3855
p < 0.0001, r² = 0.61, n = 1012
FEF warm only Δ SRT (ms)
Δ onset of saccade activity (ms)

Figure 4-5. FEF inactivation delayed the onset of saccade-related activity in both ipsilesional and contralesional iSC neurons, which strongly correlated to differences in SRT. (A) For example ipsilesional neuron O3, FEF inactivation delayed the onset of saccade-related activity (grey circles) and SRT (black circles) for matched memory-guided saccades. (B) FEF inactivation consistently delayed the onset of saccade-related activity across both ipsilesional and contralesional iSC neurons matched for saccades metrics and dynamics. For each neuron, close and filled circles indicate where SRT increased and decreased from FEF inactivation, respectively. (C) Differences in the onset of saccade-related activity strongly correlated to SRT differences across ipsilesional and contralesional iSC neurons. (D) We found similar relationships, and more importantly similar variability, across all matched trials with (top, blue line) and without FEF inactivation (bottom, red line).

Remarkably, we observed a similar influence of FEF inactivation across our sample of both ipsilesional ($p < 0.0001$) and contralesional ($p < 0.001$) iSC neurons having at least 5 saccade matches (**Fig. 4-5B**). Recall that large, unilateral FEF inactivation often increased SRTs in both directions (see **Fig. 4-1C**). As shown in **Figure 4-5B**, we observed that changes in the onset of accumulation during FEF inactivation generally corresponded to a similar increase (closed circle, which tended to cluster above the line of unity in **Fig. 4-5B**) or decrease (open circle, which tended to cluster below the line of unity in **Fig. 4-5B**). To analyze this more closely, we plotted the change in the onset of accumulation versus the change in SRTs on a neuron-by-neuron basis, and determined the variance explained by a linear correlation (**Fig. 4-5C**). Interestingly, we found robust correlations with r^2 values of 0.73 and 0.52 for ipsilesional and contralesional iSC neurons, respectively, with slopes near 1.0 (0.78 and 0.87) and intercepts near 0 (2.0 and 2.8). Thus, on a neuron-by-neuron basis, changes in the onset of accumulation of saccade-related iSC activity predicted accompanying changes in SRT in an almost one-to-one manner.

Another way of illustrating the relationship between the onset of iSC accumulation and SRT is to extend this analysis to the level of matched saccades. For each matched saccade pair, extracted either across FEF inactivation (top subplots in **Fig. 4-5D**) or only from trials without FEF inactivation (bottom subplots in **Fig. 4-5D**) and from either the ipsi- or contralesional iSC (left or right

subplots of **Fig. 4-5D** respectively), we derived both a change in the onset of accumulation and a change in SRT. Across all matched trials, and regardless of whether the FEF was inactivated or not, plotting these values against each other revealed r^2 values > 0.5, slopes near 1.0 (between 0.58 and 0.68), and intercepts near 0 (between -0.5 and 4; **Fig. 4-5D**). These results reinforce the importance of the onset of iSC accumulation in determining SRT.

4.3.6: FEF inactivation decreased the accumulation rate and threshold activity of ipsilesional iSC neurons, but such changes do not explain the accompanying SRT increases

SRT increases with FEF inactivation could also be related to increases in threshold activity, or decreases in baseline activity or rate of accumulation. While FEF inactivation did impact these parameters, the variability or direction of changes in neural activity did not relate as well to accompanying changes in bilateral SRT. For instance, FEF inactivation decreased the accumulation rate (3.9 to 3.2 spikes/s^2, $p < 0.01$), and threshold activity (264 to 229 spikes/s, $p = 0.05$) in the exemplar neuron O3 (see arrow in **Fig. 4-6A**). Across our sample, FEF inactivation only significantly decreased rate of accumulation (**Fig. 4-6B**) and threshold (**Fig. 4-6C**) for ipsilesional but not contralesional iSC neurons; baseline activity preceding the onset of accumulation did not change with FEF inactivation in either iSC (**Fig. 4-6D**). These results differ from what would have been predicted of a manipulation that increases bilateral SRTs in two ways. First,

we observed no changes in baseline, threshold or accumulation rate for the contralesional iSC despite occasional increases in ipsiversive SRT. Second, we predicted that increases in contraversive SRT would be related to increases in threshold activity in the ipsilateral iSC; instead, we observed a significant decrease in threshold activity with FEF inactivation.

To examine how well changes in the parameters of iSC activity related to accompanying changes in SRT, we employed a simple rise-to-threshold model that allowed us to extract the amount of time needed for saccade threshold be reached, based on the measured values for baseline, threshold, and accumulation rate ([threshold - baseline activity]/[accumulation rate]). Note that this time to reach threshold value does not incorporate measures of the onset of accumulation; effectively this model assumes that neural activity accumulates from baseline at some fixed time after a go cue. We then compared how changes in this time to reach threshold value with FEF inactivation related to accompanying changes in SRT.

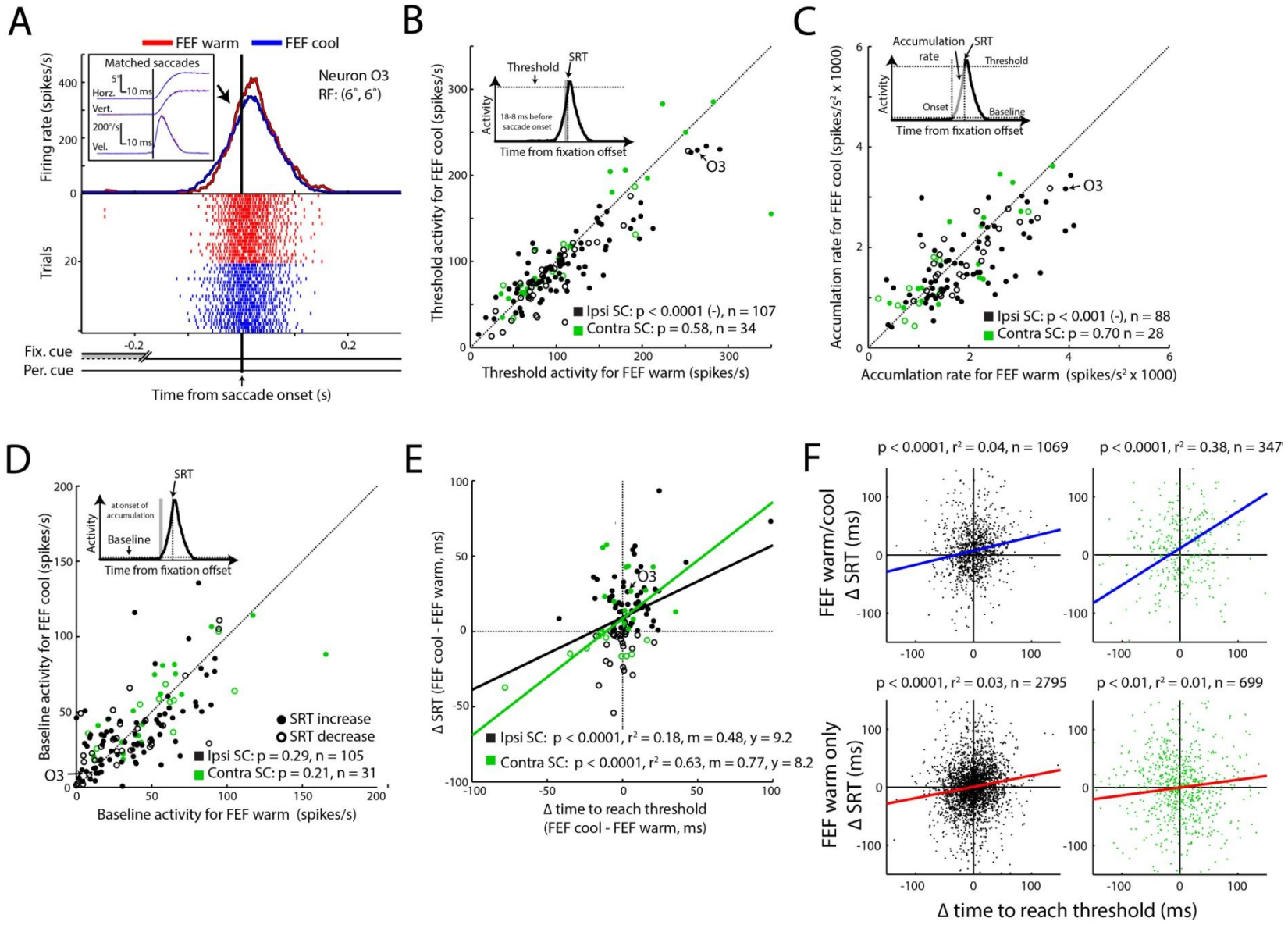
A
FEF warm
FEF cool
Matched saccades
Neuron O3
RF: (6˚, 6˚)
Firing rate (spikes/s)
Trials
Fix. cue
Per. cue
Time from saccade onset (s)
B
Threshold
SRT
Activity
18-8 ms before saccade onset
Time from fixation offset
Threshold activity for FEF cool (spikes/s)
Threshold activity for FEF warm (spikes/s)
Ipsi SC: p < 0.0001 (-), n = 107
Contra SC: p = 0.58, n = 34
C
Accumulation rate
Onset
Baseline
Accumlation rate for FEF cool (spikes/s² x 1000)
Accumlation rate for FEF warm (spikes/s² x 1000)
Ipsi SC: p < 0.001 (-), n = 88
Contra SC: p = 0.70 n = 28
D
at onset of accumulation
Baseline
Baseline activity for FEF cool (spikes/s)
Baseline activity for FEF warm (spikes/s)
SRT increase
SRT decrease
Ipsi SC: p = 0.29, n = 105
Contra SC: p = 0.21, n = 31
E
Δ SRT (FEF cool - FEF warm, ms)
Δ time to reach threshold (FEF cool - FEF warm, ms)
Ipsi SC: p < 0.0001, r² = 0.18, m = 0.48, y = 9.2
Contra SC: p < 0.0001, r² = 0.63, m = 0.77, y = 8.2
F
p < 0.0001, r² = 0.04, n = 1069
p < 0.0001, r² = 0.38, n = 347
p < 0.0001, r² = 0.03, n = 2795
p < 0.01, r² = 0.01, n = 699
FEF warm/cool Δ SRT (ms)
FEF warm only Δ SRT (ms)
Δ time to reach threshold (ms)

Figure 4-6. FEF inactivation decreased accumulation rates and threshold activities, but these changes were not compatible with SRT increases. (A) In example neuron O3, FEF inactivation decreased both the accumulation rate (difference in threshold activity and activity at the onset of saccade-related activity divided by the difference in SRT and onset of saccade-related activity) and threshold activities (18 to 8 ms before saccade onset, see arrow) for matched memory-guided saccades. (B,C) Across our sample, FEF inactivation also consistently decreased the accumulation rate and threshold activities, but only for ipsilesional iSC neurons. (D) In contrast, we found no effects on the baseline activity (activity at the onset of saccade-related activity) across our sample. (E) Differences in the time to reach threshold (difference of threshold and baseline activities divided by the accumulation rate) correlated with SRT changes, but much less so than the onset time of saccade-related activity. (F) Across all matched saccades, SRTs differences were only marginally explained by changes in the time to reach threshold with and without FEF inactivation, particularly in the ipsilesional iSC.

The results of this analysis is shown on a neuron-by-neuron basis in **Fig. 4-6E**. Although the time to reach threshold did increase with FEF inactivation (meaning that the decreases in accumulation rate more than compensated for decreases in threshold), this increases approached but did not reach significance for the ipsilesional iSC (mean values of 47.8 to 51.2 ms, or a relative increase of 11%, $p = 0.07$), and did not change for the contralesional iSC ($p = 0.37$). Moreover, the change in the time to reach threshold did not appear to relate well to accompanying changes in SRT (**Fig. 4-6E**), with increases in SRT accompanying either increases or decreases in the time to reach threshold value (e.g., note the clustering of values in the top-left and top-right quadrants). Linear regressions of these changes revealed modest correlations in both the ipsilesional and contralesional iSC (r^2 values of 0.18 and 0.63, respectively) which depended strongly a few extreme values in the upper-right or lower-left quadrants (slopes of 0.48 and 0.63, and intercepts of 9.2 and 8.2, respectively). We also used this analysis for matched-saccade pairs, and only very weak relationships between the change SRT and the change in the time to reach threshold, regardless of side of inactivation or whether the FEF was inactivated or not (**Fig. 4-6F**). The very weak relationships shown in **Fig. 4-6F** contrast sharply with what is shown in **Fig. 4-5D**, emphasizing the importance of incorporating changes in the onset of accumulation in accounting for changes in SRT.

4.3.7: FEF inactivation reduced the number of ipsilesional iSC spikes for saccades of similar metrics

Our dataset of iSC activity during FEF inactivation can also be used to test models of saccade generation. For example, a recent model (Goossens and Van Opstal, 2006; Van Opstal and Goossens, 2008) proposes that iSC neurons emit an invariant number of spikes for saccades of similar metrics; this model held even during blink-evoked saccades with highly irregular saccade trajectories. As detailed in the **Supplemental Information** and **Supplemental Fig. 4-1**, we found that FEF inactivation decreased the overall number of iSC spikes for saccades of similar metrics. This result demonstrates that the Goossens and Van Opstal model requires the integrity of the FEF.

4.4: Discussion

4.4.1: Summary of results

We showed that reversible inactivation of a large volume of the unilateral FEF decreases many aspects of ipsilesional iSC activity, consistent with a general loss of excitatory input. The magnitude of such decreases in iSC activity depended both on the functional content of the signal, with greatest decreases for saccade-related activity, and on the inferred depth of the iSC neuron, with greater decreases in visually-related activity on those ISC neurons also displaying delay- and saccade-related activity. Such results largely conform both with the

preferential distribution of frontal projections to intermediate and deeper layers of the iSC (Tigges and Tigges, 1981), and with antidromic studies of the functional content of corticotectal neurons (Segraves and Goldberg, 1987; Sommer and Wurtz, 2000; Helminski and Segraves, 2003). We also studied the neural correlates of increased SRT in both colliculi not confounded by long-term recovery or differences in saccade metrics and dynamics, and in doing so, revealed novel and unexpected findings for how the oculomotor cortex and brainstem coordinate saccade initiation. For example, seemingly paradoxical changes in saccade threshold in the iSC, which decreased rather than increased during FEF inactivation, reinforce recent findings that saccade threshold varies at the level of an individual iSC neuron (Jantz et al., 2013). Further, the primary determinant of SRT increases in either direction were delays in the onset of saccade-related activity in the iSC, demonstrating a causal role for frontal signals in when downstream saccade-related activity starts to accumulate, and the need to incorporate the onset of accumulation into neurophysiologically-inspired models of saccade initiation.

4.4.2: FEF inactivation reduces excitatory input to the ipsilesional iSC, particularly for neurons with saccade-related activity, but does not disinhibit the contralesional iSC

The functional content of cortical signals relayed directly to iSC or between nodes of the oculomotor system has been well-characterized using

antidromic identification (Finlay et al., 1976; Segraves and Goldberg, 1987; Paré and Wurtz, 1997; Everling and Munoz, 2000; Sommer and Wurtz, 2000, 2001; Wurtz et al., 2001; Ferraina et al., 2002; Helminski and Segraves, 2003). However, FEF signals to the iSC can also be relayed via indirect, polysynaptic pathways, such as through the basal ganglia (Hikosaka and Wurtz, 1983b). Inactivation studies like ours are required to causally assess how FEF signals through various routes collectively influence iSC activity. The general agreement between our results and those that would have been predicted by antidromic studies alone is encouraging, as it reaffirms the FEF's role in providing excitatory input to the ipsilateral iSC, particularly for those neurons displaying saccade-related activity.

Long-range interactions between different regions of the iSC or between the FEFs are thought to be inhibitory (Munoz and Istvan, 1998; Schlag et al., 1998). Could the general reduction in ipsilesional iSC activity during FEF inactivation arise from disinhibition of the contralesional FEF and/or iSC, or a shift toward increased activity in the rostral iSC? While we did not record from the rostral iSC or contralesional FEF, a number of observations argue against these interpretations. First, contralesional iSC activity neither increased nor decreased, contrary to what would have been expected from disinhibition or increased rostral iSC activity, respectively. Second, we recently reported that unilateral FEF inactivation decreased the peak velocity and prevalence of cue-

related microsaccades in both directions (Peel et al., 2016), which would be more consistent with decreasing, rather than increasing, levels of rostral iSC activity during FEF inactivation. Third, although FEF inactivation decreased the magnitude of visual responses on ipsilesional saccade-related iSC neurons, the latency of such responses were unchanged (**Fig. 4-2**); this is also inconsistent with a shift of activity toward the rostral iSC (Dorris et al., 1997; Marino et al., 2012).

The failure to observe disinhibition in the contralesional iSC is surprising given that focal pharmacological inactivation of the FEF can facilitate ipsiversive oculomotor behaviors (Sommer and Tehovnik, 1997; Dias and Segraves, 1999; Wardak et al., 2006). Studies using focal microstimulation (Schlag et al., 1998; Seidemann et al., 2002) or paired bilateral recordings (Cohen et al., 2010) have also supported a view wherein the two FEFs compete in a push-pull fashion. In contrast, large-volume FEF inactivation tends to delay rather than facilitate ipsiversive oculomotor behaviors (**Fig. 4-1**; (Peel et al., 2014, 2016; Kunimatsu et al., 2015)), implicating different dynamics within the oculomotor network during focal versus large-volume inactivation (see below).

4.4.3: A bilateral influence of the unilateral FEF on the onset of saccade-related accumulation in the iSC

As reported previously (REFS), unilateral FEF inactivation increased ipsiversive SRTs, although such increases were of lower magnitude and more subject-dependent than the increases in contraversive SRTs. Our recording results clarify the underlying neural substrates, demonstrating that SRT increases in either direction, when present, related best to delays in the onset of saccade-related accumulation in the iSC. While such changes within the ipsilesional iSC could relate to a loss of topographically-organized excitatory input consequent to FEF inactivation (Sommer and Wurtz, 2000), how could unilateral FEF inactivation impact the onset of saccade-related activity in the contralesional iSC? A number of scenarios are possible. Large-volume unilateral FEF inactivation may disrupt the contribution of FEF neurons that project to the contralesional iSC either directly (Distel and Fries, 1982) or indirectly through the basal ganglia (Jayaraman et al., 1977; Jiang et al., 2003; Liu and Basso, 2008), or impair the contribution of ipsilaterally-tuned neurons that are broadly dispersed throughout the FEF (Sommer and Wurtz, 2000; Izawa et al., 2009). Large-volume unilateral FEF inactivation may also produce a more broadly-disinhibited network state that, somewhat paradoxically, takes longer to start the accumulation of saccade-related activity due to altered levels of cooperative and competitive interactions. A future experiment should determine the impact of large-volume unilateral FEF inactivation on activity within the contralesional FEF,

to see if this differs from what we found in the contralesional iSC. Studies using focal microstimulation (Schlag et al., 1998; Seidemann et al., 2002), pharmacological inactivation (Sommer and Tehovnik, 1997; Dias and Segraves, 1999; Wardak et al., 2006), or paired bilateral recordings (Cohen et al., 2010) have supported a view wherein the two FEFs compete in a push-pull fashion. The observation of bilateral increases in SRTs and bilateral delays in saccade-related accumulation, neither of which appear consistent with a push-pull mechanism, may relate to the volume of tissue inactivation with our cooling loops, which we have estimated is at least four times larger than that inactivated pharmacologically (Peel et al., 2014, 2016).

The impact of large-volume FEF inactivation on iSC activity and saccadic behavior differs from that observed following large-volume inactivation of the adjacent dorso-lateral prefrontal cortex (DLPFC), emphasizing differential contributions of these structures to saccade control. In contrast to our observations, large-volume DLPFC inactivation of the gyral tissue surrounding the caudal principal sulcus did appear to produce disinhibition, increasing activity in the contralesional iSC and facilitating ipsiversive oculomotor behaviors (Koval et al., 2011; Johnston et al., 2014). DLPFC inactivation also did not lower the magnitude of saccade-related ipsilesional iSC activity (in contrast to our results), although it did delay or expedite the onset of saccade-related accumulation in both the ipsilesional or contralesional iSC, respectively.

4.4.4: New perspectives on saccade initiation

FEF inactivation altered how iSC activity relates to saccade initiation, doing so in a manner that provides new insights into how the oculomotor brainstem initiates a saccade. Importantly, the inferences that we can draw hinge critically on comparisons of saccades closely matched for metrics and kinematics; without such matching, any changes in iSC activity during FEF inactivation could relate simply to the generation of a different saccade. One fundamental observation is that less saccade-related activity is emitted by ipsilateral iSC neurons during FEF inactivation. Clearly, at the level of single iSC neurons, and with targets placed at movement field centers, saccade threshold can vary (**Fig. 4-6**). This observation complements recent observations of how saccade threshold can change in the iSC (Jantz et al., 2013) or FEF (Heitz and Schall, 2012). In the FEF, Heitz and Schall (2012) have reconciled observations of increased SRTs despite decreasing thresholds by proposing a leaky integrator mechanism where saccade-related spikes are integrated over time to produce an invariant level of cumulative activity. We also observed decreasing threshold and rates of accumulation accompanying increasing SRTs during FEF inactivation, hence such a temporal code may also apply to iSC thresholds. Additionally, iSC thresholds may relate to population coding across the entire iSC (Gandhi and Keller, 1997, 1999; Anderson et al., 1998); if so, decreases in activity from the center of the movement field may be offset by increases in the activity of other off-center iSC

neurons. We are currently mapping iSC movement fields before and during FEF inactivation to causally test this notion of population coding.

Previous evidence for fixed thresholds in the FEF (Hanes and Schall, 1996; Brown et al., 2008) and iSC (Paré and Hanes, 2003) fit well with rise-to-threshold (Carpenter and Williams, 1995; Reddi and Carpenter, 2000; Lo and Wang, 2006; Carpenter et al., 2009) and drift-diffusion models (Ratcliff et al., 2003, 2007) of saccade initiation, strengthening contentions that these models provided useful descriptions of neural activity. However, by embracing a greater subset of experimental tasks or conditions, the work of Heitz and Schall (2012) and Jantz and colleagues (2013) revealed that contemporary models failed to predict observed profiles of FEF or iSC activity. As another example, Pouget and colleagues (2011) demonstrated that post-error increases in SRT related best to delays in the onset of saccade-related activity in both the iSC and FEF, rather than decreasing threshold or rate of accumulation. Our causal findings complement the work of Pouget and colleagues (2011), by showing that FEF inactivation delays the onset of saccade-related activity in the iSC. Clearly, the onset of saccade-related activity in the iSC is a relevant metric that impacts SRT, and one that is governed by frontal inputs. Together, our results reinforce that profiles of iSC activity cannot be accommodated by current models of saccade initiation (Heitz and Schall, 2012). Modifications are required to produce a

comprehensive model that describes the changes in both neural activity and behavior.

4.5: References

Anderson RW, Keller EL, Gandhi NJ, Das S (1998) Two-dimensional saccade-related population activity in superior colliculus in monkey. J Neurophysiol 80:798–817.

Basso MA, Wurtz RH (1997) Modulation of neuronal activity by target uncertainty. Nature 389:66–69.

Basso MA, Wurtz RH (1998) Modulation of neuronal activity in superior colliculus by changes in target probability. J Neurosci 18:7519–7534.

Berman R a, Joiner WM, Cavanaugh J, Wurtz RH (2009) Modulation of presaccadic activity in the frontal eye field by the superior colliculus. J Neurophysiol 101:2934–2942.

Brown JW, Hanes DP, Schall JD, Stuphorn V (2008) Relation of frontal eye field activity to saccade initiation during a countermanding task. Exp Brain Res 190:135–151.

Bruce CJ, Goldberg ME (1985) Primate frontal eye fields. I. Single neurons discharging before saccades. J Neurophysiol 53:603–635.

Bruce CJ, Goldberg ME, Bushnell MC, Stanton GB (1985) Primate frontal eye fields. II. Physiological and anatomical correlates of electrically evoked eye movements. J Neurophysiol 54:714–734.

Carpenter RH, Williams ML (1995) Neural computation of log likelihood in control of saccadic eye movements. Nature 377:59–62.

Carpenter RHS, Reddi BAJ, Anderson AJ (2009) A simple two-stage model predicts response time distributions. J Physiol 587:4051–4062.

Cashaback JGA, Cluff T, Potvin JR (2013) Muscle fatigue and contraction intensity modulates the complexity of surface electromyography. J Electromyogr Kinesiol 23:78–83.

Cohen JY, Crowder EA, Heitz RP, Subraveti CR, Thompson KG, Woodman GF, Schall JD (2010) Cooperation and Competition among Frontal Eye Field Neurons during Visual Target Selection. J Neurosci 30:3227–3238.

Costello MG, Zhu D, Salinas E, Stanford TR (2013) Perceptual modulation of motor--but not visual--responses in the frontal eye field during an urgent-decision task. J Neurosci 33:16394–16408.

Crapse TB, Sommer MA (2009) Frontal eye field neurons with spatial representations predicted by their subcortical input. J Neurosci 29:5308–5318.

Deng SYY, Goldberg M. E, Segraves MAA, Ungerleider LGG, Mishkin M (1986) The effect of unilateral ablation of the frontal eye fields on saccadic performance in the monkey. In: Adaptive Processes in the Visual and Oculomotor Systems, pp 201–208. Elsevier.

Dias EC, Kiesau M, Segraves MA (1995) Acute activation and inactivation of macaque frontal eye field with GABA-related drugs. J Neurophysiol 74:2744–2748.

Dias EC, Segraves MA (1999) Muscimol-induced inactivation of monkey frontal eye field: effects on visually and memory-guided saccades. J Neurophysiol 81:2191–2214.

Distel H, Fries W (1982) Contralateral cortical projections to the superior colliculus in the macaque monkey. Exp brain Res 48:157–162.

Dorris MC, Paré M, Munoz DP (1997) Neuronal activity in monkey superior colliculus related to the initiation of saccadic eye movements. J Neurosci 17:8566–8579.

Everling S, Munoz DP (2000) Neuronal correlates for preparatory set associated with pro-saccades and anti-saccades in the primate frontal eye field. J Neurosci 20:387–400.

Ferraina S, Paré M, Wurtz RH (2002) Comparison of cortico-cortical and cortico-collicular signals for the generation of saccadic eye movements. J Neurophysiol 87:845–858.

Finlay BL, Schiller PH, Volman SF (1976) Quantitative studies of single-cell properties in monkey striate cortex. IV. Corticotectal cells. J Neurophysiol 39:1352–1361.

Gandhi NJ, Keller EL (1997) Spatial distribution and discharge characteristics of superior colliculus neurons antidromically activated from the omnipause region in monkey. J Neurophysiol 78:2221–2225.

Gandhi NJ, Keller EL (1999) Comparison of saccades perturbed by stimulation of the rostral superior colliculus, the caudal superior colliculus, and the omnipause neuron region. J Neurophysiol 82:3236–3253.

Goonetilleke SC, Katz L, Wood DK, Gu C, Huk AC, Corneil BD (2015) Cross-species comparison of anticipatory and stimulus-driven neck muscle activity well before saccadic gaze shifts in humans and nonhuman primates. J Neurophysiol 114:902–913.

Goossens HHLM, Van Opstal a J (2006) Dynamic ensemble coding of saccades in the monkey superior colliculus. J Neurophysiol 95:2326–2341.

Hanes DP, Patterson WF, Schall JD (1998) Role of frontal eye fields in countermanding saccades: visual, movement, and fixation activity. J Neurophysiol 79:817–834.

Hanes DP, Schall JD (1996) Neural control of voluntary movement initiation. Science 274:427–430.

Hanes DP, Thompson KG, Schall JD (1995) Relationship of presaccadic activity in

frontal eye field and supplementary eye field to saccade initiation in macaque: Poisson spike train analysis. Exp Brain Res 103:85–96.

Hanes DP, Wurtz RH (2001) Interaction of the frontal eye field and superior colliculus for saccade generation. J Neurophysiol 85:804–815.

Heitz RP, Schall JD (2012) Article Neural Mechanisms of Speed-Accuracy Tradeoff.

Helminski JO, Segraves MA (2003) Macaque Frontal Eye Field Input to Saccade-Related Neurons in the Superior Colliculus. J Neurophysiol 90:1046–1062.

Hikosaka O, Wurtz RH (1983a) Visual and oculomotor functions of monkey substantia nigra pars reticulata. III. Memory-contingent visual and saccade responses. J Neurophysiol 49:1268–1284.

Hikosaka O, Wurtz RH (1983b) Visual and oculomotor functions of monkey substantia nigra pars reticulata. IV. Relation of substantia nigra to superior colliculus. J Neurophysiol 49:1285–1301.

Horwitz GD, Newsome WT (1999) Separate signals for target selection and movement specification in the superior colliculus. Science 284:1158–1161.

Huerta MF, Krubitzer LA, Kaas JH (1986) Frontal eye field as defined by intracortical microstimulation in squirrel monkeys, owl monkeys, and macaque monkeys: I. Subcortical connections. J Comp Neurol 253:415–439.

Izawa Y, Suzuki H, Shinoda Y (2009) Response properties of fixation neurons and their location in the frontal eye field in the monkey. J Neurophysiol 102:2410–2422.

Jantz JJ, Watanabe M, Everling S, Munoz DP (2013) Threshold mechanism for saccade initiation in frontal eye field and superior colliculus. J Neurophysiol 109:2767–2780.

Jayaraman A, Batton RR, Carpenter MB (1977) Nigrotectal projections in the monkey: An autoradiographic study. Brain Res 135:147–152.

Jiang H, Stein BE, McHaffie JG (2003) Opposing basal ganglia processes shape midbrain visuomotor activity bilaterally. Nature 423:982–986.

Johnston K, Everling S (2006) Monkey dorsolateral prefrontal cortex sends task-selective signals directly to the superior colliculus. J Neurosci 26:12471–12478.

Johnston K, Koval MJ, Lomber SG, Everling S (2014) Macaque Dorsolateral Prefrontal Cortex Does not Suppress Saccade-Related Activity in the Superior Colliculus. Cereb Cortex 24:1373–1388.

Katnani HA, Gandhi NJ (2012) The relative impact of microstimulation parameters on movement generation. J Neurophysiol 108:528–538.

Katz LN, Yates JL, Pillow JW, Huk AC (2016) Dissociated functional significance of decision-related activity in the primate dorsal stream. Nature 535:285–288.

Kim JN, Shadlen MN (1999) Neural correlates of a decision in the dorsolateral prefrontal cortex of the macaque. Nat Neurosci 2:176–185.

Komatsu H, Suzuki H (1985) Projections from the functional subdivisions of the frontal eye field to the superior colliculus in the monkey. Brain Res 327:324–327.

Koval MJ, Lomber SG, Everling S (2011) Prefrontal cortex deactivation in macaques alters activity in the superior colliculus and impairs voluntary control of saccades. J Neurosci 31:8659–8668.

Kunimatsu J, Miyamoto N, Ishikawa M, Shirato H, Tanaka M, J. K, N. M, M. I, H. S, M. T (2015) Application of radiosurgical techniques to produce a primate model of brain lesions. Front Syst Neurosci 9:67.

Leichnetz GR, Spencer RF, Hardy SGP, Astruc J (1981) The prefrontal corticotectal projection in the monkey; An anterograde and retrograde horseradish peroxidase study. Neuroscience 6:1023–1041.

Liu P, Basso M a (2008) Substantia nigra stimulation influences monkey superior colliculus neuronal activity bilaterally. J Neurophysiol 100:1098–1112.

Lo C-C, Wang X-J (2006) Cortico-basal ganglia circuit mechanism for a decision threshold in reaction time tasks. Nat Neurosci 9:956–963.

Lomber SG, Payne BR, Horel JA (1999) The cryoloop: An adaptable reversible cooling deactivation method for behavioral or electrophysiological assessment of neural function. J Neurosci Methods 86:179–194.

Marino R a., Levy R, Boehnke S, White BJ, Itti L, Munoz DP (2012) Linking visual response properties in the superior colliculus to saccade behavior. Eur J Neurosci 35:1738–1752.

Mays LE, Sparks DL (1980) Dissociation of visual and saccade-related responses in superior colliculus neurons. J Neurophysiol 43:207–232.

Mazurek ME, Roitman JD, Ditterich J, Shadlen MN (2003) A Role for Neural Integrators in Perceptual Decision Making. Cereb Cortex 13:1257–1269.

McPeek RM, Keller EL (2002) Saccade target selection in the superior colliculus during a visual search task. J Neurophysiol 88:2019–2034.

Miyashita N, Hikosaka O (1996) Minimal synaptic delay in the saccadic output pathway of the superior colliculus studied in awake monkey. Exp Brain Res 112:187–196.

Munoz DP, Istvan PJ (1998) Lateral inhibitory interactions in the intermediate layers of the monkey superior colliculus. J Neurophysiol 79:1193–1209.

Munoz DP, Wurtz RH (1995) Saccade-related activity in monkey superior colliculus. I. Characteristics of burst and buildup cells. J Neurophysiol 73:2313–2333.

Pandya DN, Vignolo L a (1971) Intra- and interhemispheric projections of the precentral, premotor and arcuate areas in the rhesus monkey. Brain Res 26:217–233.

Paré M, Hanes DP (2003) Controlled movement processing: superior colliculus activity associated with countermanded saccades. J Neurosci 23:6480–6489.

Paré M, Wurtz RH (1997) Monkey posterior parietal cortex neurons

antidromically activated from superior colliculus. J Neurophysiol 78:3493–3497.

Paré M, Wurtz RH (2001) Progression in neuronal processing for saccadic eye movements from parietal cortex area lip to superior colliculus. J Neurophysiol 85:2545–2562.

Peel TR, Hafed ZM, Dash S, Lomber SG, Corneil BD (2016) A causal role for the cortical frontal eye fields in microsaccade deployment. PLoS Biol 14:775–786.

Peel TR, Johnston K, Lomber SG, Corneil BD (2014) Bilateral saccadic deficits following large and reversible inactivation of unilateral frontal eye field. J Neurophysiol 111:415–433.

Pouget P, Logan GD, Palmeri TJ, Boucher L, Paré M, Schall JD (2011) Neural Basis of Adaptive Response Time Adjustment during Saccade Countermanding. J Neurosci 31:12604–12612.

Ratcliff R, Cherian A, Segraves M (2003) A comparison of macaque behavior and superior colliculus neuronal activity to predictions from models of two-choice decisions. J Neurophysiol 90:1392–1407.

Ratcliff R, Hasegawa YT, Hasegawa RP, Smith PL, Segraves M a (2007) Dual diffusion model for single-cell recording data from the superior colliculus in a brightness-discrimination task. J Neurophysiol 97:1756–1774.

Ratcliff R, McKoon G (2008) The diffusion decision model: theory and data for two-choice decision tasks. Neural Comput 20:873–922.

Ratcliff R, Smith PL (2004) A comparison of sequential sampling models for two-choice reaction time. Psychol Rev 111:333–367.

Raybourn MS, Keller EL (1977) Colliculoreticular organization in primate oculomotor system. J Neurophysiol 40:861–878.

Reddi BA, Carpenter RH (2000) The influence of urgency on decision time. Nat Neurosci 3:827–830.

Rezvani S, Corneil BD (2008) Recruitment of a head-turning synergy by low-frequency activity in the primate superior colliculus. J Neurophysiol 100:397–411.

Schiller PH, True SD, Conway JL (1980) Deficits in eye movements following frontal eye-field and superior colliculus ablations. J Neurophysiol 44:1175–1189.

Schlag J, Dassonville P, Schlag-Rey M (1998) Interaction of the two frontal eye fields before saccade onset. J Neurophysiol 79:64–72.

Schnyder H, Reisine H, Hepp K, Henn V (1985) Frontal eye field projection to the paramedian pontine reticular formation traced with wheat germ agglutinin in the monkey. Brain Res 329:151–160.

Scudder CA, Kaneko CR, Fuchs AF (2002) The brainstem burst generator for saccadic eye movements: A modern synthesis. Exp Brain Res 142:439–462.

Segraves MA (1992) Activity of monkey frontal eye field neurons projecting to

oculomotor regions of the pons. J Neurophysiol 68:1967–1985.

Segraves MA, Goldberg ME (1987) Functional properties of corticotectal neurons in the monkey's frontal eye field. J Neurophysiol 58:1387–1419.

Seidemann E, Arieli A, Grinvald A, Slovin H (2002) Dynamics of depolarization and hyperpolarization in the frontal cortex and saccade goal. Science 295:862–865.

Shankar S, Massoglia DP, Zhu D, Costello MG, Stanford TR, Salinas E (2011) Tracking the temporal evolution of a perceptual judgment using a compelled-response task. J Neurosci 31:8406–8421.

Sommer M a, Wurtz RH (2004a) What the brain stem tells the frontal cortex. I. Oculomotor signals sent from superior colliculus to frontal eye field via mediodorsal thalamus. J Neurophysiol 91:1381–1402.

Sommer M a, Wurtz RH (2004b) What the brain stem tells the frontal cortex. II. Role of the SC-MD-FEF pathway in corollary discharge. J Neurophysiol 91:1403–1423.

Sommer MA, Tehovnik EJ (1997) Reversible inactivation of macaque frontal eye field. Exp brain Res 116:229–249.

Sommer MA, Wurtz RH (2000) Composition and topographic organization of signals sent from the frontal eye field to the superior colliculus. J Neurophysiol 83:1979–2001.

Sommer MA, Wurtz RH (2001) Frontal eye field sends delay activity related to movement, memory, and vision to the superior colliculus. J Neurophysiol 85:1673–1685.

Sparks DL (1978) Functional properties of neurons in the monkey superior colliculus: Coupling of neuronal activity and saccade onset. Brain Res 156:1–16.

Sparks DL (1986) Translation of sensory signals into commands for control of saccadic eye movements: role of primate superior colliculus. Physiol Rev 66:118–171.

Sparks DL (2002) The brainstem control of saccadic eye movements. Nat Rev Neurosci 3:952–64.

Sparks DL, Holland R, Guthrie BL (1976) Size and distribution of movement fields in the monkey superior colliculus. Brain Res 113:21–34.

Stanford TR, Freedman EG, Sparks DL (1996) Site and parameters of microstimulation: evidence for independent effects on the properties of saccades evoked from the primate superior colliculus. J Neurophysiol 76:3360–3381.

Stanford TR, Shankar S, Massoglia DP, Costello MG, Salinas E (2010) Perceptual decision making in less than 30 milliseconds. Nat Neurosci 13:379–385.

Thompson KG, Hanes DP, Bichot NP, Schall JD (1996) Perceptual and motor processing stages identified in the activity of macaque frontal eye field neurons during visual search. J Neurophysiol 76:4040–4055.

Tigges J, Tigges M (1981) Distribution of retinofugal and corticofugal axon terminals in the superior colliculus of squirrel monkey. Invest Ophthalmol Vis Sci 20:149–158.

Van Opstal a. J, Goossens HHLM (2008) Linear ensemble-coding in midbrain superior colliculus specifies the saccade kinematics. Biol Cybern 98:561–577.

Waitzman DM, Ma TP, Optican LM, Wurtz RH (1991) Superior colliculus neurons mediate the dynamic characteristics of saccades. J Neurophysiol 66:1716–1737.

Wardak C, Ibos G, Duhamel J-R, Olivier E (2006) Contribution of the monkey frontal eye field to covert visual attention. J Neurosci 26:4228–4235.

Woodman GF, Kang M-S, Thompson K, Schall JD (2008) The effect of visual search efficiency on response preparation: neurophysiological evidence for discrete flow. Psychol Sci a J Am Psychol Soc / APS 19:128–136.

Wurtz RH, Goldberg ME (1972a) Activity of superior colliculus in behaving monkey. 3. Cells discharging before eye movements. J Neurophysiol 35:575–586.

Wurtz RH, Goldberg ME (1972b) Activity of superior colliculus in behaving monkey. IV. Effects of lesions on eye movements. J Neurophysiol 35:587–596.

Wurtz RH, Sommer MA, Paré M, Ferraina S (2001) Signal transformations from cerebral cortex to superior colliculus for the generation of saccades. Vision Res 41:3399–3412.

Yoshida K, Iwamoto Y, Chimoto S, Shimazu H (1999) Saccade-related inhibitory input to pontine omnipause neurons: an intracellular study in alert cats. J Neurophysiol 82:1198–1208.

Zénon A, Krauzlis RJ (2012) Attention deficits without cortical neuronal deficits. Nature 489:434–437.

Chapter 5

General Discussion

5.1: Summary of Results

The FEF is a prime candidate for studying how cognitive and sensory processes influence visually-guided movements. In this series of experiments, I aimed to better understand the FEF's contribution to flexible oculomotor behaviour and neuronal activity in a key convergence area of cortical signals, the iSC. Moreover, given that iSC activity can be correlated to many aspects of saccade behaviour, it also provides a unique opportunity to study the neuronal mechanisms of saccade initiation and generation. Here, I provide a summary of the results from each experiment, and then I discuss how these results provide important insights into the underlying oculomotor mechanisms.

In **Chapter 2**, we found that the FEF contributes to the initiation of saccades in both directions, in addition to driving the generation of the contralateral saccades. FEF inactivation caused greater movement deficits and performance errors for memory-guided compared to visually-guided saccades, confirming that the FEF had an important role for cognitive influences on saccade behaviour.

As described in **Chapter 3**, we demonstrated that the FEF has a causal role in microsaccade generation, particularly for microsaccades deployed following peripheral cues. Regardless of the hemifield a peripheral cue appeared, unilateral FEF inactivation reduced and delayed the occurrence of rebound microsaccades. Bilateral FEF inactivation decreased microsaccades occurrence before cue onset, and further reduced the rate of rebound microsaccades, consistent with the FEF's role for microsaccade deployment following cues in both directions. Using an existing model of microsaccade deployment (Hafed and Ignashchenkova, 2013), we proposed that the lower rate of rebound microsaccades could result from a reduced cognitive excitatory influence on microsaccades. Importantly, unilateral FEF inactivation also increased amplitudes and decreased peak velocities of microsaccades in both directions, before and after cue onset, consistent with a reduction of inputs to downstream oculomotor structures. This evidence implicates the FEF as a likely substrate for how cognitive processes influence the strategic deployment of microsaccades.

Finally, in **Chapter 4**, we found that the FEF contributes to visual, delay-period, and saccade-related responses in the downstream, ipsilateral iSC, consistent with the FEF exerting its influence on saccade behaviour via the iSC. Unexpectedly, unilateral FEF inactivation also delayed onset of saccade-related activity bilaterally in the iSC, which could not be predicted based on previous antidromic studies. Interestingly, delayed onsets of saccade-related activity, but

not the accumulation rate or threshold activity, correlated with increases in bilateral SRT, suggesting that the onset of activity is an discerning factor for mechanisms of saccade initiation.

Together, our results offer new insights into the FEF's contribution to saccade and microsaccade behaviour, particularly the bilateral influence of the FEF on oculomotor behaviour. Moreover, examining iSC activity during FEF inactivation revealed how FEF inputs to the SC can govern the onset of iSC activity, and more generally, the importance of the onset of accumulation within rise-to-threshold models of saccade initiation.

5.2: Role of FEF for saccade and microsaccade behaviour in both directions

One consistent, yet surprising, result across these experiments was the bilateral influence of unilateral FEF inactivation on saccades and microsaccades behaviour. Despite the fact that electrical stimulation in the FEF can evoke saccades of various amplitudes and directions (Bruce et al., 1985), and the known existence of FEF neurons tuned in either contralateral or ipsilateral directions (Bruce and Goldberg, 1985), previous studies have found that reversible inactivation of focal FEF regions impairs the generation of only

contralesional saccades (Sommer and Tehovnik, 1997; Dias and Segraves, 1999). Interestingly, such focal FEF inactivations also decreased ipsilesional SRTs, or increased the incidence of ipsilesional saccades, suggesting that the FEF may also have a role in suppressing ipsiversive saccades. Consequently, the finding that FEF inactivation delays saccades in both directions has important implications for oculomotor mechanisms.

We attribute the bilateral effects of unilateral FEF inactivation to its large size, which provides a volume of inactivation approximately four times larger than those achieved using pharmacological modulations (see **Chapter 2**). We propose that a large-volume inactivation reveals the contribution of the more sparse and distributed ipsilateral tuned FEF neurons (Sommer and Wurtz, 2000; Izawa et al., 2009), in addition to affecting all aspects of the FEF's topographic map for contralateral-directed saccades (Robinson, 1972; Bruce et al., 1985). The manner in which the FEF directly communicates with each side of the iSC (Distel and Fries, 1982; Stanton et al., 1988; Crapse and Sommer, 2009) could be a simple explanation of why unilateral FEF inactivation produces bilateral effects on saccade and microsaccade behaviour.

However, the FEF could also indirectly influence the SC through the contralateral FEF (Pandya and Vignolo, 1971) or basal ganglia (Stanton et al., 1988), complicating the interpretation for the bilateral effects from FEF

inactivation. Indeed, visuospatial interactions between FEF neurons in one or both hemispheres (Schlag et al., 1998; Cohen et al., 2010) could be more broadly disrupted during large-volume compared to focal FEF inactivations, which usually affect a specific topographic region (Sommer and Tehovnik, 1997; Dias and Segraves, 1999). Consequently, a more general reduction in visuospatial processing amongst FEF neurons may lead to delays in target selection or coming to a consensus on any specific saccade vector. Furthermore, the FEF's connections to the basal ganglia may ultimately release the tonic inhibition of the substantia nigra pars reticulata (SNr) on each side of the iSC (Hikosaka and Wurtz, 1983; Liu and Basso, 2008). Importantly, SNr neurons with uncrossed and crossed projections to the iSC differ in several aspects, such as in their anatomical locations, spontaneous activity, and response fields (Jiang et al., 2003). In any case, the FEF's indirect connections to either side of the iSC could also account for the FEF's bilateral influence on saccade initiation.

While the FEF's excitatory influence on the downstream iSC is analogous to that of the DLPFC (Koval et al., 2011, 2014; Johnston et al., 2014), we did not observe any evidence of increased intercollicular inhibition across the bilateral iSC. In fact, FEF inactivation delayed the onset of saccade-related activity bilaterally within the iSC for visually-guided saccades, which differs from how DLPFC inactivation delayed and shortened the onset of such activity in the ipsilesional and contralesional iSC, respectively. Consequently, this evidence

suggests that frontal regions encompassing the FEF and not DLPFC facilitate the initiation of saccades in both directions. Perhaps this evidence might explain why large-volume lesions containing the DLPFC (Guitton et al., 1985; Pierrot-Deseilligny et al., 2005), but not FEF (Deng et al., 1986; Schiller and Chou, 1998; Gaymard et al., 1999), produce an inability to suppress ipsilesional saccades.

We also found that the FEF contributed to microsaccade deployment in both directions. Since FEF inactivation attenuated rebound microsaccades following peripheral cues in both the affected and intact visual hemifields, this suggests that it was not due to an impairment in detecting the visual cue. Alternatively, modulations in microsaccade rate and direction following the appearance of stimuli are thought to involve cognitive processes, such as visuospatial attention (Hafed and Clark, 2002; Engbert and Kliegl, 2003), hence inactivating the FEF could prevent such processes from influencing microsaccade behaviour. However, since our task was not suited to study shifts of covert attention, we do not know how the bilateral impairments in rebound microsaccades during FEF inactivation directly related to cognitive processes. Future studies will need to examine how specific cortical processes allow for the strategic deployment of microsaccades.

The bilateral influence of the primate FEF on saccade behaviour may explain the discrepancies between studies using different techniques. In particular, the human and primate FEF is known to bilaterally activated for saccades using functional magnetic resonance imaging (Connolly et al., 2002; Ford et al., 2005), suggesting that the FEF in each hemisphere are at least participating during saccades in both directions. Since this technique has low spatial resolution about an area of interest, the evidence that a large-volume FEF inactivation causes bilateral effects on saccade initiation could explain the discrepancies of results obtained from these functional magnetic resonance imaging and focal FEF inactivation (Sommer and Tehovnik, 1997; Dias and Segraves, 1999).

5.3: Limits of linking models to neuronal mechanisms

Studying iSC activity in the absence of its key FEF input provides an unique opportunity to directly test neuronal mechanisms of saccade initiation. An influential rise-to-fixed threshold model of saccade initiation assumes that the neuronal mechanisms underlying saccade initiation follow this framework (Carpenter and Williams, 1995; Carpenter et al., 2009). In this section, I discuss why rise-to-threshold models do not fully account for the underlying mechanism of saccade initiation.

The notion that neuronal activity rising above a certain threshold initiated saccades is supported by neurophysiological evidence demonstrating *fixed* thresholds in individual neurons (Hanes and Schall, 1996; Mazurek et al., 2003; Ratcliff et al., 2007). That is, FEF or iSC neurons display an invariant firing rate immediately before saccade onset, and changes to the baseline level or rate of accumulation account for differences in SRT (Dorris et al., 1997; Reddi and Carpenter, 2000; Ludwig et al., 2004; Lo and Wang, 2006). However recent evidence suggests that saccade thresholds can vary in speed-accuracy tradeoffs (Heitz and Schall, 2012) or based on task conditions (Jantz et al., 2013).. Consequently, we were intrigued by the fact that the onset time of saccade-related activity, but not the accumulation rate, baseline or threshold activities, in the iSC correlated with the subsequent SRT. Nonetheless, our results are in line with recent neurophysiological findings that other factors may also explain changes in SRT. For example, Pouget and colleagues (2011) found that the onset time of saccade-related activity in either FEF or iSC neurons sufficiently explained systematic increases in SRT following a countermanding trial, which entails that a saccade towards a peripheral cue must be cancelled if a stop-signal appears. Likewise, the accumulation rate or baseline or threshold activities could not account SRT differences, suggesting that saccade initiation is determined by additional factors than simply the threshold level.

Such fixed thresholds in the FEF and iSC could be due to their parallel or indirect connections to OPNs (Segraves, 1992; Keller et al., 2000), which neurons display a firing rate that is tightly coupled to the instantaneous saccade velocity (Yoshida et al., 1999). Since OPN activity should be invariant regardless of SRT, how then can we explain our paradoxical finding that accumulation rate and threshold activities decreased for similar, but longer latency, contralesional saccades, during FEF inactivation?

Because we only recorded single neurons, a simple explanation is that evidence of fixed thresholds could be attributed to a population coding within the iSC. Another intriguing explanation is that the brainstem circuitry integrates neuronal activity from upstream oculomotor areas. Since the duration between the onset times of saccade-related activity and the saccade appeared to explain at least some of the variability of SRT changes during FEF inactivation (see **Chapter 4**), such a relationship could mean that the integration of saccade-related signals occurred over a longer duration. Encouragingly, such a mechanism is also consistent with the leaky integrator mechanism proposed by Heitz & Schall (2012). These investigators reported that more accurate saccades with longer SRTs result from decreased baseline activity, accumulation rate, and threshold activities. They proposed that a leaky integrator mechanism could produce the invariant amount of activity required to silence the OPNs during speed-accuracy tradeoffs. While future studies will need to directly test the

validity of these mechanisms, it does underscore the claim that rise-to-threshold models of saccade initiation provide an overly simplistic representation of the neuronal mechanism.

5.4: Future Directions

This series of experiments set out to uncover the FEF's contribution to saccade and microsaccade behaviour, and the underlying oculomotor mechanisms involving the downstream iSC. Our results implicate the FEF in bilateral saccade generation though intriguing effects occurring in both sides of the iSC, however questions remain about how exactly the FEF influences the timing and not the magnitude of saccade-related activity in contralateral iSC. Based on the results obtained from these present experiments, I discuss some potential objectives for future studies.

First, we hypothesized that a large-volume FEF inactivation revealed the contribution of ipsilateral-tuned neurons dispersed throughout the FEF, but future studies should examine the functional pathways mediating this influence. This is particularly important since FEF corticotectal neurons projecting directly to the contralateral iSC do not appear to overlay with the dispersed ipsilateral-tuned FEF neurons (Distel and Fries, 1982; Sommer and Wurtz, 2000; Izawa et al., 2009), suggesting the involvement of indirect connections, such as those between the FEFs (Schlag et al., 1998). Coupling FEF inactivation with neuronal

recordings in the FEF of the opposite hemisphere might provide clues into whether ipsilateral-tuned neurons mediate their influence directly to downstream structures or indirectly through a cortical process.

Second, we found that the FEF is a plausible substrate for cognitive influences on microsaccade deployment, but future studies will need to address the specific cognitive processes involved. Since the FEF is directly implicated in cognitive influences on visual processing areas, such as V4 (Moore and Armstrong, 2003; Gregoriou et al., 2009), FEF's role in visual processing may also depend upon the strategic deployment of microsaccades. Measuring microsaccades before and during FEF inactivation in a more cognitively demanding task, such as in a peripheral cueing task, could help establish a relationship between cortical processes and the strategic deployment of microsaccades.

Finally, our results obtained from caudal iSC neurons do not address the impact of FEF inactivation on rostral iSC activity, nor how visual response or movement fields might have changed during FEF inactivation, important limitations of these experiments. Since we recorded iSC activity at the center of the visual response and/or movement field as determined before FEF inactivation, it is possible that FEF inactivation shifted, collapsed, or even expanded these fields. Changing fields could alter an iSC neuron's visual,

cognitive, or saccade-related activity, possibly contributing to our observed changes of iSC activity during FEF inactivation. While we cannot rule out this possibility, the robust decreases of all aspects of iSC activity suggests that reduced FEF inputs likely contributed to any changes in response fields during FEF inactivation, and similarly, lateral inhibitory pathways between the rostral and caudal iSC neurons could not simply explain our results. Interestingly, preliminary evidence indicates that FEF inactivation bilaterally disrupted local interactions occurring at specific frequencies amongst iSC neurons (Peel et al., 2013), consistent with reduced FEF inputs directly or indirectly to the iSC. Future studies investigating how FEF inactivation affects rostral iSC activity, and the response fields of iSC neurons may help clarify the FEFs contribution to the downstream iSC.

5.5: Concluding Remarks

This series of experiments reveals a novel perspective into the FEF's contribution to saccade and microsaccade generation, which is supported by correlates of neuronal activity in the downstream iSC. Consistent with previous reports (Everling and Munoz, 2000; Sommer and Wurtz, 2000; Helminski and Segraves, 2003), we found that the FEF is an important source of sensory and cognitive signals to the iSC for flexible oculomotor behaviour, but we could not predict the FEF's bilateral influence on saccade and microsaccade generation, nor the importance of the onset of iSC activity for saccade initiation. While there

is much interest in understanding the cortical processes underlying flexible saccade behaviour, future studies should also address the gap of knowledge of how such areas communicate with the downstream brainstem circuitry to initiate and generate a specific saccade vector.

5.6: References

Bruce CJ, Goldberg ME (1985) Primate frontal eye fields. I. Single neurons discharging before saccades. J Neurophysiol 53:603–635.

Bruce CJ, Goldberg ME, Bushnell MC, Stanton GB (1985) Primate frontal eye fields. II. Physiological and anatomical correlates of electrically evoked eye movements. J Neurophysiol 54:714–734.

Carpenter RH, Williams ML (1995) Neural computation of log likelihood in control of saccadic eye movements. Nature 377:59–62.

Carpenter RHS, Reddi BAJ, Anderson AJ (2009) A simple two-stage model predicts response time distributions. J Physiol 587:4051–4062.

Cohen JY, Crowder EA, Heitz RP, Subraveti CR, Thompson KG, Woodman GF, Schall JD (2010) Cooperation and Competition among Frontal Eye Field Neurons during Visual Target Selection. J Neurosci 30:3227–3238.

Connolly JD, Goodale M a, Menon RS, Munoz DP (2002) Human fMRI evidence for the neural correlates of preparatory set. Nat Neurosci 5:1345–1352.

Crapse TB, Sommer MA (2009) Frontal eye field neurons with spatial representations predicted by their subcortical input. J Neurosci 29:5308–5318.

Deng SYY, Goldberg M. E, Segraves MAA, Ungerleider LGG, Mishkin M (1986) The effect of unilateral ablation of the frontal eye fields on saccadic performance in the monkey. In: Adaptive Processes in the Visual and Oculomotor Systems, pp 201–208. Elsevier.

Dias EC, Segraves MA (1999) Muscimol-induced inactivation of monkey frontal eye field: effects on visually and memory-guided saccades. J Neurophysiol 81:2191–2214.

Distel H, Fries W (1982) Contralateral cortical projections to the superior colliculus in the macaque monkey. Exp brain Res 48:157–162.

Dorris MC, Paré M, Munoz DP (1997) Neuronal activity in monkey superior colliculus related to the initiation of saccadic eye movements. J Neurosci 17:8566–8579.

Engbert R, Kliegl R (2003) Microsaccades uncover the orientation of covert

attention. Vision Res 43:1035–1045.

Everling S, Munoz DP (2000) Neuronal correlates for preparatory set associated with pro-saccades and anti-saccades in the primate frontal eye field. J Neurosci 20:387–400.

Ford K a, Goltz HC, Brown MRG, Everling S (2005) Neural processes associated with antisaccade task performance investigated with event-related FMRI. J Neurophysiol 94:429–440.

Gaymard B, Ploner CJ, Rivaud-Péchoux S, Pierrot-Deseilligny C (1999) The frontal eye field is involved in spatial short-term memory but not in reflexive saccade inhibition. Exp Brain Res 129:288–301.

Gregoriou GG, Gotts SJ, Zhou H, Desimone R (2009) High-frequency, long-range coupling between prefrontal and visual cortex during attention. Science (80-) 324:1207–1210.

Guitton D, Buchtel H a., Douglas RM (1985) Frontal lobe lesions in man cause difficulties in suppressing reflexive glances and in generating goal-directed saccades. Exp Brain Res 58:455–472.

Hafed ZM, Clark JJ (2002) Microsaccades as an overt measure of covert attention shifts. Vision Res 42:2533–2545.

Hafed ZM, Ignashchenkova A (2013) On the dissociation between microsaccade rate and direction after peripheral cues: microsaccadic inhibition revisited. J Neurosci 33:16220–16235.

Hanes DP, Schall JD (1996) Neural control of voluntary movement initiation. Science 274:427–430.

Heitz RP, Schall JD (2012) Article Neural Mechanisms of Speed-Accuracy Tradeoff.

Helminski JO, Segraves MA (2003) Macaque Frontal Eye Field Input to Saccade-Related Neurons in the Superior Colliculus. J Neurophysiol 90:1046–1062.

Hikosaka O, Wurtz RH (1983) Visual and oculomotor functions of monkey substantia nigra pars reticulata. IV. Relation of substantia nigra to superior colliculus. J Neurophysiol 49:1285–1301.

Izawa Y, Suzuki H, Shinoda Y (2009) Response properties of fixation neurons and their location in the frontal eye field in the monkey. J Neurophysiol 102:2410–2422.

Jantz JJ, Watanabe M, Everling S, Munoz DP (2013) Threshold mechanism for saccade initiation in frontal eye field and superior colliculus. J Neurophysiol 109:2767–2780.

Jiang H, Stein BE, McHaffie JG (2003) Opposing basal ganglia processes shape midbrain visuomotor activity bilaterally. Nature 423:982–986.

Johnston K, Koval MJ, Lomber SG, Everling S (2014) Macaque Dorsolateral Prefrontal Cortex Does not Suppress Saccade-Related Activity in the Superior Colliculus. Cereb Cortex 24:1373–1388.

Keller EL, McPeek RM, Salz T (2000) Evidence against direct connections to PPRF

EBNs from SC in the monkey. J Neurophysiol 84:1303–1313.

Koval MJ, Hutchison RM, Lomber SG, Everling S (2014) Effects of unilateral deactivations of dorsolateral prefrontal cortex and anterior cingulate cortex on saccadic eye movements. J Neurophysiol 111:787–803.

Koval MJ, Lomber SG, Everling S (2011) Prefrontal cortex deactivation in macaques alters activity in the superior colliculus and impairs voluntary control of saccades. J Neurosci 31:8659–8668.

Liu P, Basso M a (2008) Substantia nigra stimulation influences monkey superior colliculus neuronal activity bilaterally. J Neurophysiol 100:1098–1112.

Lo C-C, Wang X-J (2006) Cortico-basal ganglia circuit mechanism for a decision threshold in reaction time tasks. Nat Neurosci 9:956–963.

Ludwig CJH, Gilchrist ID, McSorley E (2004) The influence of spatial frequency and contrast on saccade latencies. Vision Res 44:2597–2604.

Mazurek ME, Roitman JD, Ditterich J, Shadlen MN (2003) A Role for Neural Integrators in Perceptual Decision Making. Cereb Cortex 13:1257–1269.

Moore T, Armstrong KM (2003) Selective gating of visual signals by microstimulation of frontal cortex. Nature 421:370–373.

Pandya DN, Vignolo L a (1971) Intra- and interhemispheric projections of the precentral, premotor and arcuate areas in the rhesus monkey. Brain Res 26:217–233.

Peel TR, Womelsdorf T, Lomber SG, Corneil BD (2013) The functional contribution of the frontal eye fields to spiking activity and local field potentials in the intermediate superior colliculus. In: Society for Neuroscience Abstracts.

Pierrot-Deseilligny C, Müri RM, Nyffeler T, Milea D (2005) The role of the human dorsolateral prefrontal cortex in ocular motor behavior. Ann N Y Acad Sci 1039:239–251.

Pouget P, Logan GD, Palmeri TJ, Boucher L, Paré M, Schall JD (2011) Neural Basis of Adaptive Response Time Adjustment during Saccade Countermanding. J Neurosci 31:12604–12612.

Ratcliff R, Hasegawa YT, Hasegawa RP, Smith PL, Segraves M a (2007) Dual diffusion model for single-cell recording data from the superior colliculus in a brightness-discrimination task. J Neurophysiol 97:1756–1774.

Reddi BA, Carpenter RH (2000) The influence of urgency on decision time. Nat Neurosci 3:827–830.

Robinson D (1972) Eye movements evoked by collicular stimulation in the alert monkey. Vision Res 12:1795–1808.

Schiller PH, Chou IH (1998) The effects of frontal eye field and dorsomedial frontal cortex lesions on visually guided eye movements. Nat Neurosci 1:248–253.

Schlag J, Dassonville P, Schlag-Rey M (1998) Interaction of the two frontal eye fields before saccade onset. J Neurophysiol 79:64–72.

Segraves MA (1992) Activity of monkey frontal eye field neurons projecting to oculomotor regions of the pons. J Neurophysiol 68:1967–1985.

Sommer MA, Tehovnik EJ (1997) Reversible inactivation of macaque frontal eye field. Exp brain Res 116:229–249.

Sommer MA, Wurtz RH (2000) Composition and topographic organization of signals sent from the frontal eye field to the superior colliculus. J Neurophysiol 83:1979–2001.

Stanton GB, Goldberg ME, Bruce CJ (1988) Frontal eye field efferents in the macaque monkey: II. Topography of terminal fields in midbrain and pons. J Comp Neurol 271:493–506.

Yoshida K, Iwamoto Y, Chimoto S, Shimazu H (1999) Saccade-related inhibitory input to pontine omnipause neurons: an intracellular study in alert cats. J Neurophysiol 82:1198–1208.

Western

2007-099-10::7:

AUP Number: 2007-099-10
AUP Title: Sensory and Motor Roles for Neck Muscles in Visually-Guided Actions: Neural Mechanisms Underlying Recruitment and Kinesthesia

Yearly Renewal Date: 01/01/2015

The YEARLY RENEWAL to Animal Use Protocol (AUP) 2007-099-10 has been approved, and will be approved for one year following the above review date.

1. This AUP number must be indicated when ordering animals for this project.
2. Animals for other projects may not be ordered under this AUP number.
3. Purchases of animals other than through this system must be cleared through the ACVS office. Health certificates will be required.

REQUIREMENTS/COMMENTS
Please ensure that individual(s) performing procedures on live animals, as described in this protocol, are familiar with the contents of this document.

The holder of this Animal Use Protocol is responsible to ensure that all associated safety components (biosafety, radiation safety, general laboratory safety) comply with institutional safety standards and have received all necessary approvals. Please consult directly with your institutional safety officers.

Submitted by: Kinchlea, Will D
on behalf of the Animal Use Subcommittee

Curriculum Vitae

University Address:
Graduate Program in Neuroscience
The University of Western Ontario
Robarts Research Institute, RRI 3203
London, Ontario, Canada
N6A 3K7

Education

2009-2016 **Doctor of Philosophy Candidate - Neuroscience**
The University of Western Ontario, London, Ontario.
Thesis: Contribution of the Primate Frontal Cortex to Eye Movements and Neuronal Activity in the Superior Colliculus
Supervisor: Dr. Brian Corneil

2005-2009 **Bachelor of Medical Science (Honours) with Distinction - Pharmacology and Toxicology**
The University of Western Ontario, London, Ontario.

Publications

Peel T. R., Johnston K., Lomber S. G., and Corneil B. D. (2014) Bilateral saccadic deficits following large and reversible inactivation of unilateral frontal eye field. *J. Neurophysiol.* 111, 415-433.

Corneil B.D., Goonetilleke S.C., **Peel T.R.**, Green K.A., and Welch I.D. (2012) Ultrasound-guided insertion of intramuscular electrodes into suboccipital muscles in the non-human primate: Technique description and physiological verification. *J Electromyogr Kinesiol.* 22, 553-559.

Peel T.R., Hafed Z.M., Dash S., Lomber S.G., and Corneil B.D. (2016) A causal role for the cortical frontal eye fields in microsaccade deployment. *PLoS Biol 14:775-786*.

Manuscripts Submitted or In Preparation

Peel T.R., Dash, S., Lomber, S.G., and Corneil B.D. Mechanisms of saccade generation and initiation within the superior colliculus: insights following frontal eye fields inactivation. In preparation for *Cerebral Cortex.*

Published Abstracts

Peel T.R., Dash S., Lomber S.G., and Corneil B.D. (2016) Mechanism of saccade initiation within the superior colliculus: insights following frontal eye fields inactivation. *Neural Control of Movement Meeting*

Peel T.R., Hafed Z.M., Lomber S.G., and Corneil B.D. (2015) The frontal eye fields are necessary for bottom-up, cue-induced influences on microsaccades. *German Primate Meeting*

Peel T.R., Womelsdorf T., Lomber S.G., and Corneil B.D. (2013) The functional contribution of the frontal eye fields to spiking activity and local field potentials in the intermediate superior colliculus. *Soc Neurosci Abstr.* 373.16

Peel T.R., Womelsdorf T., Lomber S.G., and Corneil B.D. (2013) The frontal eye fields contributes to spiking activity and modulates low-frequency oscillations in the intermediate superior colliculus. *Gordon Res. Conf.*

Peel T.R., Hafed Z.M., Lomber S.G., and Corneil B.D. (2012) The frontal eye fields are necessary for bottom-up, cue-induced influences on microsaccades. *Soc Neurosci Abstr.* 373.16

Peel T.R., Lomber S.G., and Corneil B.D. (2012) The functional contribution of the frontal eye fields to activity in the intermediate superior colliculus. *Soc Neurosci Abstr.* 373.10

Peel T.R., Lomber S.G., and Corneil B.D. (2011) An analysis of saccadic reaction times by the LATER model following unilateral inactivation of the primate frontal eye fields. *Soc Neurosci Abstr.* 272.04

Peel T.R., Lomber S.G., and Corneil B.D. (2011) Saccadic deficits following unilateral cryogenic inactivation of the primate frontal eye fields. *Gordon Res. Conf.*

Peel T.R., Lomber S.G., and Corneil B.D. (2010) Behavioural effects of unilateral cryogenic inactivation of primate frontal eye fields. *Soc Neurosci Abstr.* 778.17

Invited Presentations

Peel T.R. (2012) The functional contribution of the frontal eye fields to activity in the intermediate superior colliculus. NSERC CREATE (CAN-ACT) provincial conference.

Scholarships and Grants

2013	Gordon Research Travel Fellowship Research award ($500)
2012-2013	Trainee member of CREATE grant from Natural Sciences and Engineering Research Council of Canada ($15,000)
2011	Gordon Research Travel Fellowship Research award ($500)
2011 - 2012	Queen Elizabeth II Graduate Scholarship in Science and Technology ($15,000)
2009-2014	Western Graduate Research Scholarship ($7,200 / year)
2005-2009	Queen Elizabeth II Aiming for the Top Scholarship ($3,500 / year)
2005-2006	Western Scholarship of Distinction ($1,500)

Research and Teaching Assistantships

2013-2014	Anatomy and Cell Biology 9550, University of Western Ontario, London, Ontario.
2010-2011	Physiology 3130y, University of Western Ontario, London, Ontario.
2009-2010	Physiology 3130y, University of Western Ontario, London, Ontario.
2009	Summer Student Research Assistantship, University of Western Ontario, London, Ontario. Supervisors: Corneil B.D. and Womelsdorf T.

Leadership Positions

2010-2012	Schulich Graduate Student Representative